The microcirculation in gynaecological disease

Kastelein, A.W.

Publication date
2020
Document Version
Final published version
License
Other

THE

MICROCIRCULATION

IN GYNAECOLOGICAL DISEASE

Arnoud W. Kastelein

THE MICROCIRCULATION IN GYNAECOLOGICAL DISEASE

Arnoud W. Kastelein

Colofon
The microcirculation in gynaecological disease
ISBN/EAN: 978-94-6416-071-0

Cover design by Leon Postma
Layout and design by David de Groot | www.persoonlijkproefschrift.nl
Printed by Ridderprint | www.ridderprint.nl

The microcirculation in gynaecological disease

ACADEMISCH PROEFSCHRIFT

ter verkrijging van de graad van doctor
aan de Universiteit van Amsterdam
op gezag van de Rector Magnificus
prof. dr. ir. K.I.J. Maex
ten overstaan van een door het College voor Promoties ingestelde commissie,
in het openbaar te verdedigen in de Aula der Universiteit
op vrijdag 11 december 2020, te 11.00 uur

door
Arnoud Willem Kastelein
geboren te Vancouver

Promotiecommissie

Promotores	**Prof. dr. J.P.W.R. Roovers**	AMC-UvA
	Prof. dr. ir. C. Ince	AMC-UvA
Copromotor	**Dr. C.A.R. Lok**	NKI-AvL
Overige leden	**Prof. dr. C.J.F. van Noorden**	AMC-UvA
	Prof. dr. M.J. van de Vijver	AMC-UvA
	Prof. dr. A.M.M. van Pelt	AMC-UvA
	Prof. dr. F.C.A. Amant	AMC-UvA
	Prof. dr. C.H. van der Vaart	Universiteit Utrecht
	Prof. dr. ir. T.H. Smit	Vrije Universiteit Amsterdam

Faculteit der Geneeskunde

Voor mijn ouders

TABLE OF CONTENTS

1 General introduction and thesis outline

Blood vessels are of vital importance to the human body: all tissues rely on their presence and functionality. Different types of blood vessels have different functions and characteristics. *Arteries* transport blood from heart to tissue, whereas *veins* transport blood from tissue back to the heart (1). Further away from the heart, vessels divide, branch and get smaller until they form the *microcirculation*. The microcirculation consists of all blood vessels smaller than 100 µm: *arterioles*, *venules* and *capillaries*. Capillaries are the smallest blood vessels and exchange of oxygen, carbon dioxide and nutrients between blood and tissue occurs here (2). Consequently, the microcirculation is essential for oxygenation and proper organ functioning, and plays a key role in many pathophysiological processes such as wound healing and tumor metabolism (3-5).

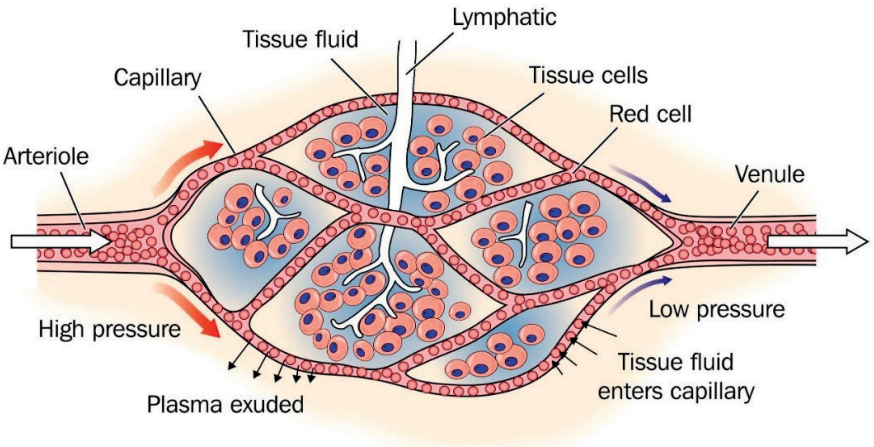

Capillary bed

Research of the microcirculation has increased drastically over the past decades and has been facilitated by the introduction of hand-held vital microscopes (6). The latest generation of these devices uses incident dark field (IDF) imaging, in which concentrically placed light-emitting diodes provide green light epi-illumination of the tissue (7, 8). The light is absorbed by hemoglobin within erythrocytes, allowing red blood cells to be imaged and recorded as a representation of the functional microcirculation. This enables non-invasive and real-time measurement of microvascular parameters such as *angioarchitecture*, *vessel density, vessel perfusion* and *focal depth* (9).

The largest body of evidence on the microcirculation comes from imaging of the sublingual microcirculation in critically ill patients (10, 11). Microcirculatory dysfunction – especially alterations in vessel perfusion – has been found to be predictive for organ failure and progress of sepsis. Abnormalities and heterogeneity in sublingual microcirculatory flow are associated with increased mortality, independent of alterations of the systemic circulation. Microvascular imaging has also been performed in various other organs, for example to investigate oral mucosal wound healing (12) or to assess the microcirculation of different human organ surfaces such as the brain, skin, intestines, conjunctiva, liver, and vagina (13-18). However, there is still much to be elucidated about the microcirculation, its function and consequences of its dysfunction.

In this thesis, we further investigate the microcirculation of the vagina and the peritoneum, because of its alleged contribution to adequate functioning of the female genital tract. Furthermore, we investigate the possible consequences of microcirculatory dysfunction in various benign and malignant gynaecological diseases. With this thesis, we improve fundamental (patho)physiological knowledge of gynaecological diseases and associated treatments. This is crucial for basic insight into treatment efficacy and inefficacy, development of new therapeutic strategies and generation of new hypotheses for future research.

PART I of this thesis investigates the microcirculation in two highly prevalent benign gynecological conditions that have significant impact on daily activity, sexual function and overall quality of life: vulvovaginal atrophy (VVA) and pelvic organ prolapse (POP). Hypoestrogenism after menopause plays a crucial role in these diseases and vaginal estrogen therapy is efficacious in treating symptoms of VVA and may also improve the outcome of POP surgery by stimulating wound healing. Estrogens may increase epithelial thickness and improve vaginal wall perfusion and oxygenation, but the actual effect of estrogens on the latter parameters is virtually unknown. We investigated the role of estrogens in vaginal wound healing, whether epithelial thickness can be reliably measured with IDF imaging as focal depth, and studied the effect of VVA and prolapse surgery on the vaginal microcirculation. If microvascular alterations and changes in focal depth can be quantified, microcirculatory assessment can be used to evaluate the effect of estrogen therapy, alternatives for estrogen therapy such as vaginal laser therapy, and (new) surgical procedures. This may ultimately improve (the outcome of) such therapies.

PART II of this thesis describes the microcirculation of the peritoneum. The peritoneum is a large serous membrane that lines the abdominal cavity and plays a crucial role in many pathological intra-abdominal conditions such as peritoneal adhesion formation, the production of ascites, and peritoneal carcinomatosis. Peritonitis carcinomatosis (PC) is often seen in patients with epithelial ovarian cancer (EOC) and has a significant effect on quality of life and prognosis. The pathophysiology of PC is not well understood and although extensive therapy is given to patients with EOC, 5-year survival remains poor and has not improved in 25 years. The peritoneal microcirculation may play an important role in the development of PC, the limited response to treatment and the growth pattern of peritoneal metastases on the peritoneum, but current knowledge on the peritoneal microcirculation is almost non-existent.

THESIS OUTLINE

PART I consist of four chapters on the vaginal microcirculation. **Chapter 2** is a systematic literature review about the effect of estrogens on vaginal wound healing. Epithelial thickness and vaginal vascularization are important factors in vaginal wound healing and are both affected by estrogen therapy. In **chapter 3**, we validate IDF focal depth measurements to non-invasively measure epithelial thickness of the vaginal wall. In **chapter 4**, the effects of estrogen therapy on the vaginal microcirculation are described, and in **chapter 5** the effects of prolapse surgery on the vaginal microcirculation are described.

PART II consists of three chapters on the peritoneal microcirculation. **Chapter 6** gives an overview of the literature on the embryology, anatomy, physiology and pathophysiology of the peritoneum and the peritoneal vasculature. In **chapter 7,** we demonstrate feasibility of intra-abdominal perioperative IDF imaging of the peritoneum, and describe the microcirculation in healthy peritoneum. Subsequently, in **chapter 8**, the microcirculation in peritoneal metastases is described in patients with peritoneal carcinomatosis of ovarian cancer.

In **chapter 9**, the results of this thesis are summarized. **Chapter 10** includes the general discussion and future recommendations.

REFERENCES

1. Martini FH. Fundamentals of Anatomy and Physiology. 2006;7th Edition.
2. Guven G, Hilty MP, Ince C. Microcirculation: Physiology, Pathophysiology, and Clinical Application. Blood purification. 2020;49(1-2):143-50.
3. Peters J, Mack GW, Lister G. The importance of the peripheral circulation in critical illnesses. Intensive Care Med. 2001;27(9):1446-58.
4. Bentov I, Reed MJ. Anesthesia, microcirculation, and wound repair in aging. Anesthesiology. 2014;120(3):760-72.
5. Ince C. The microcirculation is the motor of sepsis. Crit Care. 2005;9 Suppl 4:S13-9.
6. Ocak I, Kara A, Ince C. Monitoring microcirculation. Best practice & research Clinical anaesthesiology. 2016;30(4):407-18.
7. Aykut G, Veenstra G, Scorcella C, Ince C, Boerma C. Cytocam-IDF (incident dark field illumination) imaging for bedside monitoring of the microcirculation. Intensive care medicine experimental. 2015;3(1):40.
8. Hutchings S, Watts S, Kirkman E. The Cytocam video microscope. A new method for visualising the microcirculation using Incident Dark Field technology. Clinical hemorheology and microcirculation. 2016;62(3):261-71.
9. Ince C, Boerma EC, Cecconi M, De Backer D, Shapiro NI, Duranteau J, et al. Second consensus on the assessment of sublingual microcirculation in critically ill patients: results from a task force of the European Society of Intensive Care Medicine. Intensive Care Med. 2018;44(3):281-99.
10. Bezemer R, Bartels SA, Bakker J, Ince C. Clinical review: Clinical imaging of the sublingual microcirculation in the critically ill--where do we stand? Crit Care. 2012;16(3):224.
11. Gruartmoner G, Mesquida J, Ince C. Microcirculatory monitoring in septic patients: Where do we stand? Medicina intensiva. 2017;41(1):44-52.
12. Lindeboom JA, Mathura KR, Aartman IH, Kroon FH, Milstein DM, Ince C. Influence of the application of platelet-enriched plasma in oral mucosal wound healing. Clinical oral implants research. 2007;18(1):133-9.
13. Mathura KR, Bouma GJ, Ince C. Abnormal microcirculation in brain tumours during surgery. Lancet. 2001;358(9294):1698-9.
14. de Bruin AF, Kornmann VN, van der Sloot K, van Vugt JL, Gosselink MP, Smits A, et al. Sidestream dark field imaging of the serosal microcirculation during gastrointestinal surgery. Colorectal disease : the official journal of the Association of Coloproctology of Great Britain and Ireland. 2016;18(3):O103-10.
15. Klijn E, Van Zijderveld R, Den Uil C, Ince C, Bakker J. Conjunctival microcirculation in patients with traumatic brain injury. Critical Care. 2008;12(Suppl 2):P106-P.

16. Uz Z, Ince C, Rassam F, Ergin B, van Lienden KP, van Gulik TM. Assessment of hepatic microvascular flow and density in patients undergoing preoperative portal vein embolization. HPB : the official journal of the International Hepato Pancreato Biliary Association. 2019;21(2):187-94.
17. Weber MA, Milstein DM, Ince C, Oude Rengerink K, Roovers JP. Vaginal microcirculation: Non-invasive anatomical examination of the micro-vessel architecture, tortuosity and capillary density. Neurourology and urodynamics. 2015;34(8):723-9.
18. van Elteren HA, Ince C, Tibboel D, Reiss IKM, de Jonge RCJ. Cutaneous microcirculation in preterm neonates: comparison between sidestream dark field (SDF) and incident dark field (IDF) imaging. J Clin Monit Comput. 2015;29(5):543-8.

Part I

The vaginal microcirculation

2 The effects of estrogen on vaginal wound healing: a systematic review and meta-analysis

EV Vodegel
AW Kastelein
CHJR Jansen
J Limpens
SE Zwolsman
JPWR Roovers
C Hooijmans
Z Guler Gokce

Submitted for publication

ABSTRACT

Objective

Systematically summarizing the available literature to determine the effects of estrogen on vaginal wound healing in both women and animals.

Data sources

This systematic review was reported according to the Preferred Reporting Items for Systematic Reviews and Meta-Analyses (PRISMA) statement and was prospectively registered in PROSPERO (CRD42019156601). An information specialist performed a systematic search in OVID MEDLINE, OVID Embase and Web of Science from inception to 28 January 2020 using controlled vocabulary (including MeSH-terms) and text words to retrieve both animal and human studies on the effect of estrogen or estrogen deprivation on vaginal wound healing. Conference abstracts were excluded. No date or language restrictions were applied.

Study eligibility criteria

All original studies that compared wound healing related outcomes of estrogen exposed subjects to hypo-estrogenic subjects after vaginal surgery were included. Subjects were female animals and women.

Study appraisal and synthesis methods

Two reviewers independently selected studies, assessed bias, and extracted data. Wound healing related outcome measures were classified into the three phases of wound healing: (1) inflammatory phase, (2) proliferative phase, (3) and maturation phase. The standardized mean difference (SMD) and 95% confidence intervals were assessed by random-effects models with Hedges' g correction between intervention and control groups. Risk of bias was assessed using the Cochrane risk of bias tool for human studies and the SYRCLE risk of bias tool for animal studies.

Results

Fourteen studies were included in the systematic review and 11 studies were eligible for meta-analysis. Meta-analysis demonstrated that estrogen increased neovascularization (SMD 1.13 [0.67 – 1.60]) and granulation tissue formation (SMD 1.67 [0.54 – 2.79]), accelerated macroscopic (SMD 1.82 [1.22 – 2.42]) and microscopic (SMD 0.98 [0.66 – 1.29]) wound closure, improved collagen synthesis (SMD 1.08 [0.42 – 1.74]), and

increased tissue strength (SMD 1.26 [0.53 – 1.99]). Estrogen decreased the inflammatory response (SMD -0.58; [-1.14 – -0.02]) and reduced levels of TGF-β1 (SMD -1.68 [-2.52 – -0.83]).

Conclusions

This systematic review provides strong evidence that estrogen therapy has a positive effect on vaginal wound healing. Therefore, women undergoing vaginal surgery may benefit from perioperative estrogen therapy. Future studies should determine whether improved wound healing following estrogen therapy also improves surgical outcome and whether estrogen should be prescribed to all women undergoing vaginal surgery.

Keywords

Estrogen, wound healing, women, animal studies, vaginal surgery, pelvic organ prolapse, neovascularization, granulation, wound contraction, re-epithelialization, collagen synthesis, tissue strength, inflammatory response, TGF-β1.

ABBREVIATIONS

CI	confidence interval
CMA	Comprehensive Meta Analysis
H&E	hematoxylin & eosin
IQR	inter quartile range
PDGF	platelet-derived growth factor
POP	pelvic organ prolapse
PRISMA	Reporting Items for Systematic Reviews and Meta-Analyses
PROSPERO	prospective register of systematic reviews
SD	standard deviation
SE	standard error
SMD	standardized mean difference
SUI	stress urinary incontinence
SYRCLE	SYstematic Review Center for Laboratory animal Experimentation
TGF-β1	transforming growth factor-β1

INTRODUCTION

Postmenopausal women with pelvic floor pathology may benefit from vaginal estrogen therapy. A reduction of symptoms has been described in women with vaginal atrophy, stress urinary incontinence (SUI), overactive bladder, and recurrent cystitis when prescribed vaginal estrogens (1-3). The suggested underlying mechanism is that estrogen thickens the vaginal wall and urothelium, and improves vascularization of the pelvic floor (4). In addition, estrogen therapy may play an important role in the outcome of vaginal surgery, such as the surgical treatment of pelvic organ prolapse (POP).

Surgery for POP is associated with high recurrence rates of up to 50% (5). This stresses the need for improvement of the outcome of vaginal POP surgery. It is thought that the outcome of POP surgery may be negatively affected by impaired wound healing in postmenopausal, hypo-estrogenic women. Although vaginal wound closure often occurs without problems, tissue quality may be poor and thereby negatively affecting the outcome of surgery. It is hypothesized that treatment with vaginal estrogen may enhance vaginal wound healing, resulting in improved tissue quality and tissue strength, which is essential for long-term surgical outcome.

Estrogen and its derivatives are known to have a positive effect on cutaneous wound healing and are important for vascularization, oxygenation, tissue regeneration, epidermal function, matrix deposition, and the inflammatory response (6-9). With regard to POP surgery, wound healing is essential to re-establish tissue integrity and to restore functional, strong tissue in order to keep the pelvic organs in place and avoid recurrence of POP. Besides POP surgery, other vaginal surgeries such as surgery for urinary incontinence, episiotomy during delivery and vaginal fistula surgery may also benefit from estrogen therapy.

To date, not much is known about the effects of estrogen on vaginal wound healing specifically and the effects of promoted wound healing on the (long-term) outcome of vaginal surgery. Therefore, as a first step, we systematically reviewed the literature on the effects of estrogen on all phases of wound healing after vaginal surgery, providing an overview of all available evidence from both animal and human studies. Improved understanding of these effects may provide further opportunities to develop estrogen-related therapies to improve the outcome of vaginal surgery.

METHODS

This systematic review and meta-analysis were reported according to the Preferred Reporting Items for Systematic Reviews and Meta-Analyses (PRISMA) statement (11). Furthermore, this review was conducted in collaboration with SYstematic Review Center for Laboratory animal Experimentation (SYRCLE) and has been registered in the prospective register of systematic reviews (PROSPERO) on 29 November 2019 (CRD42019156601).

Information sources and search strategy

An information (JL) specialist performed a systematic search in OVID MEDLINE, OVID Embase and Web of Science from inception to 28 January 2020 using controlled vocabulary (i.e. MeSH-terms) and text words to retrieve both animal and human studies on the effect of estrogen on vaginal wound healing. The following concepts were searched: estrogen or animal estrogen deficient animal models combined with either (1) vaginal surgery OR (2) vagina (disorders)/AND wounds/wound healing. Studies on malignancy, reviews, editorials, and conference abstracts were excluded. There were no restrictions on language or date. Reference lists and citing articles of identified relevant papers were crosschecked for additional relevant studies using Web of Science and the search strategy was adapted in case of additional relevant records. Identified studies were imported and deduplicated using Endnote (version X9.3.3, Clarivate Analytics). See appendix S1 for the complete search strategy.

Eligibility criteria

We included original studies performed in female animals (all species) and women. Studies were eligible if they compared wound healing related outcomes in estrogen exposed subjects to hypo-estrogenic subjects after vaginal surgery. The definition and assessment of wound healing is diversely reported due to its complex and dynamic process. In order not to restrict this systematic review to predefined wound related outcomes, we included all outcomes that authors reported as wound healing related parameters and outcomes. The wound healing related outcome measures were classified into the three phases of wound healing: (1) inflammatory phase, (2) proliferative phase, (3) and maturation phase. Vaginal surgery included POP surgery, SUI surgery, hysterectomy, episiotomy during delivery, vaginal fistula surgery and experimental wounding. Estrogens considered were (ethinyl-) estradiol, estriol, estrone, epiestriol, estetrol, dienestrol, estradiol congeners and physiologic estrogens. There were no restrictions in

administration route, dosage, and frequency. Use of diethylstilbenediol was excluded from eligibility due to its carcinogenic effects (12).

Original studies concerned interventional animal studies and clinical studies using the following design: randomized controlled trial, cohort, case-control, and case series of >10 cases. We excluded studies for the following reason: (1) lack of a hypo-estrogenic control group; (2) no vaginal wound; (3) no evaluation of wound healing; (4) wounds related to complications of vaginal surgery (e.g. mesh exposure and erosion); (5) no full-text available.

Study selection

Two reviewers (EV, AK) independently screened all retrieved studies for eligibility using Rayyan web-tool (13). Studies were initially screened by title and abstract after which selected papers underwent full review to make the final selection. Reasons for excluding articles were recorded. Discrepancies were resolved by discussion between the two reviewers (EV, AK) for consensus. Any unresolved discrepancies were adjudicated by a third reviewer (ZG).

Data extraction

From the studies included, both reviewers (EV, AK) independently extracted the following data – using an in-house developed spreadsheet based on MS Office Excel: animal species, strain, age at the beginning of the study, parity, method of vaginal surgery, surgical site, wound closure, description of treatment and control group, estrogen type, estrogen dosage, frequency of estrogen administration, timing of estrogen administration relative to vaginal surgery, duration of estrogen administration, route of estrogen administration, timing of data collection, wound healing related outcome measures, therapy compliance, sample size in treatment and control group, number of subjects excluded for statistical analysis, and reason for subject exclusion. Bibliographic details such as author, journal, year of publication, original language, and country where the study was conducted were also recorded.

For all outcomes, number of events or mean, standard deviation (SD) or standard error (SE) and total number of subjects per group were recorded. When data were only presented graphically, they were measured using a digital screen ruler (ImageJ) (14) by two independent reviewers (EV, AK). In case of relevant missing data, the authors were contacted.

Assessment of risk of bias

Two reviewers independently scored the included studies on risk of bias (EV, AK). Scoring was performed using predesigned characteristic forms based on the Cochrane risk of bias tool for human studies and the SYRCLE risk of bias tool for animal studies (Figure 1). A 'yes' score indicates low risk of bias; a 'no' score indicates high risk of bias; and a '?' score indicates unknown risk of bias. To overcome the problem of judging too many items as "unclear risk of bias" because reporting of experimental details on methods and materials in animal studies is generally very poor (15,16), we added two items on reporting: reporting of any measure of randomization, reporting of any measure of blinding. For these two items, a 'yes' score indicates 'reported', and a 'no' score indicates 'unreported'.

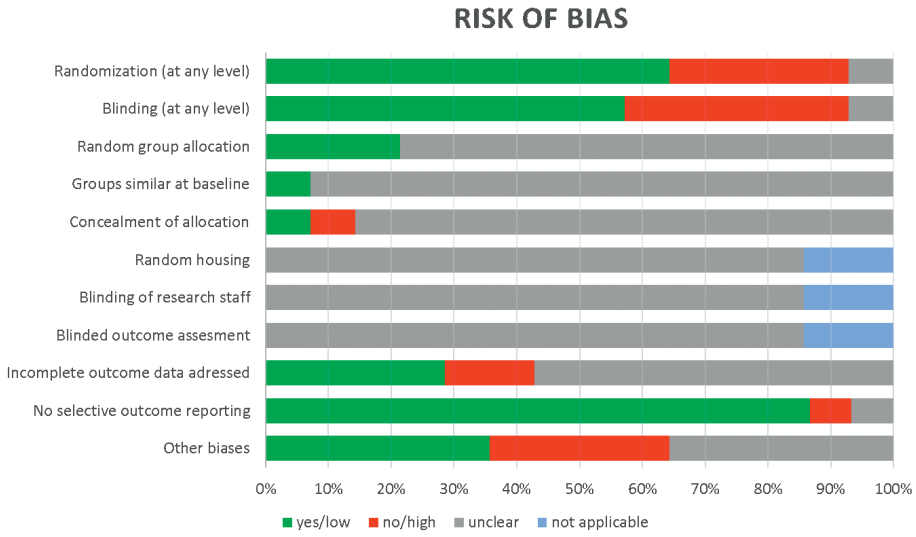

Figure 1. Risk of Bias assessment of 14 included studies.

Data synthesis

We performed a meta-analysis for each outcome with a minimum of two reporting studies. For all continuous outcome measures, SD was calculated if only the SE was reported (SD = SE x $\sqrt{n}$). Studies were excluded from meta-analysis if not all outcome data (mean, SD, and N) could be obtained. We calculated the standardized mean difference (SMD) and 95% confidence interval (95% CI) for each separate intervention-control comparison group with Hedges' g correction (17). In case of multiple experimental

groups within one study, correction for multiple use of the control group was performed (number of animals in control group divided by the number of times the control group is used; rounded up to the next whole number). In case multiple similar outcomes were reported from the same cohort of animals or women, we either extracted a single outcome (based on hierarchy of preferred outcome measures) or combined more than one outcome to provide a single outcome statistic ("nested outcome"; each outcome weighted by multiplication by the inverse of the variance for that outcome, summed for all outcomes and divided by the sum of the weights) (18). When sample sizes were presented as a range, the lowest number was used for the meta-analysis. Despite anticipated heterogeneity, the individual effect sizes were pooled to obtain an overall SMD with Hedges' g correction, with 95% CI. We used the random effects model, which takes the precision of individual studies and the variation between studies into account and weights each study accordingly. Meta-analyses were performed using Comprehensive Meta Analysis (CMA version 3.0). Forest plots were used to display the mean overall effect sizes. Subgroup analyses were planned for the following study characteristics: type of surgical procedure; route of estrogen administration, estrogen dosing, estrogen type, treatment duration, and timing of estrogen treatment related to surgery (pre/peri/post-surgery).

Sensitivity analyses and publication bias analyses

To assess the robustness of our findings, we performed a sensitivity analysis in CMA and we investigated the effect of a possible interaction based on timing of the data collection. In the analysis of all outcome measures, data collected at the time of vaginal surgery (T0) was added to the analyses. To detect publication bias, funnel plots were created and evaluated on symmetry when more than 10 studies per outcome measure were present, using Duval and Tweedie's trim and fill analysis, and Egger's regression analysis for small study effects. Because SMDs may cause funnel plot distortion we plotted the SMD against a sample size-based precision estimate ($1/\sqrt{(n)}$) (19). Heterogeneity was assessed using I^2.

RESULTS

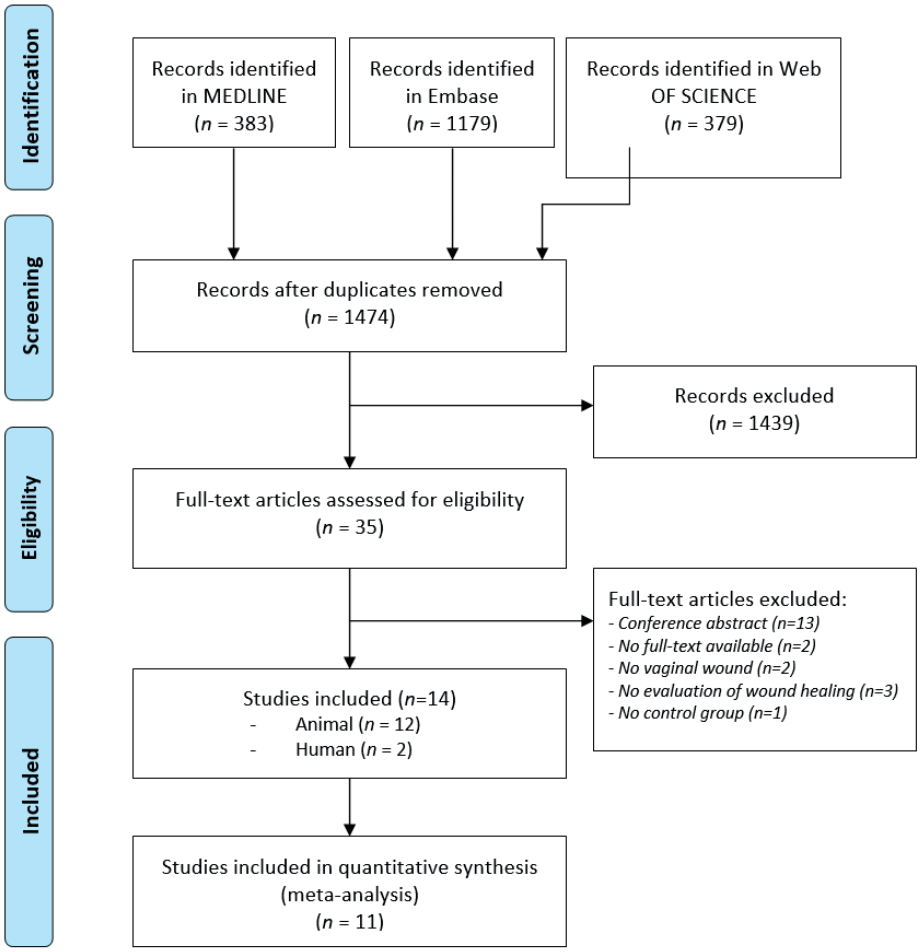

Figure 2. PRISMA flowchart

Study selection

The systematic literature search yielded 1474 unique references (Figure 2). After title and abstract screening, 35 studies met our selection criteria. After studying the full-text articles, 14 studies (12 animal studies and 2 human studies) remained (20-33). From 14 studies, 11 studies could be included in the meta-analyses which included a total of 889 female animals and 197 women in 134 comparisons across 8 outcomes.

Table 1. Study characteristics of the included studies.

Reference	Language	Species/strain	Age	Control group (days between OVX and vaginal surgery)	Intervention group(s)	n(c)/ n(int)/ n(int) / etc.	Vaginal surgery	Surgical site	Wound closure
Abramov 2012	English	Rabbit/New Zealand White	35 – 40 weeks; SM	OVX (56)	Sham OVX + physiologic E2; Physiologic E2	21/21/21	6 mm full-thickness punch biopsy	Lateral vaginal wall, 1.5 cm proximal to introitus	No closure; open wound
Abramov 2013	English	Rabbit/New Zealand White	35 – 40 weeks; SM	OVX (56)	Sham OVX + physiologic E2; Physiologic E2	21/21/21	6 mm full-thickness punch biopsy	Both lateral vaginal walls, 1.5-cm proximal to introitus	No closure; open wound
Abramov 2011	*English*	*Rabbit/New Zealand White*	*35-40 weeks; SM*	*OVX (56)*	*Sham OVX + physiologic E2; Physiologic E2*	*24/24/24*	*6 mm full-thickness punch biopsy*	*Lateral vaginal wall, 1.5 cm proximal to introitus*	*No closure; open wound*
Balgobin 2013	English	Guinea pig/Hartley	12 weeks; SM	OVX (14) + placebo	OVX (14) + oestrogen	12/12	Modified posterior colpoperineorrhaphy	Posterior vaginal wall	Closed with absorbable sutures
Cretti 1966	Polish	Rabbit/White Rat/White	SM	OVX (14-21)	OVX (14-21) + oestrogen; Physiologic E2	50/50/50 (rabbit) 58/58/58 (rat)	15 mm midline incision	Posterior vaginal wall	Closed with 3mm interval sutures
Florian-Rodriguez 2019	English	Rat/Sprague Dawley	12 weeks; SM	OVX (14) + placebo	Oestrogen (a); OVX (14) + oestrogen preop (b); OVX (14) + oestrogen periop (c)	24/20/22/20	Full thickness single linear incision	posterior vaginal wall, introitus to mid-vagina	No closure; open wound
Gale 1993	English	Canine	3 months; prepubertal	Prepubertal (N.A.)	Preopubertal + oestrogen	2/2	4 full thickness radial incisions	Vagina	No closure; open wound

Table 1. Study characteristics of the included studies (continued).

Reference	Language	Species/strain	Age	Control group (days between OVX and vaginal surgery)	Intervention group(s)	n(c)/ n(int)/ n(int) / etc.	Vaginal surgery	Surgical site	Wound closure
Higgins 2009	English	Rabbit/New Zealand White	> 6 months; SM	OVX (28) + placebo	Sham OVX + physiologic E2; OVX (28) + oestrogen preop; OVX (28) + oestrogen postop; OVX (28) + oestrogen periop	6/6/6/6/6	Vaginal mesh implantation: 1.5 x 0.8cm strip of macroporous, monofilament polypropylene mesh	Posterior distal vaginal wall; between the fibromuscular layer and vaginal epithelium	Closed with absorbable sutures
Ripperda 2017	English	Rat/Sprague Dawley	12 weeks; SM	OVX (14) + placebo	OVX (14) + oestrogen	41/47	Full thickness incision	Posterior vaginal wall; introitus to cervix	Unk
Schlaff 1987	English	Rat/Sprague Dawley	SM	OVX (0) + placebo	OVX (0) + oestrogen	24/24	Uterine horn divided and reanastomosed	Uterus	Closed in 2 layers (muscularis and serosa)
Sjovall 1947	English	Rat/White	SM	OVX (7)	OVX (7) + oestrogen	19/17	Triangular excision	Posterior vaginal wall	No closure (open wound)
Sjovall 1953	English	Rat/Mus norvegicus albus	SM	OVX)7'	Physiologic E2; OVX (7) + oestrogen a; OVX (7) + oestrogen b; OVX (7) + oestrogen c;	70/66/65/65/97	Triangular excision	Posterior vaginal wall	No closure (open wound)
Karp 2012	English	Woman	65	>2 yrs postmenopausal + placebo	>2 yrs postmenopausal + oestrogen	21/22	Vaginal reconstruction of POP (hysterectomy, native tissue, mesh) and concomitant MUS	Vagina (multiple sites possible)	Closed with absorbable sutures

Table 1. Study characteristics of the included studies (continued).

Reference	Language	Species/strain	Age	Control group (days between OVX and vaginal surgery)	Intervention group(s)	n(c)/ n(int)/ n(int) / etc.	Vaginal surgery	Surgical site	Wound closure
Sjostedt 1953	English	Woman	Unk	Postmenopausal	Postmenopausal + oestrogen	91/63	Uterine prolapse surgery	Vagina	Closed with absorbable sutures

Reference (repeated)	Country	Type of oestrogen	Route of administration	Dose	Frequency	Timing oestrogen	Duration of oestrogen therapy (days)	Compliance	Data collection (days after surgery)
Abramov 2012	USA	Physiologic	N.A.	N.A.	N.A.	N.A.	N.A.	N.A.	0, 4, 7, 14, 21, 35
Abramov 2013	USA	Physiologic	N.A.	N.A.	N.A.	N.A.	N.A.	N.A.	0, 4, 7, 10, 14, 21, 28, 35
Abramov 2011	USA	Physiologic	N.A.	N.A.	N.A.	N.A.	N.A.	N.A.	0, 4, 7, 14, 21, 35
Balgobin 2013	USA	Oestradiol	Subcutaneous (minipump)	50 ug/kg/day	Continuous	14 days before surgery	18, 35	100%	4, 21
Cretti 1966	Polen	Oestradiolum benzoicum; physiologic	Injection	4 ug/kg	Daily	3 days before surgery	4, 5, 6, 7, 8, 10, 13, 17	Unk	0.5, 1, 2, 3, 4, 5, 7, 10, 14
Florian-Rodriguez 2019	USA	Oestradiol (a); CEE cream (b,c)	Systemic injection (a); topical cream (b,c)	50ug/kg (a); 0.625ug/day (b,c)	3 days daily, then every other day (a); daily (b,c)	3 days before surgery (a); 14 days before surgery (b,c)	3.5, 4, 5, 10 (a); 14 (b); 14.5, 15, 16, 21 (c)	Unk	0.5, 1, 2, 7
Gale 1993	USA	Oestradiol (Estrace)	Topical cream	0.1 mg/gram	2x/day	At day of surgery	14	Unk	3, 7, 14, 21, 28, 35
Higgins 2009	USA	Physiologic; 17β-oestradiol	Subcutaneous pellet	200 ug/day	Continuous	-28	28; 56; 84	100%	57

Table 1. Study characteristics of the included studies (continued).

Reference (repeated)	**Country**	**Type of oestrogen**	**Route of administration**	**Dose**	**Frequency**	**Timing oestrogen**	**Duration of oestrogen therapy (days)**	**Compliance**	**Data collection** (days after surgery)
Ripperda 2017	USA	CEE cream	Topical cream	2.5 ug/kg/day	2 weeks daily, then 3x/week	At day of surgery	7, 21	Unk	7, 21
Schlaff 1987	USA	Oestradiol	Subcutaneous pellet	5 mg/day	Daily	At day of surgery	7, 14,21, 42	100%	7, 14, 21, 42
Sjovall 1947	Sweden	Oestradiolbenzoate	Subcutaneous injections	100 IbE (n=10)/ 100+100 IbE (n=2)/ 2500+2500 IbE (n=1)/ 2500 IbE (n=4)	Single and repeated	Unk	Unk	Unk	4, 5
Sjovall 1953	Sweden	Pysiologic; oestradiol benzoate (a); dienoestrol (b); ethinyloestradiol (c)	Subcutaneous injections	5 ug (c),10 ug (a), 20 ug (a), 50 ug (c),250 mg (a), 500 mg (a,b);	Single and repeated	At day of surgery or next day	1-3	Unk	4, 5
Karp 2012	USA	Oestradiol (Estring)	Vaginal ring	7.5 mg/day	Continuous	At day of surgery	84	86%; 86%	42, 84
Sjostedt 1953	Sweden	Diethylstilbenediol (stilboestrol)	Systemic (oral)	3-5 mg	Daily	2-8 days before surgery	14-20	"A few patients discontinued on account of nausea"	10-12

SM = sexually mature, OVX = ovariectomy, unk = unknown, CEE = conjugated equine estrogen, preop = preoperative, periop = perioperative (preoperative and postoperative), postop = postoperative, POP = pelvic organ prolapse, MUS = mid-urethral sling, c = control, int = intervention.

Study characteristics

A summary of the included studies is provided in Table 1. One study needed to be translated since it was published in Polish. The study characteristics varied considerably. The included studies consisted of 2 human studies, compromising 197 women, and 12 studies comprising 795 rats, 378 rabbits, 24 guinea pigs, and 4 canines. More than 10 different surgical techniques were used, and vaginal wounds varied in size and location. In six studies the vaginal wound was closed with at least one absorbable suture, whereas in seven studies the wound was not closed. One study included a wound located at the uterine horn, serving as a model for wound healing in the genital tract (30). Also type of estrogen, administration route, dosage, frequency, timing and duration of estrogen therapy varied greatly between studies. In two studies, estrogen was administered preoperatively, in six studies postoperatively, and in five studies estrogen was administered both pre- and postoperatively. The median duration of estrogen therapy was 14.3 days (inter quartile range (IQR) 6.8 – 19.3). Five studies included physiologic estrogen as part of estrogen therapy. Eleven studies used exogenous estrogens, which were administered subcutaneously (5 studies), systemically (3 studies); and vaginally (4 studies). Reported wound healing related outcome measures included inflammatory response, neovascularization, granulation formation, wound closure (defined as microscopic and macroscopic re-epithelialization), collagen synthesis, transforming growth factor (TGF)-β1 and tissue strength (Table 2).

Table 2. Wound healing reported outcomes and measures used in studies included in the meta-analysis.

	Inflammatory phase		Proliferation phase			Remodeling phase			
Reference	**Leukocytes**	**Cytokines**	**Neovascularization**	**Granulation tissue**	**Collagen synthesis**	**Macroscopic wound closure**	**Microscopic wound closure**	**Biomechanical properties**	**Others**
Abramov 2012	Presence of neutrophils (histology; H&E stain)		Neovascularization (histology; H&E stain)	Granulation tissue Δ (histology; H&E stain)	Collagen deposition (histology; MT stain)	Wound's surface area (лr2)	Re-epithelialization (histology; H&E stain)		
Abramov 2013		TGF-β1 (PCR)				Wound's surface area (лr2)			
Abramov 2011						Wound's surface area (лr2)		Young's modulus	
Balgobin 2013		TGF-β1 (PCR)			Total collagen content (hydroxyproline assay)			Young's modulus	
Cretti 1966	Intra- & extra vascular leucocytes (method unk)* Local inflammatory reaction (visual inspection)*				Collagen fibres (histology; van Gieson stain)*			Tensile strength	
Higgins 2009	Macrophages, lymphocytes, neutrophils, eosinophils, FBGC (histology; H&E stain)		Neovascularization (histology; H&E stain)		Fibroblastic proliferation (histology; H&E stain)				
Ripperda 2017		TGF-β1 (PCR)	VEGFα (PCR)		Total collagen content (hydroxyproline assay)	Area of injury (um2)		Vaginal stiffness	

Table 2. Wound healing reported outcomes and measures used in studies included in the meta-analysis (continued).

	Inflammatory phase		Proliferation phase			Remodeling phase			
Reference	**Leukocytes**	**Cytokines**	**Neovascularization**	**Granulation tissue**	**Collagen synthesis**	**Macroscopic wound closure**	**Microscopic wound closure**	**Biomechanical properties**	**Others**
Sjovall 1947						Epithelialization (visual inspection)	Epithelialization (histology; stain unk)		
Sjovall 1953							Epithelialization (histology; stain unk)		
Karp 2012	Microscopic inflammation (cytology)			Granulation tissue (macroscopic inspection)					
Sjostedt 1953						Epithelialization (visual inspection)			

Δ = nested outcome: (1) amount of granulation tissue; (2) maturation of granulation tissue (determined by the shape and alignment of the fibroblasts).* = rat cohort; not included in meta-analysis because standard deviation was not reported. H&E = Hematoxylin & Eosin, MT = Masson's Trichrome, FBLN-5 = fibulin-5, PCR = polymerase chain reaction, FBGC = multinucleated foreign body giant cells, unk = unknown.

Three studies of this systematic review were not included for meta-analyses: (1) Rodriguez et al.[25] was excluded because it reported only on fibulin-5, which is a matricellular glycoprotein that promotes elastogenesis and inhibits the matrix degrading protein MMP-9. For this systematic review, this outcome measure was too indirect to represent wound healing. (2) Gale et al. (26) was excluded because all outcome measures were presented descriptively. (3) Schlaff et al. (30) was excluded from meta-analysis because it evaluated the biomechanical properties of the uterus. Although the study states that the uterine horn model represents the genital tract, we find that the biomechanical properties from a uterus are too different from a vaginal wall to include this in the meta-analysis. (4) The rat cohort of Cretti et al. (24) could also not be included in the meta-analyses because SDs were not reported. Therefore, only the data from the rabbit cohort has been included.

Risk of Bias of included studies

The results of the risk of bias assessment of the 14 included studies are shown in Figure 1. In total, 64% of the studies reported randomization at any level. 57% reported blinding at any level, but none of the studies reported on blinding of the outcome assessor. In 29% of the studies, incomplete outcome data was adequately addressed. Figure 1 shows that many items were scored as ''unclear risk of bias'', which indicates poor reporting of mainly animal studies in scientific publications. Assessment of the risk of publication bias was not assessed because of too few studies per outcome measure.

Synthesis of results: effects of estrogen on vaginal wound healing

Inflammatory response

Fourteen comparisons from three studies were included in the meta-analysis regarding the effect of estrogen on the inflammatory response after vaginal surgery. The inflammatory response was defined as the presence of neutrophils in hematoxylin & eosin (H&E) stained sections or scored by naked eye inspection (from none to severe inflammation or yes/no presence of micro-inflammation). The inflammatory response was measured in rabbits and women, and was milder in the groups that received estrogen when compared to controls (Figure 3; SMD -0.58; [-1.14 – -0.02]). From the three included studies, one study administered estrogen therapy vaginally.

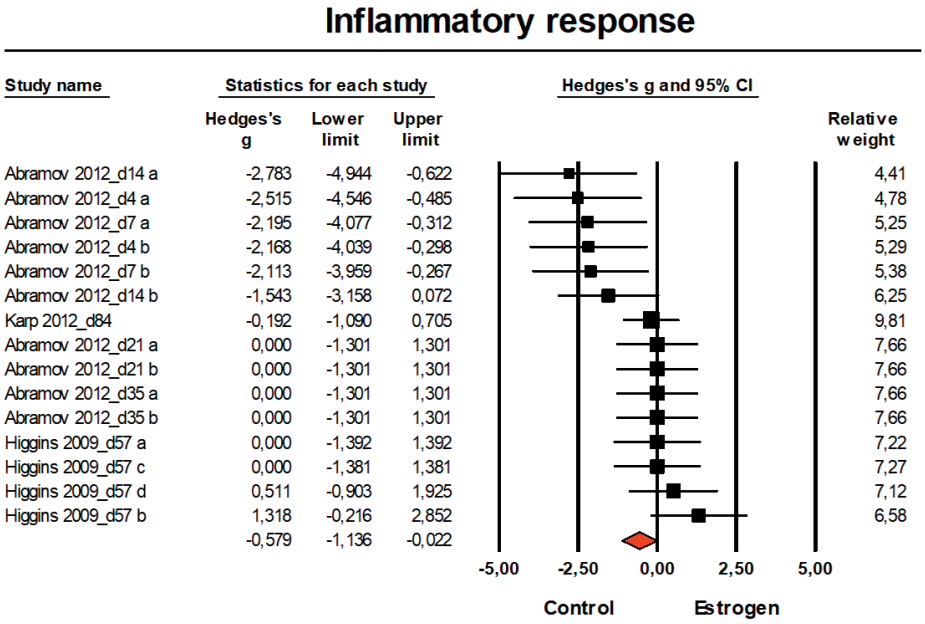

Figure 3. Effects of estrogen on the inflammatory response after vaginal wounding.
Forest plot of the data of three included studies. The forest plot displays the standardized mean difference (SMD) (Hedges' g), 95% confidence interval and relative weight of the individual studies. The diamond indicates the global estimate and its 95% confidence interval. Study names contain the moment of data collection in days after surgery (d). Heterogeneity: $Tau^2 = 0{,}613$, Q-value = 29,691, df = 14 ($p = 0{,}008$), $I^2 = 52{,}8\%$. Test for overal effect: Z = -2,038; $p = 0{,}042$

TGF-β1

TGF-β1 was measured in three studies (16 comparisons) which were included in the meta-analysis. Measurement of TGF-β1 was performed in rabbits, rats, and guinea pigs of which one study administered estrogen vaginally. Meta-analysis revealed that estrogen reduces TGF-β1 gene transcription after vaginal surgery (Figure 4; SMD -1.68 [-2.52 – -0.83]).

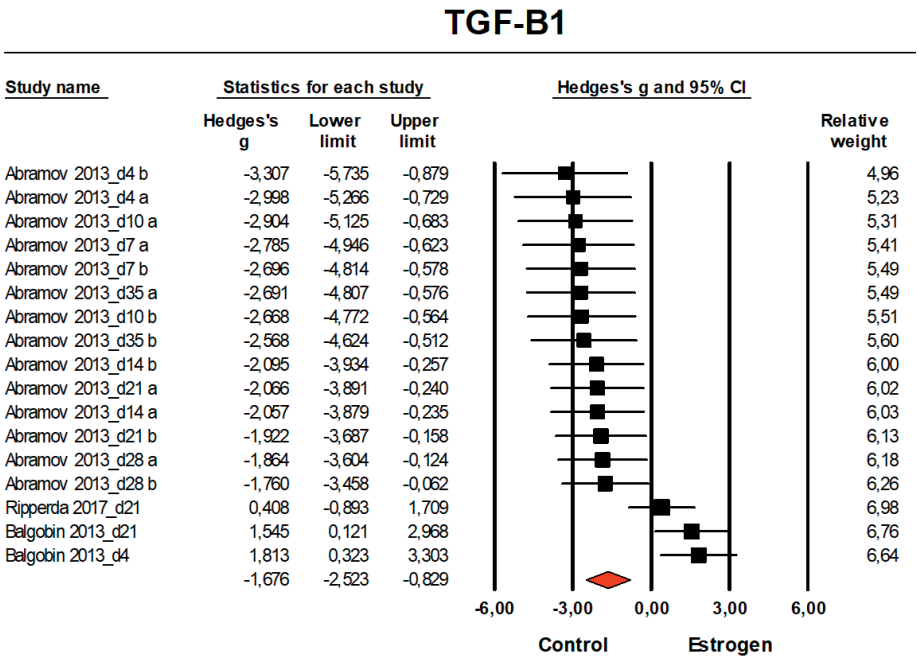

Figure 4. Effects of estrogen on TGF-β1 after vaginal wounding.
Forest plot of the data of three included studies. The forest plot displays the standardized mean difference (SMD) (Hedges' g), 95% confidence interval and relative weight of the individual studies. The diamond indicates the global estimate and its 95% confidence interval. Study names contain the moment of data collection in days after surgery (d). Heterogeneity: $Tau^2 = 2,232$, Q-value = 56,967, df = 16 ($p < 0,000$), $I^2 = 71,9\%$. Test for overal effect: Z = -3,879; $p < 0,000$

Neovascularization

Fourteen comparisons from three studies that measured the effect of estrogen on neovascularization after vaginal wounding were included. These three studies were performed in rabbits and rats of which one study administered estrogen vaginally. Meta-analysis revealed increased vascularization in animals following estrogen administration (Figure 5; SMD 1.13 [0.67 – 1.60]).

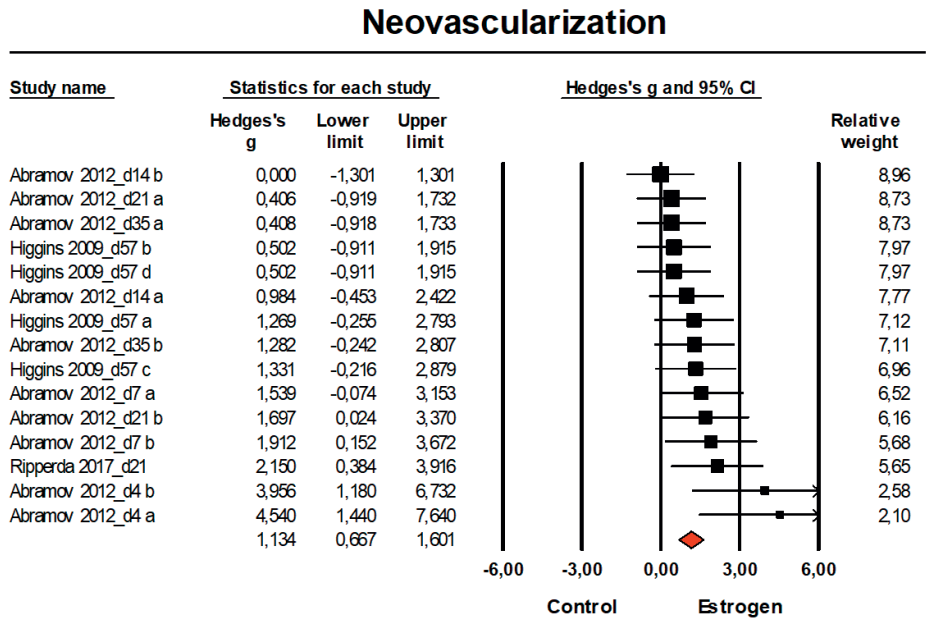

Figure 5. Effects of estrogen on neovascularization after vaginal wounding.
Forest plot of the data of three included studies. The forest plot displays the SMD (Hedges' g), 95% confidence interval and relative weight of the individual studies. The diamond indicates the global estimate and its 95% confidence interval. Study names contain the moment of data collection in days after surgery (d). Heterogeneity: Tau^2 = 0,192, Q-value = 18,169, df = 14 (p = 0,199), I^2 = 22,9%. Test for overal effect: Z = 4,763; p < 0,000

Granulation tissue

The effect of estrogen on granulation tissue after vaginal surgery was analyzed in two studies (10 comparisons), performed in rabbits and women of which one study used vaginally administered estrogen. Meta-analysis demonstrated that estrogen increased the amount of granulation tissue after vaginal surgery (Figure 6; SMD 1.67 [0.54 – 2.79]).

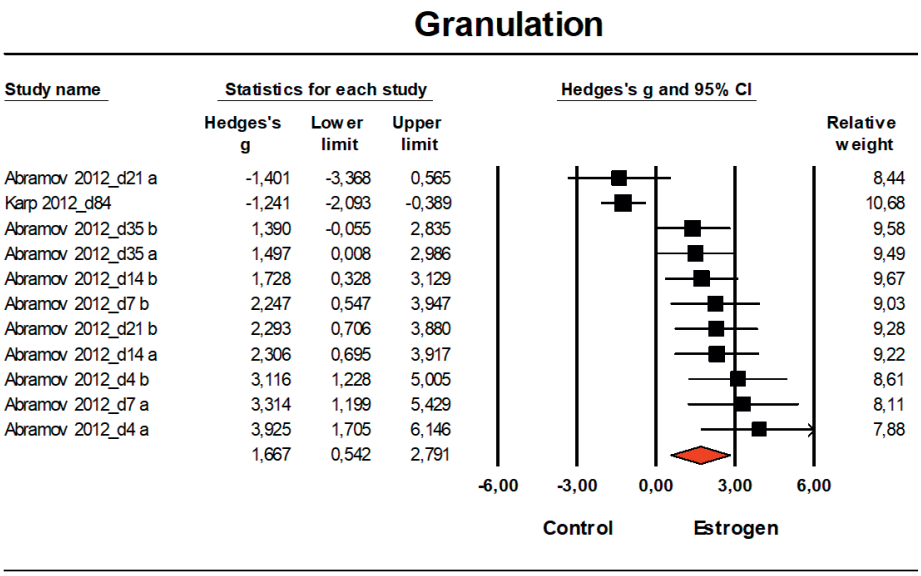

Figure 6. Effects of estrogen on granulation tissue after vaginal wounding.
Forest plot of the data of two included studies. The forest plot displays the SMD (Hedges' g), 95% confidence interval and relative weight of the individual studies. The diamond indicates the global estimate and its 95% confidence interval. Study names contain the moment of data collection in days after surgery (d). Heterogeneity: $Tau^2 = 2,895$, Q-value = 57,260, df = 10 ($p < 0,000$), $I^2 = 82,5\%$. Test for overal effect: Z = 2,904; $p = 0,004$

Wound closure (macroscopic re-epithelialization)

Overall analysis of the five studies investigating macroscopic wound closure showed that wounds recover faster under influence of estrogen (Figure 7; SMD 1.82 [1.22 – 2.42]). Macroscopic wound closure was assessed in rabbits, rats, and women of which one study administered estrogen vaginally.

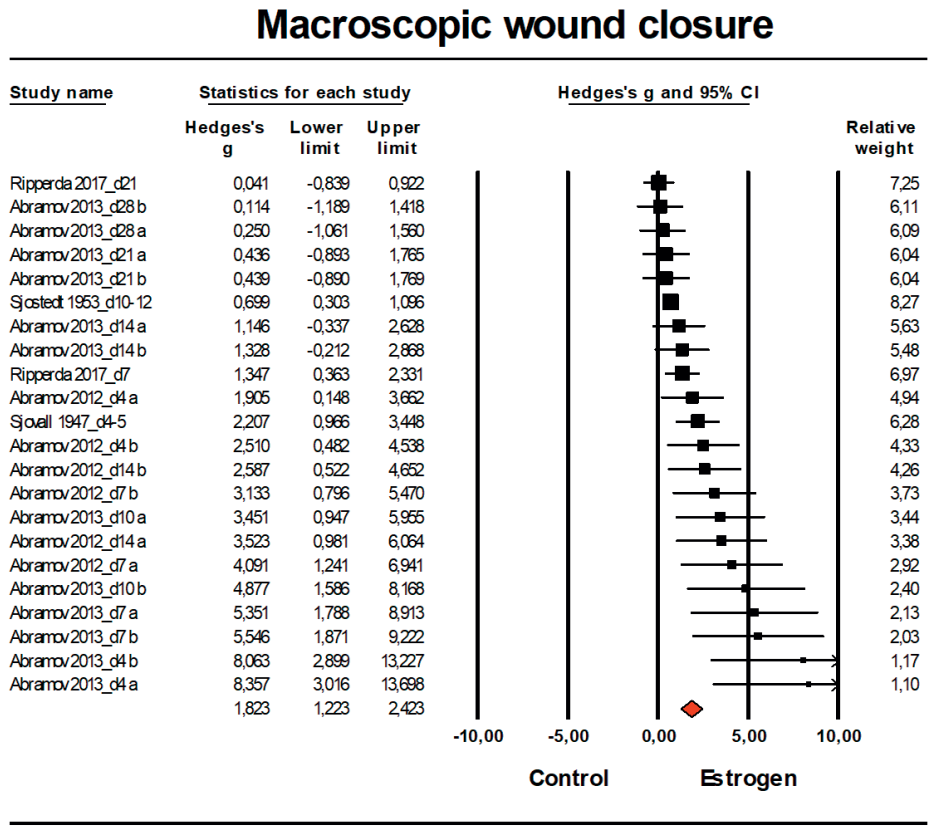

Figure 7. Effects of estrogen on macroscopic wound closure after vaginal wounding.
Forest plot of the data of five included studies. The forest plot displays the SMD (Hedges' g), 95% confidence interval and relative weight of the individual studies. The diamond indicates the global estimate and its 95% confidence interval. Study names contain the moment of data collection in days after surgery (d). Heterogeneity: $Tau^2 = 1,092$, Q-value = 67,368, df = 21 ($p < 0,000$), $I^2 = 68,8\%$. Test for overal effect: Z = 5,954; $p < 0,000$

Wound closure (microscopic re-epithelialization)

Microscopic wound closure was also accelerated under administration of estrogen, which was evaluated in three studies that included 19 comparisons. (Figure 8; SMD 0.98 [0.66 – 1.29]). Re-epithelialization was assessed in rabbits and rats. None of the studies administered estrogen therapy vaginally.

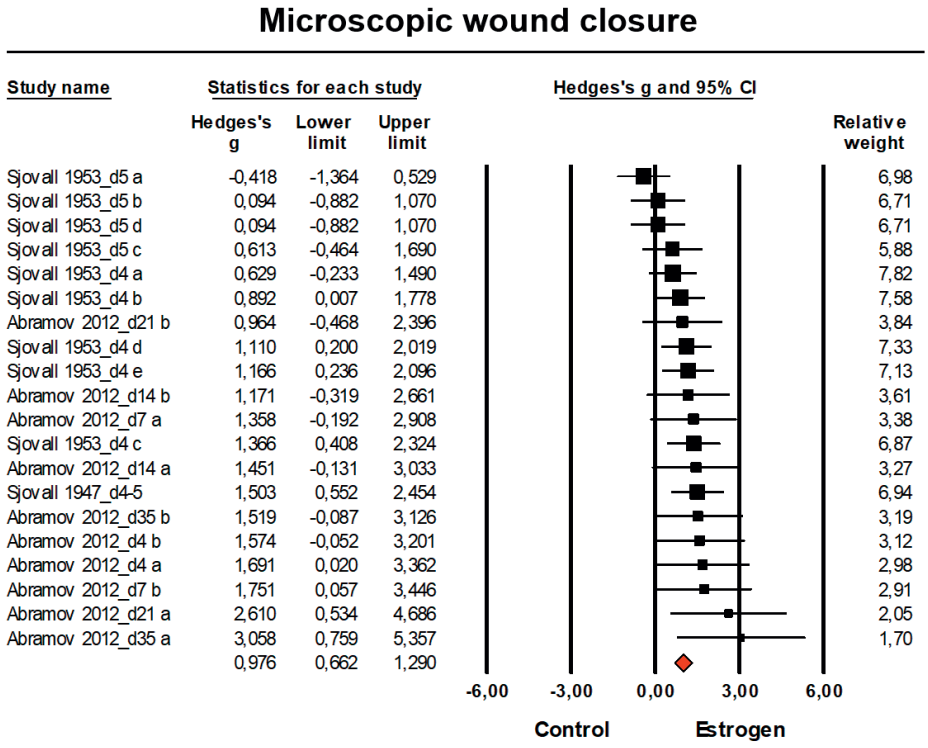

Figure 8. Effects of estrogen on microscopic wound closure after vaginal wounding.
Forest plot of the data of three included studies. The forest plot displays the SMD (Hedges' g), 95% confidence interval and relative weight of the individual studies. The diamond indicates the global estimate and its 95% confidence interval. Study names contain the moment of data collection in days after surgery (d). Heterogeneity: $Tau^2 = 0{,}135$, Q-value = 26,259, df = 19 ($p = 0{,}123$), $I^2 = 27{,}6\%$. Test for overal effect: Z = 6,086; $p < 0{,}000$

Collagen synthesis

Sixteen comparisons from four studies concerned the effect of estrogen on collagen synthesis after vaginal wounding. These studies were performed in rabbits, rats, and guinea pigs of which one study administered estrogen therapy vaginally. Analysis showed that estrogen increased the amount of newly formed collagen after vaginal surgery (Figure 9; SMD 1.08 [0.42 – 1.74]).

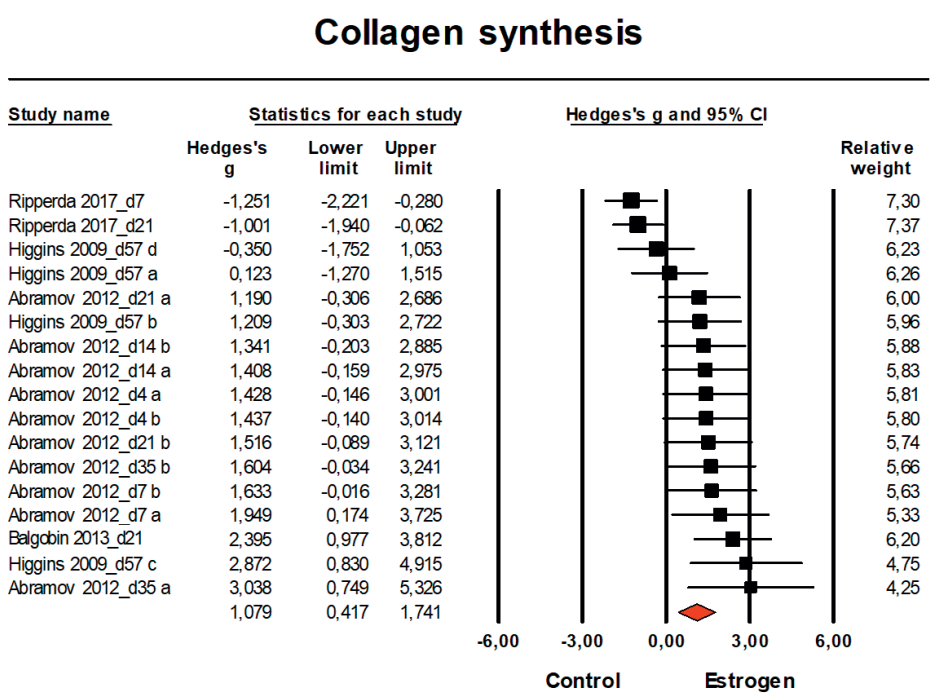

Figure 9. Effects of estrogen on collagen synthesis after vaginal wounding.
Forest plot of the data of four included studies. The forest plot displays the SMD (Hedges' g), 95% confidence interval and relative weight of the individual studies. The diamond indicates the global estimate and its 95% confidence interval. Study names contain the moment of data collection in days after surgery (d). Heterogeneity: Tau^2 = 1,318, Q-value = 54,051, df = 16 (p < 0,00), I^2 = 70,4%. Test for overal effect: Z = 3,195; p = 0,001

Biomechanical tissue properties

Sixteen comparisons from four studies concerning the effects of estrogen on biomechanical tissue strength of a vaginal wound were included in the meta-analysis. In three studies, vaginal stiffness was calculated from the slope of the linear portion of the stress-strain curves, also known as the Young's modulus. Biomechanical tests were performed in rabbits, rats, and guinea pigs of which one study administered estrogen vaginally. Results revealed an increased tissue stiffness in estrogen treated animals (Figure 10; SMD 1.26 [0.53 – 1.99]).

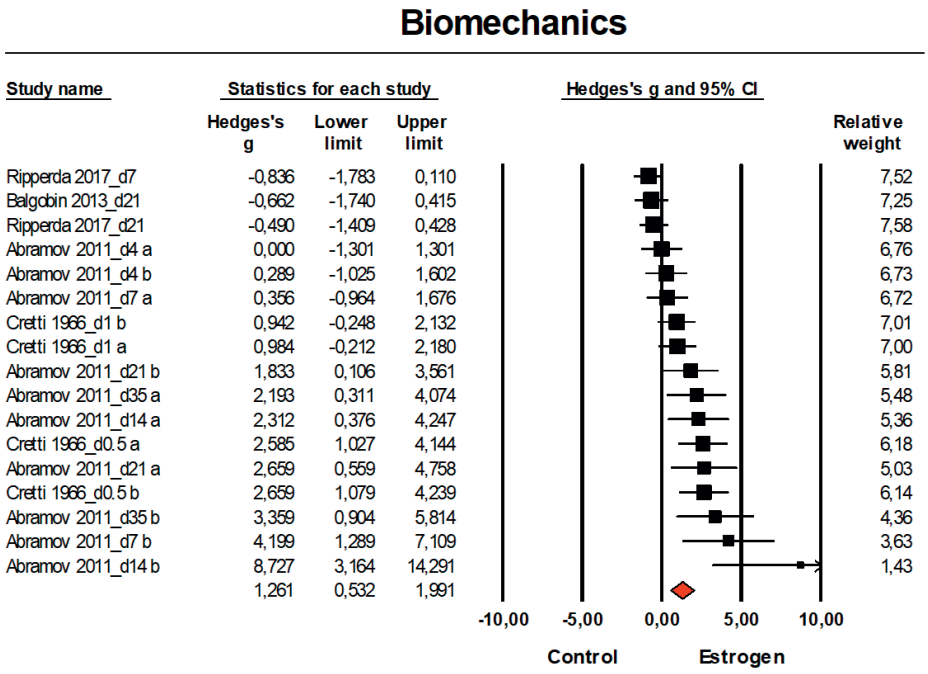

Figure 10. Effects of estrogen on vaginal tissue strength after vaginal wounding.
Forest plot of the data of four included studies. The forest plot displays the SMD (Hedges' g), 95% confidence interval and relative weight of the individual studies. The diamond indicates the global estimate and its 95% confidence interval. Study names contain the moment of data collection in days after surgery (d). Heterogeneity: $Tau^2 = 1,608$, Q-value = 64,416, df = 16 ($p < 0,000$), $I^2 = 75,2\%$. Test for overal effect: Z = 3,390; $p < 0,001$

Subgroup analyses and sensitivity analysis

Subgroup analyses for inflammatory response, TGF-β1, neovascularization, granulation formation, macroscopic wound closure, re-epithelialization, collagen synthesis, and biomechanical tissue strength could not be conducted because the number of included studies was too limited. Sensitivity analyses showed that the overall effect size slightly decreased in all outcome measures but remained clinically significant compared to the control (hypo-estrogen) group.

COMMENT

Main findings

This systematic review and meta-analysis report on the effects of estrogen on different domains of vaginal wound healing in women and animals. Meta-analyses were performed on wound healing related outcomes and provide evidence that estrogen therapy (1) increases neovascularization, (2) optimizes granulation tissue, (3) accelerates wound closure, (4) enhances collagen synthesis and (5) increases tissue strength. In addition, estrogen decreases the inflammatory response and reduces levels of TGF-β1. Since estrogen therapy improves the quality of vaginal tissue after surgery, it is likely that patients may benefit from estrogen therapy. These results from meta-analysis are in accordance with the results from the studies that were included in this systematic review, but could not be included for meta-analysis because the exact data could not be obtained (24,26). These studies also reported improved neovascularization, wound closure and collagen synthesis following estrogen therapy.

Strengths and limitations

This study is the first systematic review and meta-analysis addressing the effect of estrogen on vaginal wound healing. Both animal and human studies were systematically appraised and retrieved through an extensive literature search, without language and date restrictions. The outcomes of this study suggest that women may benefit from perioperative estrogen therapy, which may potentially improve surgical outcomes such as reduced recurrence rates of POP, and improved quality of life and sexual function. Furthermore, this study has been performed in collaboration with the Systematic Review Centre for Laboratory Animal Experimentation (SYRCLE), who are highly experienced in the conduct of systematic reviews and meta-analyses of animal studies.

Nevertheless, there are also limitations that may affect the generalizability and validity of our findings. A major limitation of the meta-analysis was the high variation between studies. Since the number of included studies was limited, it was not possible to perform subgroup analyses and thereby differentiate between (1) vaginal and systemic estrogen, (2) types of estrogen administration; (3) frequencies, doses, timing and durations of treatment, (4) type of surgical procedure, and (5) animal species and women. Although we accounted for heterogeneity by using a random effects model rather than a fixed effects model for meta-analysis, this might have affected our certainty in the evidence. Moreover, in the included studies both vaginal and systemic estrogen was used, whereas in clinical practice, low-dose vaginal estrogen is preferred over systemic estrogen, in particular because systemic estrogens are associated with an increased risk of thrombosis and endometrial cancer, breast cancer and ovarian cancer (34-36). Furthermore, a Cochrane review on estrogen therapy for urinary incontinence showed that systemic administration of estrogen increased incontinence compared to placebo, whereas vaginally administered estrogen actually improved symptoms of incontinence (3). Unfortunately, we could not restrict this systematic review to vaginally administered estrogen only. An evaluation of species, type of surgery as well as type, dosage, frequency, timing, and duration of estrogen therapy with regard to the effect on wound healing and subsequent surgical outcomes is an essential element of future research.

Another limitation of this systematic review was that studies reported incompletely on important methodological details such as randomization and blinding. This hampered reliable risk of bias assessment and may reduce the reliability of our conclusions.

Also, regarding the reported outcome on macroscopic wound closure in our meta-analysis, it was noted that two studies had an identical study set-up and were performed by the same research group (20,22). To prevent that this cohort was weighed twice with risk of duplication; only the data from one study was included in the meta-analysis. Furthermore, a study reported two data time points in the result section which were not included in the methods section (21). We decided to include all time points as reported in the result section and assumed the group sizes were identical to the other groups. The authors were contacted regarding these discrepancies, unfortunately they did not respond to confirm or refute our assumptions. One study did not report the individual group sizes (24). Therefore, individual group sizes were calculated by dividing the total group size by the number of experimental groups and the number of data time points.

Comparison with existing literature

Inflammatory phase of wound healing

This phase includes hemostasis and inflammation, characterized by platelet accumulation followed by cytokine signaling, after which platelet-derived growth factor (PDGF) and TGF-β are released, which is chemotactic for neutrophils migrating into the wound bed (37). Our meta-analysis showed a reduced inflammatory response, including reduced levels of TGF-β1 in subjects treated with estrogen. This anti-inflammatory effect of estrogen is also (partially) seen in other studies evaluating the effect of estrogen on cutaneous wound healing. Two literature reviews on this topic illustrated either no influence on the inflammatory response or a reduced inflammatory response from estrogen (6,7). Reduction was expressed by dampening purulent inflammation, decreasing neutrophil numbers, promoting alternative macrophage polarization (promoting a shift from M1 to M2 subtypes) and reducing the expression of pro-inflammatory cytokines.[7] It is hypothesized that there is an optimum dose at which estrogen is beneficial (38,39), which may also apply to the process of healing, resulting in inconsistent effects or even over-inhibitions of inflammation when excessive amount of estrogen are administered in animal experiments.

Proliferative phase of wound healing

The proliferative phase of wound healing is marked by angiogenesis, fibroplasia (during which the matrix of granulation tissue is formed), re-epithelialization, wound contraction, and collagen synthesis. Our meta-analysis showed that estrogen improved these proliferation-related outcomes of wound healing. This is also supported by evidence from literature showing accelerated cutaneous wound healing after estrogen treatment in aged women and hormone-deprived animals (40-43). Several studies addressed the underlying mechanisms and illustrated that estrogenic compounds play a prominent role in promoting the healing processes by accelerating re-epithelialization and promoting collagen deposition, granulation tissue formation and wound contraction (9, 44-46). Moreover, Trenti et al. (47) demonstrated that estrogen is a key factor in promoting endothelial healing and angiogenesis. Angiogenesis plays an important role in the supply of oxygen and nutrients to fibroblasts and catalyzes the hydroxylases for collagen synthesis (48). Therefore, angiogenesis is imperative for accelerating wound healing as well as for wound strength.

Maturation and remodeling phase of wound healing

The main feature of the maturation and remodeling phase is to organize collagen deposition in a well-mannered network (49). As the phase progresses, the tensile strength of the wound gradually increases. In case of matrix deposition failure, the wound's strength will be greatly compromised. Increased tensile strength following estrogen therapy was also seen in our meta-analysis. When compared to cutaneous wound healing, Ashcroft et al. (40) also showed increased strength of cutaneous wounds in elderly women treated with estrogen. In perspective to surgery for POP, maintenance of the tissue integrity and tissue strength of the vaginal wall is essential to keep pelvic organs in place and may therefore also prevent recurrence of POP.

Conclusions and implications

Optimal wound healing after vaginal surgery is essential to re-establish tissue integrity and to restore functional, strong tissue. In case of POP surgery, strong tissue is especially important to keep the pelvic organs in place and avoid recurrence of POP. Other vaginal surgeries, such as surgery for urinary incontinence, episiotomy during delivery, and vaginal fistula surgery, may also benefit from optimal wound healing.

Postmenopausal women are considered to have an impaired wound healing capacity because of their hypo-estrogenic state. Such women may benefit from strategies that improve wound healing, which may ultimately improve surgical outcomes.

This systematic review and meta-analysis provide strong evidence that estrogen therapy has a beneficial effect on vaginal wound healing, which improves tissue quality and tissue strength after vaginal surgery. Consequently, it could be hypothesized that long-term surgical outcomes may be enhanced in postmenopausal women when treated with estrogen.

The outcomes of this study justify further research evaluating the effect of estrogen-induced improved vaginal wound healing on surgical outcomes, such as recurrence rates of POP, vaginal health, quality of life and sexual function, but also implant related complications such as mesh exposure and erosion. Future research should determine whether estrogen should be prescribed to all women undergoing vaginal surgery.

ACKNOWLEDGEMENTS

We are grateful for the support of ZonMw (project number 114024902, the Netherlands) who provided SYRCLE a grant to promote Synthesis of Evidence of animal studies.

REFERENCES

1. Lethaby A, Ayeleke RO, Roberts H. Local oestrogen for vaginal atrophy in postmenopausal women. *The Cochrane database of systematic reviews.* 2016(8):Cd001500.
2. Weber MA, Kleijn MH, Langendam M, Limpens J, Heineman MJ, Roovers JP. Local Oestrogen for Pelvic Floor Disorders: A Systematic Review. *PLoS One.* 2015;10(9):e0136265.
3. Cody JD, Jacobs ML, Richardson K, Moehrer B, Hextall A. Oestrogen therapy for urinary incontinence in post-menopausal women. *The Cochrane database of systematic reviews.* 2012;10:Cd001405.
4. Krause M, Wheeler TL, Snyder TE, Richter HE. Local Effects of Vaginally Administered Estrogen Therapy: A Review. *J Pelvic Med Surg.* 2009;15(3):105-114.
5. Denman MA, Gregory WT, Boyles SH, Smith V, Edwards SR, Clark AL. Reoperation 10 years after surgically managed pelvic organ prolapse and urinary incontinence. *Am J Obstet Gynecol.* 2008;198(5):555.e551-555.
6. Calvin M. Oestrogens and wound healing. *Maturitas.* 2000;34(3):195-210.
7. Horng HC, Chang WH, Yeh CC, et al. Estrogen Effects on Wound Healing. *Int J Mol Sci.* 2017;18(11).
8. Guo S, Dipietro LA. Factors affecting wound healing. *J Dent Res.* 2010;89(3):219-229.
9. Mukai K, Urai T, Asano K, Nakajima Y, Nakatani T. Evaluation of Effects of Topical Estradiol Benzoate Application on Cutaneous Wound Healing in Ovariectomized Female Mice. *PLoS One.* 2016;11(9):e0163560.
10. Reinke JM, Sorg H. Wound repair and regeneration. *Eur Surg Res.* 2012;49(1):35-43.
11. Liberati A, Altman DG, Tetzlaff J, et al. The PRISMA statement for reporting systematic reviews and meta-analyses of studies that evaluate health care interventions: explanation and elaboration. *J Clin Epidemiol.* 2009;62(10):e1-34.
12. Marselos M, Tomatis L. Diethylstilboestrol: I, Pharmacology, Toxicology and carcinogenicity in humans. *Eur J Cancer.* 1992;28a(6-7):1182-1189.
13. Ouzzani M, Hammady H, Fedorowicz Z, Elmagarmid A. Rayyan-a web and mobile app for systematic reviews. *Syst Rev.* 2016;5(1):210.
14. *ImageJ* [computer program]. Bethesda, Maryland, USA: https://imagej.nih.gov/ij/; 1997-2020.
15. Kilkenny C, Parsons N, Kadyszewski E, et al. Survey of the quality of experimental design, statistical analysis and reporting of research using animals. *PLoS One.* 2009;4(11):e7824.
16. Avey MT, Moher D, Sullivan KJ, et al. The Devil Is in the Details: Incomplete Reporting in Preclinical Animal Research. *PLoS One.* 2016;11(11):e0166733.
17. Hedges LV, Olkin I. *Statistical Methods for Meta-Analysis.* New York: Academic Press; 1985.
18. Vesterinen HM, Sena ES, Egan KJ, et al. Meta-analysis of data from animal studies: a practical guide. *J Neurosci Methods.* 2014;221:92-102.
19. Zwetsloot PP, Van Der Naald M, Sena ES, et al. Standardized mean differences cause funnel plot distortion in publication bias assessments. *Elife.* 2017;6.

20. Abramov Y, Golden B, Sullivan M, Goldberg RP, Sand PK. Vaginal incisional wound healing in a rabbit menopause model: a histologic analysis. *International Urogynecology Journal.* 2012;23(12):1763-1769.
21. Abramov Y, Hirsch E, Ilievski V, Goldberg RP, Sand PK. Transforming growth factor beta1 gene expression during vaginal wound healing in a rabbit menopause model. *Bjog-an International Journal of Obstetrics and Gynaecology.* 2013;120(2):251-256.
22. Abramov Y, Webb AR, Botros SM, Goldberg RP, Ameer GA, Sand PK. Effect of bilateral oophorectomy on wound healing of the rabbit vagina. *Fertil Steril.* 2011;95(4):1467-1470.
23. Balgobin S, Montoya TI, Shi H, et al. Estrogen alters remodeling of the vaginal wall after surgical injury in guinea pigs. *Biol Reprod.* 2013;89(6):138.
24. Cretti A. The influence of oestradiol and progesterone on wound healing. [Polish]. *Roczn Akad Med Marchlewskiego.* 1966;14.
25. Florian-Rodriguez M, Chin K, Hamner J, Acevedo J, Keller P, Word RA. Effect of Protease Inhibitors in Healing of the Vaginal Wall. *Sci Rep.* 2019;9(1):12354.
26. Gale CL, Muram D, Adamec TA. The effects of exogenous estrogen on wound healing in dogs. *Adolesc Pediatr Gynecol.* 1993;6(3):160-163.
27. Higgins EW, Rao A, Baumann S, et al. Effect of estrogen replacement on the histological response to polypropylene mesh implanted in the rabbit vagina model. *Journal of Pelvic Medicine and Surgery.* 2009;15:63.
28. Karp DR, Jean-Michel M, Johnston Y, Suciu G, Aguilar VC, Davila GW. A randomized clinical trial of the impact of local estrogen on postoperative tissue quality after vaginal reconstructive surgery. *Female Pelvic Med Reconstr Surg.* 2012;18(4):211-215.
29. Ripperda C, Maldonado PA, Acevedo JF, Keller P, Word RA. Vaginal estrogen: A dual edged sword in postoperative healing of the vaginal wall. *Female Pelvic Medicine and Reconstructive Surgery.* 2016;22:S15.
30. Schlaff WD, Cooley BC, Shen W, Gittlesohn AM, Rock JA. A rat uterine horn model of genital tract wound healing. *Fertil Steril.* 1987;48(5):866-872.
31. Sjostedt S. The effect of diethylstilbenediol on the healing of wounds in the human vagina. *Acta Endocrinol (Copenh).* 1953;12(3):260-263.
32. Sjovall A. The influence of oestrogen upon the healing of vaginal wounds in rats. *Acta Obstet Gynecol Scand.* 1947;27(1):1-10.
33. Sjovall A. The influence of oestrogens upon the healing of vaginal wounds in rats. *Acta Endocrinol (Copenh).* 1953;12(3):249-259.
34. Suckling J, Lethaby A, Kennedy R. Local oestrogen for vaginal atrophy in postmenopausal women. *The Cochrane database of systematic reviews.* 2006(4):Cd001500.
35. Krause M, Wheeler TL, 2nd, Richter HE, Snyder TE. Systemic effects of vaginally administered estrogen therapy: a review. *Female Pelvic Med Reconstr Surg.* 2010;16(3):188-195.
36. Crandall C. Vaginal estrogen preparations: a review of safety and efficacy for vaginal atrophy. *Journal of women's health (2002).* 2002;11(10):857-877.

37. Childs DR, Murthy AS. Overview of Wound Healing and Management. *Surg Clin North Am.* 2017;97(1):189-207.
38. Shahrad P, Marks R. A pharmacological effect of oestrone on human epidermis. *Br J Dermatol.* 1977;97(4):383-386.
39. Brincat M, Versi E, Moniz CF, Magos A, de Trafford J, Studd JW. Skin collagen changes in postmenopausal women receiving different regimens of estrogen therapy. *Obstet Gynecol.* 1987;70(1):123-127.
40. Ashcroft GS, Greenwell-Wild T, Horan MA, Wahl SM, Ferguson MW. Topical estrogen accelerates cutaneous wound healing in aged humans associated with an altered inflammatory response. *Am J Pathol.* 1999;155(4):1137-1146.
41. Brufani M, Rizzi N, Meda C, et al. Novel Locally Active Estrogens Accelerate Cutaneous Wound Healing-Part 2. *Sci Rep.* 2017;7(1):2510.
42. Hardman MJ, Emmerson E, Campbell L, Ashcroft GS. Selective estrogen receptor modulators accelerate cutaneous wound healing in ovariectomized female mice. *Endocrinology.* 2008;149(2):551-557.
43. Midgley AC, Morris G, Phillips AO, Steadman R. 17β-estradiol ameliorates age-associated loss of fibroblast function by attenuating IFN-γ/STAT1-dependent miR-7 upregulation. *Aging Cell.* 2016;15(3):531-541.
44. Emmerson E, Hardman MJ. The role of estrogen deficiency in skin ageing and wound healing. *Biogerontology.* 2012;13(1):3-20.
45. Thornton MJ. Estrogens and aging skin. *Dermatoendocrinol.* 2013;5(2):264-270.
46. Mukai K, Nakajima Y, Urai T, et al. 17β-Estradiol administration promotes delayed cutaneous wound healing in 40-week ovariectomised female mice. *Int Wound J.* 2016;13(5):636-644.
47. Trenti A, Tedesco S, Boscaro C, Trevisi L, Bolego C, Cignarella A. Estrogen, Angiogenesis, Immunity and Cell Metabolism: Solving the Puzzle. *Int J Mol Sci.* 2018;19(3).
48. Gantwerker EA, Hom DB. Skin: histology and physiology of wound healing. *Facial Plast Surg Clin North Am.* 2011;19(3):441-453.
49. Broughton G, 2nd, Janis JE, Attinger CE. The basic science of wound healing. *Plast Reconstr Surg.* 2006;117(7 Suppl):12s-34s.

APPENDIX S1 – COMPLETE SEARCH STRATEGY

Database(s): **Ovid MEDLINE(R) and Epub Ahead of Print, In-Process & Other Non-Indexed Citations and Daily** 1946 to January 27, 2020

Search Strategy: **2020-01-28**

#	Searches	Results
1	estrogens/ or estradiol congeners/ or estradiol/ or "estrogens, conjugated (usp)"/ or estrone/ or ethinyl estradiol/ or estrogens, non-steroidal/ or dienestrol/ or exp estriol/	147492
2	estrogen replacement therapy/	15024
3	(estrogen* or oestrogen* or estradiol* or oestradiol* or ethinylestradiol* or ethinyloestradiol* or estriol* or oestriol* or epi?estriol or estetrol* or oestetrol* or estrone* or oestrone* or dienestrol* or dienoestrol* or TEHRT*).tw,ot,kf.	220908
4	(Ovestin* or Vivelle or Estrace or Aerodiol or Estraderm or Ovocyclin* or hydroxyestriol* or hydroxyoestriol* or Menorest or VAGIFEM or FemSeven or Fem7 or Fem-7 or Estring or Promestrien* or Cenestin* or SCE-A or Ortho-Gynes* or Premarin or Synapause).tw,ot,kf.	944
5	**or/1-4 [estrogens]**	**258382**
6	exp ovariectomy/	25114
7	menopause/	27238
8	(ovar*tom* or OVX or oophorectom* or ovar*hysterect* or salpingo?ophorectom* or spaying or speying or ((speyed or spayed) adj6 (dogs or bitches or cats or females)) or immun*sp#ying or immun*castrat* or (remov* adj3 (ovary or ovaries or horn*)) or (castrat* adj3 (femal* or ovar*))).tw,kf.	41996
9	(menopau* or hypo?estrogen* or hypo-?estrogen* or (hormon* adj2 (depriv* or deficien*)) or hormon*deficien*).tw,kf.	58579
10	uter*-horn-model*.tw,kf.	88
11	**or/6-10 [estrogen-deficient/ female castration]**	**113973**
12	(animal experimentation/ or laboratory animal science/ or models, animal/ or disease models, animal/ or exp animals, genetically modified/ or exp animals, laboratory/ or animals, outbred strains/ or (animals/ not humans/) or exp sheep/ or exp lagomorpha/ or exp rodentia/ or (animals or animal study or animal experiment or dam or dams or rodent* or marmoset* or mice or mouse or murine or C57BL* or Balb-c or Balbc or Bl6 or C57Bl6 or BL-6 or C3H* or rat or rats or wistar or dawley or rabbit* or lambs or ewes or pigs or piglet* or sows or gilts or dogs or bitches or beagles or canine or cats or baboon* or macac* or macaq* or ((animal or ovine or sheep or porcine or sus or swine* or pig or sow or cat or feline or dog or primate* or monkey*) adj3 model*)).tw,kf. or (porcine or ovine).ti.) not (case reports/ or case report*.jw. or (("we-report" adj3 case) or our case).tw. or (case-report or "one case" or two cases or (porcine* adj4 (dermis or skin or graft* or matrix or collagen* or sheet* or implant*))).ti.) [animal filter]	6022043
13	**11 and 12 [estrogen-deficient animals]**	**37367**
14	**5 or 13 [estrogens/ estrogen-deficient animals]**	**273838**

#	Searches	Results
15	exp *uterine hemorrhage/ or exp *uterine neoplasms/ or vaginal neoplasms/ or *leiomyoma/ or *myoma/ or *myosarcoma/ or male urogenital diseases/ or genital diseases, male/ or exp genital neoplasms, male/ or exp penile diseases/ or exp prostatic diseases/ or exp testicular diseases/ or (male/ not female/) or (neoplas* or cancer* or carcinom* or mammacarcinom* or adenocarcinom* or malignan* or tumor* or tumour* or leukem* or lymphom* or lymph*sarcom* or sarcom* or myosarcom* or rhabdomyosarcom* or leiomyom* or myoma* or fibrom* or fibroid* or adenomyo* or endometriom* or hydatidiform or metasta* or lymph* spread* or metaplas* or bleed* or blood loss* or h?emorrhag* or diethylstilbestrol or stilbestrol or stilboestrol or genital mutilat* or childhood or erectile or penile or penis or prostrat* or ((male or males or men) not (female* or women))).ti,ot. or DES.ti.	5065966
16	**14 not 15 [estrogen (deficient) not cancer in title]**	**196259**
17	(editorial or "systematic review").pt. or exp guideline/ or (committee or editorial or reply or guideline*).ti. or cochrane.jw. or ((review.pt. or review.ti.) not (exp records/ or ((review adj2 cases) or case-series or case-control or cohort study or case-cohort or trial).ti,ot. or exp cohort studies/ or case-control studies/ or exp controlled clinical trial/ or ((chart* or record* or retrospectiv*) adj3 review*).tw,kf.)) [study-exclusion filter]	3343393
18	**16 not 17 [estrogen (deficient) not cancer in title, not reviews/editorials]**	**171674**
19	vagina/in not (exp burns/ or exp radiation injuries/)	721
20	exp vaginal fistula/	4755
21	suburethral slings/	3002
22	((fascia lata/ or intestinal mucosa/ or intestine, small/) and ((cadaver* or scaffold* or bioscaffold* or polypropylen* or POP or pelvic organ prolaps* or pelvis floor or colpoc?el* or vaginoc?el* or cystoc?el* or rectoc?el*or stress incontin*).mp. or ((exp swine/ or pig.hw.) and (graft* or xenograft* or collagen-matrix or implant* or POP or prolaps*).mp.))) or ((exp dermis/ and (exp swine/ or pig.hw. or (polypropylen* or prolaps* or POP).mp.)) not ((pig or porcine) adj2 skin).mp.)	1567
23	hysterectomy, vaginal/	2868
24	episiotomy/	2115
25	(colpotomy/ or (colpotom* or culdotom* or vaginotom*).tw,kf.) not (cow or cows or bovine or cattle or heifer* or mare or mares or horse* or equine).ti,ot.	640
26	(genit* wound heal*.mp. or ((wound* adj3 (heal* or repair* or dehisc* or closur*)).mp. and (genitalia, female/ or (((genit* or urogenit*) adj2 (tract* or system* or organ* or wound* or injur* or prolap*)) or reproductive tract*).mp.))) and ((female* not (male or males)) or women or vagina or vaginal or vaginally or vulvovag* or vesicovag* or cervicovag* or uterovag* or urethrovagin* or rectovagin* or transvagin* or uterine horn*).mp. [female genital tract wound]	105
27	(Gynemesh* or Restorell* or Polyform or Dexon or Vypro or Pelvicol or Pelvisoft or Pelvitex or Mersuture or Ugytex or UltraPro or SmartMesh* or Dynamesh* or Coloplast or TiMeSH or Prolift or SPMM or SPMW or surgipro or Avaulta or Surgisis or Marlex or InteXen or Perigee or Zenoderm or BARD or Matristem or Parietene).tw,kf. or ((Elevate or SPM or Apogee or Prolene).tw,kf. and (mesh or meshes or prolaps* or vault* or POP or SUI or incontin*).mp.)	3793
28	((transobtur* or obturat* or miduret* or mid-uret* or tension-free or tensionless or Advantage) adj3 (tape or tapes)).tw,kf.	1912

#	Searches	Results
29	(AJUST or AJUSTTM or MiniArc* or Mini-arc* or Altis or AltisTM or SECUR or SECURTM or Monarc or Ophira or Solyx or RetroArc or Desara or Supris or Obtryx* or Abbrevo or Pelvilac*).tw,kf.	345
30	((TVT or TOT or ARIS or Lynx or SPM or SIMS or Align).tw,kf. and (tape or SUI or incontinen* or transobturat* or obturat* or miduret* or mid-uret*).mp.) or (TVT-O or (single-incis* adj3 TOT) or Advantage-Fit).tw,kf.	1699
31	(((fascia lat* or (small intestin* adj2 (submucosa* or mucosa*)) or SIS or dermis) adj3 (cadaver* or porcine or graft* or xenograft*)) or porcine dermal xenograft* or (porcine intestin* adj6 (scaffold* or matrix))).tw,kf.	1732
32	(sling or slings or minisling* or sling?plast* or PIVS or ((IVS or PVS) adj proced*)).tw,kf.	7313
33	((pubovagin* or retropubic* or retro-pubic* or transobturat* or obturat* or midurethr* or mid-urethr*) adj9 (procedur* or techniq* or method* or approach or route or placement or insert* or implant* or incis* or anchor* or fixat*)).tw,kf.	5010
34	(colporrhaph* or colporaph* or colpoplast* or vaginotom* or (vagin* adj9 (wall or anterior or posterior) adj5 (repair* or incis* or injur* or insert* or implant*)) or colposusp*).tw,kf.	2205
35	(perineoplasty or perineoplasties or vestibuloplast* or perineolevatoroplast* or native tissue repair* or ((sacrospin* or sacro-spin* or vault) adj3 (fixat* or suspen*)) or (SSF and (vagin* or transvagin* or vault* or TVT or prolaps* or POP)) or ((uterosacr* or utero-sacr*) adj3 ligament* adj2 suspen*) or Manchester-Fothergill).tw,kf.	1338
36	((vagin* or transvagin*) adj6 (hysterectom* or (uter* adj2 remov*))).tw,kf.	5145
37	episiotom*.tw,kf.	2811
38	((vagina or vaginal or intravagin* or vesicovag* or cervicovag* or uterovag* or urethrovagin* or rectovagin* or genit* tract* or genito* or urogenit* or ((genital or uterine) adj2 prolaps*)) adj6 (postop* or postsurg* or surger* or surgic* or operat* or perioperat* or perisurg* or preoperat* or presurg*) adj6 (estrogen* or oestrogen* or estradiol* or oestradiol* or ethinylestradiol* or ethinyloestradiol* or estriol* or oestriol* or epiestriol or estetrol* or oestetrol* or estrone* or oestrone* or dien?estrol* or TEHRT* or Ovestin or Vivelle or Estrace or Aerodiol or Estraderm or Ovocyclin or hydroxy?estriol or Menorest or VAGIFEM or FemSeven or Fem7 or Fem-7 or Estring or Promestriene or Cenestin or SCE-A or Ortho-Gynes* or Premarin or Synapause)).tw,kf.	55
39	**or/19-38 [vaginal wound /surgery /mesh/sling I]**	**35492**
40	(vagina/ or vaginal diseases/ or administration, intravaginal/ or (vagina or vaginal or vaginally or paravagin* or transvag* or vulvovag* or vesicovag* or cervicovag* or uterovag* or ureth* or rectovag* or intravag* or paravag* or extravagin* or transvagin* or pubovagin* or retropubic* or retro-pubic* or transobturat* or obturat* or midurethr* or mid-urethr*).tw,kf.) not ((((burn or burns or radiat* or irradiat* or chemical) adj2 (injur* or traum*)) or ((caustic or vagina*) adj2 (burn or burns))).mp. or (lichen or chemical or burn or burns).ti.)	200901
41	wound healing/ or *regeneration/ or granulation tissue/ or scar formation/ or "wounds and injuries"/ or lacerations/ or surgical wound/ or prosthesis failure/ or prosthesis-related infections/ or surgical wound dehiscence/ or surgical wound infection/ or wound closure techniques/ or prosthesis implantation/ or bioprosthesis/ or tissue scaffolds/ or exp host vs graft reaction/	391680
42	surgical mesh/ or polypropylenes/ or polyglactin 910/	18933

#	Searches	Results
43	((exp pelvic organ prolapse/ or pelvic floor disorders/ or pelvic floor/ or urinary incontinence/ or urinary incontinence, stress/ or (POP or ((pelvic or pelvis) adj2 (organ* or floor* or support*)) or prolaps* or vault* or colpoptos* or colpoc?el* or vaginoc?el* or cystoc?el* or rectoc?el* or enteroc?el* or ((vagin* or vulvovag* or vesicovag* or cervicovag*) adj4 (extrusion* or extrude* or eviscerat* or descen* or prociden* or ptos* or herni* or bulg*)) or ((uter* or urinary or urethr* or genit* or urogenit* or rect* or pelvic) adj4 (extrusion* or extrude* or eviscerat* or descen* or prociden* or ptos* or herni* or bulg*)) or SUI or incontinen*).tw,kf.) and (exp pelvic organ prolapse/su or pelvic floor disorders/su or pelvic floor/su or exp urinary incontinence/su or vagina/su or vaginal diseases/su or abdominal wall/su or urinary incontinence/su or urinary incontinence, stress/su or "gynecologic surgical procedures"/ or urogenital surgical procedures/ or urologic surgical procedures/ or urinary tract/su or surgery, plastic/or device removal/ or postoperative complications/ or intraoperative complications/or pain, postoperative/ or exp perioperative care/ or exp perioperative period/ or reconstructive surgical procedures/ or reoperation/ or ((pelvic* or genit* or POP or prolaps* or vault* or colpoptos* or colpoc?el* or vaginoc?el* or cystoc?el* or rectoc?el* or enteroc?el* or vagina or vaginal or vaginally or transvagin* or paravagin* or vesicovag*) adj3 (reconstr* or repair* or surger* or operation* or postoperat* or postsurg* or preoperat* or presurg* or perioperat* or perisurg* or reinforc* or implanted or implantat* or incis* or graft* or flap or flaps or PP)).tw,kf.)) not ((case report or one-case or two cases or bitch or dog or cat or queen or bongo or pseudohermaphr* or hermaphr* or neovag*).ti. or (("we-report" adj3 case) or our case).tw.)	26598
44	(wound* or healing or healed or dehisc* or eros* or erod* or debrid* or epibol* or granulat* or (tissue adj2 (disrupt* or damag*)) or excoriat*).tw,kf.	447485
45	(((vagina or vaginal or vaginally or paravagin* or transvag* or vulvovag* or vesicovag* or cervicovag* or uterovag* or ureth* or rectovag* or intravag* or paravag* or extravagin* or transvagin*) adj12 (lacerat* or fissur* or scar or scars or scarring or fistul* or injur*)) or (obstetr* adj3 (fistul* or lacerat*)) or (trauma adj2 vagin*)).tw,kf.	12192
46	(((mesh or meshes) not ((wire or search* or medline or pubmed) adj5 mesh*)) or polypropylen* or polylactic or PLA or polyglac* or scaffold* or bioscaffold* or biologic graft* or ((acellular or collagen) adj3 matrix)).tw,kf.	154560
47	**or/41-46 [wound, mesh,sling, vaginal surgery II]**	**891798**
48	**40 and 47 [vaginal wound/surgery/mesh/sling II]**	**29179**
49	**39 or 48 [vaginal wound/surgery/mesh/sling II]**	**52688**
50	**49 and 18 [estrogens + vaginal wound/ surgery/mesh/sling]**	**384**
51	**remove duplicates from 50 [I II estrogens + wound healing/vaginal surgery models - deduplicated]**	**383**

Database(s): **Embase Classic+Embase** 1947 to 2020 January 27
Search Strategy: **2020-01-28**

#	Searches	Results
1	((*estrogen/ or exp *estradiol derivative/) not (estrogen/ec or exp estradiol derivative/ec)) or estrogen/ad, ae, cb, cm, do, dt, im, va, po, pd, sc, tp, td or exp estradiol derivative/ad, ae, cb, cm, do, dt, im, va, po, pd, sc, tp, td or ((estrogen/ or exp estradiol derivative/) and (low drug dose/ or treatment duration/ or treatment outcome/ or drug efficacy/ or drug therapy/ or drug effect/ or hormone substitution/ or major clinical study/ or controlled study/ or exp controlled clinical trial/ or intravaginal drug administration/ or topical drug administration/ or oral drug administration/ or intramuscular drug administration/)) or estrogen derivative/ or conjugated estrogen/ or **dienestrol/** or exp estrone derivative/ or estriol/ or promestriene/	218587
2	estrogen therapy/	25078
3	(estrogen* or oestrogen* or estradiol* or oestradiol* or ethinylestradiol* or ethinyloestradiol* or estriol* or oestriol* or epi?estriol or estetrol* or oestetrol* or estrone* or oestrone* or dienestrol* or dienoestrol* or TEHRT*).tw,ot,kw.	293282
4	(Ovestin* or Vivelle or Estrace or Aerodiol or Estraderm or Ovocyclin* or hydroxyestriol* or hydroxyoestriol* or Menorest or VAGIFEM or FemSeven or Fem7 or Fem-7 or Estring or Promestrien* or Cenestin* or SCE-A or Ortho-Gynes* or Premarin or Synapause).tw,ot,kw,tn,dq,dv.	5542
5	**or/1-4 [estrogens]**	**367787**
6	estrogen deficiency/	4919
7	castrated female/ or ovariectomy/ or salpingooophorectomy/	53585
8	***menopause/**	20848
9	(ovar*tom* or OVX or oophorectom* or ovar*hysterect* or salpingo?ophorectom* or spaying or speying or ((speyed or spayed) adj6 (dogs or bitches or cats or females)) or immun*sp#ying or immun*castrat* or (remov* adj3 (ovary or ovaries or horn*)) or (castrat* adj3 (femal* or ovar*))).tw,kw.	57776
10	(**menopau*** or hypo?estrogen* or hypo-?estrogen* or (hormon* adj2 (depriv* or deficien*)) or hormon*deficien*).tw,kw.	93764
11	uter*-horn-model*.tw,kw.	96
12	**or/6-11 [estrogen-deficient/ female castration]**	**169475**
13	(animal experiment/ or exp animal model/ or exp experimental animal/ or exp glires/ or rabbit*.hw. or rat/ or exp experimental rat/ or mouse/ or exp experimental mouse/ or (animal/ not human/) or sheep/ or exp experimental sheep/ or (animals or animal study or animal experiment or dam or dams or rodent* or marmoset* or mice or mouse or murine or C57BL* or Balb-c or Balbc or Bl6 or C57Bl6 or BL-6 or C3H* or rat or rats or wistar or dawley or rabbit* or lambs or ewes or pigs or piglet* or sows or gilts or dogs or bitches or beagles or canine or cats or baboon* or macac* or macaq* or ((animal or ovine or sheep or porcine or sus or swine* or pig or sow or cat or feline or dog or primate* or monkey*) adj3 model*)).tw,kw. or (porcine or ovine).ti.) not (case report/ or case report*.jw. or ((“we-report” adj3 case) or our case).tw. or (case-report or “one case” or two cases or (porcine* adj4 (dermis or skin or graft* or matrix or collagen* or sheet* or implant*))).ti.) [animal filter]	6588578
14	**12 and 13 [estrogen-deficient animals]**	**48754**

#	Searches	Results
15	**5 or 14 [estrogens/ estrogen-deficient animals]**	**388164**
16	*genital bleeding/ or *uterus bleeding/ or (vagina bleeding/ and exp child/) or exp *uterus cancer/ or *female genital tract cancer/ or *leiomyoma/ or *myoma/ or *myosarcoma/ or **exp male genital system disease/ or exp male genital system/ or (exp male/ not exp female/)** or (neoplas* or cancer* or carcinom* or mammacarcinom* or adenocarcinom* or malignan* or tumor* or tumour* or leukem* or lymphom* or lymph*sarcom* or sarcom* or myosarcom* or rhabdomyosarcom* or leiomyom* or myoma* or fibrom* or fibroid* or adenomyo* or endometriom* or hydatidiform or metasta* or lymph* spread* or metaplas* or LLETZ or LEEP or bleed* or blood loss* or h?emorrhag* or diethylstilbestrol or stilbestrol or stilboestrol or genital mutilat* or childhood or erectile or penile or penis or prostrat* or ((male or males or men) not (female* or women))).ti,ot. or DES.ti.	6325861
17	**15 not 16 [estrogen (deficient) not cancer in title]**	**271970**
18	editorial/ or "systematic review"/ or (editorial or note).pt. or practice guideline/ or consensus development/ or (committee or editorial or reply or guideline*).ti. or cochrane.jw. or ((review.pt. or review/ or review.ti.) not (exp medical records/ or ((review adj2 cases) or case-series or case-control or cohort study or case-cohort or trial).ti,ot. or cohort analysis/ or cohort analysis/ or longitudinal study/ or prospective study/ or retrospective study/ or case-control studies/ or exp controlled clinical trial/ or ((chart* or record* or retrospectiv*) adj3 review*).tw,kw.)) [study-exclusion filter]	4773753
19	**17 not 18 [estrogen (deficient) not cancer in title, not reviews/editorials]**	**236380**
20	vaginal injury/ not (exp chemical injury/ or radiation injury/)	588
21	cystovaginal fistula/ or rectovaginal fistula/	6374
22	vaginal mesh/ or exp mesh sling/	9325
23	((fascia lata/ or small intestine mucosa/ or small intestine/ or submucosa/) and ((cadaver* or scaffold* or bioscaffold* or polypropylen* or POP or pelvic organ prolaps* or pelvis floor or colpoc?el* or vaginoc?el* or cystoc?el* or rectoc?el*or stress incontin*).mp. or ((swine/ or pig.hw.) and (graft* or xenograft* or collagen-matrix or implant* or POP or prolaps*).mp.))) or ((dermis/ and (swine/ or pig.hw. or (polypropylen* or prolaps* or POP).mp.)) not ((pig or porcine) adj2 skin).mp.)	2510
24	anterior intravaginal slingplasty/ or exp colporrhaphy/ or colposuspension/ or posterior intravaginal slingplasty/ or pubovaginal sling procedure/	2340
25	vaginal hysterectomy/	7631
26	episiotomy/	4821
27	(colpotomy/ or (colpotom* or culdotom* or vaginotom*).tw,kw.) not (cow or cows or bovine or cattle or heifer* or mare or mares or horse* or equine).ti,ot.	1343
28	(genit* wound heal*.mp. or ((wound* adj3 (heal* or repair* or dehisc* or closur*)).mp. and (female genital tract parameters/ or female genital system/ or (((genit* or urogenit*) adj2 (tract* or system* or organ* or wound* or injur* or prolap*)) or reproductive tract*).mp.))) and ((female* not (male or males)) or women or vagina or vaginal or vaginally or vulvovag* or vesicovag* or cervicovag* or uterovag* or urethrovagin* or rectovagin* or transvagin* or uterine horn*).mp. [female genital tract wound]	444

#	Searches	Results
29	(Gynemesh* or Restorell* or Polyform or Dexon or Vypro or Pelvicol or Pelvisoft or Pelvitex or Mersuture or Ugytex or UltraPro or SmartMesh* or Dynamesh* or Coloplast or TiMeSH or Prolift or SPMM or SPMW or surgipro or Avaulta or Surgisis or Marlex or InteXen or Perigee or Zenoderm or BARD or Matristem or Parietene).tw,kw,dv,dq,dm. or ((Elevate or SPM or Apogee or Prolene).tw,kw,dv,dm,mf,dq. and (mesh or meshes or prolaps* or vault* or POP or SUI or incontin*).mp.)	13061
30	((transobtur* or obturat* or miduret* or mid-uret* or tension-free or tensionless or Advantage) adj3 (tape or tapes)).tw,kw.	3301
31	(AJUST or AJUSTTM or MiniArc* or Mini-arc* or Altis or AltisTM or SECUR or SECURTM or Monarc or Ophira or Solyx or RetroArc or Desara or Supris or Obtryx* or Abbrevo or Pelvilac*).tw,kw.	875
32	((TVT or TOT or ARIS or Lynx or SPM or SIMS or Align).tw,kw. and (tape or SUI or incontinen* or transobturat* or obturat* or miduret* or mid-uret*).mp.) or (TVT-O or (single-incis* adj3 TOT) or Advantage-Fit).tw,kw.	3542
33	((((fascia lat* or (small intestin* adj2 (submucosa* or mucosa*)) or SIS or dermis) adj3 (cadaver* or porcine or graft* or xenograft*)) or porcine dermal xenograft* or (porcine intestin* adj6 (scaffold* or matrix))).tw,kw.	2462
34	(sling or slings or minisling* or sling?plast* or PIVS or ((IVS or PVS) adj proced*)).tw,kw.	13054
35	((pubovagin* or retropubic* or retro-pubic* or transobturat* or obturat* or midurethr* or mid-urethr*) adj9 (procedur* or techniq* or method* or approach or route or placement or insert* or implant* or incis* or anchor* or fixat*)).tw,kw.	8210
36	(colporrhaph* or colporaph* or colpoplast* or vaginotom* or (vagin* adj9 (wall or anterior or posterior) adj5 (repair* or incis* or injur* or insert* or implant*)) or colposusp*).tw,kw.	4443
37	(perineoplasty or perineoplasties or vestibuloplast* or perineolevatoroplast* or native tissue repair* or ((sacrospin* or sacro-spin* or vault) adj3 (fixat* or suspen*)) or (SSF and (vagin* or transvagin* or vault* or TVT or prolaps* or POP)) or ((uterosacr* or utero-sacr*) adj3 ligament* adj2 suspen*) or Manchester-Fothergill).tw,kw,dq.	2655
38	((vagin* or transvagin*) adj6 (hysterectom* or (uter* adj2 remov*))).tw,kw.	8987
39	episiotom*.tw,kw.	4152
40	((vagina or vaginal or intravagin* or vesicovag* or cervicovag* or uterovag* or urethrovagin* or rectovagin* or genit* tract* or genito* or urogenit* or ((genital or uterine) adj2 prolaps*)) adj6 (postop* or postsurg* or surger* or surgic* or operat* or perioperat* or perisurg* or preoperat* or presurg*) adj6 (estrogen* or oestrogen* or estradiol* or oestradiol* or ethinylestradiol* or ethinyloestradiol* or estriol* or oestriol* or epiestriol or estetrol* or oestetrol* or estrone* or oestrone* or dien?estrol* or TEHRT* or Ovestin or Vivelle or Estrace or Aerodiol or Estraderm or Ovocyclin or hydroxy?estriol or Menorest or VAGIFEM or FemSeven or Fem7 or Fem-7 or Estring or Promestriene or Cenestin or SCE-A or Ortho-Gynes* or Premarin or Synapause)).tw,kw.	144
41	**or/20-40 [vaginal wound /surgery /mesh/sling]**	**64808**

#	Searches	Results
42	(vagina/ or vagina epithelium/ or vagina mucosa/ or vagina tissue/ or vagina disease/ or colpocele/ or vagina pain/ or vagina ulcer/ or vaginal vault prolapse/ or intravaginal drug administration/ or exp estrogen/va or vagina reconstruction/ or (vagina or vaginal).dq. or (vagina or vaginal or vaginally or paravagin* or transvag* or vulvovag* or vesicovag* or cervicovag* or uterovag* or ureth* or rectovag* or intravag* or paravag* or extravagin* or transvagin* or pubovagin* or retropubic* or retro-pubic* or transobturat* or obturat* or midurethr* or mid-urethr*).tw,kw.) not ((((burn or burns or radiat* or irradiat* or chemical) adj2 (injur* or traum*)) or ((caustic or vagina*) adj2 (burn or burns))).mp. or (lichen or chemical or burn or burns).ti.) [vaginal]	301039
43	exp wound healing/ or *healing/ or tissue repair/ or ulcer healing/ or healing impairment/ or wound healing impairment/ or wound/ or chronic wound/ or exp surgical wound/ or wound complication/ or wound dehiscence/ or wound infection/ or wound care/ or wound closure/ or tissue regeneration/ or *regeneration/ or erosion/ or surgical injury/ or surgical infection/ or tissue injury/ or prosthesis implantation/ or exp bioprosthesis/ or collagen implant/ or tissue scaffold/ or graft dysfunction/ or graft failure/ or graft infection/ or graft rejection/ or prosthesis complication/	549283
44	surgical mesh/ or polypropylene/ or polyglactin/	39166
45	((pelvic organ prolapse/ or cystocele/ or anterior vaginal wall prolapse/ or apical prolapse/ or colpocele/ or uterus prolapse/ or vaginal vault prolapse/ or enterocele/ or exp posterior vaginal wall prolapse/ or exp pelvic floor disorder/ or pelvis floor/ or stress incontinence/ or urine incontinence/ or incontinence/ or (POP or ((pelvic or pelvis) adj2 (organ* or floor* or support*)) or prolaps* or vault* or colpoptos* or colpoc?el* or vaginoc?el* or cystoc?el* or rectoc?el* or enteroc?el* or ((vagin* or vulvovag* or vesicovag* or cervicovag*) adj4 (extrusion* or extrude* or eviscerat* or descen* or prociden* or ptos* or herni* or bulg*)) or ((uter* or urinary or urethr* or genit* or urogenit* or rect* or pelvic) adj4 (extrusion* or extrude* or eviscerat* or descen* or prociden* or ptos* or herni* or bulg*)) or SUI or incontinen*).tw,kw.) and (pelvic organ prolapse/su or cystocele/su or anterior vaginal wall prolapse/su or apical prolapse/su or colpocele/su or uterus prolapse/su or vaginal vault prolapse/ su or enterocele/su or exp posterior vaginal wall prolapse/su or exp pelvic floor disorder/su or pelvis floor/su or vagina/su or vagina diseases/su or abdominal wall/ su or abdominal wall musculature/su or stress incontinence/su or urine incontinence/ su or *gynecologic surgery/ or vagina reconstruction/ or pelvis surgery/ or urologic surgery/ or urinary tract surgery/ or perioperative period/ or plastic surgery/ or surgical technique/ or device removal/ or excision/ or incision/ or intraoperative period/ or peroperative care/ or peroperative complication/ or postoperative period/ or postoperative care/ or preoperative period/ or preoperative care/ or preoperative treatment/ or reconstructive surgery/ or reoperation/ or ((pelvic* or genit* or POP or prolaps* or vault* or colpoptos* or colpoc?el* or vaginoc?el* or cystoc?el* or rectoc?el* or enteroc?el* or vagina or vaginal or vaginally or transvagin* or paravagin* or vesicovag*) adj3 (reconstr* or repair* or surger* or operation* or postoperat* or postsurg* or preoperat* or presurg* or perioperat* or perisurg* or reinforc* or implanted or implantat* or incis* or graft* or flap or flaps or PP)).tw,kw.)) not ((case report or one-case or two cases or bitch or dog or cat or queen or bongo or pseudohermaphr* or hermaphr* or neovag*).ti. or ((“we-report” adj3 case) or our case).tw.)	44413
46	(wound* or healing or healed or dehisc* or eros* or erod* or debrid* or epibol* or granulat* or (tissue adj2 (disrupt* or damag*)) or excoriat*).tw,kw.	606945

#	Searches	Results
47	(((vagina or vaginal or vaginally or paravagin* or transvag* or vulvovag* or vesicovag* or cervicovag* or uterovag* or ureth* or rectovag* or intravag* or paravag* or extravagin* or transvagin*) adj12 (lacerat* or fissur* or scar or scars or scarring or fistul* or injur*)) or (obstetr* adj3 (fistul* or lacerat*)) or (trauma adj2 vagin*)).tw,kw.	18941
48	(((mesh or meshes) not ((wire or search* or medline or pubmed) adj5 mesh*)) or polypropylen* or polylactic or PLA or polyglac* or scaffold* or bioscaffold* or biologic graft* or ((acellular or collagen) adj3 matrix)).tw,kw,dq.	204553
49	**or/43-48 [wound, mesh,sling, vaginal surgery II]**	**1152759**
50	**42 and 49 [vaginal wound/surgery/mesh/sling II]**	**51069**
51	**41 or 50 [vaginal wound/surgery/mesh/sling II]**	**94084**
52	**51 and 19 [estrogens + vaginal wound/ surgery/mesh/sling]**	**1268**
53	**remove duplicates from 52 [I estrogens + wound healing/vaginal surgery models - deduplicated]**	**1254**
54	**53 not medline.cr. [I estrogens + wound healing/vaginal surgery models - deduplicated - embase records only]**	**1179**

Web of Science 2020-01-28 (reverse order of search history)

# 30	379	#28 NOT #29
		Indexes=SCI-EXPANDED, SSCI, A&HCI, ESCI Timespan=All years
# 29	941161	TI=("committee" or "editorial" or "reply" or "guideline*" or "review") not (TI=(("review" NEAR/2 "cases") or "case-series" or "case-control" or "cohort-study" or "case-cohort" or "trial") OR TS=(("chart*" or "record*" or "retrospectiv*") NEAR/3 "review*"))
		Indexes=SCI-EXPANDED, SSCI, A&HCI, ESCI Timespan=All years
# 28	**393**	**#26 NOT #27**
		Indexes=SCI-EXPANDED, SSCI, A&HCI, ESCI Timespan=All years
# 27	3142105	TI=("neoplas*" or "cancer*" or "carcinom*" or "mammacarcinom*" or "adenocarcinom*" or "malignan*" or "tumor*" or "tumour*" or "leukem*" or "lymphom*" or "lymph*sarcom*" or "sarcom*" or "myosarcom*" or "rhabdomyosarcom*" or "leiomyom*" or "myoma*" or "fibrom*" or "fibroid*" or "adenomyo*" or "endometriom*" or "hydatidiform" or "metasta*" or "lymph*-spread*" or "metaplas*" or "bleed*" or "blood-loss*" or "h$emorrhag*" or "diethylstilbestrol" or "stilbestrol" or "stilboestrol" or "DES" or "genital-mutilat*" or "childhood" or "erectile" or "penile" or "penis" or "prostrat*" or (("male" or "males" or "men") not ("female*" or "women")))
		Indexes=SCI-EXPANDED, SSCI, A&HCI, ESCI Timespan=All years
# 26	**440**	**#18 OR #25**
		Indexes=SCI-EXPANDED, SSCI, A&HCI, ESCI Timespan=All years
# 25	**279**	**#10 AND #19 AND #24**
		Indexes=SCI-EXPANDED, SSCI, A&HCI, ESCI Timespan=All years

# 24	**894827**	**#20 OR #21 OR #22 OR #23**
		Indexes=SCI-EXPANDED, SSCI, A&HCI, ESCI Timespan=All years
# 23	358555	(TS=("mesh" or "meshes") NOT TS=(("wire" or "search*" or "medline" or "pubmed") NEAR/5 "mesh*")) OR TS=("polypropylen*" or "polylactic" or "PLA" or "polyglac*" or "scaffold*" or "bioscaffold*" or "biologic-graft*" or (("acellular" or "collagen") NEAR/3 "matrix"))
		Indexes=SCI-EXPANDED, SSCI, A&HCI, ESCI Timespan=All years
# 22	9083	TS=(("vagina" or "vaginal" or "vaginally" or "paravagin*" or "transvag*" or "vulvovag*" or "vesicovag*" or "cervicovag*" or "uterovag*" or "ureth*" or "rectovag*" or "intravag*" or "paravag*" or "extravagin*" or "transvagin*") NEAR/12 ("lacerat*" or "fissur*" or "scar" or "scars" or "scarring" or "fistul*" or "injur*")) or ("obstetr*" NEAR/3 ("fistul*" or "lacerat*")) or ("trauma" NEAR/2 "vagin*"))
		Indexes=SCI-EXPANDED, SSCI, A&HCI, ESCI Timespan=All years
# 21	541097	TS=("wound*" or "healing" or "healed" or "dehisc*" or "eros*" or "erod*" or "debrid*" or "epibol*" or "granulat*" or ("tissue" NEAR/2 ("disrupt*" or "damag*")) or "excoriat*")
		Indexes=SCI-EXPANDED, SSCI, A&HCI, ESCI Timespan=All years
# 20	8388	(TS=("POP" or (("pelvic" or "pelvis") NEAR/2 ("organ*" or "floor*" or "support*")) or "prolaps*" or "vault*" or "colpoptos*" or "colpoc$el*" or "vaginoc$el*" or "cystoc$el*" or "rectoc$el*" or "enteroc$el*" or (("vagin*" or "vulvovag*" or "vesicovag*" or "cervicovag*") NEAR/4 ("extrusion*" or "extrude*" or "eviscerat*" or "descen*" or "prociden*" or "ptos*" or "herni*" or "bulg*")) or (("uter*" or "urinary" or "urethr*" or "genit*" or "urogenit*" or "rect*" or "pelvic") NEAR/4 ("extrusion*" or "extrude*" or "eviscerat*" or "descen*" or "prociden*" or "ptos*" or "herni*" or "bulg*")) or "SUI" or "incontinen*") AND TS=(("pelvic*" or "genit*" or "POP" or "prolaps*" or "vault*" or "colpoptos*" or "colpoc?el*" or "vaginoc?el*" or "cystoc?el*" or "rectoc?el*" or "enteroc?el*" or "vagina" or "vaginal" or "vaginally" or "transvagin*" or "paravagin*" or "vesicovag*") NEAR/3 ("reconstr*" or "repair*" or "surger*" or "operation*" or "postoperat*" or "postsurg*" or "preoperat*" or "presurg*" or "perioperat*" or "perisurg*" or "reinforc*" or "implanted" or "implantat*" or "incis*" or "graft*" or "flap" or "flaps" or "PP"))) NOT (TI=("case-report" or "one-case" or "two-cases" or "bitch" or "dog" or "cat" or "queen" or "bongo" or "pseudohermaphr*" or "hermaphr*" or "neovag*") OR TS=(("we-report" NEAR/3 "case") or "our-case"))
		Indexes=SCI-EXPANDED, SSCI, A&HCI, ESCI Timespan=All years
# 19	175591	(TS=("vagina" or "vaginal" or "vaginally" or "paravagin*" or "transvag*" or "vulvovag*" or "vesicovag*" or "cervicovag*" or "uterovag*" or "ureth*" or "rectovag*" or "intravag*" or "paravag*" or "extravagin*" or "transvagin*" or "pubovagin*" or "retropubic*" or "retro-pubic*" or "transobturat*" or "obturat*" or "midurethr*" or "mid-urethr*")) NOT (TS=(("burn" or "burns" or "radiat*" or "irradiat*" or "chemical") NEAR/2 ("injur*" or "traum*")) or (("caustic" or "vagina*") NEAR/2 ("burn" or "burns"))) OR TI=("lichen" or "chemical" or "burn" or "burns"))
		Indexes=SCI-EXPANDED, SSCI, A&HCI, ESCI Timespan=All years

# 18	**259**	**#10 AND #17**
		Indexes=SCI-EXPANDED, SSCI, A&HCI, ESCI Timespan=All years
# 17	29451	**#11 OR #12 OR #13 OR #14 OR #15 OR #16**
		Indexes=SCI-EXPANDED, SSCI, A&HCI, ESCI Timespan=All years
# 16	46	TS=((“vagina” or “vaginal” or “intravagin*” or “vesicovag*” or “cervicovag*” or “uterovag*” or “urethrovagin*” or “rectovagin*” or ((“genital” or “uterine”) NEAR/2 “prolaps*”) or “genit*-tract*” or “genito*” or “urogenit*”) NEAR/6 (“postop*” or “postsurg*” or “surger*” or “surgic*” or “operat*” or “perioperat*” or “perisurg*” or “preoperat*” or “presurg*”) NEAR/6 (“estrogen*” or “oestrogen*” or “estradiol*” or “oestradiol*” or “ethinylestradiol*” or “ethinyloestradiol*” or “estriol*” or “oestriol*” or “epi$estriol” or “estetrol*” or “oestetrol*” or “estrone*” or “oestrone*” or “dienestrol*” or “dienoestrol*” or “TEHRT*” or “Ovestin*” or “Vivelle” or “Estrace” or “Aerodiol” or “Estraderm” or “Ovocyclin*” or “hydroxyestriol*” or “hydroxyoestriol*” or “Menorest” or “VAGIFEM” or “FemSeven” or “Fem7” or “Fem-7” or “Estring” or “Promestrien*” or “Cenestin*” or “SCE-A” or “Ortho-Gynes*” or “Premarin” or “Synapause”))
		Indexes=SCI-EXPANDED, SSCI, A&HCI, ESCI Timespan=All years
# 15	14642	TS=(((“transobtur*” or “obturat*” or “miduret*” or “mid-uret*” or “tension-free” or “tensionless”) near/3 “tape*”) or “AJUST” or “AJUSTTM” or “MiniArc*” or “Mini-arc*” or “Altis” or “AltisTM” or “SECUR” or “SECURTM” or “Monarc” or “Ophira” or “Solyx” or “RetroArc” or “Desara” or “Supris” or “Obtryx*” or “Abbrevo” or “Pelvilac*” or “TVT-O” or (“single-incis*” NEAR/3 “TOT”) or (“Advantage” NEAR/6 (“tape” or “SUI”)) or “Advantage-Fit” or ((“fascia-lat*” or (“small-intestin*” NEAR/2 (“submucosa*” or “mucosa*”)) or “SIS” or “dermis”) NEAR/3 (“cadaver*” or “porcine” or “graft*” or “xenograft*”)) or “porcine-dermal-xenograft*” or (“porcine-intestin*” NEAR/6 (“scaffold*” or “matrix”)) or “sling” or “slings” or “minisling*” or “sling$plast*” or “PIVS” or “IVS-proced*” or “PVS-proced*” or ((“pubovagin*” or “retropubic*” or “retro-pubic*” or “transobturat*” or “obturat*” or “midurethr*” or “mid-urethr*”) NEAR/9 (“procedur*” or “techniq*” or “method*” or “approach” or “route” or “placement” or “insert*” or “implant*” or “incis*” or “anchor*” or “fixat*”))) OR (TS=(“TVT” or “TOT” or “ARIS” or “Lynx” or “SPM” or “SIMS” or “Align”) AND TS=(“tape” or “SUI” or “incontinen*” or “transobturat*” or “obturat*” or “miduret*” or “mid-uret*”))
		Indexes=SCI-EXPANDED, SSCI, A&HCI, ESCI Timespan=All years

# 14	10519	TS=(“colporrhaph*” or “colporaph*” or “colpoplast*” or “vaginotom*” or (“vagin*” NEAR/9 (“wall” or “anterior” or “posterior”) NEAR/5 (“repair*” or “incis*” or “injur*” or “insert*” or “implant*”)) or “colposusp*” or “perineoplasty” or “perineoplasties” or “vestibuloplast*” or “perineolevatoroplast*” or “native-tissue-repair*” or ((“sacrospin*” or “sacro-spin*” or “vault”) NEAR/3 (“fixat*” or “suspen*”)) or (“SSF” and (“vagin*” or “transvagin*” or “vault*” or “TVT” or “prolaps*” or “POP”)) or ((“uterosacr*” or “utero-sacr*”) NEAR/3 “ligament*” NEAR/2 “suspen*”) or “Manchester-Fothergill” or ((“vagin*” or “transvagin*”) NEAR/6 (“hysterectom*” or (“uter* NEAR/2 remov*”))) or “episiotom*”)
		Indexes=SCI-EXPANDED, SSCI, A&HCI, ESCI Timespan=All years
# 13	5564	TS=(“Gynemesh*” or “Restorell*” or “Polyform” or “Dexon” or “Vypro” or “Pelvicol” or “Pelvisoft” or “Pelvitex” or “Mersuture” or “Ugytex” or “UltraPro” or “SmartMesh*” or “Dynamesh*” or “Coloplast” or “TiMeSH” or “Prolift” or “SPMM” or “SPMW” or “surgipro” or “Avaulta” or “Surgisis” or “Marlex” or “InteXen” or “Perigee” or “Zenoderm” or “BARD” or “Matristem” or “Parietene”) OR (TS=(“Elevate” or “SPM” or “Apogee” or “Prolene”) AND TS=(“mesh” or “meshes” or “prolaps*” or “vault*” or “POP” or “SUI” or “incontin*”))
		Indexes=SCI-EXPANDED, SSCI, A&HCI, ESCI Timespan=All years
# 12	60	(TS=(“genit*-wound-heal*”) or (TS=(“wound*” NEAR/3 (“heal*” or “repair*” or “dehisc*” or “closur*”)) and TS=(((“genit*” or “urogenit*”) NEAR/2 (“tract*” or “system*” or “organ*” or “wound*” or “injur*” or “prolap*”)) or “reproductive-tract*”))) and TS=((“female*” not (“male” or “males”)) or “women” or “vagina” or “vaginal” or “vaginally” or “vulvovag*” or “vesicovag*” or “cervicovag*” or “uterovag*” or “urethrovagin*” or “rectovagin*” or “transvagin*” or “uterine-horn*”)
		Indexes=SCI-EXPANDED, SSCI, A&HCI, ESCI Timespan=All years
# 11	339	TS=(“colpotom*” or “culdotom*” or “vaginotom*”) NOT TI=(“cow” or “cows” or “bovine” or “cattle” or “heifer*” or “mare” or “mares” or “horse*” or “equine”)
		Indexes=SCI-EXPANDED, SSCI, A&HCI, ESCI Timespan=All years
# 10	258824	**#3 OR #9**
		Indexes=SCI-EXPANDED, SSCI, A&HCI, ESCI Timespan=All years
# 9	35198	**#7 AND #8**
		Indexes=SCI-EXPANDED, SSCI, A&HCI, ESCI Timespan=All years

# 8	4218251	(TS=(“animals” or “animal-study” or “animal-experiment” or “dam” or “dams” or “rodent*” or “marmoset*” or “mice” or “mouse” or “murine” or “C57BL*” or “Balb-c” or “Balbc” or “Bl6” or “C57Bl6” or “BL-6” or “C3H*” or “rat” or “rats” or “wistar” or “dawley” or “rabbit*” or “lambs” or “ewes” or “pigs” or “piglet*” or “sows” or “gilts” or “dogs” or “bitches” or “beagles” or “canine” or “cats” or “baboon*” or “macac*” or “macaq*” or ((“animal” or “ovine” or “sheep” or “porcine” or “sus” or “swine*” or “pig” or “sow” or “cat” or “feline” or “dog” or “primate*” or “monkey*”) near/3 “model*”)) or TI=(“porcine” or “ovine”)) NOT (TS=((“we-report” NEAR/3 “case”) or “our-case”) or TI=(“case-report” or “one-case” or “two-cases” or (“porcine*” NEAR/4 (“dermis” or “skin” or “graft*” or “matrix” or “collagen*” or “sheet*” or “implant*”))))
		Indexes=SCI-EXPANDED, SSCI, A&HCI, ESCI Timespan=All years
# 7	**101158**	**#4 OR #5 OR #6**
		Indexes=SCI-EXPANDED, SSCI, A&HCI, ESCI Timespan=All years
# 6	195	TS= “uter*-horn-model*”
		Indexes=SCI-EXPANDED, SSCI, A&HCI, ESCI Timespan=All years
# 5	63929	TS=(“menopau*” or “hypo$estrogen*” or “hypo-$estrogen*” or (“hormon*” NEAR/2 (“depriv*” or “deficien*”)) or “hormon*deficien*”)
		Indexes=SCI-EXPANDED, SSCI, A&HCI, ESCI Timespan=All years
# 4	42024	TS=(“ovar*tom*” or “OVX” or “oophorectom*” or “ovar*hysterect*” or salpingo$ophorectom* or “spaying” or “speying” or ((“speyed” or “spayed”) NEAR/6 (“dogs” or “bitches” or “cats” or “females”)) or “immun*sp$ying” or “immun*castrat*” or (“remov*” NEAR/3 (“ovary” or “ovaries” or “horn*”)) or (“castrat*” NEAR/3 (“femal*” or “ovar*”)))
		Indexes=SCI-EXPANDED, SSCI, A&HCI, ESCI Timespan=All years
# 3	242252	**#1 OR #2**
		Indexes=SCI-EXPANDED, SSCI, A&HCI, ESCI Timespan=All years
# 2	806	TS=(“Ovestin*” or “Vivelle” or “Estrace” or “Aerodiol” or “Estraderm” or “Ovocyclin*” or “hydroxyestriol*” or “hydroxyoestriol*” or “Menorest” or “VAGIFEM” or “FemSeven” or “Fem7” or “Fem-7” or “Estring” or “Promestrien*” or “Cenestin*” or “SCE-A” or “Ortho-Gynes*” or “Premarin” or “Synapause”)
		Indexes=SCI-EXPANDED, SSCI, A&HCI, ESCI Timespan=All years
# 1	241952	TS=(“estrogen*” or “oestrogen*” or “estradiol*” or “oestradiol*” or “ethinylestradiol*” or “ethinyloestradiol*” or “estriol*” or “oestriol*” or “epi$estriol” or “estetrol*” or “oestetrol*” or “estrone*” or “oestrone*” or “dienestrol*” or “dienoestrol*” or “TEHRT*”)
		Indexes=SCI-EXPANDED, SSCI, A&HCI, ESCI Timespan=All years

3 Validation of noninvasive focal depth measurements to determine epithelial thickness of the vaginal wall

AW Kastelein
CM Diedrich
CHJR Jansen
SE Zwolsman
C Ince
JPWR Roovers

Menopause. 2019 Oct;26(10):1160-1165.

ABSTRACT

Objective

This study investigates whether noninvasive focal depth (FD) measurements correlate with vaginal wall epithelial thickness (ET). If FD accurately reflects ET of the vaginal wall, this would allow noninvasive longitudinal assessment of (newly developed) treatment modalities aiming to increase ET, without the need for invasive biopsies.

Methods

Fourteen women, median age 62 years (inter quartile ranges: 57-65), undergoing vaginal prolapse surgery because of anterior and/or posterior compartment pelvic organ prolapse were included. We used the CytoCam, a handheld video microscope based on incident dark field imaging, and performed FD measurements of the vaginal wall before surgery. Histology was performed on tissue that was removed during the surgical procedure, and ET was measured in stained sections. We compared ET with FD interindividually, and determined the expected linear correlation and agreement between the two measurements.

Results

Seventeen ET measurements (mean 125 μm ± 38.7, range 48-181 μm) were compared with 17 FD measurements (mean 128 μm ± 34.3, range 68-182 μm). The linear correlation between the two measurements was strong ($r = 0.902$, $P < 0.01$). Bland-Altman analysis demonstrated a mean difference of 13.5 μm when comparing ET to FD.

Conclusions

The results demonstrate good agreement between ET and FD measurements. We consider the mean difference demonstrated with Bland-Altman analysis acceptable for these measurements. This suggests that FD accurately reflects ET, which further supports the use of FD to measure ET of the vaginal wall. For a complete assessment of the vaginal wall, FD measurements are preferably combined with the assessment of vaginal angioarchitecture.

INTRODUCTION

Vulvovaginal atrophy (VVA) is a common ageing condition, affecting an estimated 40% of postmenopausal women (1). As a consequence of vaginal discomfort and pain, VVA has significant impact on daily activity, sexual function, and overall quality of life (2). The diagnosis and evaluation of treatment are predominantly done by clinical assessment (3). Objective measures such as the vaginal maturation index or vaginal pH are either expensive and time-consuming or inaccurate in the case of the latter (4). Clinicians and researchers would benefit from a method that accurately and directly measures VVA, for objective assessment and evaluation of (newly developed) treatment modalities.

As VVA is characterized by a thin epithelium, measuring epithelial thickness (ET) has been suggested as a method (4, 5). Previous histological studies have demonstrated that ET increases after treatment with topical estrogen (6, 7), and possibly also after vaginal laser therapy (8). Histology, however, requires invasive tissue sampling and is therefore not easily applicable in a daily clinical or research setting.

In a previous study, it was suggested that ET can be measured in vivo and noninvasively with the use of incident dark field (IDF) imaging (5). This technique is primarily used to investigate the microcirculation (9-11). It uses green light that is absorbed by hemoglobin in red blood cells, allowing visualization of the microcirculation (9). In addition, the IDF-device records the distance from the tip of the device to the point where the microcirculation is in optimal focus, defined as focal depth (FD). Because the vaginal vasculature is located in the subepithelial layers of the vagina (lamina propria) and the epithelium is not directly vascularized, FD is considered to be a reflection of ET (5).

It was demonstrated that FD increases significantly after application of topical estrogen (5), but it is unknown whether FD measurements reflect the actual thickness of the epithelium. Therefore, we compared vaginal wall FD measurements with ET measured in participant-derived tissue samples from imaged sites, and determined correlation and agreement between the measurements. A good correlation between these two measures would further rationalize the use of FD and justify replacement of histology by noninvasive FD measurements, not only for VVA, but in many other (fibrotic, sclerosing) conditions that affect the epithelium. In case of VVA, this would allow noninvasive, longitudinal assessment of (newly developed) treatment modalities aiming to increase ET.

MATERIALS AND METHODS

Participants and settings

In this prospective, single-center observational study, we recruited women with (1) pelvic organ prolapse stage 2 or more, (2) undergoing anterior and/or posterior colporrhaphy at the Department of Obstetrics and Gynaecology who (3) could be informed about study procedures and guidelines in their native language. Medical history was obtained and women with history of vaginal surgery were excluded from participation. Women received verbal explanation of the study and written informed consent was obtained from each participant. All approached women (n = 14) agreed to participate in our study. This study was reviewed by the Medical Ethics Committee under number W17_040, and permission was granted on February 2, 2017.

Focal depth measurements

Focal depth measurements were performed using incident dark field (IDF) imaging (CytoCam, Braedius Medical, Huizen, The Netherlands) (9). The CytoCam is a commercially available hand-held video microscope, predominantly used for assessment of the sublingual microcirculation in critically ill patients. In addition, the CytoCam has been used for assessment of the microcirculation of different organ surfaces, including the vagina. CytoCam measurements are noninvasive and safe: no adverse events or complications have been reported as a consequence of measurements performed with the CytoCam. In previous studies, vaginal measurements were well tolerated by study participants. The CytoCam is lightweight (120 g) and shaped like a pen (length 220 mm, diameter 23 mm), and uses green light, emitted from high-brightness LEDs located at the tip of the device. Green light is absorbed by hemoglobin in the red blood cell, allowing visualization of the microcirculation. The CytoCam measures the distance from the tip of the device to the point where the microcirculation is in optimal focus (ie, when individual erythrocytes can be discriminated). In practice, this is the distance between the subepithelial microcirculation and the epithelial surface, in micrometers. The CytoCam can focus between 0 and 400 μm and the focus can be adjusted with steps of 1 μm. The CytoCam was connected to a device controller which, in turn, was connected to a powerful laptop (P50, Lenovo, Peking, China) that was used for visualization and storage of the images. All measurements were performed on participants in the operating room before surgery by one researcher (AK) experienced in measuring the vaginal microcirculation and performing FD measurements. All measurements were performed while patients were under general anesthesia. The CytoCam was placed into contact

with the mucosa of the vaginal wall without applying excessive pressure, at 3 cm above the hymen at the surgical site. Subsequently, the CytoCam was adjusted for optimal focus. Optimal focus was acquired in micrometers for the most superficially located blood vessels (ie, the smallest value at which the microcirculation was in focus, was noted as the focal depth). In all participants, the complete measurement took less than 3 minutes.

Tissue retrieval and histological assessment of epithelial thickness

After hydrodissection with a saline solution with 24% adrenaline, a midline incision of the vaginal wall tended by four Allis clamps was performed. After plication, excessive and redundant vaginal tissue was trimmed and removed. We avoided clamping of the imaged part of the redundant tissue, in order not to manipulate the epithelium. From the removed tissue, a tissue sample of approximately 10 × 10 mm was taken, which was formerly located 3 cm above the hymen. Tissue samples were fixed in 10% neutral-buffered formalin immediately after harvesting, for 48 hours. After fixation and dehydration, tissue samples were embedded in paraffin, cut into 5 µm thick sections and stained with hematoxylin and eosin (H&E) staining (Benchmark ULTRA, Roche Diagnostics, Indianapolis, IN) for histological analysis. Stained sections were analyzed by light microscopy and images were acquired using the Olympus cellSense Standard software (Olympus, Leiderdorp, The Netherlands) and an Olympus BX51 microscope (Olympus) with ×20 objective. In the acquired images, ET (ie, stratified squamous epithelium, superficial layer until lamina propria) was measured with ImageJ software (ImageJ, NIH and LOCI, University of Wisconsin, Madison, WI) (12). From each section, ET was measured at crypts, where the distance from the surface of the vaginal wall to the vasculature in the lamina propria was the smallest. When no crypts were present, the thinnest measure of ET in that sample was used. Measurements of ET were performed by two individual researchers (AK, CD) who were blinded for sample identity, and measurements were averaged.

Statistical analysis

The primary outcome was the agreement between the two measurement techniques. The thinnest ET measured in sections was the reference measurement. Descriptive statistics were used for data summaries, that is, a mean with SD when normally distributed and median with inter quartile ranges (IQRs) when not normally distributed. We used a d'Agostino and Pearson test to determine distribution of data. The correlation between ET in histological slides and FD measured with the CytoCam was examined as r by

calculating the Pearson correlation coefficient (PCC). A correlation coefficient of 0.9 to 1.0 will be considered a very high positive correlation, 0.7 to 0.9 as a high positive correlation, 0.5 to 0.7 as a moderate positive correlation, and so on (13). A minimal sample size of 13 participants was determined for a correlation coefficient of 0.7, with the alpha level set at 0.05 and the beta level set at 0.20. The level of agreement and the 95% limits of agreement between the two measurements were determined using the Bland-Altman method (14). All results were analyzed in SPSS Statistics 25 (IBM Corp. Released 2017. IBM SPSS Statistics for Windows, Version 25.0. Armonk, NY: IBM Corp.).

RESULTS

Fourteen women provided written and verbal informed consent and were included in this study. The median age was 62 years (IQR 57-65) and participants had no relevant comorbidity (ASA I-II). All participants were operated for an anterior and/or posterior compartment pelvic organ prolapse, POP-Q stage 2 or more. In total, 17 locations were imaged: 13 measurements of the anterior vaginal wall, and 4 measurements of the posterior vaginal wall. Three women were operated for both an anterior and posterior compartment prolapse, in which case both the anterior vaginal wall and the posterior vaginal wall were measured.

Focal depth and epithelial thickness measurements

Focal depth could be determined in all participants. Different types of microvascular morphology, also known as angioarchitecture (10), were observed during FD measurements (Fig. 1). The mean FD measured with the CytoCam in all participants was 128 µm (SD 34.3 µm, range 68-182 µm) (Table 1). In all HE-stained sections, a normal structure of vaginal tissue was observed, including the epithelium, the lamina propria, a muscularis layer, and the adventitia (15). The mean ET measured in all histological samples was 125 µm (SD 38.7, range 48-181 µm) (Table 1). Within a section, ET was often heterogeneous. Figure 2 illustrates a histological sample with heterogeneous ET ranging from 160 to 320 µm. In this case, the thinnest measure of ET in that sample (160 µm) was used for comparison.

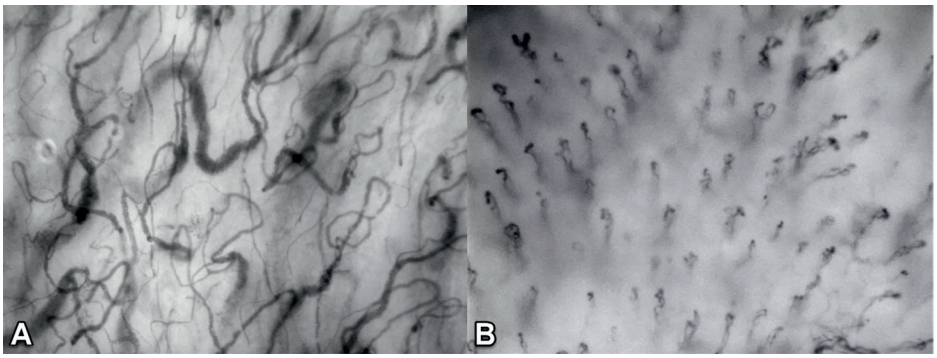

Figure 1. Screenshots of CytoCam images with different types of angioarchitecture.
Each image represents an area of 1.55 × 1.16 mm. (A) The focal depth is 80 µm. (B) The focal depth is 160µm.

Table 1. Overview of study participants and the performed measurements

Subject number	Histology epithelial thickness (µm)	CytoCam Focal depth (µm)
1	160	160
2	83	100
3	174	170
4	115	92
5	154	156
6	126	128
7	119	106
8	160	182
9-1	110	124
9-2	48	83
10-1	134	124
10-2	86	68
11	181	172
12	123	127
13-1	168	157
13-2	65	93
14	119	137
$\dot{X}$	125	128
SD (range)	38.7 (48-181)	34.3 (68-182)

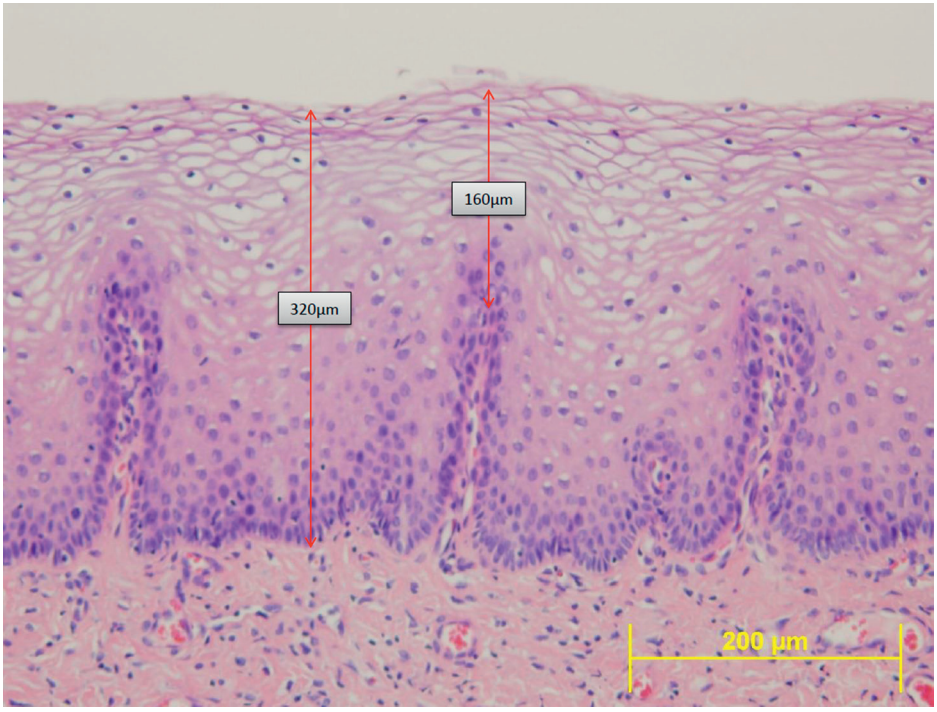

Figure 2. Hemotoxylin and eosin (H&E) staining of the vaginal wall.
The epithelial thickness is heterogeneous and ranges from 160 to 320 µm. In this participant, the CytoCam focal depth was 160 µm.

Correlation and agreement between measurements

Comparison of ET with FD demonstrated a very high positive correlation ($r = 0.902$, $P < 0.01$) (Table 2). Figure 3 graphically displays this positive linear relationship between the two measurements. The Bland-Altman plot in Figure 4 shows the level of agreement between the two measurements and the 95% limits of agreement. This analysis demonstrated that the mean observed difference between the two measurements was 13.5 µm with a 95% CI of –5.9 to 32.9 µm.

Table 2. Mean difference and SD in micrometers between measurements of epithelial thickness and focal depth

	Ẋ	SD (range)	Pearson *r*
Δ Histology – CytoCam	13.5	9.9 (0-35)	0,9

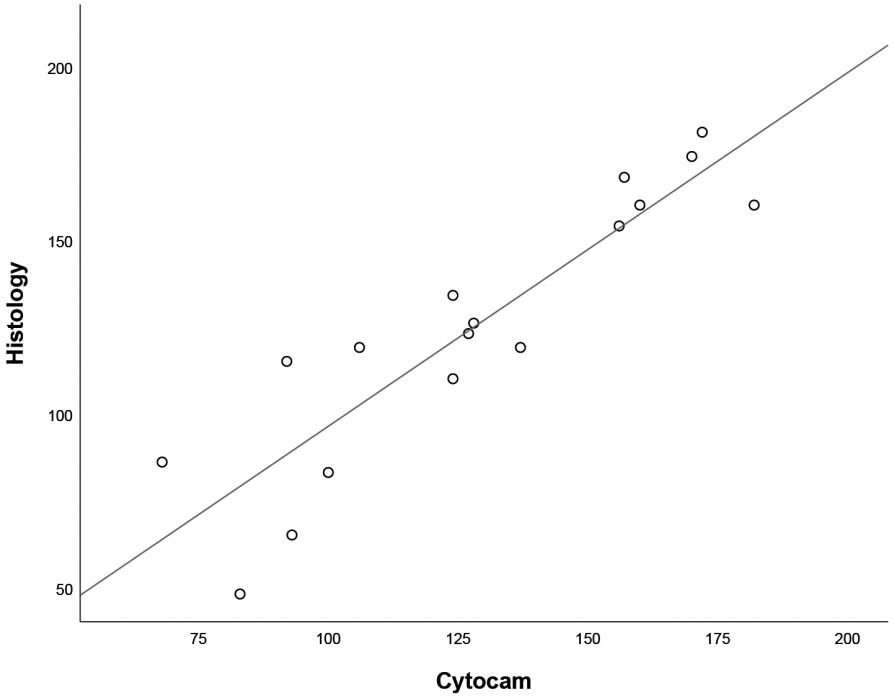

Figure 3. Scatterplot comparing epithelial thickness (histology) to focal depth (CytoCam)

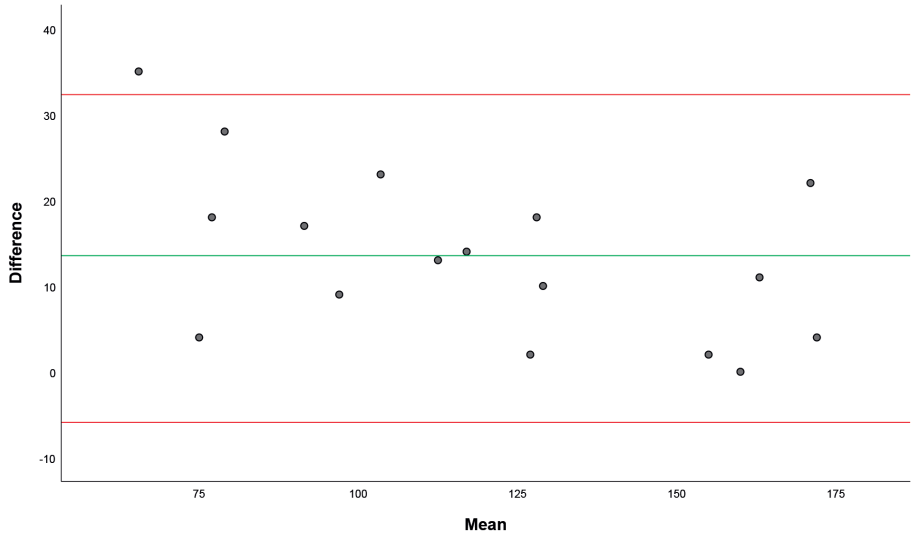

Figure 4. Bland-Altman plot of the difference between epithelial thickness (histology) and focal depth (CytoCam).

DISCUSSION

Main findings

The results of this study suggest that FD measurements have a strong correlation with vaginal wall ET. We have demonstrated that FD accurately reflects the thinnest measure of ET within an individual.

Strengths and limitations

The study design allowed us to acquire vaginal tissue for histological analysis and ET measurements, without the need for additional invasive procedures. Double, independent, and blinded ET measurements were performed in sections and compared with FD measurements. Because no strict inclusion and exclusion criteria were used, the possibility for sampling bias was reduced.

This study also has several limitations. A relatively small sample size was used, which increases the possibility that our findings are based on chance. Also, all participants were women with pelvic organ prolapse, which makes our sample a specific selection of women. The fact that participants had no relevant comorbidity and a median age

of 62 years increases the generalizability of this sample to the broader population with VVA.

Limitations with respect to the measurements have to be considered as well. We did not mark the location that was imaged. Therefore, the selected tissue sample might not exactly be the imaged location. By standardizing the FD measurements as much as possible (midline, 3 cm above the hymen), we, however, limited this chance. In addition, we determined ET measurements in sections as the gold standard. There are, however, some factors that could affect the thickness of the epithelium in sections, or the way it is measured. First, fixation in formalin can hypothetically alter the dimensions of tissue (16). Nevertheless, research in other tissues demonstrated that these changes are not observed or are very limited (17, 18). Second, when tissue samples are embedded and subsequently sectioned, sectioning is never performed in an exact 90° perpendicular position. The less this 90° position is respected and the more oblique the section is made, the thicker the epithelium will appear in a section (19). Third, placement of Allis clamps and traction on the tissue could affect the dimensions.

There are also factors that can affect FD measurements. First, FD is a subjective measure, in which the user has to determine the optimal focus of the camera. Because of practical reasons, only one trained investigator performed the FD measurements, which would ideally have been done by two independent researchers. As also mentioned for ET in sections, a non-90° position of the CytoCam would hypothetically also affect FD and a 90° position cannot be guaranteed.

Interpretation of results

The vaginal wall is composed of four layers: the epithelium, the lamina propria, a muscularis layer and the adventitia (15). The epithelial layer is not directly vascularized, but is provided with oxygen via diffusion from the vasculature in the subepithelial layers (19). The fact that the epithelium is avascular provides the rationale for measuring FD by using the distance from basal membrane to vascular network as proxy for ET (5). VVA is characterized by a thin epithelium, whereas a thick epithelium is observed in women without VVA (20). In previous studies that evaluated ET in biopsies, the reported ET ranged from 200 to 2.5 mm (21). In our study, the ET measured in tissue samples ranged from 48 to 405 µm, with great intraparticipant-variation. The large variation within participants can be explained by crypts and rugae, causing the epithelium to fold strongly. Figure 2 demonstrates ET ranging from 160 to 320 µm in one tissue sample.

In this case, the FD measured by the CytoCam was 160 µm. This demonstrates that FD reflects the thickness of the epithelium where the capillary bed is most superficial (ie, the thinnest part of the epithelium). In the present study, FD measurements ranged from 68 to 182 µm, which is within the same range as our previous study (5). It should also be noted that the imaged area with the CytoCam is approximately 1.8 mm2, indicating that FD is an average of that area, from which only a small region is measured in a section. Interestingly, the epithelium of the posterior vaginal wall was thinner in all participants than the epithelium of the anterior vaginal wall.

Clinical implications

Currently, measurements of ET are mainly performed in a research setting to evaluate new treatment modalities for VVA, such as vaginal laser therapy. This study further supports the use of noninvasive FD measurements to replace these invasive, histological measurements of ET. Although we have now demonstrated that FD measurements underestimate the mean ET, our previous study demonstrated that significant changes in FD after treatment could be measured. This suggests that not only the mean ET increases after treatment, but that the thinnest measure of ET increases as well. It should, however, be noted that the true increase of (mean) ET might be more significant than is measured with FD.

To perform a more complete and even more reliable assessment of the vaginal wall, FD can be combined with assessment of the vaginal angioarchitecture (ie, structure and layout of vascular network). In a previous study, we demonstrated that an altered angioarchitecture is observed in women with VVA (22). In these participants, we observed a loss of capillary loops, and appearance of a vascular network. We also demonstrated that estrogen has the potential to restore these alterations. When combining FD measurements and assessment of angioarchitecture, a more complete assessment of the vaginal wall can be performed. We argue that treatment for VVA should not only increase ET, but also improve vaginal angioarchitecture.

We suggest that CytoCam-IDF imaging can be used in research as well as in clinical practice. For a broader application in clinical practice, the costs and cost-effectiveness of this method would have to be analysed. The relatively expensive one-time purchase of a CytoCam system would have to be balanced against the advantages of this method, such as direct and accurate diagnosis of VVA. This could be a subject of future research.

CONCLUSIONS

Focal depth measurements can be used as an accurate and noninvasive measure of epithelial thickness. Focal depth measurements reflect the thinnest measure of the epithelium within an individual.

Acknowledgments

We thank Robert Evers for his assistance in sample preparation, staining, and sectioning.

REFERENCES

1. Dennerstein L, Dudley EC, Hopper JL, Guthrie JR, Burger HG. A prospective population-based study of menopausal symptoms. Obstetrics and gynecology. 2000;96(3):351-8.
2. Nappi RE, Kokot-Kierepa M. Women's voices in the menopause: results from an international survey on vaginal atrophy. Maturitas. 2010;67(3):233-8.
3. Bachmann GA, Nevadunsky NS. Diagnosis and treatment of atrophic vaginitis. American family physician. 2000;61(10):3090-6.
4. Nilsson K, Risberg B, Heimer G. The vaginal epithelium in the postmenopause--cytology, histology and pH as methods of assessment. Maturitas. 1995;21(1):51-6.
5. Weber MA, Diedrich CM, Ince C, Roovers JP. Focal depth measurements of the vaginal wall: a new method to noninvasively quantify vaginal wall thickness in the diagnosis and treatment of vaginal atrophy. Menopause (New York, NY). 2016;23(8):833-8.
6. Felding C, Mikkelsen AL, Clausen HV, Loft A, Larsen LG. Preoperative treatment with oestradiol in women scheduled for vaginal operation for genital prolapse. A randomised, double-blind trial. Maturitas. 1992;15(3):241-9.
7. Krause M, Wheeler TL, 2nd, Snyder TE, Richter HE. Local Effects of Vaginally Administered Estrogen Therapy: A Review. Journal of pelvic medicine & surgery. 2009;15(3):105-14.
8. Arunkalaivanan A, Kaur H, Onuma O. Laser therapy as a treatment modality for genitourinary syndrome of menopause: a critical appraisal of evidence. International urogynecology journal. 2017;28(5):681-5.
9. Aykut G, Veenstra G, Scorcella C, Ince C, Boerma C. Cytocam-IDF (incident dark field illumination) imaging for bedside monitoring of the microcirculation. Intensive care medicine experimental. 2015;3(1):40.
10. Weber MA, Milstein DM, Ince C, Oude Rengerink K, Roovers JP. Vaginal microcirculation: Non-invasive anatomical examination of the micro-vessel architecture, tortuosity and capillary density. Neurourology and urodynamics. 2015;34(8):723-9.
11. Weber MA, Milstein DM, Ince C, Roovers JP. Is pelvic organ prolapse associated with altered microcirculation of the vaginal wall? Neurourology and urodynamics. 2016;35(7):764-70.
12. Collins TJ. ImageJ for microscopy. BioTechniques. 2007;43(1 Suppl):25-30.
13. Mukaka MM. Statistics corner: A guide to appropriate use of correlation coefficient in medical research. Malawi medical journal : the journal of Medical Association of Malawi. 2012;24(3):69-71.
14. Bland JM, Altman DG. Statistical methods for assessing agreement between two methods of clinical measurement. Lancet. 1986;1(8476):307-10.
15. Kerkhof MH, Ruiz-Zapata AM, Bril H, Bleeker MC, Belien JA, Stoop R, et al. Changes in tissue composition of the vaginal wall of premenopausal women with prolapse. American journal of obstetrics and gynecology. 2014;210(2):168.e1-9.

16. Boonstra H, Oosterhuis JW, Oosterhuis AM, Fleuren GJJVAA. Cervical tissue shrinkage by formaldehyde fixation, paraffin wax embedding, section cutting and mounting. 1983;402(2):195-201.
17. Vent J, Zimmermann C, Drebber U, Wedemeyer I, Eckel HE, Huettenbrink KB, et al. Influence of formalin fixation on tissue dimensions in palatal tonsils. Pathology, research and practice. 2014;210(1):59-61.
18. Holda MK, Klimek-Piotrowska W, Koziej M, Piatek K, Holda J. Influence of different fixation protocols on the preservation and dimensions of cardiac tissue. Journal of anatomy. 2016;229(2):334-40.
19. De Landsheere L, Munaut C, Nusgens B, Maillard C, Rubod C, Nisolle M, et al. Histology of the vaginal wall in women with pelvic organ prolapse: a literature review. International urogynecology journal. 2013;24(12):2011-20.
20. Mac Bride MB, Rhodes DJ, Shuster LT. Vulvovaginal Atrophy. Mayo Clinic Proceedings. 2010;85(1):87-94.
21. Hoyle CH, Stones RW, Robson T, Whitley K, Burnstock G. Innervation of vasculature and microvasculature of the human vagina by NOS and neuropeptide-containing nerves. Journal of anatomy. 1996;188 (Pt 3):633-44.
22. Diedrich CM, Kastelein AW, Verri F, Weber MA, Ince C, Roovers JPWR. Effects of topical estrogen therapy on the vaginal microcirculation in women with vulvovaginal atrophy. Neurourology and urodynamics. 2019.

4 Effects of topical estrogen therapy on the vaginal microcirculation in women with vulvovaginal atrophy

CM Diedrich
AW Kastelein
F Verri
MA Weber
C Ince
JPWR Roovers

Neurourol Urodyn. 2019 Jun;38(5):1298-1304.

ABSTRACT

Aims

This study aims to assess vaginal wall angioarchitecture and function in women with vulvovaginal atrophy (VVA) and determine the effect of topical estrogen on the vaginal microcirculation.

Materials and Methods

In this prospective observational study, incident dark field imaging was used to assess the vaginal microcirculation. In patients with VVA, measurements were performed before and after treatment with topical estrogen and compared to measurements performed in women without VVA. Vaginal angioarchitecture was studied by assessing microcirculatory architecture and capillary tortuosity scores at four regions of the vaginal wall. In addition, the capillary density and microvascular flow index (MFI) were obtained.

Results

Seventeen women were included in this study. Of these, eight women were diagnosed with VVA and nine women were considered healthy controls. Significant differences were observed between groups with regard to microcirculatory architecture scores. The architecture of the microvasculature in women with VVA was characterized by the appearance of a vascular network without capillary loops, whereas an array of capillary loops was predominantly seen in women without VVA. After estrogen treatment, no difference in architecture scores between patients and healthy controls was observed. Capillary tortuosity, capillary density, and MFI were similar in both groups before and after estrogen treatment.

Conclusions

The architecture of vaginal microvasculature is altered in patients with VVA. In case of similar vascular architecture, capillary tortuosity and density seem to be comparable. Treatment with topical estrogen results in restoration of the angioarchitecture.

INTRODUCTION

Vulvovaginal atrophy (VVA) is a common condition in postmenopausal women. The prevalence of VVA dramatically increases during the menopausal transition, whereas most postmenopausal women suffer from their associated symptoms (1). As a consequence of vaginal discomfort and pain, VVA has a significant impact on daily activity, sexual function, and overall quality of life (2). VVA is characterized by dryness, erythema, and petechiae of the vaginal wall and is associated with a thin and pale epithelium resulting from low estrogen levels specific for menopause (3).

It is well known that vaginal estrogen therapy is efficacious in treating symptoms of VVA (4). Therapy with estrogen thickens the epithelium, decreases vaginal dryness, and seems to optimize vaginal blood flow (5). Since sufficient estrogen levels support the proliferation of vascular and nonvascular smooth muscle cells in the subepithelial layers of the vagina, estrogen is considered to affect vaginal wall perfusion and oxygenation (6). The actual perfusion of vaginal tissue and the exchange of nutrients and gases (ie, O2 and CO2) between the intravascular space and the vaginal tissue occurs at the level of the microcirculation (ie, in the capillaries). Therefore, the capillary vessel bed should be considered essential for a healthy vaginal environment (7).

To what extent VVA affects the vaginal microcirculation is not well objectified, and it is unknown whether treatment with vaginal estrogen results in changes to the microcirculation. Therefore, assessment of the vaginal microcirculation before and after estrogen treatment can improve understanding of the working mechanism of vaginal estrogen therapy.

With the use of handheld microscopy imaging, human microcirculation can be assessed in great detail (8). This imaging technique has been used to assess the microcirculatory status of different human organ surfaces (9-11). Incident dark field (IDF) imaging was used to assess the vaginal microcirculation in healthy subjects (12) and in patients with prolapse (13). IDF imaging uses high-brightness green LEDs. The emitted green light is absorbed by hemoglobin in the red blood cell, allowing visualization of the microcirculation (8). In another study, the same authors demonstrated that topical estrogen therapy results in thickening of the epithelial layer and that it could be assessed noninvasively with IDF imaging (14).

It is hypothesized that topical estrogen therapy has an effect on the vaginal microcirculation in women with VVA: therapy possibly changes the angioarchitecture and quantity of capillaries, thereby improving the diffusion and convection of oxygen to the vaginal tissue. To test these hypotheses, this study compares the microcirculation between women with and without VVA and objectifies the effects of topical estrogen on the vaginal microcirculation.

MATERIALS AND METHODS

Participants and settings

We performed a prospective, single-center observational study at the outpatient clinic of the Department of Obstetrics and Gynecology of a University Medical Center. Women enrolled in this study received a full explanation of the study guidelines and procedures. Written informed consent was obtained from each participant.

Postmenopausal women that were meant to receive treatment with topical estrogen for VVA were recruited. Synapause-E3 ovules 0.5 mg were self-administered at home daily for 2 weeks followed by two times per week for at least 4 consecutive weeks. Medical history was obtained and women with cardiovascular (eg, angina pectoris, uncontrolled hypertension), inflammatory (eg, rheumatoid arthritis, eczema), other systemic illness (eg, inadequately controlled [non-] insulin-dependent diabetes mellitus) or those taking medication (eg, anticoagulants, anti-inflammatory, or immunosuppressive agents) that could affect the microcirculation were excluded from participation. Women with a history of vaginal surgery were also excluded, because of its uncertainty to what extent vaginal surgery affects the vaginal microcirculation.

VVA was diagnosed based on the following three characteristics: (1) the presence of a most bothersome symptom involving at least one of the following symptoms: vaginal dryness, vaginal itching or irritation, dyspareunia (15); (2) the presence of one or more of the following signs at physical examination: vaginal wall pallor and petechiae, friability of the vaginal wall (defined as any bleeding occurring during examination), conization (markedly decreased elasticity), or the absence of rugae (16); and (3) a vaginal pH of at least 5.5 (17). pH was measured using a pH strip with a pH range of 3.8 to 5.5 with intervals of 0.3 (Dosatest; Prolabo; VWR International, Leuven, Belgium).

The control group consisted of women aged 40 years or older with no signs or symptoms of VVA, attending the outpatient clinic because of bothersome pelvic floor symptoms and no previous history of vaginal surgery or use of topical estrogen.

Microcirculation imaging

The vaginal microcirculatory assessment was performed using IDF imaging (Cytocam; Braedius Medical, Huizen, the Netherlands). This technique has been described in detail previously (8). In summary, IDF imaging contains high-brightness LEDs with a very short illumination pulse time of 2 ms. Greenlight is absorbed by hemoglobin in the red blood cell, allowing visualization of the microcirculation. The device is a lightweight (120 g) and pen-like instrument (length 220 mm, diameter 23 mm). The combination of factor 4 optical magnification and a large sensor image area provides a field of view of 1.55 × 1.16 mm, which equates 1.80 mm2. The optical system provides an optical resolution of more than 300 lines/mm. The camera is connected to a device controller on a computer that is used for image storage and off-line analysis.

Microcirculatory examination and data acquisition procedure

Participants were examined in a gynecological chair in a stable 45° semi-reclined position in a room kept at a constant temperature. An experienced researcher, skilled in measuring the vaginal microcirculation, conducted all measurements. The CytoCam was placed into contact with the vaginal wall at exactly 3 cm above the hymen. The pressure of the device on the vaginal wall was avoided to prevent pressure-induced flow-artifacts, and the CytoCam was adjusted for optimal focus and contrast. The anterior, posterior, and lateral vaginal walls were measured to calculate a general vaginal measurement. All measurements were stored as video clips which were directly saved as digital AVI-DV files to a hard drive. Videos were blinded and anonymized so that the observer was not aware of the intervention and time point. Image assessment was performed in a random fashion.

Quality score assessment

Each video clip was assessed through a scoring system based on six parameters (illumination, focus, content, stability, pressure, duration); failure to meet a parameter disqualified a video clip from the analysis (18).

Tissue angioarchitecture

This scoring system allows for classification of subepithelial vascular patterns (12, 13). Microvascular architecture scores from each measurement site were examined and systematically classified with a score of 1, 2, or 3. Score 1, defines the appearance of an array of capillary loops; in score 2, both capillary loops and vascular network are visible, and score 3, is defined by the appearance of a vascular network with a complete absence of capillary loops. The overall microcirculatory architecture score per anatomical region per subject was determined by selecting the most frequently observed architecture score in the available frames.

Capillary tortuosity score

Additional description of the microvasculature is the capillary tortuosity (number of twists per capillary). Capillary tortuosity is a microvascular feature which has previously been associated with chronic disease (19). A frame was judged suitable for assessment if capillary loops and the presence or absence of twists could be clearly identified. Capillary tortuosity was classified as score 0: no twists (or pinhead capillaries) to 4: four or more twists (12). The overall tortuosity score per anatomical region per subject was determined by selecting the most frequently observed tortuosity score in the available frames.

Assessment of capillary density

Assessment of the capillary density was performed by counting the number of capillary loops per visual field from the video clips from each of the four anatomical regions. The capillary density obtained from one isolated image frame expressed as the median number of capillary loops per square millimeter (cpll/mm2), was used to quantify the vaginal microcirculation at each of the associated vaginal wall regions. Each image frame provides a field of view of 1.55×1.16 mm, which equates 1.80 mm2. Capillary density was assessed in each frame where capillary loops could be clearly identified and calculated by counting the number of capillary loops per field of view area and divided by 1.80 to obtain a unit cpll/mm2.

Microvascular flow index

Microvascular flow characteristics were assessed using the microvascular flow index (MFI). This score was previously developed and tested for reproducibility by Boerma et al (20) and is based on the determination of the predominant type of flow in four quadrants. Flow is characterized as absent (0), intermittent (1), sluggish (2), or continuous

(normal) (3). The MFI score per region was calculated by averaging the MFI scores over four quadrants per frame per region.

Statistical analysis

The aim of the analysis was (1) to compare microcirculatory parameters between women with and without VVA, and (2) to compare microcirculatory parameters in women before and after treatment with topical estrogen. Significant differences were found in a previous study on this topic using a small sample size (14), therefore, this study used the same sample size. Descriptive statistics were used to present the demographic variables. Non-normally distributed data are presented as medians with interquartile ranges. Normally distributed data are presented as means and standard deviations. For differences between the two groups in tissue microcirculatory architecture and capillary tortuosity scores, the $\chi 2$ test was used. Capillary density was compared between groups using the Mann–Whitney U test for non-normal distribution. A two-sided $P < 0.05$ was considered statistically significant. All data were analyzed using SPSS, version 23.0 for Windows (IBM Corp, Armonk, NY).

Ethical approval

This study was approved by the Medical Ethics Committee of the Amsterdam UMC.

RESULTS

Participants

A total of 17 women were included in this study. Of these women, 8 women were diagnosed with VVA (median age 65 years; interquartile range [IQR] 56-74 years) and 9 women were considered healthy controls (median age 49 years; IQR 45-59). Women in both groups were comparable with regard to parity (VVA median 2 [range 1-3] vs without VVA 2 [range 1-3]). In the control group, women had no signs or symptoms of VVA and visited the clinic because of an abnormal pap smear (n = 2), urinary incontinence (n = 4), recurrent urinary tract infections (n = 1), and/or pelvic organ prolapse (n = 4). A few patients did not undergo the second measurement in the VVA group (n = 1) and control group (n = 2).

Physical examination

Before treatment, there was a statistically significant difference between the median vaginal pH in the VVA and healthy control group (5.5 vs 5.1, respectively; $P < 0.01$). pH of the VVA group did change from 5.5 to 5.0, however, this results was not significant ($P = 0.07$). No significant difference was found in the control group over time (5.1 vs 5.2; $P = 0.32$). Clinical signs of VVA (eg, vaginal wall pallor and petechiae, friability of the vaginal wall, conization, or the absence of rugae) improved in six out of seven patients in the VVA group.

Tissue angioarchitecture

Vaginal angioarchitecture differed significantly between women with and without VVA (Table 1). In women with VVA, a score 3 was predominantly seen (Figure 1A), whereas a score 1 architecture was predominantly seen in healthy controls (Figure 1B). After treatment with estrogen, a significant change in architecture score was observed, resulting in angioarchitecture that was comparable to the angioarchitecture seen in the control group (Table 1).

Table 1. Microcirculatory architecture scores of patients and controls at both time points.

	Microcirculatory architecture score at baseline (t=0)			Microcirculatory architecture score, 2nd measurement (t=1)		
	Patients (n=8)	**Control (n=9)**	***P*-value***	**Patients (n=7)**	**Control (n=7)**	***P-value****
Anterior						
Score 1	2 (25%)	8 (89%)	**0.02**	6 (86%)	7 (100%)	0.30
Score 2	4 (50%)	0 (0%)		1 (14%)	0 (0%)	
Score 3	2 (25%)	1 (11%)		0 (0%)	0 (0%)	
Left						
Score 1	2 (25%)	8 (89%)	**0.02**	4 (57%)	3 (43%)	0.84
Score 2	2 (25%)	1 (11%)		2 (29%)	3 (43%)	
Score 3	4 (50%)	0 (0%)		1 (14%)	1 (14%)	
Posterior						
Score 1	2 (25%)	7 (78%)	0.07	5 (71%)	4 (57%)	0.58
Score 2	4 (50%)	2 (22%)		2 (29%)	3 (43%)	
Score 3	2 (25%)	0 (0%)		0 (0%)	0 (0%)	
Right						
Score 1	2 (25%)	6 (67%)	0.08	2 (33%)**	6 (86%)	0.08
Score 2	3 (37.5%)	3 (33%)		3 (50%)	0 (0%)	
Score 3	3 (37.5%)	0 (0%)		1 (17%)	1 (14%)	

Score 1: appearance of an array of capillary loops; Score 2: both capillary loops and vascular network are visible, and Score 3: appearance of a vascular network, absence of capillary loops. Values are number (percentage).
Bold values <0.05 are considered statistically significant.
* The $\chi 2$ test.
** Only six measurements, clips from one patient were extracted because of a low-quality score

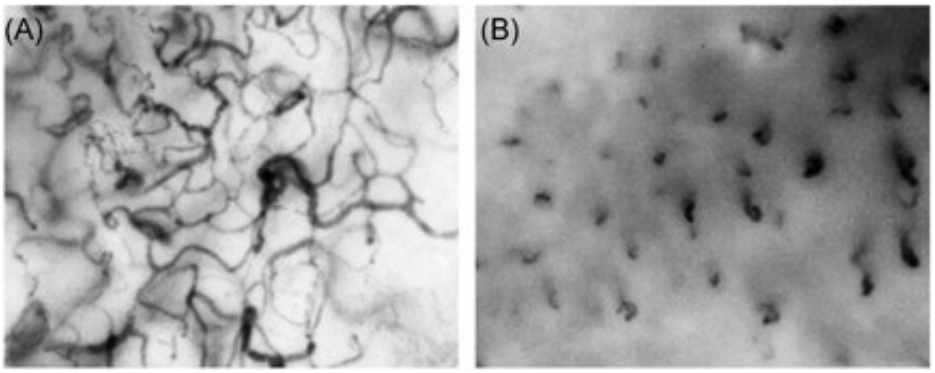

Figure 1. Incident dark-field illumination images of the vaginal microcirculation.
A, Architecture score 3 (appearance of the vascular network without capillary loops) seen in vulvovaginal atrophy. B, Architecture score 1 (appearance of an array of capillary loops) seen in healthy controls.

Capillary tortuosity score

Capillary tortuosity score was assessed in all frames except for frames with hardly identifiable capillary loops and mainly the appearance of the underlying vascular network (architecture score 3). Capillary tortuosity scores were similar in both groups before and after treatment with estrogen. Score 1 and 2, illustrating one or two capillary loop twists subsequently, were most frequently found (Tables S1 and S2).

Assessment of capillary density

Assessment of capillary density was performed on all frames including an array of capillary looks, architecture score 1. Capillary density was similar during the first measurement for all anatomical regions (anterior vaginal wall VVA 16.2 cpll/mm2 [13.2-17.3] vs control 12.8 cpll/mm2 [11.4-15.1]; P = 0.20). Also after treatment with estrogen, no significant differences were seen in capillary density between the two sites for all anatomical regions (anterior vaginal wall VVA 12.4 cpll/mm2 [11.4-15.8] vs control 13.3 cpll/mm2 [12.1-17.2]; P = 0.93) (Table S1).

Microvascular flow index

All patients and controls had at both time point an MFI score of 3.0 [confidence interval, 3.0 to 3.0] corresponding to continuous flow.

DISCUSSION

This is the first study to report on the effects of VVA and topical estrogen therapy on the architecture of vaginal microcirculation using an in vivo noninvasive technique. Our results demonstrate that in women with VVA, angioarchitecture in the subepithelial layer of the vagina is altered. Treatment with estrogen has a distinct effect on the architecture of the vaginal microcirculation and has the potential to reverse the vascular alterations observed in VVA to normal angioarchitecture as observed in women without VVA.

Four layers characterize vaginal tissue: the epithelium, the lamina propria, a muscularis layer, and the adventitia (21). The epithelial layer is not directly vascularized but receives nutrients and oxygen via capillary loops and diffusion from the vascular network beneath, located in the lamina propria. In this case, IDF imaging shows a thick epithelial layer and a lamina propria with a pattern of capillary loops (architecture score 1), without a visible background of the vascular network. However, in women with VVA, a significantly higher degree of architecture scores 2 and 3 were observed at baseline: a vascular network without capillary loops. After treatment with estrogen, a score 1 architecture was also predominant in the VVA group. This is graphically illustrated in Figure 2.

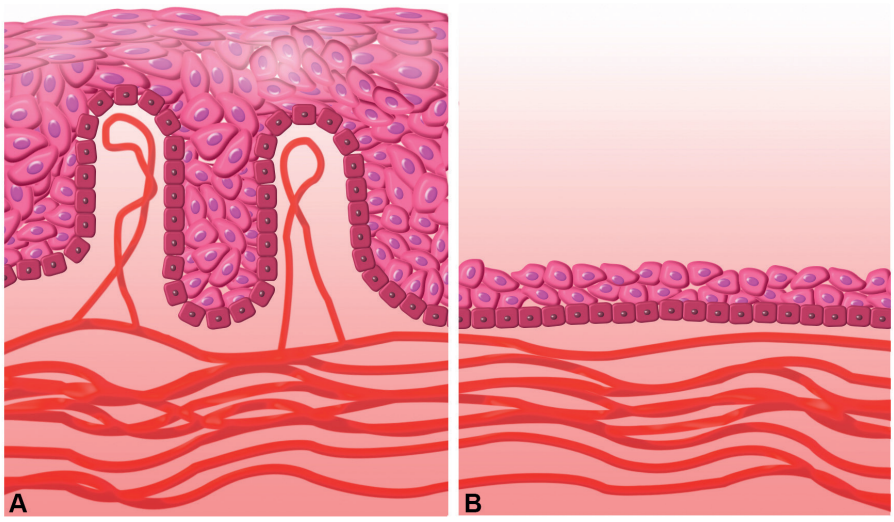

Figure 2. A, Illustration of healthy vaginal tissue with a dense epithelial layer including crypts and capillary loops originating from the vascular network (architecture score 1). B, Illustration of atrophic vaginal tissue, a thin layer of epithelium with loss of crypts and capillary loops, residual vascular network visible (architecture score 3).

It is unknown why a hypoestrogenic state alters vaginal vasculature. The altered angioarchitecture could be an effect of a thinner epithelium and loss of crypts, for which delivery of oxygen and nutrients through capillary loops is no longer necessary. However, since estrogen regulates the growth and function of vascular and nonvascular smooth muscle cells in the subepithelial layers in the vagina (22), another explanation could be that the lack of estrogen has a direct negative effect on the vaginal vasculature. The absence of capillary loops in the vaginal microcirculation can have clinical consequences. Capillary loops are also present in the skin, where this form of vascularization is considered to be better resistant against trauma, and protects the larger vessel bed beneath and facilitates thermal regulation by constriction and dilation of the capillary loops (23). Similar features can possibly be attributed to the vaginal epithelium with capillary loops. Among other functions, capillary loops could play a role in vaginal lubrication under the mediation of endothelial nitric oxide synthases and a hypoestrogenic state (24). Hypothetically, a microvasculature without capillary loops can also cause vaginal dryness with itching or irritation as result.

Analysis of the capillary density and microvascular flow showed no statistically significant differences between patients and controls, neither before nor after treatment. Capillary density and flow are both parameters for tissue perfusion, which depends on the number and distribution of the capillaries in combination with blood viscosity and pressure. The two main hemodynamic principles that determine oxygen supply to tissue are convection and diffusion. Convection is quantified by flow, whilst diffusion is normally quantified by the density of the perfused microvessels. However, it can be argued if this also applies to the vagina, where angioarchitecture might be a more important factor facilitating oxygen diffusion rather than a high density of the microvessels. In addition, we analyzed capillary tortuosity. This morphologic characteristic has been associated with pathology such as diabetes, but its biological explanation is currently unknown (19). We observed no differences in tortuosity scores between groups, and these scores were comparable to nondiabetic patients. Future research should be focused on the relationship between the qualitative aspect of microvessels and their ability to deliver oxygen to the cells.

Potential limitations of this study need to be addressed. First of all, although the CytoCam has the largest field of view among existing handheld video microscopes, its field of view is still relatively small (1.55 × 1.16 mm). Therefore, it can be debated if the imaged area is an adequate representation of the entire vaginal wall or vaginal canal. In a future study, it could be interesting to more extensively map microvascular changes throughout the

vagina in patients with VVA. A thorough mapping could also provide information on the course of VVA and how and when it affects the microcirculation in different parts of the vagina. Secondly, the assessment of the vaginal vessel density is challenging with analysis programs that are currently available (eg, automated vascular analysis). Such programs can calculate total vessel densities, but not when capillary loops are present. Therefore, it is not possible to use these programs for analysis of vaginal images, and it is impossible to compare density parameters between different architecture scores. In this study, we calculated capillary density by manually counting loops per field of view in architecture score 1 and 2 dominant tissue (as was validated by Weber et al (12)). Unfortunately, with this method, capillary density cannot be calculated in architecture score 2 and 3 tissue, since capillary loops were limited to absent. This limits the report on vaginal capillary density. Thirdly, since this is the first study on this topic, no data from previous studies were available. Consequently, we could not perform a power calculation. Therefore, we should be cautious to generalize these findings, which were observed in a relatively small patient population.

CONCLUSIONS

The architecture of the vaginal microvasculature is altered in women with VVA. In case of similar vascular architecture, capillary tortuosity, and density seem to be comparable. Treatment with topical estrogen results in restoration of the vaginal angioarchitecture. From other studies we have learned that vaginal estrogen therapy improves the quality of the vaginal epithelium, and apparently, qualitative aspects of the microcirculation play an important role as well. Future research should be focused on how to preserve the quality of the microcirculation in women who are exposed to events like aging, vaginal delivery, and pelvic floor surgery.

SUPPLEMENTARY MATERIAL

Supplementary table 1A. Microcirculatory tortuosity scores and capillary density of patients and controls at baseline (T0).

	Patient	**Control**	***P*-value**
Anterior			
*Tortuosity**	n=6	n=8	0.20***
Score 0	0 (0)	0 (0)	
Score 1	5 (83)	4 (50)	
Score 2	1 (17)	4 (50)	
Score 3	0 (0)	0 (0)	
Score 4	0 (0)	0 (0)	
*Capillary density (cpll/mm2)***	16.2 [13.2-17.3]	12.8 [11.4-15.1]	0.20****
Left lateral			
*Tortuosity**	n=6	n=9	0.30***
Score 0	0 (0)	1 (11)	
Score 1	5 (83)	6 (67)	
Score 2	0 (0)	2 (22)	
Score 3	0 (0)	0 (0)	
Score 4	1 (17)	0 (0)	
*Capillary density (cpll/mm2)***	13.6 [10.8-13.6]	13.3 [10.3-15.3]	0.73****
Posterior			
*Tortuosity**	n=7	n=9	0.65***
Score 0	0 (0)	0 (0)	
Score 1	5 (71)	6 (67)	
Score 2	2 (29)	2 (22)	
Score 3	0 (0)	1 (11)	
Score 4	0 (0)	0 (0)	
*Capillary density (cpll/mm2)***	13.1 [10.6-13.1]	11.1 [10.2-14.8]	0.83****
Right lateral			
*Tortuosity**	n=6	n=9	0.30***
Score 0	0 (0)	0 (0)	
Score 1	4 (67)	5 (56)	
Score 2	1 (17)	4 (44)	
Score 3	0 (0)	0 (0)	
Score 4	1 (17)	0 (0)	
*Capillary density (cpll/mm2)***	11.9 [11.7-11.9]	11.1 [9.1-15.0]	0.38****

Score 0: no twists; Score 1: 1 twist; Score 2: 2 twists; Score 3: 3 twists, and score 4: 4 or more twists. Tortuosity scores were calculated in patients showing architecture sore 1 and 2. Capillary density was calculated by counting the number of capillary loops per field of view area in all images with an array of capillary loops and divided by 1.80 (architecture score 1). Cpll/mm2= Capillary loops / mm2. * Values are number (percentage) ** Values are median [range] *** Chi-square test **** Mann–Whitney U test.

Supplementary table 1B. Microcirculatory tortuosity scores and capillary density of patients and controls at baseline (T1).

	Patient	**Control**	***P*-value**
Anterior			
*Tortuosity**	n=7	n=7	0.57***
Score 0	0 (0)	0 (0)	
Score 1	4 (57)	5 (71)	
Score 2	2 (29)	2 (29)	
Score 3	1 (14)	0 (0)	
Score 4	0 (0)	0 (0)	
*Capillary density (cpll/mm2)***	12.4 [11.4-15.8]	13.3 [12.1-17.2]	0.83****
Left lateral			
*Tortuosity**	n=7	n=7	0.60***
Score 0	0 (0)	0 (0)	
Score 1	2 (29)	3 (43)	
Score 2	4 (57)	2 (29)	
Score 3	1 (14)	1 (14)	
Score 4	0 (0)	1 (14)	
*Capillary density (cpll/mm2)***	12.9 [9.1-20.7]	15.7 [8.7-15.7]	0.72****
Posterior			
*Tortuosity**	n=7	n=7	1.00***
Score 0	0 (0)	0 (0)	
Score 1	2 (29)	2 (29)	
Score 2	4 (57)	4 (57)	
Score 3	1 (14)	1 (14)	
Score 4	0 (0)	0 (0)	
*Capillary density (cpll/mm2)***	10.6 [7.8-12.8]	13.5 [9.8-16.9]	0.09****
Right lateral			
*Tortuosity**	n=5	n=7	0.53***
Score 0	0 (0)	0 (0)	
Score 1	4 (80)	3 (43)	
Score 2	0 (0)	1 (14)	
Score 3	1 (20)	2 (29)	
Score 4	0 (0)	1 (14)	
*Capillary density (cpll/mm2)***	13.8 [10.0-20.1]	12.2 [9.8-16.8]	1.00****

Score 0: no twists; Score 1: 1 twist; Score 2: 2 twists; Score 3: 3 twists, and score 4: 4 or more twists. Tortuosity scores were calculated in patients showing architecture sore 1 and 2. Capillary density was calculated by counting the number of capillary loops per field of view area in all images with an array of capillary loops and divided by 1.80 (architecture score 1). Cpll/mm2= Capillary loops / mm2. * Values are number (percentage) ** Values are median [range] *** Chi-square test **** Mann–Whitney U test.

Supplementary table 2. Microcirculatory tortuosity scores were compared over time per site. No significant change was found over time in patients and controls.

Tortuosity	*Anterior* *T0 vs. T1*	*Left* *T0 vs. T1*	*Posterior* *T0 vs. T1*	*Right* *T0 vs. T1*
	P-value (Wilcoxon Signed Ranks Test)			
Patient	*P*=0.32	*P*=0.71	*P*=0.18	*P*=0.66
Control	*P*=0.32	*P*=0.14	*P*=0.26	*P*=0.19

REFERENCES

1. Dennerstein L, Dudley EC, Hopper JL, Guthrie JR, Burger HG. A prospective population-based study of menopausal symptoms. Obstetrics and gynecology. 2000;96(3):351-8.
2. Nappi RE, Kokot-Kierepa M. Women's voices in the menopause: results from an international survey on vaginal atrophy. Maturitas. 2010;67(3):233-8.
3. Pandit L, Ouslander JG. Postmenopausal vaginal atrophy and atrophic vaginitis. The American journal of the medical sciences. 1997;314(4):228-31.
4. Lethaby A, Ayeleke RO, Roberts H. Local oestrogen for vaginal atrophy in postmenopausal women. The Cochrane database of systematic reviews. 2016(8):Cd001500.
5. Bachmann G, Lobo RA, Gut R, Nachtigall L, Notelovitz M. Efficacy of low-dose estradiol vaginal tablets in the treatment of atrophic vaginitis: a randomized controlled trial. Obstetrics and gynecology. 2008;111(1):67-76.
6. Forsberg JG. A morphologist's approach to the vagina--age-related changes and estrogen sensitivity. Maturitas. 1995;22 Suppl:S7-s15.
7. Peters J, Mack GW, Lister G. The importance of the peripheral circulation in critical illnesses. Intensive Care Med. 2001;27(9):1446-58.
8. Aykut G, Veenstra G, Scorcella C, Ince C, Boerma C. Cytocam-IDF (incident dark field illumination) imaging for bedside monitoring of the microcirculation. Intensive care medicine experimental. 2015;3(1):40.
9. Puhl G, Schaser KD, Vollmar B, Menger MD, Settmacher U. Noninvasive in vivo analysis of the human hepatic microcirculation using orthogonal polorization spectral imaging. Transplantation. 2003;75(6):756-61.
10. Mathura KR, Bouma GJ, Ince C. Abnormal microcirculation in brain tumours during surgery. Lancet. 2001;358(9294):1698-9.
11. de Bruin AF, Kornmann VN, van der Sloot K, van Vugt JL, Gosselink MP, Smits A, et al. Sidestream dark field imaging of the serosal microcirculation during gastrointestinal surgery. Colorectal disease : the official journal of the Association of Coloproctology of Great Britain and Ireland. 2016;18(3):O103-10.
12. Weber MA, Milstein DM, Ince C, Oude Rengerink K, Roovers JP. Vaginal microcirculation: Non-invasive anatomical examination of the micro-vessel architecture, tortuosity and capillary density. Neurourology and urodynamics. 2015;34(8):723-9.
13. Weber MA, Milstein DM, Ince C, Roovers JP. Is pelvic organ prolapse associated with altered microcirculation of the vaginal wall? Neurourology and urodynamics. 2016;35(7):764-70.
14. Weber MA, Diedrich CM, Ince C, Roovers JP. Focal depth measurements of the vaginal wall: a new method to noninvasively quantify vaginal wall thickness in the diagnosis and treatment of vaginal atrophy. Menopause (New York, NY). 2016;23(8):833-8.

15. Ettinger B, Hait H, Reape KZ, Shu H. Measuring symptom relief in studies of vaginal and vulvar atrophy: the most bothersome symptom approach. Menopause (New York, NY). 2008;15(5):885-9.
16. Johnston SL, Farrell SA, Bouchard C, Farrell SA, Beckerson LA, Comeau M, et al. The detection and management of vaginal atrophy. Journal of obstetrics and gynaecology Canada : JOGC = Journal d'obstetrique et gynecologie du Canada : JOGC. 2004;26(5):503-15.
17. Nilsson K, Risberg B, Heimer G. The vaginal epithelium in the postmenopause--cytology, histology and pH as methods of assessment. Maturitas. 1995;21(1):51-6.
18. Massey MJ, Larochelle E, Najarro G, Karmacharla A, Arnold R, Trzeciak S, et al. The microcirculation image quality score: development and preliminary evaluation of a proposed approach to grading quality of image acquisition for bedside videomicroscopy. J Crit Care. 2013;28(6):913-7.
19. Djaberi R, Schuijf JD, de Koning EJ, Wijewickrama DC, Pereira AM, Smit JW, et al. Non-invasive assessment of microcirculation by sidestream dark field imaging as a marker of coronary artery disease in diabetes. Diab Vasc Dis Res. 2013;10(2):123-34.
20. Boerma EC, Mathura KR, van der Voort PH, Spronk PE, Ince C. Quantifying bedside-derived imaging of microcirculatory abnormalities in septic patients: a prospective validation study. Crit Care. 2005;9(6):R601-6.
21. Kerkhof MH, Ruiz-Zapata AM, Bril H, Bleeker MC, Belien JA, Stoop R, et al. Changes in tissue composition of the vaginal wall of premenopausal women with prolapse. American journal of obstetrics and gynecology. 2014;210(2):168.e1-9.
22. Bachmann GA, Leiblum SR. The impact of hormones on menopausal sexuality: a literature review. Menopause (New York, NY). 2004;11(1):120-30.
23. Landis EM. The Capillaries of the Skin11Paper read in part at the First Annual Meeting of the Society for Investigative Dermatology, Inc., New York City, April 30, 1938.: A Review. Journal of Investigative Dermatology. 1938;1(4):295-311.
24. Musicki B, Liu T, Lagoda GA, Bivalacqua TJ, Strong TD, Burnett AL. Endothelial nitric oxide synthase regulation in female genital tract structures. The journal of sexual medicine. 2009;6 Suppl 3:247-53.

5 The vaginal microcirculation after prolapse surgery

AW Kastelein
CM Diedrich
L de Waal
C Ince
JPWR Roovers

Neurourol Urodyn. 2020 Jan;39(1):331-338.

ABSTRACT

Aims

Oxygen plays a crucial role in wound healing after prolapse surgery. Trauma to the vaginal vasculature might limit the delivery of oxygen to the surgical wound, which may negatively affect wound healing and regeneration of connective tissue. This possibly increases the future risk of recurrence. We aimed to determine the effects of vaginal prolapse surgery on the microcirculation of the vaginal wall.

Methods

We evaluated the vaginal microcirculation in healthy participants without known vascular disease undergoing anterior and/or posterior colporrhaphy. We used incident dark-field imaging for in vivo assessment before and after (1 day, 2 weeks, and 6 weeks) surgery. We studied perfusion (microvascular flow index [MFI]), angioarchitecture (morphology/layout of microvessels) and capillary density.

Results

Ten women were included. Interindividual differences were observed 1 day postoperatively with regard to perfusion and angioarchitecture. Microvascular flow at the surgical site was absent or significantly reduced in some participants, whereas normal microvascular flow was observed in others (MFI range 0–3). Perfusion and angioarchitecture had been restored in all participants after 6 weeks (MFI range 2–3), regardless of the extent of vascular trauma 1 day postoperatively.

Conclusions

The difference in the extent of vascular trauma between women undergoing seemingly identical surgical procedures suggests that some individuals are more susceptible to vascular trauma than others. Delivery of oxygen to the wound and subsequent wound healing may be compromised in these cases, which could be related to the development of anatomical recurrence. Future studies should investigate whether there is a relationship between the vaginal microvasculature and the recurrence of prolapse.

Keywords: cystocele, microcirculation, microvasculature, native tissue repair, pelvic organ prolapse, rectocele, recurrence, vaginal surgery

INTRODUCTION

Pelvic organ prolapse (POP) is the descent of the pelvic organs to or beyond the vaginal walls (1). It is a common condition that can result in micturition symptoms, defecation symptoms, and sexual dysfunction (2). The lifetime risk for women to undergo surgery for POP is estimated to be as high as 10% (3). Reconstructive native tissue repair (NTR) is the most commonly performed surgical procedure but unfortunately, high recurrence rates of up to 50% are reported after NTR (4, 5). Procedures with a synthetic implant have been shown to be more effective, but are currently under scrutiny because the risk of serious adverse events (6-8). The high recurrence rates and lack of safe alternatives stress the need for improvement of NTR.

Vaginal wound healing may affect the outcome of NTR. Wound healing can be divided into four phases: hemostasis, inflammation, proliferation, and remodeling (9). Especially in the proliferative phase, collagen is deposited to re-establish tissue integrity and strength (9, 10). For effective wound healing, with optimal production of collagen, oxygenation of the wound at a cellular level is essential (11-13). The delivery of oxygen primarily depends on the capillaries of the microcirculation, and the delivery rate depends on the hemodynamic principles convection and diffusion (14). Convection is quantified by flow, and diffusion is quantified by the spatial arrangement of capillaries. In other words, the higher the capillary density and the more continuous the flow, the better the delivery of oxygen.

Therefore, a microcirculation postoperatively in which flow is suboptimal or even absent may compromise oxygenation of the wound resulting from NTR, which in turn would compromise wound healing, thereby increasing the risk of recurrent POP. The importance of the microvasculature in postoperative wound repair and wound dehiscence has also been described in other (pre)clinical studies (15-17).

It is currently unknown to what extent the vaginal microcirculation is damaged during surgery, and whether this damage is reversible. If we can accurately and quantitatively determine such vascular damage, it can be investigated whether there is a relationship between vascular trauma and the recurrence of POP. It would also allow comparison of vascular damage from different surgical techniques, and it could be investigated whether strategies aimed to improve angiogenesis (estrogen, vaginal laser therapy) can limit vascular damage, or enhance vascular restoration.

The vaginal microcirculation was studied previously with a handheld video microscope based on the incident dark field (IDF) imaging (18-21). This technique allows for reproducible, noninvasive and in vivo assessment of the vaginal microcirculation. In the present explorative pilot study, we assessed the vaginal microcirculation with IDF imaging before and after prolapse surgery. We aimed to determine if the microcirculation can be studied postoperatively, whether surgery affects microvascular perfusion and angioarchitecture and whether the vasculature can be restored to a presurgical level.

METHODS

An explorative pilot study was performed at the outpatient clinic of the Department of Obstetrics and Gynecology of a University Medical Center. The Institutional Review Board approved the study protocol under number METC 2014_137. The study was registered in a database for registration and publication of medical research involving human subjects under number NL49122.018.14.

Participants

Women undergoing primary anterior or posterior colporraphy because of prolapse POP-Q stage 2 or more in either the anterior and/or posterior compartment were eligible for participation. Women received verbal and written explanation of the study guidelines and procedures. Written informed consent was obtained from all participants. Baseline characteristics were obtained from the electronic patient records. Women were excluded when they suffered from cardiovascular diseases (eg, uncontrolled hypertension, angina pectoris), inflammatory diseases (eg, rheumatoid arthritis, eczema) or diabetes mellitus, because these conditions can affect the microcirculation. Also, women were excluded when they were taking medications that could affect the microcirculation such as anticoagulants, anti-inflammatory- or immunosuppressive agents.

Surgical procedures

All participants were operated under general anesthesia. Prolapse surgery was performed according to standardized surgical protocol. Hydrodissection with a saline solution with 1:200.000 adrenaline was performed in all participants, and running Vicryl 2.0 sutures were used for closure of the vaginal epithelium in all participants. All participants received a single administration of cefazoline/metronidazol and nadroparine per-operatively. A vaginal pack and indwelling catheter were given for the first 24 hours after surgery.

Incident dark-field imaging

Imaging of the microcirculation was performed with the CytoCam (Braedius Medical, Huizen, The Netherlands), which is a handheld video microscope on the IDF imaging (22). This technique was previously used for assessment of the vaginal microvasculature (18-20). It was also used to study other surgical procedures and wound healing (17). In short, IDF imaging enables visualization of the organ surface microcirculation by using epi-illumination. Greenlight is absorbed by hemoglobin in the red blood cells flowing in the microcirculation. Hereby, magnified moving images can be recorded, representing the space that these flowing red blood cells occupy and thus demonstrate the functional microcirculation. This technique is built into an easy-to-use device that is composed of aluminum and titanium, has the shape and size of a pen (length 220 mm, diameter 23 mm, weight 120 g) and is commercially available. The CytoCam is connected to a device controller, which in turn is connected to a laptop (P50, Lenovo, Peking, China) that is used for image storage and analysis.

Imaging procedures

The CytoCam was covered with a disposable cap and the tip of the camera was placed 3 cm above the hymen. The camera was adjusted for optimal focus and contrast, and measurements were recorded clockwise: starting from the midline of the anterior vaginal wall, left lateral, the midline of the posterior vaginal wall and right lateral. At each position, three 100-frame measurements were performed. Imaging 1 day postoperatively was performed at least 1 hour after removal of the vaginal tampon that was placed after surgery. On the operated vaginal wall (either the anterior or posterior wall) measurements were performed on the scar tissue, in the midline and up to 1 cm to the right and left of the scar, from 3 cm above the hymen to a maximum of 8 cm above the hymen. In total, twelve videos were recorded per patient per time point. The pressure of the device on the vaginal wall was avoided to prevent pressure artefacts (ie, disturbance of capillary flow). Participants were instructed to indicate if measurements were painful. Participants underwent measurements at different time points. Before the surgery (T0), 1 day postoperatively (T1), 2 weeks postoperatively (T2), and 6 weeks postoperatively (T3). Measurements were performed by two experienced investigators (AWK and CMD).

Quality score assessment

Each video clip was assessed through a scoring system based on six parameters (illumination, focus, content, stability, pressure, duration); failure to meet a parameter disqualified a video clip from the analysis.

Analysis of microcirculatory parameters

We analysed the parameters (a) microvascular flow index; (b) tissue angioarchitecture scores; and (c) capillary density. All parameters were validated in previous studies (18-21, 23). Scoring of the microcirculation was performed by one investigator who was blinded for the clinical data (LdW). Another investigator with extensive experience in scoring microcirculation (AWK) provided close supervision and was available as an independent arbiter when there was doubt during scoring. AWK also performed an additional analysis of 10% of the data, which demonstrated high agreement with the initial analysis by LdW. We qualitatively described the angioarchitecture that was observed at the surgical sites. All videos that could not be scored according to the normal tissue angioarchitecture scores, were discussed and described by at least two investigators.

Microvascular flow

The microvascular flow was assessed to determine perfusion. Flow characteristics were assessed using the MFI. The MFI was developed and validated by Boerma and coworkers and tested for reproducibility (23). This score is based on the determination of the predominant type of flow in four quadrants. This scoring system quantifies the microcirculatory perfusion as absent (0), intermittent (1), sluggish (2) or normal (3), providing an index for microcirculatory blood flow velocity. The MFI score per region was the score that occurred the most. When the MFI was 3 in all quadrants, this was considered a normally perfused microvasculature. Perfusion was reduced when the MFI was 1 or 2, and perfusion was absent when we observed an MFI of 0.

Tissue angioarchitecture

Tissue angioarchitecture is the morphology or lay-out of the vascular network. This scoring method was devised and validated to provide rapid recognition of subepithelial vascular patterns and showed a high agreement between observers in a previous study with complete agreement in 93% of frames and ICC between observers of 0.78.18 Three types of predefined sub-epithelial vascular patters may be recognized and classified with a score 1, 2, or 3 (18). In score 1 capillary loops are predominantly observed. This is considered to be the most favorable angioarchitecture score, which is most frequently seen in premenopausal women with a thicker vaginal epithelium (20). The capillary loops are necessary to supply the avascular epithelium with oxygen and nutrients. In score 2, capillary loops and vascular networks are both seen. In score 3, the vascular network without capillary loops is seen. Score 3 angioarchitercure is associated with a thin epithelium of the vaginal wall. Figure 1 shows these three types

of angioarchitecture. When the angioarchitecture did not meet one of these predefined patterns, we qualitatively described the angioarchitecture.

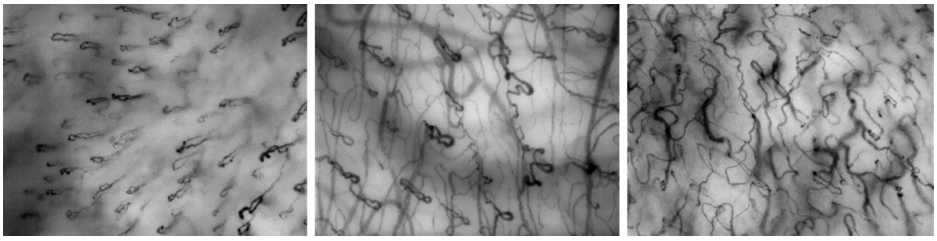

Figure 1. Screenshots of CytoCam videos with different types of angioarchitecture.
Each image represents an area of 1.55 × 1.16 mm. Left: angioarchitecture score 1. Middle: angioarchitecture score 2. Right: angioarchitecture score 3

Capillary density

When the vascularization was classified as a microvascular architecture score of 1 or 2 (ie, capillary loops were identifiable), the video was judged suitable for the assessment of capillary density. The capillary density was determined by counting the number of capillary loops per visual field and expressed as the mean number of capillary loops per square millimeter (cpll/mm2). The frame of each image was 1.55 mm × 1.16 mm, resulting in a total area of 1.8 mm^2. The capillary density score per region was calculated by averaging the frames and divided by 1.8 to obtain the unit cpll/mm2. Assessment of capillary density was performed in the same way in previous studies regarding the vaginal microcirculation (18-20).

Sample size calculation

We did not perform a sample size calculation. We determined a convenient sample of 10 participants suitable for this explorative pilot study where within-subject effects were studied. We also considered this small sample size to be sufficient based on the findings of a previous study in nine healthy female volunteers, where it was concluded that the vaginal microcirculation can be consistently and reliably measured in a small sample (18).

Statistical analysis

We compared baseline measurements with postoperative measurements to determine surgical trauma and restoration of vascularization. Descriptive statistics were used to present the demographic variables. Non-normally distributed data were presented as

medians with interquartile ranges. Normally distributed data were presented as means and standard deviations. Postoperative measurements (T1, T3) were compared to baseline measurements (T0) using a Wilcoxon signed-rank test for paired numerical data (capillary density) and McNemar test for paired categorical data (MFI and angioarchitecture). A $P \leq .05$ was considered to be statistically significant. All analyses were performed using the statistical software SPSS (IBM SPSS Statistics for Windows, Version 24.0).

RESULTS

Participants

Ten participants with a POP-Q stage ≥2 were included in this study. In these participants, there were 14 vaginal walls involved in the surgical procedures (9× anterior colporrhaphy, 5× posterior colporrhaphy). The mean age was 64 ± 7.5 years. All participants were Caucasian, parous and postmenopausal. Three participants used vaginal estrogens perioperatively, no participants were active smokers. No participants had known the vascular disease. It was feasible to perform IDF imaging with the CytoCam before and after surgery in all participants. In some participants, imaging 1 day postoperatively was complicated by excessive vaginal discharge or vaginal blood loss. Careful cleaning with a vaginal swab and repositioning of the CytoCam enabled correct imaging in all cases. The T2 measurement was only performed in four participants, mostly due to difficulties with the hospital visit in the postoperative recovery period. Therefore, we only report on the T0, T1, and T3 measurements, which were performed in all participants.

The microcirculation 1 day postoperatively

In 2 of 10 participants, remarkable changes were observed between the microcirculation at T0 and T1. In these cases, a severely altered angioarchitecture with a dilated and expanded vascular network was observed at the surgical site 1 day postoperatively (Figure 2). In these individuals, we were not able to identify risk factors that could be associated with this damage. These participants did not use vaginal estrogen, did not smoke and the surgical procedures were identical to the procedures performed in other participants. It concerned one anterior vaginal wall and one posterior vaginal wall. We also observed areas with expanded capillary loops (Figure 2). At these locations, the capillary flow was absent and individual erythrocytes could not be identified within the microvessels. In other participants, smaller areas with extravasation of erythrocytes were observed, often next to a normally perfused microcirculation with a normal angioarchitecture (score

1, 2 or 3) (Figure 3, left). In these participants, the microcirculation appeared normally perfused (MFI 3) at the surgical site, all the way up to the incision (Figure 3, right).

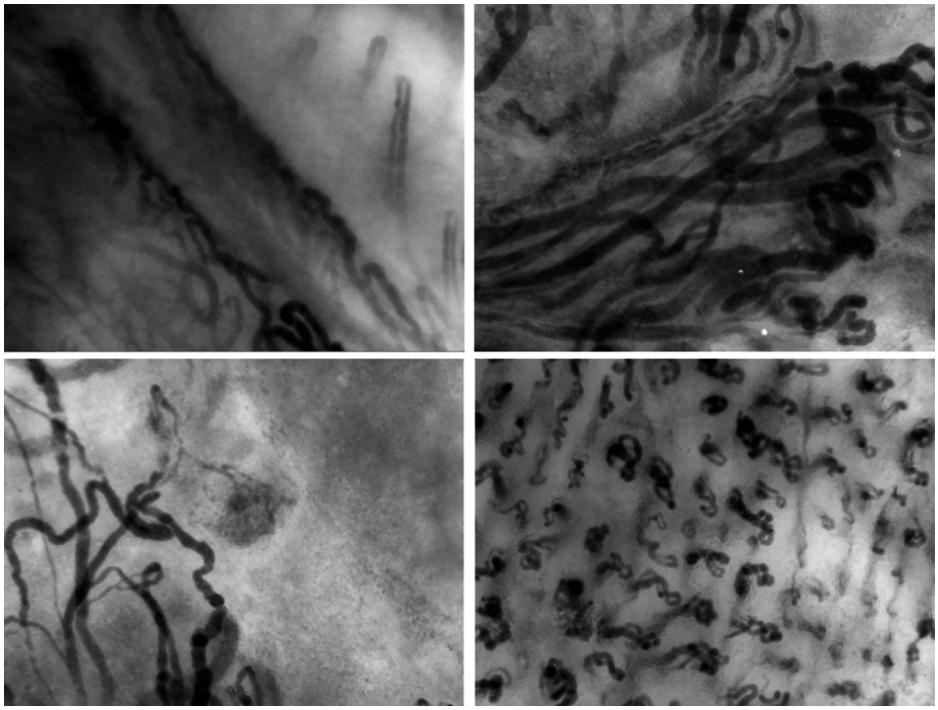

Figure 2. Screenshots of CytoCam videos, each image representing an area of 1.55 × 1.16 mm. A severely altered angioarchitecture with a dilated and expanded vascular network at the surgical site 1 day postoperatively. The capillary flow was absent and individual erythrocytes could not be discriminated. Bottom right: angioarchitecture type 1 with capillary loops can be distinguished, but the capillary loops are dilated and flow is absent.

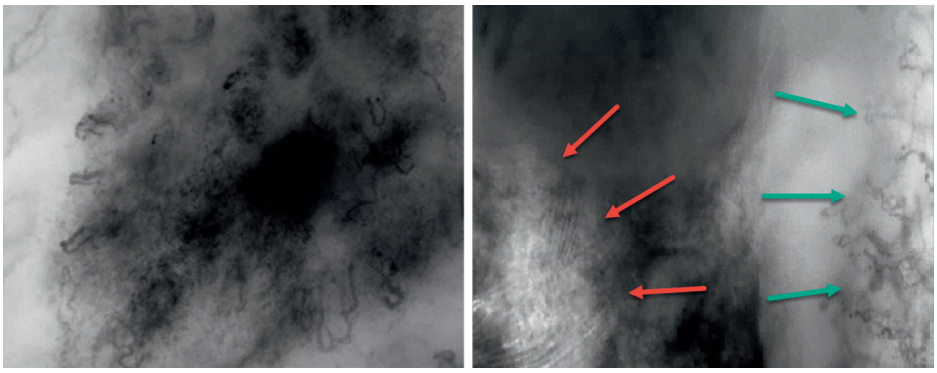

Figure 3. Screenshots of CytoCam videos. Each image represents an area of 1.55 × 1.16 mm. Left: areas with extravasation of erythrocytes are observed, imposing as a hematoma. The adjacent microcirculation was perfused normally. Right: video was taken at the surgical site one day postoperatively. Red arrows: suture (Vicryl 2.0) at the incision. Green arrows: normal flow (MFI 3) in the microcirculation and normal, type 2 angioarchitecture.

Analysis of microcirculatory parameters

Microvascular flow index

The microvascular flow index (MFI) demonstrated differences between individuals and locations. In some participants, the MFI at the surgical site at T1 was 0, illustrating the absence of capillary flow and no perfusion of the microvasculature. In others, the MFI at the surgical site at T1 was 3, illustrating normal capillary flow and a normally perfused microcirculation. Overall, the MFI at the surgical site 1 day postoperatively was significantly lower than before surgery (P = .03). Microvascular flow at the nonsurgical sites was unaffected in all participants. After 6 weeks, the MFI scores of the surgical sites were comparable to the pre-surgical MFI scores of the surgical sites.

Tissue angioarchitecture and capillary density

No differences were observed between T0, T1, and T3 regarding angioarchitecture scores (P = .22) and capillary density scores (P = .48). Surgery did not affect microvascular parameters of the nonsurgical sites in any of the participants.

DISCUSSION

Main findings

We demonstrated that vaginal angioarchitecture, microvascular perfusion, and recovery can be studied in vivo after prolapse surgery. We showed that prolapse surgery can have a significant effect on the vaginal microcirculation and that effects vastly differed between subjects. Regardless of the extent of the vascular changes observed 1 day postoperatively, quantitative and qualitative parameters had been restored to a pre-surgical level in all participants 6 weeks after surgery, suggesting the microvasculature of the vaginal wall has the significant regenerative capacity.

Interpretation of results

We have observed an altered angioarchitecture and an obvious reduction in vaginal wall microvascular flow in some participants 1 day postoperatively. The vascular damage may be the consequence of dissection and tissue handling during surgery, and the reduction in flow may be the consequence of intravascular coagulation and hemostasis to the incision. The interindividual differences in vascular damage are remarkable, since participants underwent seemingly identical surgical procedures. It could suggest that some individuals are more susceptible to vascular trauma than others. We were not able to identify specific risk factors in these participants that explain the vascular damage.

Because estrogen has vasoactive effects, it possibly also improves the resilience of the vaginal microcirculation, which makes vascular damage during surgery less likely to occur. All participants that were using vaginal estrogen (n = 3), had normal angioarchitecture and flow at T1. The sample size of the current study is however too small to draw conclusions from this, and it should be investigated in a larger patient sample whether vascular damage is less likely to occur in women using estrogen. Based on the aforementioned numbers, a study comparing an estrogen-exposed group to a nonestrogen group should have a sample of at least 40 participants to have an 80% chance of detecting a relevant decrease in alteration of angioarchitecture 1 day postoperatively.

The fact that no significant differences were observed when comparing microcirculatory parameters before and 6 weeks after surgery, suggests that the vaginal microcirculation has significant capacity to recover. Given the apparent regenerative capacity of the microcirculation, it can be argued that microvascular damage will be of limited effect

on surgical outcome, since the microcirculation was restored in all participants at 6 weeks. However, it can also be argued that a damaged microcirculation in the first days after the operation is in fact detrimental, since the synthesis of collagen has been shown to start 48 hours after surgery, and continues until day 7 (9, 10). Therefore, when the microcirculation is dysfunctional in the first week after surgery, the delivery of oxygen to the surgical wound could be limited. Consequently, the synthesis of collagen would be inhibited, leading to a weaker vaginal wall (11, 13). While this may not cause problems in an early stage, a weaker vaginal wall could be more prone to anatomical recurrence years later.

Clinical implications and future perspectives

This study demonstrated that IDF imaging can be used to study vaginal microcirculation after prolapse surgery. Therefore, it can be studied if there is a correlation between vascular damage and long term surgical outcome. Also, (novel) strategies that aim to improve the outcome of prolapse surgery by enhancing vascularization and oxygenation, can be evaluated. Future studies evaluating the effect of such therapies could include assessment of the microcirculation, as objective, noninvasive outcome measurement of vaginal surgery. Other future applications include microcirculatory assessment of (newly developed) vaginal implants, in which case angiogenesis can be studied as a key representative of scaffold integration (24). Also, a recent study demonstrated that IDF imaging can be used to study leukocyte recruitment and adhesion to the endothelium, as hallmarks of systemic inflammation (25). This is potentially interesting when the inflammatory response to vaginal implants is studied.

Strengths and limitations

The current study allowed us to noninvasively study the vaginal microcirculation perioperatively and in vivo. Limitations of this study include the small sample size, which allowed us to merely perform an explorative analysis. Larger sample size would be necessary to define the magnitude and clinical relevance of the observed changes in the microcirculation, and to identify which factors are predictors of these changes. Second, it was difficult for participants to come to the hospital 2 weeks after surgery, because of prescribed restrictions in activities, such as traveling and driving a car. Consequently, we did not study this data point. Third, the focal depth of the CytoCam is limited to 300 µm, indicating that imaging of the deeper, fibromuscular layers of the vaginal wall, is not optimal. Healing of these deeper layers is especially important in prolapse repair and prevention of recurrent POP. Unfortunately, to date, there are no alternative techniques

that allow imaging of the microvasculature in this detail of deeper layers. Nevertheless, we consider the status of the more superficial vasculature to be a representative of the vascularization of the deeper layers of the vaginal wall. Fourth, images with a severely altered angioarchitecture could not be assigned an angioarchitecture score and were therefore excluded from quantitative angioarchitecture analysis. Therefore, the overall angioarchitecture scores at T1 underestimate the true effect of surgery on angioarchitecture.

CONCLUSIONS

Incident dark-field imaging can be used to study vaginal microcirculation after prolapse surgery. Microvascular flow and angioarchitecture show interindividual differences after prolapse surgery, suggesting that some women are more susceptible to surgically-induced vascular trauma than others. Future studies should investigate whether there is a relationship between vascular damage and long term surgical outcome, and explore the potential of therapies such as vaginal estrogen therapy to decrease vascular damage during surgery.

REFERENCES

1. Jelovsek JE, Maher C, Barber MD. Pelvic organ prolapse. Lancet. 2007;369(9566):1027-38.
2. Fritel X, Varnoux N, Zins M, Breart G, Ringa V. Symptomatic pelvic organ prolapse at midlife, quality of life, and risk factors. Obstetrics and gynecology. 2009;113(3):609-16.
3. Olsen AL, Smith VJ, Bergstrom JO, Colling JC, Clark AL. Epidemiology of surgically managed pelvic organ prolapse and urinary incontinence. Obstetrics and gynecology. 1997;89(4):501-6.
4. Maher C, Feiner B, Baessler K, Schmid C. Surgical management of pelvic organ prolapse in women. The Cochrane database of systematic reviews. 2013(4):Cd004014.
5. Denman MA, Gregory WT, Boyles SH, Smith V, Edwards SR, Clark AL. Reoperation 10 years after surgically managed pelvic organ prolapse and urinary incontinence. American journal of obstetrics and gynecology. 2008;198(5):555.e1-5.
6. Altman D, Vayrynen T, Engh ME, Axelsen S, Falconer C. Anterior colporrhaphy versus transvaginal mesh for pelvic-organ prolapse. The New England journal of medicine. 2011;364(19):1826-36.
7. Maher C FB, Baessler K, Christmann-Schmid C, Haya N, Marjoribanks J. Transvaginal mesh or grafts compared with native tissue repair for vaginal prolapse. Cochrane Database of Systematic Reviews. 2016(2).
8. Dällenbach P. To mesh or not to mesh: a review of pelvic organ reconstructive surgery. International Journal of Women's Health. 2015;7:331-43.
9. Zhou S, Salisbury J, Preedy VR, Emery PW. Increased collagen synthesis rate during wound healing in muscle. PloS one. 2013;8(3):e58324.
10. Emery PW, Ghusain-Choueiri A. Effect of surgical trauma on muscle protein synthesis in the rat. The British journal of surgery. 1994;81(4):539-42.
11. Gottrup F. Oxygen in wound healing and infection. World journal of surgery. 2004;28(3):312-5.
12. Li J, Ollague Sierra J, Zhu L, Tang L, Rahill K, El-Sabawi B, et al. Effects of a topical aqueous oxygen emulsion on collagen deposition and angiogenesis in a porcine deep partial-thickness wound model. Experimental Dermatology. 2013;22(10):674-6.
13. Sen CK. Wound healing essentials: let there be oxygen. Wound repair and regeneration : official publication of the Wound Healing Society [and] the European Tissue Repair Society. 2009;17(1):1-18.
14. Jacob M, Chappell D, Becker BF. Regulation of blood flow and volume exchange across the microcirculation. Critical Care. 2016;20(1):319.
15. Kaner D, Zhao H, Terheyden H, Friedmann A. Improvement of microcirculation and wound healing in vertical ridge augmentation after pre-treatment with self-inflating soft tissue expanders - a randomized study in dogs. Clinical oral implants research. 2015;26(6):720-4.
16. Bentov I, Reed MJ. Anesthesia, microcirculation, and wound repair in aging. Anesthesiology. 2014;120(3):760-72.

17. Lindeboom JA, Mathura KR, Aartman IH, Kroon FH, Milstein DM, Ince C. Influence of the application of platelet-enriched plasma in oral mucosal wound healing. Clinical oral implants research. 2007;18(1):133-9.
18. Weber MA, Milstein DM, Ince C, Oude Rengerink K, Roovers JP. Vaginal microcirculation: Non-invasive anatomical examination of the micro-vessel architecture, tortuosity and capillary density. Neurourology and urodynamics. 2015;34(8):723-9.
19. Weber MA, Milstein DM, Ince C, Roovers JP. Is pelvic organ prolapse associated with altered microcirculation of the vaginal wall? Neurourology and urodynamics. 2016;35(7):764-70.
20. Diedrich CM, Kastelein AW, Verri F, Weber MA, Ince C, Roovers JPWR. Effects of topical estrogen therapy on the vaginal microcirculation in women with vulvovaginal atrophy. Neurourology and urodynamics. 2019.
21. Kastelein AW, Diedrich CM, Jansen C, Zwolsman SE, Ince C, Roovers JWR. Validation of noninvasive focal depth measurements to determine epithelial thickness of the vaginal wall. Menopause (New York, NY). 2019.
22. Aykut G, Veenstra G, Scorcella C, Ince C, Boerma C. Cytocam-IDF (incident dark field illumination) imaging for bedside monitoring of the microcirculation. Intensive care medicine experimental. 2015;3(1):40.
23. Boerma EC, Mathura KR, van der Voort PH, Spronk PE, Ince C. Quantifying bedside-derived imaging of microcirculatory abnormalities in septic patients: a prospective validation study. Crit Care. 2005;9(6):R601-6.
24. Shafaat S, Mangir N, Regureos SR, Chapple CR, MacNeil S. Demonstration of improved tissue integration and angiogenesis with an elastic, estradiol releasing polyurethane material designed for use in pelvic floor repair. Neurourology and urodynamics. 2018;37(2):716-25.
25. Uz Z, van Gulik TM, Aydemirli MD, Guerci P, Ince Y, Cuppen D, et al. Identification and quantification of human microcirculatory leukocytes using handheld video microscopes at the bedside. J Appl Physiol (1985). 2018;124(6):1550-7.

Part II

The peritoneal microcirculation

6 Embryology, anatomy, physiology and pathophysiology of the peritoneum and the peritoneal vasculature

AW Kastelein
LMC Vos
KH de Jong
JOAM van Baal
R Nieuwland
CJF van Noorden
JPWR Roovers
CAR Lok

Semin Cell Dev Biol. 2019 Aug;92:27-36.

ABSTRACT

The peritoneum is a large serous membrane with both epithelial and mesenchymal features, and is essential for maintaining an intra-abdominal homeostatic equilibrium. The peritoneum plays a central role in the pathogenesis of a number of disorders. Pathological processes affecting the peritoneum such as inflammation and carcinomatosis can have serious clinical consequences, but the pathophysiology of these conditions is poorly understood. Understanding peritoneal embryology, anatomy and physiology is crucial to comprehend pathophysiological mechanisms and to devise a new focus for research. The vascular response to pathological processes appears to be of considerable importance, since the peritoneal vasculature plays a pivotal role in most associated diseases. Therefore, this review summarizes currently available literature with special emphasis on the development, anatomy and function of the peritoneal vasculature. Pathological processes are described to illustrate physiological and pathophysiological characteristics of the peritoneum.

HIGHLIGHTS

- The peritoneum is an extensive serous membrane with both epithelial and mesenchymal features, essential for maintaining an intra-abdominal homeostatic equilibrium.
- The peritoneum covers the abdominal walls and all intra-abdominal structures, with exception of the bare area of the liver. Comprehension of the anatomy of the peritoneum and its reflections is essential for surgeons performing intra-abdominal surgery.
- The peritoneum and the peritoneal vasculature play a central role in many intra-abdominal conditions such as peritoneal adhesions, the production of ascites and peritoneal carcinomatosis.
- The peritoneal microcirculation is located in submesothelial stroma and is characterized by a relatively low vessel density, but this may alter under pathological conditions.
- Understanding of the interaction between cancer cells, the peritoneum and the peritoneal vasculature is crucial for the development of new treatment strategies for peritoneal carcinomatosis.

INTRODUCTION

The peritoneum is a large serous membrane, essential for maintaining an intra-abdominal homeostatic equilibrium. Peritoneal structure and function can be affected by the following pathological processes: 1) adhesion formation as a consequence of surgical trauma, inflammation (peritonitis) or endometriosis, which in turn complicates surgical interventions and can lead to abdominal symptoms and female infertility; 2) fibrosis due to inflammation or long-term peritoneal dialysis and that can decrease the peritoneal diffusion capacity; 3) gynecologic or gastro-intestinal malignancies that can cause peritoneal carcinomatosis, which in turn can lead to ascites and impaired bowel function. However, the pathophysiology of the above-mentioned processes is not well understood. Despite extensive research and proposed interventions, peritoneal adhesions and fibrosis cannot be adequately prevented or treated. Additionally, peritoneal susceptibility for metastases in patients with cancer is still an enigma, and the behavior of carcinoma cells on the peritoneal membrane remains largely unexplained. This stresses the need for new insights into peritoneal physiology and pathophysiology. In turn these may guide research and development of new treatment strategies. Understanding basic principles is a necessary first step. We previously reviewed the literature on the histophysiology and pathophysiology of the peritoneum (1). However, current knowledge on the peritoneal vasculature has not previously been reviewed, even though the vascular response to peritoneal pathology seems of considerable clinical importance. Therefore, this review summarizes currently available literature with special emphasis on the development, anatomy and function of the peritoneal vasculature.

EMBRYOLOGY

Embryology of the peritoneum

Embryonic development of the peritoneum starts during the gastrulation stage, at which point a 3-layered disc is formed and a layer of endoderm, ectoderm and mesoderm emerge (1-4). The mesodermal layer consists of cells that have an irregular shape with large intercellular spaces and no recognizable extracellular matrix. Around Carnegie Stage (CS) 9 (25 days development), mesodermal cells start to transform into cuboidally shaped cells. This causes the intercellular spaces to merge and form larger cavities. These cavities, the so-called coelomic vesicles, eventually consolidate to one coelomic cavity, lined with a layer of cuboidal mesodermal cells. The caudal part of the coelomic cavity

will give rise to the peritoneal cavity, and the layer of mesodermal cells will form the peritoneal membrane (Figure 1) (5, 6).

In later stages of the embryonic development, the shape of the embryo changes from a 2-dimensional embryonic disk to a 3-dimensional embryo (CS 10, 28 days development). In the cranial part of the embryonic coelomic cavity, the primitive pericardial region is formed first. From here, two extensions develop in a caudal direction: the pericardioperitoneal canals (Figure 1). These expanding canals connect to the extraembryonic coelomic cavity (chorionic cavity). In this process, part of this extraembryonic coelom is incorporated in the embryo. This will form the future peritoneal cavity below the umbilicus (5, 6) (Figure 2).

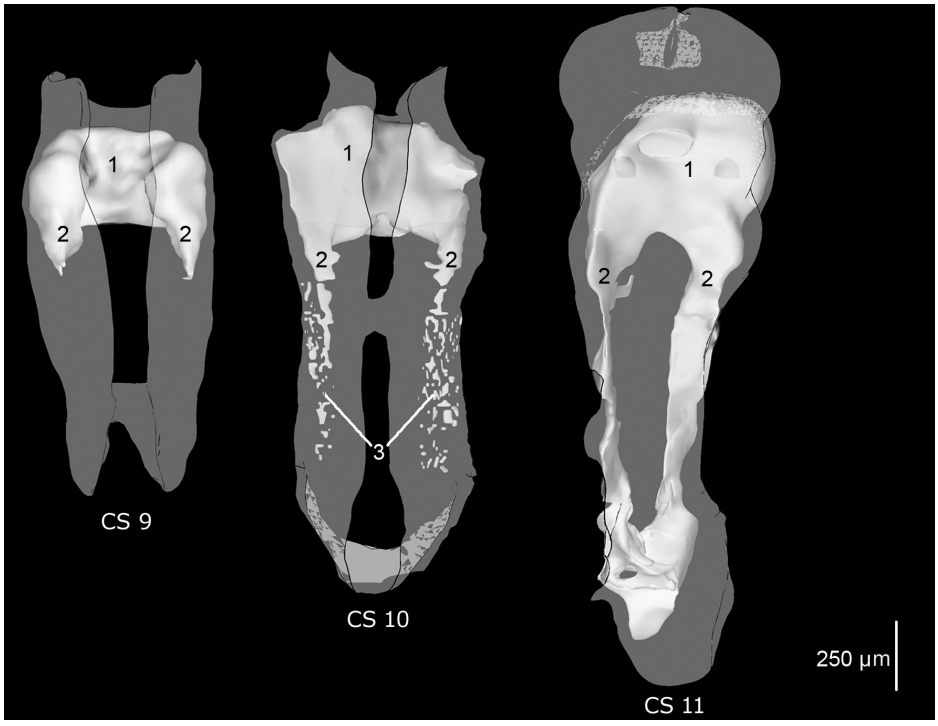

Figure 1. Ventral view of reconstructions of human embryos.
The coelom is reconstructed in white, the embryo is transparent. 1: pericardial cavity, 2: pericardioperitoneal canals, 3: coelomic vesicles. From https://www.3dembryoatlas.com/ with permission of Bernadette de Bakker, Amsterdam UMC

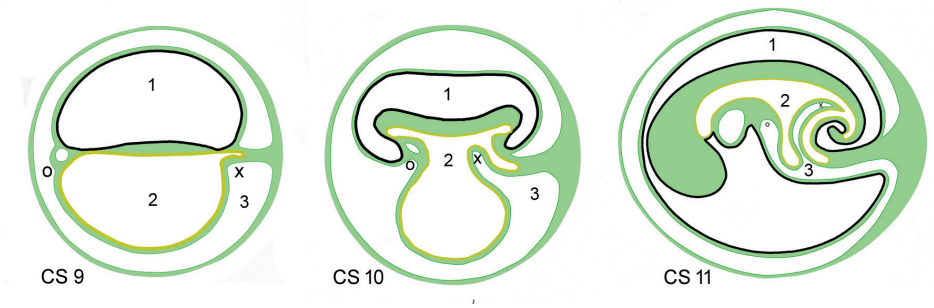

Figure 2. Schematic drawing of a mid-sagittal section through a human embryo.
1: amniotic cavity, 2: yolk sac/gut, 3: coelom, o and x: parts of the extra-embryonic coelom that, due to the folding of the embryonic disc, become situated in the embryo as part of the embryonic coelom.
■ ectoderm
■ mesoderm
■ mesothelium coelomic cavity
■ endodermal lining yolksac and gut

The embryonic peritoneal cavity is separated from the pleural cavity by the formation of pleuroperitoneal membranes halfway along the pericardioperitoneal canals. These membranes are the cranial parts of the urogenital ridges. They do not contribute to the urogenital organs, but instead form part of the adult diaphragm. Once the peritoneal cavity is separated from the pleural cavity, a right and left cavity is present above the level of the umbilicus (which has developed from the pericardioperitoneal canals) and an undivided cavity is present below the level of the umbilicus (which has developed from the extraembryonic coelom) (5, 6).

The peritoneal cavity is empty, but the embryonic gut protrudes in it. Mesodermal cells that line the protruding embryonic gut will form the future visceral peritoneum, and mesodermal cells that line the body wall and the septum transversum will form the future parietal peritoneum. Cells in the transition zone between visceral and parietal peritoneum (which become peritoneal 'reflections' in the adult) are "aggressive" towards their microenvironment, digesting underlying mesodermal cells. Therefore, the coelomic cavity has the ability to enlarge at the expense of non-differentiated sub-coelomic tissue. In this way, the liver (which will form in the septum transversum) is separated from the diaphragm, the foregut (i.e. esophagus, stomach and proximal duodenum) and the ventral body wall. Only the falciform ligament, the bare area of the liver (area nuda hepatis) with the surrounding coronary ligament and the lesser omentum persist. In the adult human, remnants of the septum transversum occur in these structures anterior to the embryonic

foregut and below the embryonic pericardial cavity. The fact that the liver originates from the septum transversum explains why the future peritoneum covering the liver is derived from the embryologic parietal peritoneum instead of the visceral peritoneum (which covers most other abdominal organs) (5, 6).

In the dorsal body wall, two genital ridges develop from the mesonephros. The mesonephros is initially situated retroperitoneally and therefore covered with parietal peritoneum. Consequently, when the mesonephros proliferates and differentiates into ovaries or testes, these organs are covered with parietal peritoneum as well. The left and right genital ridges form a V-shape in the dorsal body wall, meeting in the midline at the caudal boundary of the peritoneal cavity. The peritoneal cavity enlarges in a caudal direction, and the caudal ends of the two genital ridges enlarge in a cranial direction, and move from a subperitoneal to an intraperitoneal position. As the caudal end of the genital ridges contains the fused genital ridges (which will from two Fallopian tubes, the uterus and the cranial part of the vagina in women) the latter moves in a similar manner. Consequently, these structures are covered with peritoneum of parietal origin (5, 6).

The sensory innervation of the peritoneum is derived from migrating neural crest cells. An important difference in the number and type of sensory nerve receptors arises between parietal and visceral peritoneum. Precisely when receptor differentiation occurs and whether this is preceded by an embryologic event, is not clear yet (5, 6). Anatomical differences and nerve trajectories are discussed in more detail in paragraph 3.3.

Development of the (peritoneal) vasculature

The vascular system starts to develop when gastrulation is completed. Mesodermal cells differentiate into hemangioblasts in embryonic and extraembryonic mesoderm. The latter overlies the outer surface of the ectoderm (of the amniotic cavity) and endoderm of the yolk sac. At CS 6 (embryonic day 13 to 15), these cells form small clusters in a process known as blood island formation (Figure 3). Around embryonic day 16, cells in the blood islands further differentiate into angioblasts (which will differentiate into endothelial cells) and hematopoietic precursors (which will differentiate into blood cells). Blood islands fuse and create a primitive vascular network of primordial blood vessels. The formation of endothelial cells from mesodermal cell precursors is defined as vasculogenesis (7-10) (Figure 3).

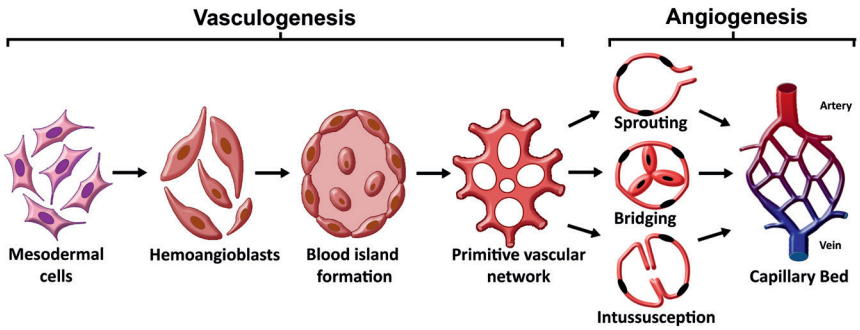

Figure 3. Schematic drawing of the development of the vascular system within the mesoderm.

From embryonic day 18 onwards, new blood vessels arise from vessels initially formed by vasculogenesis. When capillaries arise from pre-existing vessels, the process is called sprouting angiogenesis. During 'intussusceptive angiogenesis' an intussusceptive cylindrical tissue pillar is formed within an existing vessel, thus splitting the lumen of that vessel into two vessels. This form of angiogenesis is not well understood, partly because (and in contrast with sprouting angiogenesis) it is an intravascular process which cannot be visualized by light microscopy (11). Intussusceptive angiogenesis can radically alter the structure of the microvasculature. During 'bridging angiogenesis', endothelial cells form bridges between capillary walls, thus creating two or more capillaries from one vessel (Figure 3). Angiogenesis is responsible for the formation of the majority of the embryonic blood vessels and for vascularization of organs of endoderm and ectoderm origin (12-14).

Vasculogenesis is regulated by various growth factors. Fibroblast growth factors induce differentiation of mesodermal cells into hemangioblasts and signaling through Hedgehog ligands and their receptors is considered crucial for blood island formation (15). Transforming growth factor-β (TGFβ) plays a critical role in vasculogenesis as well (15, 16). Three TGFβ ligands have been identified (TGFβ1, TGFβ2 and TGFβ3) that can bind to receptors on endothelial cells (type 1 receptor TGFβRII and type 2 receptors Alk1 and Alk5) (15, 17). When TGFβ signaling is altered, for example because of deletion of a ligand or receptor, this results in embryo lethality due to defective vasculogenesis in the yolk sac (18).

Vascular endothelial growth factor (VEGF) is a signaling protein that is essential in vasculogenesis and angiogenesis. The VEGF family consists of 6 members (VEGF-A, VEGF-B, VEGF-C, VEGF-D, VEGF-E and placental growth factor), of which VEGF-A is the most potent angiogenic factor. Three VEGF receptors have been identified, namely VEGFR1, VEGFR2 and VEGFR3 (14). Signaling through VEGFR2 is considered the most important initiator of sprouting angiogenesis (19). Knocking out a VEGF receptor in mice results in lethal vascular defects during embryonic development. Deletion of a single VEGF allele results in lethal blood vessel formation defects (20).

Other signaling pathways are also involved in angiogenesis. For example, neuropilins act as co-receptors for VEGF-A and can bind VEGF ligands (21, 22). Notch receptors and ligands regulate proliferation and differentiation of endothelial cells (23). Tie receptors in conjunction with angiopoietin ligands, regulate angiogenesis and vessel maturation (24).

In the dorsal mesentery, endothelial cells develop into dorsal-ventral cords during gut rotation. These cords become the major arteries supplying the midgut. To avoid strangulation of these vessels, vascular development is adapted to gut-rotation. Hence, formation of dorsal-ventral cords occurs solely in the left side of the dorsal mesentery. Asymmetrical development of the vasculature is regulated by the transcription factor pituitary homeobox 2 (Pitx2) (25).

ANATOMY

General anatomy

The peritoneum has a surface area of approximately 1.8 m^2 (26). Parietal peritoneum lines the abdomino-pelvic cavity whereas visceral peritoneum covers most visceral organs. As a consequence, the abdominal walls and all intra-abdominal structures are covered with peritoneum, with exception of the bare area of the liver. Most caudally in the abdomino-pelvic cavity, the peritoneum covers the dome of the bladder and the anterior rectal surface. Hence, the bladder and rectum are located 'under' the peritoneum, in the subperitoneal space. The uterus and uterine tubes are situated between rectum and bladder. These organs are initially situated in the sub- and retroperitoneal spaces, covered with parietal peritoneum. As these organs develop they will protrude into the intra-abdominal cavity and are therefore covered for a large part by parietal peritoneum

(27, 28). The double layers of peritoneum on the lateral sides of the uterus are identified as the broad ligament (consisting of mesometrium), the mesosalpinx and the mesovarium (29).

The uterus, Fallopian tubes and ovaries are covered with parietal peritoneum. The peritoneum covering the ovaries is also known as ovarian surface epithelium. This epithelium is continuous with the parietal peritoneum that covers the fallopian tubes, but has different properties (1). The peritoneum is discontinuous at the fimbrial openings. Consequently, in women, there is a connection between the peritoneal cavity and the outer world, allowing transport of an oocyte from the peritoneal cavity, through the fallopian tubes to the uterus after ovulation. In contrast, the male reproductive organs are situated outside the peritoneal cavity. Therefore, in men the peritoneal cavity is a completely closed sac, continuously covered by peritoneum (27, 28).

Several virtual spaces can be distinguished between the pelvic organs. Males exhibit a recto-vesical pouch situated between the rectum and bladder. In women, the uterus divides this space into the vesico-uterine and recto-uterine pouch (or Douglas' pouch). In an upright position, the recto-vesical and recto-uterine pouches are the lowest parts of the peritoneal cavity (28). Consequently, intra-abdominal fluid, e.g. peritoneal fluid, ascites, and blood, tends to accumulate here. Therefore, this region requires special clinical attention, for instance, when imaging the abdominal cavity (30, 31).

A series of peritoneal 'folds' are situated at the anterior abdominal wall, below the umbilicus, where the peritoneum is reflected over (obliterated) structures. The median fold is formed by the obliterated urachus, the medial folds are formed by the obliterated umbilical arteries and the lateral folds overlie the inferior epigastric vessels.

The peritoneum also covers the intestines and contributes to the mesentery. The mesentery consists of connective tissue, adipocytes, the intestinal vasculature, lymphatics and two layers of mesenteric peritoneum, which are a further region of the visceral peritoneum (32). The mesentery suspends the intestines and is characterized by a 'root', where the parietal peritoneal lining of the abdominal wall detaches, and where the celiac trunk branches and the superior and inferior mesenteric arteries enter the mesentery. The small intestinal mesentery, the transverse mesocolon and lateral mesosigmoid are mobile, whereas the left and right mesocolon and the medial mesosigmoid are flattened against the posterior abdominal wall (32).

The mesentery of the small intestine and colon have been considered separate entities, with the right and left mesocolon being 'fused' with the underlying retroperitoneum. However, between the right and left mesocolon and the underlying retroperitoneum, a separating layer of connective tissue (also known as Toldt's fascia) can be identified. This means that the mesentery is in fact continuous, from duodenum to rectum (32, 33).

The transition zone between the visceral and parietal peritoneum is also termed 'peritoneal reflection'. In regards to the mesentery, the peritoneal reflection is important for colorectal surgeons, because dissection provides access to surgical planes, for example when detaching the mesentery during mesocolic or mesorectal surgery (33). Toldt's fascia is also continuous, but has different names at different anatomic locations (32). In the pelvis, surgeons know this fascia as the 'holy plane' of rectal surgery. Superior to the mesenteric root, the peritoneum contributes to the greater omentum and forms the anterior layer of the lesser omentum.

The peritoneum almost covers the entire liver, except for the bare area of the liver (area nuda hepatis), where the liver is attached directly to the diaphragm. The peritoneum around the bare area forms the coronary ligament, and the peritoneum around the obliterated umbilical vein (ligamentum teres hepatis) forms the falciform ligament, which is the most anterior remnant of the septum transversum, that forms the embryonic ventral mesentery. Finally, the peritoneum lines the lesser sac and contributes to the lieno-renal and gastro-splenic ligaments and covers the posterior wall of the stomach, where it folds into the greater omentum and continues posteriorly towards the posterior abdominal wall (27, 28). The described ligaments are mostly located where the peritoneum is reflected and changes from parietal to visceral peritoneum. In this sense, these ligaments can be considered as a transition zone between the two different types of peritoneum.

Microscopic anatomy

The peritoneum is often defined in literature as a 3-layer structure: a mesothelial cell layer, a basal lamina and submesothelial stroma (1, 34). In contrast, the peritoneum is sometimes defined as a single layer of mesothelial cells. According to the latter definition, the basal lamina and submesothelial stroma are not considered to be part of the peritoneum (27, 35). In the present review, the first definition is used because of the important role of the basal lamina and structures such as blood and lymphatic vessels in the submesothelial stroma in physiological and pathological processes.

Mesothelium

The mesothelial layer is the innermost layer of the peritoneum, and is in contact with the abdominal cavity. Mesothelial cells are mesodermal in origin and possess both epithelial and mesenchymal features. Three types of mesothelial cells have been described (36-38). Flattened mesothelial cells are characteristic of the intestinal, omental and parietal mesothelia. A cuboidal cell type occurs in visceral peritoneum whilst the diaphragm and gastric peritoneum have an intermediate mesothelial cell type (34). Morphologic heterogeneity suggests there are functional differences between mesothelial cells at different anatomical locations. Cuboidal cells contain more mitochondria and endoplasmic reticulum, a well-developed Golgi apparatus, microtubules and a greater number of microfilaments, suggesting increased metabolic activity in these cells (39).

Mesothelial cells are linked by intercellular junctions, including tight junctions, gap junctions and desmosomes (Figure 4) (1, 40-42). At the junction of two or more mesothelial cells, stomatal openings may be present. These openings are 3-12 mm in diameter and provide direct access to the submesothelial lymphatic system, allowing rapid transportation of fluid (1, 43-46). It is suggested that stomata provide a gateway between pleural and peritoneal cavities (46). Lymphatic stomata are extensively present in the mesothelium, but the distribution of stomata has not been characterized for all mesothelial regions (e.g. for different regions of the mesentery) (43).

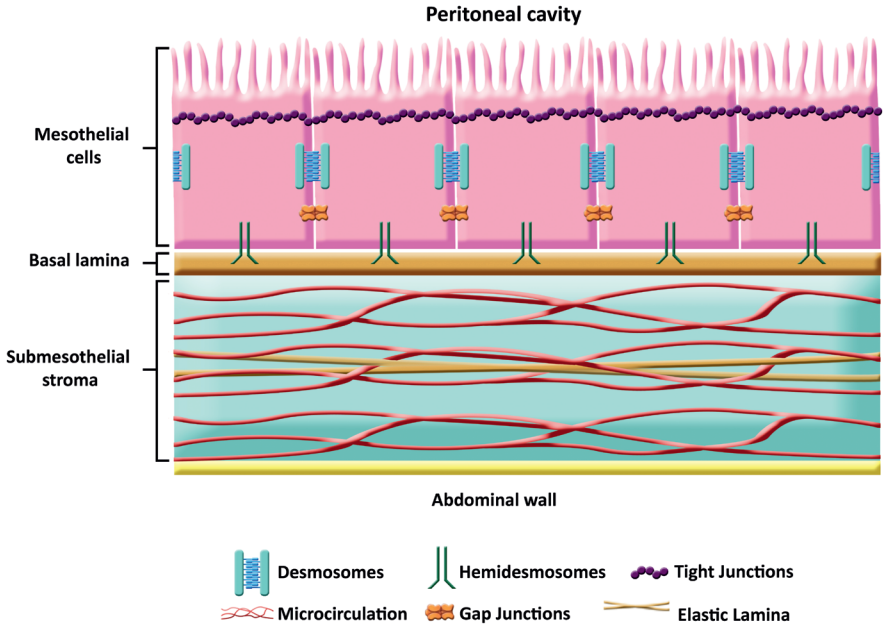

Figure 4. Schematic representation of the peritoneum.

At the apical mesothelial cell membrane, numerous microvilli are present (46, 47). On top of these microvilli, a glycocalyx is present, which creates a stagnant fluid layer consisting of proteoglycans and glycosaminoglycans to promote lubrication (39). This glycocalyx has an anti-inflammatory function and plays an important role in intercellular contacts, tissue remodeling and possibly transport of growth factors and nutrients across the peritoneal membrane (46, 48).

Mesothelial cells contain a number of intracellular vesicles with secretory products. These vesicles can be excreted as exosomes at the apical cell membrane (49). The exact function of mesothelium-derived exosomes is unknown, but they may play a role in intercellular communication (50). Mesothelial cells also contain lamellar bodies. These organelles have a lipid storage function (34). In fact, the main function of lamellar bodies is to supply lipid components to the apical membrane (51). Lamellar bodies in general were first identified in type 2 pneumocytes. In these cells, lamellar bodies store alveolar surfactant. In mesothelial cells, lamellar bodies produce a similar surfactant-like substance, that helps to provide a friction-free peritoneal surface (52, 53). Besides lubrication, surfactant proteins may also have immunological functions (1).

A recent study has suggested that mesothelial cells are also a potential source of adipocytes. The authors demonstrated that visceral fat depots (which are associated with metabolic dysfunction) have a layer of mesothelial cells, that can differentiate into adipocytes (54).

Basal lamina

The basal lamina supports mesothelial cells. It is less than 100 nm thick and consists of an extracellular matrix, mainly composed of collagen type IV and laminin (1). The collagen type IV fiber network acts as a skeleton of the basal lamina, whereas laminin provides binding sites for adhesion of mesothelial cells via hemi-desmosomes (55). Binding of mesothelial cells to the basal lamina is not strong, explaining why minor injuries can result in cellular detachment (56).

Submesothelial stroma

Stroma underneath mesothelial cells and basal lamina provides support to the mesothelial cell layer. This layer consists of collagen type I fibers, laminin, fibronectin, proteoglycans, glycosaminoglycans, fibroblasts, adipocytes, blood and lymph vessels and nerves (57). The thickness and composition of submesothelial stroma varies with age (58) and can change in response to disease (59). Within the stroma, a continuous layer of elastic fibers is present as elastic lamina (60). Knowledge of its function is limited, but a relation has been described between the thickness of the elastic lamina and motility of the organ the peritoneum covers (60). Organs with peristaltic movements are covered by peritoneum with a more prominent elastic lamina, whereas the elastic lamina is thinner in static organs. In some organs, such as the omentum and bladder, the elastic lamina is absent, although it is not clear whether this holds for both lesser and greater omentum.

The submesothelial stroma can also be described as 'interstitium'. A recent study has suggested that the interstitium consists of macroscopically visible spaces within tissues through which interstitial fluid flows (61). These authors consider the submesothelial layer of the mesentery an interstitium, that functionally communicates with the lymphatic drainage of the gastrointestinal tract. Another study also demonstrated that the submesothelial stroma of the mesentery is connected to the intestinal serosa, which means that intestinal and mesenteric connective tissues are continuous (32). These findings are of clinical importance, for example in inflammatory bowel disease or with respect to the spread of cancer cells.

In the mesentery, adipose tissue in the submesothelial layer has been identified as a source of C-reactive protein (CRP). This protein is widely used as marker for inflammation and previously was considered as exclusively produced by the liver. However, emerging data suggests that mesenteric fat tissue can also contribute to the inflammatory response by producing CRP, and that this may be relevant in patients with Crohn's Disease [61].

Anatomy of the peritoneal (micro)vasculature, lymphatics and nerves

Microvascular anatomy

The blood supply of the parietal peritoneum is provided by arteries of the abdominal wall and by parietal pelvic arteries. In contrast, blood flow to the visceral peritoneum comes from mesenteric, coeliac and visceral pelvic arteries. Venous blood from the visceral peritoneum drains into the portal vein, whereas vessels of the parietal peritoneum drain into the inferior vena cava (62).

The peritoneal microcirculation is located in submesothelial stroma and comprises arterioles, venules and capillaries. The morphology of these vessel types differs: arterioles have a round lumen of 20-130 mm, whereas the lumen of venules is often not round and can be larger than that of arterioles. Capillaries located between arterioles and venules have a diameter of 5-10 mm (63). The walls of arterioles and venules consist of several layers. From lumen to adventitia, the following layers can be identified: endothelium, tunica elastica interna, tunica media, tunica elastica externa and tunica adventitia. The thickness of the tunica media differs between arterioles (thick) and venules (thin). The wall of a capillary is morphologically different from that of arterioles and venules and consists of a single endothelial cell layer, on top of which pericytes are located (63, 64). Pericytes are morphologically heterogenous cells that play a key role in blood flow regulation and endothelial proliferation (65). Trans-sectional imaging of the peritoneal submesothelial stroma demonstrates that vascular networks are situated in three horizontal planes (58) (Figure 4).

Arterioles and venules are transport vessels, which means that no exchange of substances between these vessels and surrounding tissues occurs (63). Exchange of substances occurs in capillaries. In the capillary bed, hormones, gases, (like oxygen and carbon dioxide), immune cells, nutrients, water and waste products are exchanged between the capillary lumen and surrounding tissue (66).

The solute and water transport capacity of the peritoneum depends on the capillary density (the spatial arrangement of capillaries) and perfusion of these (67). The peritoneal microcirculation is characterized by a relatively low vessel density (68), but this can be altered under pathological conditions. The density of peritoneal microvasculature under physiological conditions depends on age. The highest density is found in infants younger than 1 year, the lowest density is found in children 7-12 years of age, and density increases again in adults older than 18 years of age (58). The thickness of the endothelial wall also varies with age. The endothelium is thickest in children 7-12 years of age, and thinnest in infants younger than 1 year and adults older than 18 years of age (58). It is hypothesized that the reduced capillary density in childhood is caused by stretching of the growing peritoneal surface, in which angiogenesis cannot keep up with the rapid expansion of the peritoneal surface (58). With regard to the mesenteric peritoneum, Culligan *et al.* have described that certain submesothelial areas of the mesocolon are highly vascularized (69).

Lymphatic anatomy

Different pathways of fluid drainage have been described by which fluid drains from the peritoneal cavity (70, 71). Fluid can be transported across the mesothelial lining of the peritoneum (i.e. through lymphatic stomata), into the celiac, superior mesenteric, and periportal lymph node groups. Subsequently, lymphatic fluid is transported to the thoracic duct by efferent visceral lymphatics (72, 73). Fluid in the abdominal cavity can also drain via diaphragmatic lymphatic channels towards the caudal and anterior mediastinal lymph nodes (1). These channels may explain the occurrence of isolated mediastinal lymph node metastases in patients with ovarian cancer.

Nerve anatomy

Sensory nerve fibers arising from the abdominal wall and (partially) from the parietal peritoneum reach the central nervous system (CNS) via segmental spinal nerves. The most cranial part of the parietal peritoneum (covering the diaphragm) is innervated by the phrenic nerve and its fibers connect to corresponding cervical segments C4, C5 and C6. More caudally, parietal peritoneum derives its nerve supply from thoraco-abdominal nerves, segmental spinal nerves, subcostal and lumbosacral nerves. The obturator nerve innervates parietal peritoneum in the pelvis.

Sensory nerve fibers of the intestine (and the visceral peritoneum) have a more complex route to the CNS. Depending on the location, nerve fibers reach the CNS via the superior

celiac and mesenteric plexus as well as via vagus and splanchnic nerves (74, 75). The sensory innervation of the viscera is derived from neural crest cells and consists mostly of small, thinly myelinated or unmyelinated afferents that appear in a mesh-like complex (76). The majority of mesenteric afferents are located near or on blood vessels (77). An important difference between parietal and visceral peritoneum is the amount and type of sensory nerve receptors. In the parietal peritoneum, pain receptors, stretch receptors and temperature receptors are found. These receptors have a relative low threshold and are therefore very sensitive to pressure, pain, temperature and laceration. In the visceral peritoneum only stretch receptors are present. The visceral peritoneum is insensitive to pain, but sensitive to stretch and chemical irritation (78). These differences explain why movements in hollow organs (i.e. intestines) covered by visceral peritoneum do not cause pain, but are registered by stretch receptors.

PHYSIOLOGY AND PATHOPHYSIOLOGY

Tissue repair and adhesion formation

Peritoneal injury (for example due to surgery or peritonitis) activates the coagulation cascade, which generates fibrin that is deposited on the injured peritoneal surface (79). Fibrin deposition is part of normal tissue repair, but complete degradation of fibrin (fibrinolysis) is necessary for adequate peritoneal healing. The balance between fibrin deposition and its degradation is crucial for normal peritoneal healing.

The conversion of plasminogen into plasmin is an important step in fibrinolysis, since plasmin is highly effective in the degradation of fibrin. Mesothelial cells produce tissue-type plasminogen activator (tPA) and urokinase-type plasminogen activator (uPA), which are both plasminogen activators (80). However, mesothelial cells also produce plasminogen-activating inhibitor (PAI), which inhibits plasminogen activation and thus prevents fibrin degradation. When fibrin is not degraded completely, the fibrin matrix forms a scaffold for collagen-secreting fibroblasts and capillary ingrowth, contributing to peritoneal adhesion formation (81). Peritoneal adhesions can cause pelvic pain, intestinal obstruction and female infertility, and complicate abdominal surgical interventions. Despite extensive research, peritoneal adhesions still represent an important clinical challenge and as yet there is no definitive strategy to prevent their formation (82).

There are considerable inter-individual differences in susceptibility to develop peritoneal adhesions. Various factors have been identified that increase the risk of post-operative adhesion development, such as genetic polymorphisms in PAI and the interleukin-1 receptor antagonist (83). In addition, the formation of adhesions may be affected by the levels of hypoxia that occur during or after surgery.

The role of hypoxia and angiogenesis in adhesion formation

During laparoscopic surgery, carbon dioxide is used for insufflation of the peritoneal cavity in order to visualize intra-abdominal organs. In this way, a so-called pneumoperitoneum is established. Pneumoperitoneum may cause local tissue hypoxia due to the use of carbon dioxide and the increase in intra-abdominal pressure, compression of capillaries and decreased blood flow. Hypoxia, with attendant oxidative stress, free radical production and angiogenesis, may induce formation of peritoneal adhesions (84, 85). Free radicals are toxic to cells at higher concentrations and impair cellular functions. Free radicals can modify proteins, affect proper functioning of organelles and disturb intracellular signal transduction pathways. Induction of oxidative damage contributes to vascular dysfunction and remodelling, and can initiate and stimulate the development of adhesions (85). Therapeutic strategies that target free radicals in preventing adhesion formation, are emerging. Pneumoperitoneum-induced adhesions were absent in mice that not expressing genes encoding for factors regulated by hypoxia, such as VEGF, hypoxia inducible factors and PAI-1 (86-90). Moreover, *in vitro* studies demonstrate that exposure of peritoneal fibroblasts to hypoxia modulates expression of TGF-β, a major profibrotic factor (91-94). These studies suggest that mesothelial hypoxia plays a key role in adhesion formation and that prevention of hypoxia or the use of antiangiogenic drugs may prevent or reduce peritoneal adhesion formation (95).

Peritoneal fibrosis and mesothelial-to-mesenchymal transition

Peritoneal fibrosis is often observed in patients undergoing peritoneal dialysis, and partially arises from dialysate with high glucose levels and low pH. Dialysis-induced fibrosis significantly decreases diffusion capacity, leading to failure of ultrafiltration. Peritoneal fibrosis is characterized by submesothelial thickening, vasculopathy, and autocrine proliferation (96, 97).

Epithelial-to-mesenchymal transition of mesothelial cells can be triggered by factors affecting mesothelial cells, and plays a central role in peritoneal fibrosis (Figure 5). During this so-called mesothelial-to-mesenchymal transition (MMT), mesothelial cells

lose intercellular adhesions, microvilli and apical-basolateral polarity. Subsequently, they transform into migratory and invasive cells with a myofibroblastic phenotype (98) (Figure 5). These express high levels of cyclooxygenase-2, connective tissue growth factor and VEGF, and induce angiogenesis. MMT is initiated by cytokines and growth factors such as TGF-β1, interleukin 1β and hepatocyte growth factor (99). TGF-β1 has been suggested to be a key player in the induction of peritoneal fibrosis, whereas inhibition of TGF-β1 protects the peritoneum from dialysis-induced fibrosis (100).

Fluid transport across the peritoneal membrane and the formation of ascites

Under physiological conditions, the peritoneal cavity contains approximately 5 - 20 ml of peritoneal fluid. Peritoneal fluid is for the larger part produced by the peritoneal capillaries. From the peritoneal cavity, peritoneal fluid is transported through lymphatic stomata to the thoracic duct and back into the intravascular space. Renewal of the peritoneal fluid occurs every 1-2 hours (67). Pathological disturbance of this equilibrium can lead to accumulation of peritoneal fluid, called ascites. Severe ascites causes abdominal distention and reduced quality of life as it impairs intestinal function, and leads to abdominal pain, anorexia and restrictive breathing. Ascites can be categorized based on the presence of high (exudate) or low levels of albumin (transudate). The amount of albumin present depends on the underlying pathophysiological process. Obstruction of the portal vein is a common cause of ascites. In this setting fluid with low levels of albumin (transudate) leaks directly from the liver surface and mesenteric vessels, through the peritoneum into the peritoneal cavity (101, 102). In addition, increased intra-abdominal pressure often decreases the absorptive capacity of the peritoneal surface and lymphatic system (102). Other pathological conditions such as peritonitis and peritoneal carcinomatosis cause ascites without obstruction of the portal or hepatic vein. In these cases, ascites results from increased permeability of the capillary endothelium in the submesothelial layer of the peritoneum. In general, this fluid is an exudate, because albumin also leaks out of the capillaries and thus colloid osmotic pressure cannot counteract the formation of ascites (103).

Cellular signaling inducig vascular leakage in peritoneum

Increased vascular permeability can be induced by various intercellular and intracellular signaling pathways that target the endothelial barrier (104). One of the most potent inducers of such signaling pathways is VEGF. Once VEGF binds to VEGFR2 on endothelial cells, an intracellular signaling pathway triggers β-arrestin dependent endocytosis of VE-cadherin (Figure 6). Since VE-cadherin is a key adhesion molecule, endocytosis of VE-

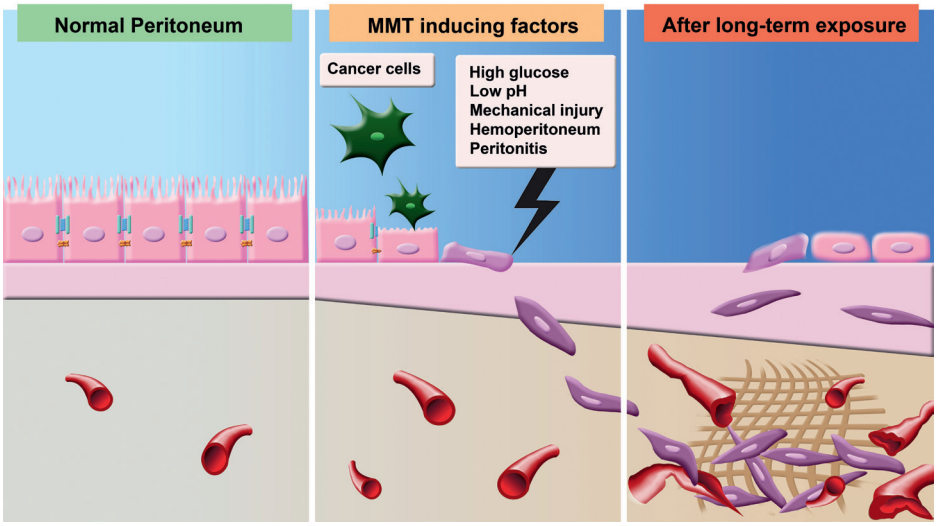

Figure 5. Schematic representation of a cross-section of the peritoneum showing mesothelial-to-mesenchymal transition (MMT) as a consequence of cancer or, for example, long-term peritoneal dialysis.

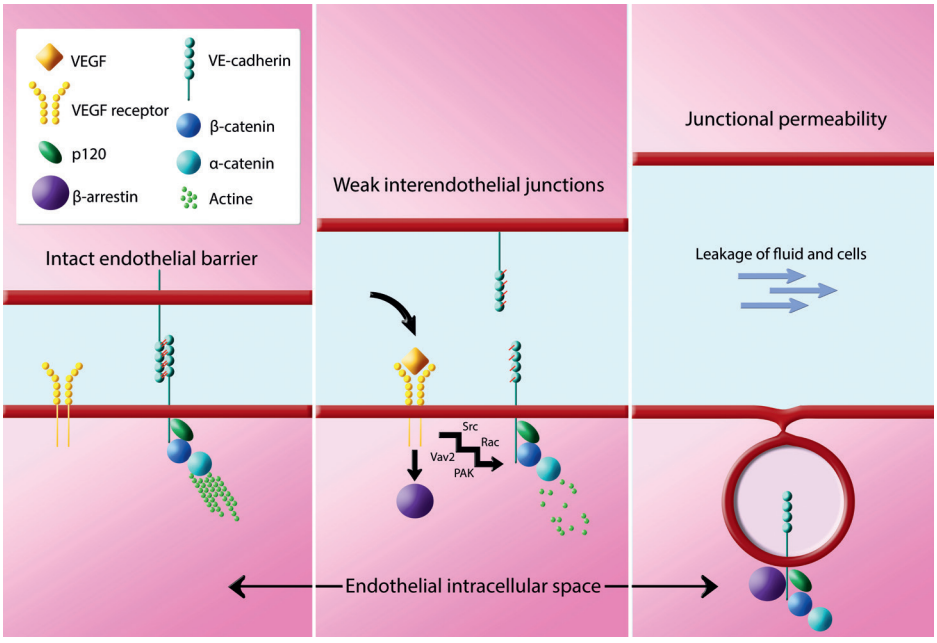

Figure 6. Schematic representation of VEGF induced VE-cadherin endocytosis that increases vascular permeability in the peritoneum.

cadherin reduces the adhesion capacity of endothelial cells, thus increasing permeability of the capillaries (104).

Blockade of VEGFR2 in patients with peritoneal carcinomatosis can restore the endothelial barrier and prevent production of ascites. Therefore, the VEGF receptor antagonist bevacizumab, currently used in the treatment of epithelial ovarian cancer, can affect the production of ascites (105). Alternatively, inhibition of tyrosine kinase phosphorylation of VEGFR2 decreases receptor activity, thus inhibiting VEGF-induced processes such as angiogenesis and aforementioned endocytosis of VE-cadherin. When a tyrosine kinase inhibitor is administered to mice with peritoneal implants of ovarian cancer, peritoneal dissemination and ascites formation are inhibited (106, 107). Moreover, intraperitoneal administration of monoclonal antibodies directed against VEGF receptors in mice with peritoneal carcinomatosis prevents recurrence of malignant ascites (108).

The role of the peritoneal vasculature in peritoneal carcinomatosis

Gastro-intestinal or gynecologic cancer that metastasizes intra-abdominally can cause peritoneal carcinomatosis, a condition in which the peritoneum is affected by numerous small-sized lesions. The role of the peritoneum in metastatic tumor spread has been studied extensively. Peristaltic bowel movements and respiratory movements contribute to dissemination of peritoneal fluid in the peritoneal cavity, enabling exfoliated cancer cells to adhere to peritoneal surfaces. Ovarian cancer cells express surface integrins which can bind efficiently to components of the ECM, such as collagen, laminin, fibronectin, fibrinogen and vitronectin. Once adhesion is established, the submesothelial stroma supplies mediators enabling metastatic cancer cells survive, proliferate and invade the peritoneum. Subsequently, a tumor-supportive microenvironment is created by attraction of inflammatory and stromal cells and chemokines. However, despite this tumor-supportive environment, peritoneal metastases remain small-sized with only superficial invasion of the submesothelial stroma. Mechanisms underlying this restrictive growth and invasion are still virtually unknown, but this phenomenon points to a complex interaction between cancer cells, peritoneal cells and the microenvironment. The process of peritoneal metastasis in epithelial ovarian cancer was recently summarized by van Baal et al (4). Few studies investigated peritoneal vasculature in the presence of cancer deposits. Increased vascularization occurs in biopsies from peritoneum surrounding tumour depositions, a finding that can be explained by the fact that angiogenesis is initiated by cancer cells and 'cancer-associated mesothelial cells' (109). Moreover, peritoneal deposits are more frequently observed at locations with immune cell aggregates, referred to as 'milky spots'. Milky spots contain mesothelial cells that secrete

VEGF and they have a high capillary density. Studies in mice demonstrated improved survival of deposits in proximity with milky spots (110, 111). Hypothetically, increased vessel density in the peritoneum is important for attachment, survival and growth of peritoneal metastases (112).

CONCLUDING REMARKS

The peritoneum is a complex structure with a variety of functions. This review provides an overview of current knowledge of embryonic development, anatomy, physiology and pathophysiology of the peritoneal membrane with special emphasis on microvasculature. The vascular response in pathological processes such as adhesion formation, inflammation and cancer is of considerable clinical importance and remodeling of peritoneal vasculature is involved in almost all associated diseases. The exact role of peritoneum in pathological conditions requires further elucidation. In order to develop new therapeutic strategies, it is imperative that the peritoneum, its physiology and pathophysiology are studied in detail.

ACKNOWLEDGEMENTS

We like to express our gratitude to Yasin Ince, for his creative assistance in composing the figures in this article.

FUNDING

This research did not receive any specific grant from funding agencies in the public, commercial or not-for-profit sectors.

REFERENCES

1. van Baal JO, Van de Vijver KK, Nieuwland R, van Noorden CJ, van Driel WJ, Sturk A, et al. The histophysiology and pathophysiology of the peritoneum. Tissue Cell. 2017;49(1):95-105.
2. T.W. Sadler JL. Langmans Medical Embryology. Wolters Kluwer Health/Lippincott Williams & Wilkins, Philadelphia 2012.
3. Hesseldahl H, Larsen JF. Ultrastructure of human yolk sac: endoderm, mesenchyme, tubules and mesothelium. The American journal of anatomy. 1969;126(3):315-35.
4. van Baal J, van Noorden CJF, Nieuwland R, Van de Vijver KK, Sturk A, van Driel WJ, et al. Development of Peritoneal Carcinomatosis in Epithelial Ovarian Cancer: A Review. The journal of histochemistry and cytochemistry : official journal of the Histochemistry Society. 2018;66(2):67-83.
5. de Bakker BS, de Jong KH, Hagoort J, de Bree K, Besselink CT, de Kanter FE, et al. An interactive three-dimensional digital atlas and quantitative database of human development. Science (New York, NY). 2016;354(6315).
6. Gary C. Schoenwolf SBB, Philip R Brauer, Philippa H Francis-West. Larsen's Human Embryology. 5th Edition ed2015.
7. Risau W, Flamme I. Vasculogenesis. Annual review of cell and developmental biology. 1995;11:73-91.
8. Moore KL. The Developing Human, clinically oriented embryology. 1982(Third edition).
9. Goldie LC, Nix MK, Hirschi KK. Embryonic vasculogenesis and hematopoietic specification. Organogenesis. 2008;4(4):257-63.
10. Noden DM. Embryonic origins and assembly of blood vessels. The American review of respiratory disease. 1989;140(4):1097-103.
11. Mentzer SJ. Intussusceptive Angiogenesis: Expansion and Remodeling of Microvascular Networks. 2014;17(3):499-509.
12. Adair TH MJ. Angiogenesis. San Rafael (CA): Morgan & Clapypool Life Sciences; 2010.
13. Mentzer SJ, Konerding MA. Intussusceptive angiogenesis: expansion and remodeling of microvascular networks. Angiogenesis. 2014;17(3):499-509.
14. Dallinga MG, Boas, Sonja EM, Klaassen, Ingeborg, Merks, Roeland HM, van Noorden, Cornelis JF, and Schlingemann, Reinier O. Tip Cells in Angiogenesis. eLS. 2015.
15. Patel-Hett S, D'Amore PA. Signal transduction in vasculogenesis and developmental angiogenesis. The International journal of developmental biology. 2011;55(4-5):353-63.
16. Pepper MS. Transforming growth factor-beta: vasculogenesis, angiogenesis, and vessel wall integrity. Cytokine Growth Factor Rev. 1997;8(1):21-43.
17. Cooley JR, Yatskievych TA, Antin PB. Embryonic Expression of the Transforming Growth Factor Beta Ligand and Receptor Genes in Chicken. Developmental dynamics : an official publication of the American Association of Anatomists. 2014;243(3):497-508.

18. Oshima M, Oshima H, Taketo MM. TGF-beta receptor type II deficiency results in defects of yolk sac hematopoiesis and vasculogenesis. Developmental biology. 1996;179(1):297-302.
19. Koch S, Claesson-Welsh L. Signal transduction by vascular endothelial growth factor receptors. Cold Spring Harbor perspectives in medicine. 2012;2(7):a006502.
20. Carmeliet P, Ferreira V, Breier G, Pollefeyt S, Kieckens L, Gertsenstein M, et al. Abnormal blood vessel development and lethality in embryos lacking a single VEGF allele. Nature. 1996;380(6573):435-9.
21. Takashima S, Kitakaze M, Asakura M, Asanuma H, Sanada S, Tashiro F, et al. Targeting of both mouse neuropilin-1 and neuropilin-2 genes severely impairs developmental yolk sac and embryonic angiogenesis. Proceedings of the National Academy of Sciences of the United States of America. 2002;99(6):3657-62.
22. Koch S. Neuropilin signalling in angiogenesis. Biochemical Society transactions. 2012;40(1):20-5.
23. Aster JC. In brief: Notch signalling in health and disease. The Journal of pathology. 2014;232(1):1-3.
24. Teichert M, Milde L, Holm A, Stanicek L, Gengenbacher N, Savant S, et al. Pericyte-expressed Tie2 controls angiogenesis and vessel maturation. Nature communications. 2017;8:16106.
25. Mahadevan A, Welsh IC, Sivakumar A, Gludish DW, Shilvock AR, Noden DM, et al. The left-right Pitx2 pathway drives organ-specific arterial and lymphatic development in the intestine. Developmental cell. 2014;31(6):690-706.
26. van Baal JOAM, Van de Vijver KK, Nieuwland R, van Noorden CJF, van Driel WJ, Sturk A, et al. The histophysiology and pathophysiology of the peritoneum. Tissue and Cell. 2017;49(1):95-105.
27. Blackburn SC, Stanton MP. Anatomy and physiology of the peritoneum. Seminars in pediatric surgery. 2014;23(6):326-30.
28. Gray's Anatomy. 41st Edition ed. Standring S, editor2015 09/2015.
29. Miller A, Hong MK, Hutson JM. The broad ligament: a review of its anatomy and development in different species and hormonal environments. Clinical anatomy (New York, NY). 2004;17(3):244-51.
30. Healy JC, Reznek RH. The peritoneum, mesenteries and omenta: normal anatomy and pathological processes. European radiology. 1998;8(6):886-900.
31. Tirkes T, Sandrasegaran K, Patel AA, Hollar MA, Tejada JG, Tann M, et al. Peritoneal and retroperitoneal anatomy and its relevance for cross-sectional imaging. Radiographics : a review publication of the Radiological Society of North America, Inc. 2012;32(2):437-51.
32. Coffey JC, O'Leary DP. The mesentery: structure, function, and role in disease. The lancet Gastroenterology & hepatology. 2016;1(3):238-47.
33. Coffey JC, Dillon M, Sehgal R, Dockery P, Quondamatteo F, Walsh D, et al. Mesenteric-Based Surgery Exploits Gastrointestinal, Peritoneal, Mesenteric and Fascial Continuity from Duodenojejunal Flexure to the Anorectal Junction--A Review. Digestive surgery. 2015;32(4):291-300.

34. Michailova KN, Usunoff KG. Serosal membranes (pleura, pericardium, peritoneum). Normal structure, development and experimental pathology. Advances in anatomy, embryology, and cell biology. 2006;183:i-vii, 1-144, back cover.
35. Melichar B, Freedman RS. Immunology of the peritoneal cavity: relevance for host-tumor relation. Int J Gynecol Cancer. 2002;12(1):3-17.
36. Barberini F, Carpino F, Renda T, Motta P. [Observations by scanning electron microscopy (SEM) on the surface of mesothelial cells of different peritoneal areas of rat (author's transl)]. Anatomischer Anzeiger. 1977;142(5):486-96.
37. Michailova KN. A combined electron microscopic investigation of the peritoneal mesothelium in the rat. European journal of morphology. 1995;33(3):265-77.
38. Michailova KN. Mesothelial lamellar bodies in norm and experimental conditions. Transmission and scanning electron microscopic observations on the peritoneum, pleura and pericardium. Anatomy and embryology. 2004;208(4):301-9.
39. Mutsaers SE. The mesothelial cell. The international journal of biochemistry & cell biology. 2004;36(1):9-16.
40. Pelin K, Hirvonen A, Linnainmaa K. Expression of cell adhesion molecules and connexins in gap junctional intercellular communication deficient human mesothelioma tumour cell lines and communication competent primary mesothelial cells. Carcinogenesis. 1994;15(11):2673-5.
41. Ito T, Yorioka N, Yamamoto M, Kataoka K, Yamakido M. Effect of glucose on intercellular junctions of cultured human peritoneal mesothelial cells. Journal of the American Society of Nephrology : JASN. 2000;11(11):1969-79.
42. Simionescu M, Simionescu N. Organization of cell junctions in the peritoneal mesothelium. The Journal of cell biology. 1977;74(1):98-110.
43. Wang ZB, Li M, Li JC. Recent advances in the research of lymphatic stomata. Anatomical record (Hoboken, NJ : 2007). 2010;293(5):754-61.
44. Li YY, Li JC. Ultrastructure and three-dimensional study of the lymphatic stomata in the costal pleura of the rabbit. Microscopy research and technique. 2003;62(3):240-6.
45. Li J, Zhao Z, Zhou J, Yu S. A study of the three-dimensional organization of the human diaphragmatic lymphatic lacunae and lymphatic drainage units. Annals of Anatomy - Anatomischer Anzeiger. 1996;178(6):537-44.
46. Mutsaers SE. Mesothelial cells: their structure, function and role in serosal repair. Respirology (Carlton, Vic). 2002;7(3):171-91.
47. Baradi AF, Rao SN. A scanning electron microscope study of mouse peritoneal mesothelium. Tissue Cell. 1976;8(1):159-62.
48. Evanko SP, Tammi MI, Tammi RH, Wight TN. Hyaluronan-dependent pericellular matrix. Advanced drug delivery reviews. 2007;59(13):1351-65.
49. Li J, Chen X, Yu S. The ultrastructure of vesicle-containing cells and ER-cells of human peritoneum. Annals of anatomy = Anatomischer Anzeiger : official organ of the Anatomische Gesellschaft. 1996;178(4):365-7.

50. van der Pol E, Boing AN, Harrison P, Sturk A, Nieuwland R. Classification, functions, and clinical relevance of extracellular vesicles. Pharmacological reviews. 2012;64(3):676-705.
51. Schmitz G, Muller G. Structure and function of lamellar bodies, lipid-protein complexes involved in storage and secretion of cellular lipids. Journal of lipid research. 1991;32(10):1539-70.
52. Dobbie JW. Surfactant protein A and lamellar bodies: a homologous secretory function of peritoneum, synovium, and lung. Peritoneal dialysis international : journal of the International Society for Peritoneal Dialysis. 1996;16(6):574-81.
53. Dobbie JW. New concepts in molecular biology and ultrastructural pathology of the peritoneum: their significance for peritoneal dialysis. American journal of kidney diseases : the official journal of the National Kidney Foundation. 1990;15(2):97-109.
54. Chau Y-Y, Bandiera R, Serrels A, Martínez-Estrada OM, Qing W, Lee M, et al. Visceral and subcutaneous fat have different origins and evidence supports a mesothelial source. Nature cell biology. 2014;16:367.
55. Yurchenco PD. Basement membranes: cell scaffoldings and signaling platforms. Cold Spring Harbor perspectives in biology. 2011;3(2).
56. Raftery AT. Regeneration of parietal and visceral peritoneum: an electron microscopical study. Journal of anatomy. 1973;115(Pt 3):375-92.
57. Witz CA, Montoya-Rodriguez IA, Cho S, Centonze VE, Bonewald LF, Schenken RS. Composition of the extracellular matrix of the peritoneum. Journal of the Society for Gynecologic Investigation. 2001;8(5):299-304.
58. Schaefer B, Bartosova M, Macher-Goeppinger S, Ujszaszi A, Wallwiener M, Nyarangi-Dix J, et al. Quantitative Histomorphometry of the Healthy Peritoneum. Scientific reports. 2016;6:21344.
59. Williams JD, Craig KJ, Topley N, Von Ruhland C, Fallon M, Newman GR, et al. Morphologic changes in the peritoneal membrane of patients with renal disease. Journal of the American Society of Nephrology : JASN. 2002;13(2):470-9.
60. Knudsen PJ. The peritoneal elastic lamina. Journal of anatomy. 1991;177:41-6.
61. Benias PC, Wells RG, Sackey-Aboagye B, Klavan H, Reidy J, Buonocore D, et al. Structure and Distribution of an Unrecognized Interstitium in Human Tissues. Scientific reports. 2018;8(1):4947.
62. Khanna R, Krediet, R.T. Chapter 4: the peritoneal microcirculation in peritoneal dialysis. Nolph and Gokal's Textbook of Peritoneal Dialysis, 3d ed Springer. 2009.
63. Kierszenbaum A. Histology and cell biology: an introduction to pathology. St Louis, MI: Mosby. 2002.
64. Hira VVV, Aderetti DA, van Noorden CJF. Glioma Stem Cell Niches in Human Glioblastoma Are Periarteriolar. The journal of histochemistry and cytochemistry : official journal of the Histochemistry Society. 2018;66(5):349-58.
65. Hirschi KK, D'Amore PA. Pericytes in the microvasculature. Cardiovascular research. 1996;32(4):687-98.
66. Peters J, Mack GW, Lister G. The importance of the peripheral circulation in critical illnesses. Intensive Care Med. 2001;27(9):1446-58.

67. Krediet RT, Lindholm B, Rippe B. Pathophysiology of peritoneal membrane failure. Peritoneal dialysis international : journal of the International Society for Peritoneal Dialysis. 2000;20 Suppl 4:S22-42.
68. Uz Z, Kastelein AW, Milstein DMJ, Liu D, Rassam F, Veelo DP, et al. Intraoperative Incident Dark Field Imaging of the Human Peritoneal Microcirculation. Journal of vascular research. 2018;55(3):136-43.
69. Culligan K, Walsh S, Dunne C, Walsh M, Ryan S, Quondamatteo F, et al. The mesocolon: a histological and electron microscopic characterization of the mesenteric attachment of the colon prior to and after surgical mobilization. Annals of surgery. 2014;260(6):1048-56.
70. Abernethy NJ, Chin W, Hay JB, Rodela H, Oreopoulos D, Johnston MG. Lymphatic drainage of the peritoneal cavity in sheep. The American journal of physiology. 1991;260(3 Pt 2):F353-8.
71. Shibata S, Yamaguchi S, Kaseda M, Ichihara N, Hayakawa T, Asari M. The time course of lymphatic routes emanating from the peritoneal cavity in rats. Anatomia, histologia, embryologia. 2007;36(1):78-82.
72. Feldman GB, Knapp RC. Lymphatic drainage of the peritoneal cavity and its significance in ovarian cancer. American journal of obstetrics and gynecology. 1974;119(7):991-4.
73. Parungo CP, Soybel DI, Colson YL, Kim SW, Ohnishi S, DeGrand AM, et al. Lymphatic drainage of the peritoneal space: a pattern dependent on bowel lymphatics. Ann Surg Oncol. 2007;14(2):286-98.
74. Tanaka K, Matsugami T, Chiba T. The origin of sensory innervation of the peritoneum in the rat. Anatomy and embryology. 2002;205(4):307-13.
75. Florian Struller F-JW, Philipp Horvath et al. peritoneal innervation: embryology and functional anatomy. Pleura and Peritoneum. 2017;2(4):153 - 61.
76. Christianson JA DB. The Role of Visceral Afferents in Disease. Kruger L LA, editor: CRC Press/ Taylor & Francis; 2010.
77. Brunsden AM, Jacob S, Bardhan KD, Grundy D. Mesenteric afferent nerves are sensitive to vascular perfusion in a novel preparation of rat ileum in vitro. American journal of physiology Gastrointestinal and liver physiology. 2002;283(3):G656-65.
78. diZerega G. Chapter 1: peritoneum and peritoneal repair. Peritoneal Surgery (1st ed), Springer-Verleg, New York (2000). 2000.
79. Holmdahl L. The role of fibrinolysis in adhesion formation. The European journal of surgery Supplement : = Acta chirurgica Supplement. 1997(577):24-31.
80. Sikkink CJJM, Reijnen MMPJ, Falk P, van Goor H, Holmdahl L. Influence of monocyte-like cells on the fibrinolytic activity of peritoneal mesothelial cells and the effect of sodium hyaluronate. Fertility and Sterility. 2005;84(Supplement 2):1072-7.
81. Cheong YC, Laird SM, Li TC, Shelton JB, Ledger WL, Cooke ID. Peritoneal healing and adhesion formation/reformation. Human reproduction update. 2001;7(6):556-66.
82. Arung W, Meurisse M, Detry O. Pathophysiology and prevention of postoperative peritoneal adhesions. World journal of gastroenterology. 2011;17(41):4545-53.

83. Fortin CN, Saed GM, Diamond MP. Predisposing factors to post-operative adhesion development. Human reproduction update. 2015;21(4):536-51.
84. Koninckx PR, Gomel V, Ussia A, Adamyan L. Role of the peritoneal cavity in the prevention of postoperative adhesions, pain, and fatigue. Fertil Steril. 2016;106(5):998-1010.
85. Awonuga AO, Belotte J, Abuanzeh S, Fletcher NM, Diamond MP, Saed GM. Advances in the Pathogenesis of Adhesion Development: The Role of Oxidative Stress. Reproductive sciences (Thousand Oaks, Calif). 2014;21(7):823-36.
86. Bigatti G, Boeckx W, Gruft L, Segers N, Brosens I. Experimental model for neoangiogenesis in adhesion formation. Human reproduction (Oxford, England). 1995;10(9):2290-4.
87. Molinas CR, Mynbaev O, Pauwels A, Novak P, Koninckx PR. Peritoneal mesothelial hypoxia during pneumoperitoneum is a cofactor in adhesion formation in a laparoscopic mouse model. Fertil Steril. 2001;76(3):560-7.
88. Molinas CR, Koninckx PR. Hypoxaemia induced by CO(2) or helium pneumoperitoneum is a co-factor in adhesion formation in rabbits. Human reproduction (Oxford, England). 2000;15(8):1758-63.
89. Molinas CR, Campo R, Dewerchin M, Eriksson U, Carmeliet P, Koninckx PR. Role of vascular endothelial growth factor and placental growth factor in basal adhesion formation and in carbon dioxide pneumoperitoneum-enhanced adhesion formation after laparoscopic surgery in transgenic mice. Fertil Steril. 2003;80 Suppl 2:803-11.
90. Molinas CR, Elkelani O, Campo R, Luttun A, Carmeliet P, Koninckx PR. Role of the plasminogen system in basal adhesion formation and carbon dioxide pneumoperitoneum-enhanced adhesion formation after laparoscopic surgery in transgenic mice. Fertil Steril. 2003;80(1):184-92.
91. Saed GM, Munkarah AR, Abu-Soud HM, Diamond MP. Hypoxia upregulates cyclooxygenase-2 and prostaglandin E(2) levels in human peritoneal fibroblasts. Fertil Steril. 2005;83 Suppl 1:1216-9.
92. Saed GM, Abu-Soud HM, Diamond MP. Role of nitric oxide in apoptosis of human peritoneal and adhesion fibroblasts after hypoxia. Fertil Steril. 2004;82 Suppl 3:1198-205.
93. Saed GM, Collins KL, Diamond MP. Transforming growth factors beta1, beta2 and beta3 and their receptors are differentially expressed in human peritoneal fibroblasts in response to hypoxia. American journal of reproductive immunology (New York, NY : 1989). 2002;48(6):387-93.
94. Saed GM, Zhang W, Diamond MP. Effect of hypoxia on stimulatory effect of TGF-beta 1 on MMP-2 and MMP-9 activities in mouse fibroblasts. Journal of the Society for Gynecologic Investigation. 2000;7(6):348-54.
95. Molinas CR, Binda MM, Koninckx PR. Angiogenic factors in peritoneal adhesion formation. Gynecological Surgery. 2006;3(3):157-67.
96. Aguilera A, Yáñez-Mo M, Selgas R, Sánchez-Madrid F, López-Cabrera M. Epithelial to mesenchymal transition as a triggering factor of peritoneal membrane fibrosis and angiogenesis in peritoneal dialysis patients. Curr Opin Investig Drugs. 2005;6(3):262-8.

97. Margetts PJ, Kolb M, Yu L, Hoff CM, Holmes CJ, Anthony DC, et al. Inflammatory cytokines, angiogenesis, and fibrosis in the rat peritoneum. Am J Pathol. 2002;160(6):2285-94.
98. Yanez-Mo M, Lara-Pezzi E, Selgas R, Ramirez-Huesca M, Dominguez-Jimenez C, Jimenez-Heffernan JA, et al. Peritoneal dialysis and epithelial-to-mesenchymal transition of mesothelial cells. The New England journal of medicine. 2003;348(5):403-13.
99. Thiery JP. Epithelial-mesenchymal transitions in development and pathologies. Current opinion in cell biology. 2003;15(6):740-6.
100. Loureiro J, Aguilera A, Selgas R, Sandoval P, Albar-Vizcaino P, Perez-Lozano ML, et al. Blocking TGF-beta1 protects the peritoneal membrane from dialysate-induced damage. Journal of the American Society of Nephrology : JASN. 2011;22(9):1682-95.
101. Cardenas A, Bataller R, Arroyo V. Mechanisms of ascites formation. Clinics in liver disease. 2000;4(2):447-65.
102. Moore CM, Van Thiel DH. Cirrhotic ascites review: Pathophysiology, diagnosis and management. World Journal of Hepatology. 2013;5(5):251-63.
103. Sangisetty SL, Miner TJ. Malignant ascites: A review of prognostic factors, pathophysiology and therapeutic measures. World Journal of Gastrointestinal Surgery. 2012;4(4):87-95.
104. Gavard J, Gutkind JS. VEGF controls endothelial-cell permeability by promoting the beta-arrestin-dependent endocytosis of VE-cadherin. Nature cell biology. 2006;8(11):1223-34.
105. Pujade-Lauraine E, Hilpert F, Weber B, Reuss A, Poveda A, Kristensen G, et al. Bevacizumab combined with chemotherapy for platinum-resistant recurrent ovarian cancer: The AURELIA open-label randomized phase III trial. Journal of clinical oncology : official journal of the American Society of Clinical Oncology. 2014;32(13):1302-8.
106. Machida S, Saga Y, Takei Y, Mizuno I, Takayama T, Kohno T, et al. Inhibition of peritoneal dissemination of ovarian cancer by tyrosine kinase receptor inhibitor SU6668 (TSU-68). International journal of cancer. 2005;114(2):224-9.
107. Xu L, Yoneda J, Herrera C, Wood J, Killion JJ, Fidler IJ. Inhibition of malignant ascites and growth of human ovarian carcinoma by oral administration of a potent inhibitor of the vascular endothelial growth factor receptor tyrosine kinases. International journal of oncology. 2000;16(3):445-54.
108. Stoelcker B, Echtenacher B, Weich HA, Sztajer H, Hicklin DJ, Mannel DN. VEGF/Flk-1 interaction, a requirement for malignant ascites recurrence. Journal of interferon & cytokine research : the official journal of the International Society for Interferon and Cytokine Research. 2000;20(5):511-7.
109. Sandoval P, Jimenez-Heffernan JA, Rynne-Vidal A, Perez-Lozano ML, Gilsanz A, Ruiz-Carpio V, et al. Carcinoma-associated fibroblasts derive from mesothelial cells via mesothelial-to-mesenchymal transition in peritoneal metastasis. The Journal of pathology. 2013;231(4):517-31.
110. Gerber SA, Rybalko VY, Bigelow CE, Lugade AA, Foster TH, Frelinger JG, et al. Preferential attachment of peritoneal tumor metastases to omental immune aggregates and possible role of a unique vascular microenvironment in metastatic survival and growth. Am J Pathol. 2006;169(5):1739-52.

111. Masoumi Moghaddam S, Amini A, Morris D, Pourgholami M. Significance of vascular endothelial growth factor in growth and peritoneal dissemination of ovarian cancer2011. 143-62 p.

112. Liu J, Geng X, Li Y. Milky spots: omental functional units and hotbeds for peritoneal cancer metastasis. Tumour biology : the journal of the International Society for Oncodevelopmental Biology and Medicine. 2016;37(5):5715-26.

7 Intraoperative incident dark field imaging of the human peritoneal microcirculation

Z Uz
AW Kastelein
DMJ Milstein
D Liu
F Rassam
DP Veelo
JPWR Roovers
C Ince
TM van Gulik

J Vasc Res. 2018;55(3):136-143.

ABSTRACT

Background/Aims

This study describes the peritoneal microcirculation, compares quantitative parameters and angioarchitecture to the standard of sublingual microcirculatory assessment, and determines the practical feasibility of this method.

Methods

Incident dark field imaging was performed of the peritoneum and sublingually to determine angioarchitecture, total and perfused vessel density (TVD and PVD), the proportion of perfused vessels (PPV), the microvascular flow index (MFI) and image acquisition time.

Results

Peritoneal angioarchitecture was characterized by a quadrangular network of longitudinally oriented capillaries, often flanked by fat cells. Differences between peritoneal and sublingual microcirculation were observed with regard to TVD (peritoneum 12 mm/mm2 [95% CI 10–14] vs. sublingual 23 mm/mm2 [95% CI 21–25]; $p < 0.0001$), PVD (peritoneum 11 mm/mm2 [95% CI 9–13] vs. sublingual 23 mm/mm2 [95% CI 21–25]; $p < 0.0001$), PPV (peritoneum 88% [95% CI 79–97] vs. sublingual 99% [95% CI 99–100]; $p = 0.014$), and MFI (peritoneum 3 [IQR 2.3–3.0] vs. sublingual 3 [IQR 3.0–3.0]; $p = 0.012$). There was no difference in image acquisition time (peritoneum 2:34 min [95% CI 1: 49–3: 19] vs. sublingual 2:38 min [95% CI 1: 37–3: 32]; $p = 0.916$).

Conclusion

The peritoneal microcirculation was characterized by a low capillary density and a distinctive angioarchitecture. The possibility of peritoneal microcirculatory assessment offers promise for the study of peritoneal (patho-)physiology and (monitoring or detection of) associated diseases.

Keywords

In vivo microcirculation, Peritoneal microcirculation, Incident dark field imaging

INTRODUCTION

The peritoneum lines the abdominopelvic cavity and covers the majority of visceral organs(1). It is essential for the regulation of the intra-abdominal inflammatory response (2), exchange of peritoneal fluid (3), and prevention of fibrosis (4). Many pathological processes can affect the function of the peritoneal membrane. For instance, surgical trauma or inflammation and subsequent adhesion formation and fibrosis can decrease diffusion capacity, cause pain, impair female fertility, and hamper surgical interventions (4-6). If the peritoneum is affected by metastases of gastrointestinal or gynecological malignancies, this ultimately leads to peritoneal carcinomatosis, which is associated with a poor clinical outcome (7, 8). In case of endometriosis, endometrial tissue can affect the pelvic peritoneum, occasionally requiring surgery because of pain and infertility (9). The previous are examples of processes that are not sufficiently understood and for which optimal and effective treatment is often not possible. This stresses the necessity for improved understanding of peritoneal (patho-)physiology.

When peritoneal structure and function are compromised in response to pathological processes, this is expected to result in changes to the vasculature (1, 6, 10). Generally, the peritoneum is expected to have a relatively low blood vessel density; this can however be altered in response to disease (1, 11, 12). Therefore, improved understanding of peritoneal vascularization patterns can facilitate insight into associated pathology, detection of disease, and development of new treatment strategies (13).

Assessment of the peritoneal microcirculation should be considered a necessary first step. The introduction of handheld video microscopy imaging instruments has enabled direct visualization of the human microcirculation and creates an opportunity for imaging of the peritoneal microvasculature intraoperatively. So far, these devices were predominantly applied sublingually, to determine microvascular dysfunction in critically ill patients (14, 15). They have also been used to assess oral mucosal wound healing and appraise the microcirculatory characteristics of different human organ surfaces such as the brain, skin, gut, intestines, conjunctiva, vagina, and liver (16-24). This multitude of data emphasizes the importance of organ microcirculation and illustrates the broad applicability and potential advantages of these imaging modalities.

The current study aimed to use the CytoCam (25), a recently introduced third-generation handheld microscope based on incident dark field (IDF) imaging, for visualization and

assessment of the human peritoneal microcirculation. Measurements were performed during hepatic surgery in patients in which the peritoneum was not affected by pathology. It is hypothesized that peritoneal microcirculation is characterized by a relatively low vessel density and a distinctive vascular architecture. In order to be able to put such remarks into context, peritoneal microangioarchitecture and related quantitative parameters were compared to the current standard of sublingual microcirculatory examination.

MATERIALS AND METHODS

Patients

In this single-center observational study, men and women undergoing major liver surgery were recruited at the Department of Surgery of the Academic Medical Center of the University of Amsterdam. Surgical procedures were performed in accordance with established institutional protocols and standards of care. The study complied with ethical principles and appropriate regulatory requirements of the European Union and the Netherlands. All patients received full explanation of the study procedures and provided informed consent. The protocol was reviewed and approved by the Institutional Review Board of the Academic Medical Center under number W17_259.

Hemodynamic Parameters

Hemodynamic parameters such as heart rate, arterial blood pressure and peripheral capillary oxygen saturation were acquired. Stroke volume and central venous pressure parameters were assessed with the FloTrac system (FloTrac, Edwards Lifesciences, Irvine, CA, USA) (26). Arterial blood gas samples were collected to determine hemoglobin, pH and oxygen hemoglobin.

Microcirculatory Imaging

Peritoneal and sublingual microcirculation assessments were performed using IDF imaging (CytoCam Video Microscope System, Braedius Medical, Huizen, the Netherlands). This technique has been described extensively elsewhere (25, 27). In summary, the CytoCam uses green light (530 nm) produced from a ring of light-emitting diodes arranged near the tip of the probe. This green light epi-illuminates the tissue of interest and is absorbed by oxygenated and deoxygenated hemoglobin in red blood cells. Unabsorbed light is scattered into the surrounding tissues as red blood cells appear as

dark globules and can be recorded flowing within the lumen of the microvasculature. This results in sharp contour visualization of the microcirculation. The CytoCam is a digital computer-controlled camera that is lightweight (120 g) and shaped like a pen (length 220 mm, diameter 23 mm). It uses high-brightness green light-emitting diodes with a short illumination pulse time (2 ms) and a high spatial (14 megapixels) and temporal (60 fps) resolution. The combination of a factor 4 optical magnification and a large image area provides a field of view of 1.55 × 1.16 mm. The optical system provides an optical resolution of more than 300 lines/mm. The camera is connected to a device controller based on a powerful medical grade computer. Video clips are directly saved as digital AVI-DV files to a hard drive (25).

Data Acquisition

Measurements were performed 10 min after laparotomy, before the start of the surgery. Three peritoneal measurements were performed on the right lateral peritoneal side of the abdominal cavity. The region of interest was at least 20 cm away from the laparotomy incision site. During peritoneal measurements, the CytoCam was covered with a laparoscopy camera cover (Camera Cover, Microtek Medical BV, Zutphen, the Netherlands) to create a sterile work field. The camera was placed into contact with the peritoneal surface gently and perpendicularly, in order to prevent pressure-induced artifacts. Subsequently, 3 sublingual measurements were performed according to a standardized procedure (28). The sublingual microcirculation was assessed in the floor of the mouth, between the lingual frenulum and the sublingual fold.

Assessment of Angioarchitecture

The layout of the peritoneal and sublingual microcirculation was described and compared. Peritoneal angioarchitecture was examined and classified as 1 of 3 types of vascular patterns, as validated and described by Weber et al. (23). These vascular patterns include the appearance of capillary loops (score 1), the appearance of capillary loops in combination with capillary networks (score 2), and the appearance of only capillary networks (score 3).

Quantifying Microcirculation and Comparison of Microcirculatory Parameters

Tissue perfusion depends on the number, distribution, and diameters of the capillaries in combination with blood viscosity and driving pressure across the capillaries. The two main hemodynamic principles governing oxygen supply to tissue are convection and diffusion. Convection is quantified by flow, and diffusion is quantified by the

density of the perfused (= functional) microvessels. Flow is calculated by scoring the predominant type of flow across the microvasculature; this generates the microvascular flow index (MFI), a semiquantitative score ranging from 0 (no flow) to 3 (continuous flow) (29). To quantify diffusion, the total and perfused vessel densities (TVD and PVD, respectively) and the proportion of perfused vessels (PPV) were determined. The PPV was calculated by scoring all vessels with a flow score greater than 1, see Figure 1. PVD can be calculated by multiplying TVD by PPV. Both TVD and PVD are expressed in millimeters per square millimeter. Each score was determined for small microvessels with a cutoff diameter of 25 μm.

Practical Feasibility

Image acquisition time was recorded and used as an indicator of practical feasibility. This feasibility was defined as the time it took to acquire 3 stable video sequences of the microcirculation. This applied to both peritoneal and sublingual measurements.

Image Analysis

After image acquisition, video clips were saved to a hard drive, and subsequent image analysis was performed off-line and blinded by the 2 investigators (Z.U. and A.W.K.). Aforementioned parameters TVD, PVD, PPV, and MFI were determined by software-assisted analysis (AVA v3.2; Automated Vascular Analysis, Microvision, the Netherlands).

Statistical Analysis

Descriptive statistics was used to present the demographic variables. Non-Gaussian data sets are presented as medians and interquartile ranges (IQR), and normal Gaussian data sets are presented as means ± standard deviation. A nonparametric test was used for MFI (Wilcoxon signed-rank) and a paired t test was used for all other data. A 2-sided p value <0.05 was considered statistically significant. All data were analyzed using SPSS, version 23.0 for Windows (IBM Corp., Armonk, NY, USA).

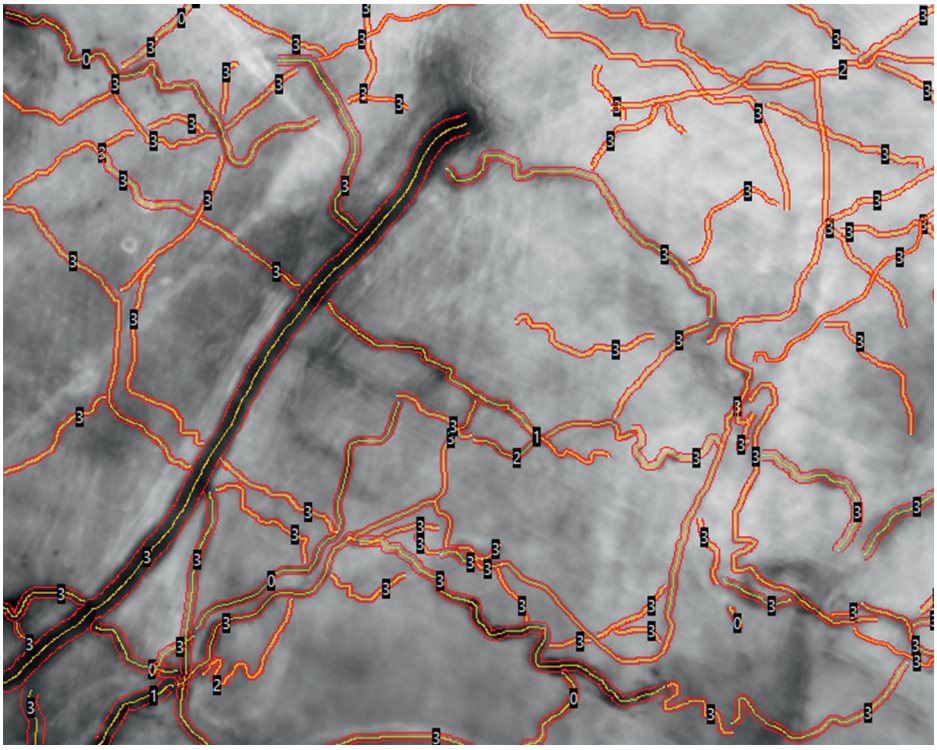

Figure 1. Peritoneal microcirculation in automated vascular analysis (AVA) analysis.
The proportion of perfused vessels (PPV), the perfused vessel density (PVD), and total vessel density (TVD) are determined by AVA software, as shown in this image. The PPV is calculated by scoring all vessels with a flow score greater than 1. PVD can be calculated by multiplying TVD and PPV. Both PVD and TVD are expressed as millimeters per square millimeter. Each score was determined for small microvessels with a cutoff diameter of 25 μm. The red lines show the vessel wall, the yellow lines show the vessel centerline. The numbers on the vessels show the flow within each vessel.

RESULTS

Patient Characteristics and Hemodynamic Parameters

Eighteen patients aged 32–78 years were enrolled in this study. The majority of patients (50%) were diagnosed with a cholangiocarcinoma for which they underwent a left or right hemihepatectomy (89%). Baseline characteristics of patients are presented in Table 1. Table 2 summarizes the hemodynamic conditions during surgery. A total of 108 measurements were obtained; 6 measurements were performed in each patient, of which 3 were on the peritoneum and 3 sublingually. Of these measurements, 10 peritoneal (9%) and 8 sublingual (7%) measurements were excluded for analysis due to poor image quality; the final data set was based on a total 90 measurements.

Table 1. Baseline characteristics. Data presented as medians or absolute numbers.

Sex (male/female), n	13/5	
Median age, years (IQR)	68	(55-73)
Median body mass index (IQR)	24.4	(21.3-27.6)
Smoker, *n* (%)	2	(11.1)
Diabetes, *n* (%)	3	(16.7)
Hypertension, *n* (%)	3	(16.7)
COPD, *n* (%)	0	(0)
Pathology, *n* (%)	2	(11.1)
CRLM	4	(22.2)
PHC	9	(50)
CGC	1	(5.6)
HCC	1	(5.6)
LA	1	(5.6)
NET		
Procedures, *n* (%)	9	(50)
Right hemihepatectomy	7	(38.8)
Left hemihepatectomy	1	(5.6)
Resection liver segment 4 and 8	1	(5.6)
Cholecystectomy		

COPD, chronic obstructive pulmonary disease; CRLM, colerectal liver metastasis; PHC, perihilar cholangiocarcinoma; CGC, cholangiocarcinoma; HCC, hepatocellular carcinoma; LA, liver adenoma; NET, neuroendocrine tumor.

Table 2. Hemodynamic parameters.

Systemic		73 ± 12
	Heart rate, *beats/min*	106 ± 21
	Systolic arterial pressure, *mmHg*	58 ± 11
	Diastolic arterial pressure, *mmHg*	73 ± 10
	Mean arterial pressure, *mmHg*	66 ± 17
	Stroke volume, *mL/beat*	7 ± 4
	Central venous pressure, *mmHg*	99 ± 1
	Peripheral oxygen saturation, *%*	36.4 ± 0.4
	Core temperature, *°C*	
Blood		7.8 ± 0.9
	Hemoglobin, *mmol/l*	7.40 ± 0.04
	pH	97.6 ± 0.9
	Oxygen hemoglobin, *%*	

Data are presented as means ± SD. Stroke volume: measurement obtained from 14/18 patients.

Assessment of Angioarchitecture and Morphological Features: Peritoneal versus Sublingual Microcirculation

Peritoneal Microcirculation

The peritoneal microcirculation is characterized by a quadrangular network of large, parallel vessels and their longitudinally orientated capillary branches (Fig. 2). The capillaries have a tortuous structure and make longer distances without connecting to other capillaries compared to the sublingual capillaries. The peritoneal microcirculation can be classified as a score 3 angioarchitecture: a vascular network is observed without the appearance of capillary loops. The peritoneal microcirculation was often flanked by fatty tissue; fat cells were therefore seen and appeared as large globular transparent structures. The quantity of fat cells varied between patients and was not consistent overall. The peritoneal microcirculation was flanked by fat cells in 10 (53% of the study population) patients. In 4 (21% of the study population) patients 100% of the field of view showed fat cells, and in 6 (32% of the study population) patients less than 50% of the field of view showed fat cells. Regardless of the presence of fat cells, microcirculatory assessment of the peritoneal microvasculature was easily possible due to their transparent appearance.

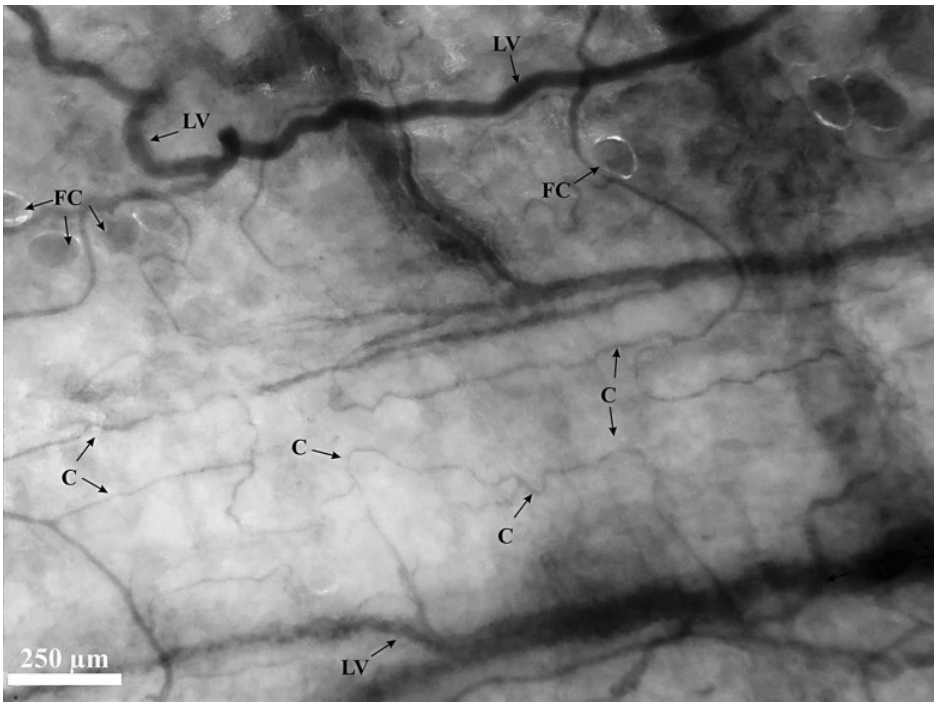

Figure 2. IDF image of the peritoneal microcirculation.
A screenshot from a CytoCam video clip of the peritoneal microcirculation. Quadrangular network of large parallel vessels (LV) and their longitudinally orientated tortuous capillary (C) branches. The peritoneal microcirculation is often flanked by fat cells (FC).

Sublingual Microcirculation

A sample of the sublingual microcirculation obtained with the CytoCam is shown in Figure 3. The large vessels of the microcirculation (diameter >25 µm) appear curly in structure. The capillaries had a less tortuous structure and make shorter distances with more interconnections to other capillaries as compared to the peritoneal microcirculation. The sublingual microcirculation also showed capillary loops (type 2 angioarchitecture); these loops primarily appeared in the most superficial layers just beneath the subepithelium of the mucosa, the papillary layer. These capillary loops do not appear in the deeper layers of the sublingual mucosa beyond the papillary layer, the microcirculation of this reticular layer is of a network type (type 3 angioarchitecture). According to the image quality score (17), only 30% of the image should contain capillary loops for a good quality sublingual microcirculatory assessment. These capillary loops were not observed in the peritoneal microcirculation.

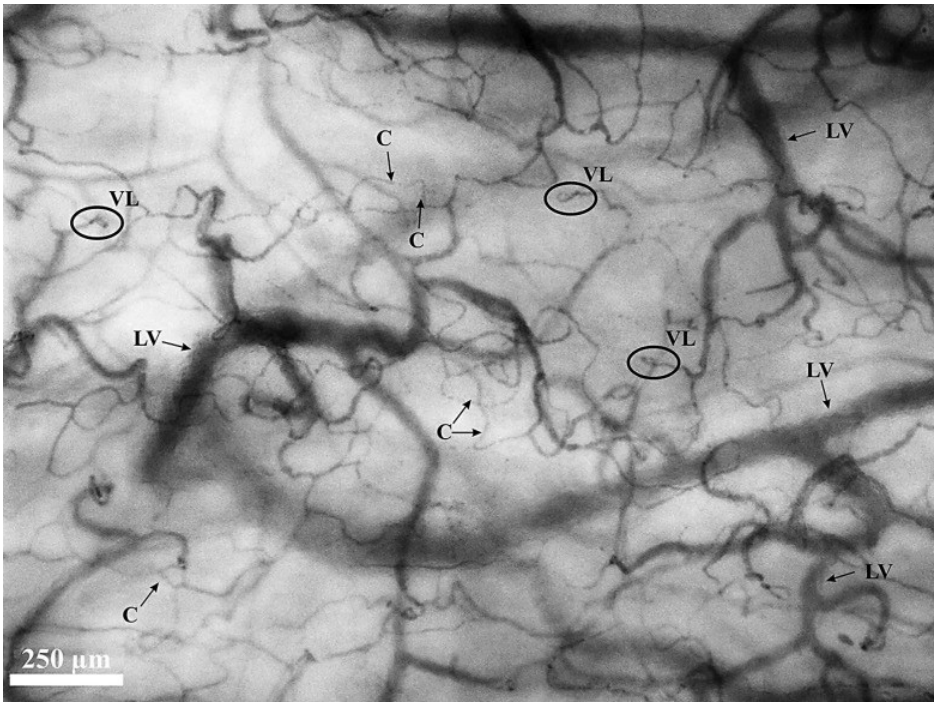

Figure 3. IDF image of the sublingual microcirculation.
A screenshot from a CytoCam video clip of the sublingual microcirculation. The large vessels (LV) of the microcirculation (diameter > 25 µm) show a curly structure. The capillaries (C) are randomly organized with the appearance of capillary vessel loops (VL) and make short distances that interconnect with other capillary vessels.

Microcirculatory Parameters

The peritoneal microcirculation was quantitatively characterized by low microvascular densities (Table 3). It showed a significantly lower TVD (peritoneum 12 mm/mm2 [95% CI 10.4--13.6] vs. sublingual 23 mm/mm2 [95% CI 21.1--24.7]; $p < 0.0001$) and PVD (peritoneum 11 mm/mm2 [95% CI 8.6--12.6] vs. sublingual 23 mm/mm2 [95% CI 20.9--24.5]; $p < 0.0001$). Moreover, differences between sublingual and peritoneal microcirculation were also observed with regard to PPV (peritoneum 88% [95% CI 78.5--96.6] vs. sublingual 99% [95% CI 98.5--99.7]; $p = 0.014$) and MFI (peritoneum 3 [IQR 2.3--3.0] vs. sublingual 3 [IQR 3.0--3.0]; $p = 0.012$). No significant differences with regard to image acquisition (i.e., time to 3 stable measurement acquisitions) were observed (peritoneum 2:34 min [95% CI 1:49--3:19] vs. sublingual 2:38 [95% CI 1:37--3:32]; $p = 0.916$).

Table 3. Microcirculatory parameters and image acquisition.

	Peritoneum	**Sublingual**	**Difference (95% CI)**	***p* value**
Median MFI (IQR)	3 (2.3 – 3.0)	3 (3.0 – 3.0)	0	0.012
PPV, %	88	99	-11 (-20,4 to -2.6)	0.014
TVD, *mm/mm2*	12.0	22.9	-10.9 (-13.5 to -8.4)	<0.0001
PVD, *mm/mm2*	10.6	22.7	-12.1 (-14.9 to -9.1)	<0.0001
Image acquisition, *min*	2:34	2:38	-0.04 (-1:09 to 1:02)	0.916

Data presented as means, unless otherwise indicated. CI: confidence interval (difference of the means). MFI: microvascular flow Index; PPV: proportion of perfused vessels; TVD: total vessel density; PVD: perfused vessel density.

In the oldest patient (79 years old) the peritoneal microcirculation was characterized by a lower microvascular density (peritoneal microcirculation: TVD 11.9 mm/mm2, PVD 11 mm/mm2, PPV 92.9%, MFI 2.7; sublingual microcirculation: TVD 27 mm/mm2, PVD 26.2 mm/mm2, PPV 97%, MFI 3) when compared to the peritoneal microvascular density of the youngest patients (33 years old) (peritoneal microcirculation: TVD 19.2 mm/mm2, PVD 18 mm/mm2, PPV 94%, MFI 2.7; sublingual microcirculation: TVD 25.4 mm/mm2, PVD 25.4 mm/mm2, PPV 100%, MFI 3).

When analyzing the microcirculatory parameters in groups with different intraoperative hemodynamic parameters (lower and higher median for stroke volume and central venous pressure), no significant differences between the groups were observed.

DISCUSSION

This study is the first to report on human peritoneal microcirculation assessed intraoperatively with IDF imaging. When compared to the sublingual microcirculation, assessment reveals significantly lower microvascular density and flow parameters, different morphological characteristics, and equal image acquisition times for each tissue. In order to discover the clinical value of the peritoneal microcirculation and to better understand the (patho-)physiology associated with the peritoneum, the ability to measure the peritoneal microcirculation is a necessary first step. These results demonstrate that assessment of peritoneal quantitative microcirculatory parameters and microcirculatory architecture is feasible, providing an opportunity for future research.

Within the scope of this study, the peritoneal tissue revealed a significantly lower microvessel density when compared to the sublingual microcirculation. This difference in density parameters (TVD, PVD) is most likely due to a different anatomy. The submesothelial stroma contains the peritoneal vasculature, of which vessels with a diameter of <100 µm (i.e., arterioles, capillaries, and venules) form the peritoneal microcirculation (1). The vasculature is organized in a single layer and the microvessels are arranged relatively spaciously, resulting in a low vessel density. This low vessel density possibly affects pathological processes such as the restrictive growth of metastases on the peritoneal membrane (8, 10). Interestingly, not only the density, but also the peritoneal flow parameters (PPV, MFI) were significantly lower when compared to the sublingual microcirculation.

In another study by de Bruin et al. (17), sidestream dark field imaging was used to examine and measure the microcirculation of the intestinal serosa. This study also revealed lower density parameters when compared to the sublingual microcirculation. However, the authors do not describe lower flow parameters. Hypothetically, the lower PPV and MFI could be the consequence of congestive pressure caused by the tip of the CytoCam. However, such pressure would be noticed by the researcher operating the device. This would be visible as compression of larger vessels and consequently as absence of flow in these vessels. No absence of flow was observed in the larger vessels. Another explanation might be the time point of the measurements. In our study, the measurements were obtained just after the laparotomy skin incision, whereas de Bruin et al. obtained measurements at the end of the surgery. This might lead to redistributed flow in the microcirculation. However, since our results regarding quantitative parameters of the sublingual microcirculation are in agreement with previous studies (19, 20, 25, 28), it seems that these differences cannot be attributed to the time point at which the measurements were performed.

The time for image acquisition was similar for peritoneal and sublingual assessments. The region of interest was easily accessible at both surfaces and there were no major movements that interfered with the stability of the device. In the case of sublingual assessments, removal of excessive saliva to avoid content artifacts took longest and determined the time to acquire a sublingual image. The difficulty that determined the time to acquire a peritoneal image was pressure artifacts. Use of an image or surface contact stabilizer, described previously by Balestra et al. (30) and validated by Bruin et al. (31), could help to avoid such pressure artifacts. This contact stabilizer is attached to

the tip of the device as a ring and adheres to the region of interest by applying a mild negative pressure. The surface of the imaging probe tip does not adhere to the surface and protects it from pressure artifacts and movements.

Some points of consideration should be addressed regarding study design and practicality. Firstly, the assessment of the peritoneal microcirculation with IDF imaging is only possible when patients undergo laparotomy. Therefore, these measurements can only be performed in a limited selection of patients. This illustrates a practical disadvantage of IDF imaging. With the devices that are currently available, intra-abdominal measurements can only be performed after laparotomy. Possibly, development of a laparoscopic device can facilitate future research and the clinical application of measuring intra-abdominal microcirculation during less invasive (laparoscopic) surgical procedures. On the other hand, it should be taken into account that the increased intra-abdominal pressure during laparoscopic surgery, i.e. the prolonged mechanical forces pushing against the peritoneum, could affect the peritoneal microcirculation.

Secondly, in an ideal situation, measurements would have been performed in a healthy control group. Nevertheless, we considered patients with liver pathology a relatively suitable patient population for measurements of unaffected peritoneum. In contrast to the visceral peritoneal veins that drain into the portal vein, parietal peritoneal veins drain directly into the vena cava, and flow is therefore not expected to be affected by liver pathology (32).

Thirdly, the measurements were performed during liver surgery in patients under general anesthesia. Some literature suggests this could cause anesthesia-induced tissue perfusion changes and affect microcirculatory parameters (33). Therefore, the measurements of the peritoneal and sublingual microcirculation were performed at the very beginning of the surgery, in order to minimize the effects of the surgery and the general anesthesia.

As mentioned above, this is the first study to report on the human peritoneal microcirculation assessed with IDF imaging. It provides unique data on in vivo dynamic and quantitative microvascular parameters and microvascular architecture. Such assessment in a pathological context should be considered a next step in future research regarding peritoneal tissue; it could facilitate the detection of pathology (peritoneal metastasis), assess reaction to treatment (the development of fibrosis after peritoneal dialysis, the effect of hyperthermal intraperitoneal chemotherapy) or contribute to

improved understanding of the pathophysiology of peritoneum-associated disease (peritoneal carcinomatosis, endometriosis).

In conclusion, IDF imaging is a promising technique for the visualization and assessment of the peritoneal microcirculation. Imaging of the peritoneal membrane reveals a distinctive microvascular layout in which angioarchitecture is characterized by a quadrangular network of longitudinally oriented capillaries, often flanked by fat cells. Microvascular density and flow parameters are significantly lower than parameters measured in the sublingual microcirculation.

Acknowledgments

The authors would like to express their gratitude to all subjects willing to participate in this research. They would also like to thank operating room personnel for their participation and facilitation of researchers performing measurements.

Disclosure Statement

Prof. Ince has developed SDF imaging and is listed as inventor on related patents commercialized by MicroVision Medical (MVM) under a license from the Academic Medical Center (AMC). He receives no royalties or benefits from this license. He has been a consultant for MVM in the past, but has not been involved with this company for more than five years now and holds no shares or stock. Braedius Medical, a company owned by a relative of Prof. Ince, has developed and designed a handheld microscope called CytoCam-IDF imaging. Prof. Ince has no financial relation with Braedius Medical of any sort, i.e., never owned shares, or received consultancy or speaker fees from Braedius Medical. Prof. Ince runs an internet site https.microcirculationacademy.org which offers services (e.g. training, courses, analysis) related to clinical microcirculation. The other authors declare that they have no competing interests

REFERENCES

1. van Baal JO, Van de Vijver KK, Nieuwland R, van Noorden CJ, van Driel WJ, Sturk A, et al. The histophysiology and pathophysiology of the peritoneum. Tissue Cell. 2017;49(1):95-105.
2. Topley N, Williams JD. Role of the peritoneal membrane in the control of inflammation in the peritoneal cavity. Kidney international Supplement. 1994;48:S71-8.
3. Fedorko ME, Hirsch JG. Studies on transport of macromolecules and small particles across mesothelial cells of the mouse omentum. I. Morphologic aspects. Experimental cell research. 1971;69(1):113-27.
4. de Lima SM, Otoni A, Sabino Ade P, Dusse LM, Gomes KB, Pinto SW, et al. Inflammation, neoangiogenesis and fibrosis in peritoneal dialysis. Clinica chimica acta; international journal of clinical chemistry. 2013;421:46-50.
5. Gomel V, Koninckx PR. Microsurgical principles and postoperative adhesions: lessons from the past. Fertil Steril. 2016;106(5):1025-31.
6. Koninckx PR, Gomel V, Ussia A, Adamyan L. Role of the peritoneal cavity in the prevention of postoperative adhesions, pain, and fatigue. Fertil Steril. 2016;106(5):998-1010.
7. Lee K TF, Prat J. Tumors of the ovary and peritoneum. World Health Organization Classification of Tumours: Pathology and Genetics of Tumours of the Breast and Female Genital Organs. 2003:117.
8. Lemoine L, Sugarbaker P, Van der Speeten K. Pathophysiology of colorectal peritoneal carcinomatosis: Role of the peritoneum. World journal of gastroenterology. 2016;22(34):7692-707.
9. Mahmood TA, Templeton A. Prevalence and genesis of endometriosis. Human reproduction (Oxford, England). 1991;6(4):544-9.
10. Solass W, Horvath P, Struller F, Königsrainer I, Beckert S, Königsrainer A, et al. Functional vascular anatomy of the peritoneum in health and disease2016.
11. Blackburn SC, Stanton MP. Anatomy and physiology of the peritoneum. Seminars in pediatric surgery. 2014;23(6):326-30.
12. Rippe B, Rosengren BI, Venturoli D. The peritoneal microcirculation in peritoneal dialysis. Microcirculation (New York, NY : 1994). 2001;8(5):303-20.
13. Flessner MF, Lofthouse J, Zakaria ER. Improving contact area between the peritoneum and intraperitoneal therapeutic solutions. Journal of the American Society of Nephrology : JASN. 2001;12(4):807-13.
14. Spronk PE, Ince C, Gardien MJ, Mathura KR, Oudemans-van Straaten HM, Zandstra DF. Nitroglycerin in septic shock after intravascular volume resuscitation. Lancet. 2002;360(9343):1395-6.
15. Goedhart PT, Khalilzada M, Bezemer R, Merza J, Ince C. Sidestream Dark Field (SDF) imaging: a novel stroboscopic LED ring-based imaging modality for clinical assessment of the microcirculation. Opt Express. 2007;15(23):15101-14.

16. Mathura KR, Bouma GJ, Ince C. Abnormal microcirculation in brain tumours during surgery. Lancet. 2001;358(9294):1698-9.
17. de Bruin AF, Kornmann VN, van der Sloot K, van Vugt JL, Gosselink MP, Smits A, et al. Sidestream dark field imaging of the serosal microcirculation during gastrointestinal surgery. Colorectal disease : the official journal of the Association of Coloproctology of Great Britain and Ireland. 2016;18(3):O103-10.
18. Klijn E, Van Zijderveld R, Den Uil C, Ince C, Bakker J. Conjunctival microcirculation in patients with traumatic brain injury. Critical Care. 2008;12(Suppl 2):P106-P.
19. Edul VSK, Ince C, Navarro N, Previgliano L, Risso-Vazquez A, Rubatto PN, et al. Dissociation between sublingual and gut microcirculation in the response to a fluid challenge in postoperative patients with abdominal sepsis. Annals of Intensive Care. 2014;4:39-.
20. Boerma EC, Kuiper MA, Kingma WP, Egbers PH, Gerritsen RT, Ince C. Disparity between skin perfusion and sublingual microcirculatory alterations in severe sepsis and septic shock: a prospective observational study. Intensive Care Med. 2008;34(7):1294-8.
21. Puhl G, Schaser KD, Vollmar B, Menger MD, Settmacher U. Noninvasive in vivo analysis of the human hepatic microcirculation using orthogonal polorization spectral imaging. Transplantation. 2003;75(6):756-61.
22. De Backer D, Creteur J, Preiser JC, Dubois MJ, Vincent JL. Microvascular blood flow is altered in patients with sepsis. American journal of respiratory and critical care medicine. 2002;166(1):98-104.
23. Weber MA, Milstein DM, Ince C, Oude Rengerink K, Roovers JP. Vaginal microcirculation: Non-invasive anatomical examination of the micro-vessel architecture, tortuosity and capillary density. Neurourology and urodynamics. 2015;34(8):723-9.
24. Lindeboom JA, Mathura KR, Aartman IH, Kroon FH, Milstein DM, Ince C. Influence of the application of platelet-enriched plasma in oral mucosal wound healing. Clinical oral implants research. 2007;18(1):133-9.
25. Aykut G, Veenstra G, Scorcella C, Ince C, Boerma C. Cytocam-IDF (incident dark field illumination) imaging for bedside monitoring of the microcirculation. Intensive care medicine experimental. 2015;3(1):40.
26. Manecke GR. Edwards FloTrac sensor and Vigileo monitor: easy, accurate, reliable cardiac output assessment using the arterial pulse wave. Expert review of medical devices. 2005;2(5):523-7.
27. Hutchings S, Watts S, Kirkman E. The Cytocam video microscope. A new method for visualising the microcirculation using Incident Dark Field technology. Clinical hemorheology and microcirculation. 2016;62(3):261-71.
28. Ocak I, Kara A, Ince C. Monitoring microcirculation. Best practice & research Clinical anaesthesiology. 2016;30(4):407-18.
29. Boerma EC, Mathura KR, van der Voort PH, Spronk PE, Ince C. Quantifying bedside-derived imaging of microcirculatory abnormalities in septic patients: a prospective validation study. Crit Care. 2005;9(6):R601-6.

30. Balestra GM, Bezemer R, Boerma EC, Yong Z-Y, Sjauw KD, Engstrom AE, et al. Improvement of Sidestream Dark Field Imaging with an Image Acquisition Stabilizer. BMC Medical Imaging. 2010;10(1):15.
31. de Bruin AF, Tavy A, van der Sloot K, Smits A, Van Ramshorst B, Boerma CE, et al. Use of an Image Acquisition Stabilizer Improves Sidestream Dark Field Imaging of the Serosa during Open Gastrointestinal Surgery. Journal of vascular research. 2016;53(3-4):121-7.
32. Khanna R, Krediet, R.T. Chapter 4: the peritoneal microcirculation in peritoneal dialysis. Nolph and Gokal's Textbook of Peritoneal Dialysis, 3d ed Springer. 2009.
33. Turek Z, Sykora R, Matejovic M, Cerny V. Anesthesia and the microcirculation. Seminars in cardiothoracic and vascular anesthesia. 2009;13(4):249-58.

8 Poor perfusion of the microvasculature in peritoneal metastases of ovarian cancer

AW Kastelein
LMC Vos
JOAM van Baal
JJ Koning
VVV Hira
R Nieuwland
WJ van Driel
Z Uz
TM van Gulik
J van Rheenen
C Ince
JPWR Roovers
CJF van Noorden
CAR Lok.

Clin Exp Metastasis. 2020 Apr;37(2):293-304.

ABSTRACT

Most women with epithelial ovarian cancer (EOC) suffer from peritoneal carcinomatosis upon first clinical presentation. Extensive peritoneal carcinomatosis has a poor prognosis and its pathophysiology is not well understood. Although treatment with systemic intravenous chemotherapy is often initially successful, peritoneal recurrences occur regularly. We hypothesized that insufficient or poorly-perfused microvasculature may impair the therapeutic efficacy of systemic intravenous chemotherapy but may also limit expansive and invasive growth characteristics of peritoneal EOC metastases. In 23 patients with advanced EOC or suspicion thereof, we determined the angioarchitecture and perfusion of the microvasculature in peritoneum and in peritoneal metastases using incident dark field (IDF) imaging. Additionally, we performed immunohistochemical analysis and 3-dimensional (3D) whole tumor imaging using light sheet fluorescence microscopy of IDF-imaged tissue sites. In all metastases, microvasculature was present but the angioarchitecture was chaotic and the vessel density and perfusion of vessels was significantly lower than in unaffected peritoneum. Immunohistochemical analysis showed expression of vascular endothelial growth factor and hypoxia inducible factor 1α, and 3D imaging demonstrated vascular continuity between metastases and the vascular network of the peritoneum beneath the elastic lamina of the peritoneum. We conclude that perfusion of the microvasculature within metastases is limited, which may cause hypoxia, affect the behavior of EOC metastases on the peritoneum and limit the response of EOC metastases to systemic treatment.

Keywords
Microvasculature, microcirculation, EOC, peritonitis carcinomatosa, incident dark field imaging.

ABBREVIATIONS

AVI	audio video interleave
CD31	cluster of differentiation 31
DCM	dichloromethane
EOC	epithelial ovarian cancer
HGSC	high grade serous carcinoma
HIF-1α	hypoxia inducible factor 1α
HIPEC	hyperthermic intraperitoneal chemotherapy
IDF	incident dark field
IP	intraperitoneal
IV	intravenous
LEDs	light emitting diodes
PAX8	paired box gene 8
PBS	phosphate buffered saline
PC	peritoneal carcinomatosis
PEL	peritoneal elastic lamina
PPV	proportion of perfused vessels
PTwH	phosphate buffered saline Tween with heparin
PVD	perfused vessel density
RT	room temperature
TVD	total vessel density
VEGF	vascular endothelial growh factor

INTRODUCTION

Epithelial ovarian cancer (EOC) has the highest mortality of all gynecological malignancies. Worldwide, an estimated 140,000 women die annually from this type of cancer (1, 2). At the time of first clinical presentation, over 70% of women with EOC have advanced stage disease that has spread beyond the pelvis to the peritoneum of the abdominal cavity. This peritoneal carcinomatosis (PC) produces malignant ascites and impairs bowel movements, which has a severe impact on quality of life and survival (3, 4).

PC poses a challenge for clinicians and researchers. Complete cytoreductive surgery is difficult, especially when the small bowel is affected by PC. Although systemic intravenously (IV)-administered chemotherapy is often initially effective, recurrences occur in more than 60% of women (3, 5). Moreover, interactions between metastatic EOC cells and the peritoneum are still an enigma: it is unclear why peritoneal metastases of EOC remain small (1-2 mm^3) and why spontaneous invasive growth of EOC cells through the parietal peritoneal layers does not occur (6-8).

Formation of new blood vessels (angiogenesis) and a new vascular network is required for tumors to grow larger than 1-2 mm^3 and is considered a prerequisite for tumor progression (9-13). Previous immunohistochemical studies reported increased vascularization in metastases and the surrounding peritoneum (14-16). However, the perfusion of the microvasculature was not investigated in these *ex vivo* studies and it has not been clearly described whether there is vascular continuity between peritoneal metastases and the vascular network of the submesothelial stroma of the peritoneum (6).

Incident dark field (IDF) imaging enables real-time *in vivo* visualization of the human microvasculature, allowing quantification of perfusion (17). We recently visualized the peritoneal microvasculature with IDF imaging and we showed that the peritoneal microvasculature consists of well-perfused vessels forming a quadrangular network, often embedded in fat tissue (18).

We hypothesized that the microvasculature in peritoneal EOC metastases is insufficient, which may not only limit expansive and invasive growth, but also impair the therapeutic efficacy of systemic IV chemotherapy. Therefore, the present study aimed to investigate the angioarchitecture and perfusion of the microvasculature in peritoneum and peritoneal

metastases of EOC. We performed IDF imaging in patients with and without EOC and/or PC and we performed histology and immunohistochemistry on tissue derived from IDF-imaged sites. Three-dimensional (3D) whole tumor imaging was performed using light sheet fluorescence microscopy, to allow a circumferential analysis of metastases and to investigate whether the microvasculature of metastases is continuous with that of the surrounding submesothelial stroma.

MATERIALS AND METHODS

Participants

In this prospective single-center observational study, we recruited women undergoing either cytoreductive surgery for advanced EOC or exploratory laparotomy because of a suspicious adnexal mass. This study was performed at the Department of Gynecological Oncology of the Netherlands Cancer Institute, Antoni van Leeuwenhoek Hospital, Amsterdam, The Netherlands. Participant characteristics were retrieved from medical charts. Exclusion criteria were recent cardiovascular events, use of anticoagulant or immunosuppressant medication and language barriers compromising informed consent. Participants that were treated with neoadjuvant chemotherapy were not excluded. The study was in compliance with ethical principles and regulatory requirements according to the Declaration of Helsinki. All study participants received a verbal and written explanation of the study procedures. Informed consent was obtained from all individual participants included in the study. The protocol was reviewed by the Institutional Review Board of the Antoni van Leeuwenhoek Hospital and permission was granted on August 16, 2017.

Vital parameters

Parameters such as heart rate, blood pressure, body temperature, hemoglobin levels and hematocrit were acquired at the time of microcirculatory imaging. An hypotensive event was characterized as a drop of >20% in mean arterial pressure or a mean arterial pressure of <60 mm Hg (19). Use of inotropic medicine was recorded as total quantity of administered drug until time of imaging.

Microcirculatory imaging

The microcirculation was visualized with IDF imaging (CytoCam; Braedius Medical, Huizen, the Netherlands) (20). The CytoCam is a third-generation hand-held video

microscope which weighs 120 g and is shaped like a pen (length 220 mm, diameter 23 mm). The CytoCam produces green light (530 nm) produced by concentrically placed light-emitting diodes (LEDs), providing epi-illumination of the tissue. The green light is absorbed by hemoglobin in erythrocytes, allowing erythrocytes to be imaged and recorded as a real-time representation of the local microcirculation (21). The CytoCam uses a short illumination pulse time (2 ms) and a high spatial (14 megapixels) and temporal (60 frames per second) resolution. A total field of view of 1.55×1.16 mm was recorded at a x4 optical magnification. The system provides an optical resolution of more than 300 lines/mm. The CytoCam is connected to a device controller which in turn is connected to a laptop, to record and store video clips as digital audio video interleave (AVI) files (20).

Data acquisition

Microcirculatory imaging was performed during surgery as soon as the surgical retractor (Omni-Tract Surgical, St. Paul, MN, USA) was positioned, either before cytoreductive surgery or after removal of the enlarged adnexa. The latter was sometimes necessary to obtain clear vision and access to the pelvic peritoneum. During imaging, the CytoCam was covered with a sterile latex-free probe cover (Microtek Medical, Zutphen, the Netherlands). The camera was operated by trained researchers (AWK, LMCV or CARL). Excess peritoneal fluid was removed using gauze or suction. To prevent pressure-induced artefacts, the camera was placed in light contact with the peritoneal surface in a perpendicular position. In case of a macroscopically normal aspect of the peritoneum, a total of 6 video clips were recorded on specific locations: 1) the paracolic gutter left and right, 2) the ovarian fossa left and right, 3) on top of the bladder left and right. In participants with PC, video clips were recorded by placing the CytoCam directly on top of metastatic depositions, and adjacent to the tumors (<1-2 cm). All imaged metastases had a diameter ≥ 1 mm. Aforementioned specific locations of the peritoneum were also imaged in participants with PC. At each area of interest, one recording of 3 seconds was made, unless imaging was suboptimal (e.g. due to image drifting or loss of focus; in those cases, a second or even third recording was performed).

Quality score

The quality of each video clip was assessed using a scoring system based on 6 parameters (illumination, focus, content, stability, pressure, duration) (22). When not all 6 parameters scored positively, the recording was not analyzed.

Quantification of the microcirculation and comparison of microcirculatory parameters

The microcirculation was quantified in the capillaries only, since these are the (functional) exchange vessels (23). We considered any vessel with a diameter of <20 μm to be a capillary, which is also the general consensus in the literature (23-25). We calculated the total vessel density (TVD, mm/mm^2) and the quality of the blood flow in the capillaries (0, no flow; 1, sluggish flow; 2, intermittent flow; 3, continuous flow). Subsequently, the perfused vessel density (PVD, mm/mm^2) was determined and the percentage of perfused vessels (PPV, %) was calculated as ratio of all vessels with flow (score ≥ 1) and TVD.

Image analysis

Analysis of images was performed offline. The analyst was blinded for the macroscopic aspects of the imaged sites. Above-mentioned parameters PVD, PPV and TVD were calculated with the use of software-assisted analysis (AVA 3.2; Automated Vascular Analysis, Amsterdam UMC, location AMC, Amsterdam, the Netherlands).

Statistical analysis

Descriptive statistics were used to analyze the demographic variables. Non-normally distributed data were presented as medians with interquartile ranges. The non-parametric Mann-Whitney-U test was used for comparing medians of TVD, PVD and PPV across the different non-normally distributed groups. Normally-distributed data were presented as means with standard deviations. A two-sided P value <0.05 was considered to indicate statistically significant differences. All data were analyzed using SPSS, version 23.0 for Windows (IBM, Armonk, NY, USA). We did not perform a power calculation prior to the study, since this was a first pilot study with unknown effect sizes. We aimed to include at least 10 participants with PC. However, because it was not always known prior to inclusion whether PC was present, it was unknown how many participants had to be included to reach the target of 10 participants with PC.

Histology

Biopsies were taken from metastases and from peritoneum with a normal aspect (control), all from different patients. Prior to resection of the biopsies, their localization was imaged with the CytoCam. Tissue samples were fixed using buffered 4% para-formaldehyde immediately after harvesting. Samples were either used for 1) immunohistochemistry and conventional 2D microscopy or 2) 3D whole tumor imaging using light sheet fluorescence microscopy.

Immunohistochemistry

Chromogenic immunohistochemistry was performed on 5 µm-thick paraffin sections of the tissue samples using Benchmark ULTRA staining (Roche Diagnostics, Indianapolis, MN, USA), using the method that was recently shown to be the optimum immunohistochemical method to be applied to paraffin sections (26). Dewaxing was performed by incubation of the sections in xylene (VWR Chemicals, Atlanta, GA, USA) for 10 min and rinsing in 100% ethanol (Merck, Darmstadt, Germany). Sections were treated with 100% methanol (Merck) containing 0.3% hydrogen peroxide (Merck) for 10 min to block endogenous peroxidase activity and to reduce non-specific background staining, followed by a washing step in distilled water. Antigen-retrieval was performed using Tris-EDTA buffer (pH 8.5) followed by a washing step in distilled water and 3 washing steps of 5 min each using Tris-buffered saline (TBS; pH = 7.6) containing 0.1% Triton-X (Sigma-Aldrich, St. Louis, MO, USA). Sections were encircled with a PAP pen (Dako, Glostrup, Denmark) and incubated using TBS containing 3% normal goat serum (Dako) and 0.1% Triton-X for 1 h to further reduce non-specific background staining and for permeabilization of the sections. Sections were subsequently incubated overnight at 4 °C with primary antibodies against paired-box gene 8 (PAX-8 363M-15; clone MRQ50, dilution 1:50; Cellmarque, Rocklin, CA, USA), which specifically stains EOC cells, VEGF (sc-152; Santa Cruz, TX, USA), cluster of differentiation 31 (CD31; M0823, clone JC70A, dilution 1:250, Dako), which specifically stains endothelial cells (26-29). Next, sections were incubated with 3,3'-diaminobenzidine (Dako) for 10 min, followed by one washing step with tap water to stop the peroxidase enzyme reaction. Sections were then incubated for 30 sec in hematoxylin (Sigma-Aldrich) for nuclear counterstaining. Sections were again placed in running tap water for 5 min and then in distilled water. Finally, sections were dehydrated by subsequently dipping in 70%, 96% and 100% ethanol (Merck) and 3 times dipping in xylene (VWR Chemicals). All incubations were performed at room temperature (RT) unless stated otherwise. An amplification step with a secondary horseradish peroxidase (HRP) antibody (poly-HRP) was performed on the PAX-8-stained sections. Finally, sections were covered with the synthetic mountant Pertex (Histolab, Götenburg, Sweden).

Fluorescence immunohistochemical staining of HIF-1α was performed, following the method as described by Hira et al. (30). Paraffin sections were dewaxed by incubation of the sections in xylene (VWR) for 5 min, followed by rinsing in 100%, 96% and 70% ethanol (Merck), respectively. Antigen-retrieval was performed in a microwave using 100 mM citrate buffer containing 0.1% Triton-X, pH 6.0, for 20 min at 98 °C,

followed by cooling for 20 min and a washing step in PBS. Sections were encircled with a PAP pen (Dako) and incubated with PBS containing 10% normal goat serum (Dako) and 0.1% Triton-X for 1 hr at RT, to reduce non-specific background staining and for permeabilization of the sections. Sections were subsequently incubated overnight at 4 °C with primary antibody (mouse anti-human HIF-1α, Abcam (ab8366), dilution 1:100) diluted in PBS containing 1% BSA. Sections were washed 3 times using PBS containing 1% BSA. Alexa Fluor 546-conjugated goat anti-mouse antibodies were used as secondary antibodies in a dilution of 1:200 in PBS containing 1% BSA for 1 hr at RT. Next, sections were washed in PBS for 5 min and coverslipped using Prolong Gold (Life Technologies, Carlsbad, CA, USA) mounting medium. Afterwards, sections were sealed with nail polish and dried overnight.

Control incubations were performed in the absence of the primary antibody. Chromogenic stained sections were analyzed by light microscopy (Olympus BX51 microscope, Leiderdorp, the Netherlands) and images were acquired using the Olympus cellSense Standard software. Fluorescence imaging was performed using a Nikon Eclipse Ti-E inverted microscope (Nikon Instruments, Melville, NY, USA) and the Nikon NIS-Elements AR 4.13.04 software.

3D whole tumor imaging using light sheet fluorescence microscopy

For 3D imaging, samples were treated according to the iDisco protocol with minor adaptions (31). Samples were dehydrated with methanol/H_2O series: 20%, 40%, 60%, 80%, 100%, 100%; 1 h each and were incubated overnight in 66% dichloromethane (DCM)/33% methanol at RT under continuous slow shaking. Samples were then washed twice in 100% methanol at RT, subsequently chilled at 4°C and overnight bleached in fresh 5% H_2O_2 in methanol. Next day, samples were rehydrated with methanol/H_2O series: 80%, 60%, 40%, 20%, PBS; 1 h each at RT and subsequently washed 2x for 1 h in PBS + 0.2% Triton X-100 at RT. For immunolabeling, samples were incubated for 2 days in permeabilization solution (PBS, 0.4% Triton X-100, 20% DMSO, 0.3 M glycine) at 37 °C and subsequently blocked in blocking solution (PBS/0.2% Triton X-100/10% DMSO/6% donkey serum) for 1 day at 37 °C. Samples were washed in PBS/0.2% Tween-20 with 10 µg/ml heparin (PTwH) for 1 h twice, then incubated in mouse anti-human CD31 antibodies (clone EN4; dilution 1:200; Monosan; Sanbio; Uden) in PTwH/5% DMSO/3% donkey serum at 37 °C for 4 days under continuous shaking. Samples were washed with PTwH for 10 min, 15 min, 30 min, 1 h and every 2 h until the end of the day and incubated with secondary antibody in PTwH, 3% donkey serum for 4 days at 37°, under continuous slow shaking. Samples were washed in PTwH for 10 min,

15 min, 30 min, 1 h, every 2 h and overnight at RT. After immunolabeling, samples were embedded in 2% low melting agarose (Sigma-Aldrich) to facilitate handling of the samples and dehydrated in methanol/H_2O series: 20%, 40%, 60%, 80%, 100%, 1 h each at RT. Samples were left overnight in 100% methanol and the next day incubated for 3 h in 66% DCM/33% methanol at RT, 2x in 100% DCM (Sigma) for 15 min and finally incubated in dibenzyl ether (Sigma) (no shaking) until samples were transparent. Upon clearing, samples were immediately imaged with light sheet fluorescence microscopy using the Ultramicroscope (LaVision BioTec, Bielefeld, Germany) (28). Inspector Software (LaVision, BioTec) was used for settings adjustment and image acquisition. Image analysis was performed using Imaris 9.2 or higher (28).

RESULTS

Twenty-three participants were included in the study. Participant and disease characteristics as well as perioperative parameters that may have affected the peritoneal microcirculation are summarized in Table 1.

A total of 199 video clips were recorded, of which 118 videos were accepted for analysis after quality assessment. Exclusion of videos most often occurred because of insufficient stability (32). Based on histopathology of the tumor and macroscopic aspects of the peritoneum, participants were divided into 3 groups: benign (n=3, 17 video clips), EOC with no visible PC (n=10, 55 video clips) and EOC with visible PC (n=10, 46 video clips).

Table 1. Characteristics and perioperative parameters of the participants and the disease state.

	All participants (n=23)	Benign (n=3)	EOC (n=10)	PC of EOC (n=10)
Participant characteristics				
Age, years	69 (58 – 75)	69 (68 – x)	60 (50 – 72)	66 (71 – 80)
Smoking, n (%)	3 (13.0)	1 (33.3)	2.5 (0 – 21.3)	0 (0 –11)
Diabetes, n (%)	4 (17.3)	1 (33.3)	0 (0)	3 (30)
Hypertension, n (%)	5 (21.7)	0 (0)	2 (20)	3 (30)
Cardiovascular event, n (%)	8 (34.8)	2 (66.7)	1 (10)	5 (50)
History abdominal surgery, n (%)	15 (65.2)	2 (66.7)	8 (80)	5 (50)
Disease characteristics				
Histotype				
Serous, n (%)	15 (65.2)	0 (0)	7 (70)	8 (80)
Clear-cell, n (%)	1 (4.3)	0 (0)	1 (10)	0 (0)
Granulosa-cell, n (%)	1 (4.3)	0 (0)	1 (10)	0 (0)
Mucinous, n (%)	1 (4.3)	0 (0)	1 (10)	1 (10)
Endometrioid, n (%)	1 (4.3)	0 (0)	0 (0)	0 (0)
Unknown PAX8-positive, n (%)	1 (4.3)	0 (0)	1 (10)	1 (10)
Grade, high grade, n (%)	14 (60.9)	0 (0)	6 (60)	8 (80)
FIGO stage				
Ic, n (%)	4 (17.4)	0 (0)	4 (40)	0 (0)
IIb, n (%)	1 (4.3)	0 (0)	0 (0)	1 (10)
IIIc, n (%)	9 (39.1)	0 (0)	2 (20)	7 (70)
Iva, n (%)	3 (13.0)	0 (0)	1 (10)	2 (20)
IVb, n(%)	3 (13.0)	0 (0)	3 (30)	0 (0)
Peritoneal involvement, n (%)	10 (43.5)	0 (0)	0 (0)	10 (100)
Simplified PCI	3 (0 – 6.75)	0 (0)	3 (0 – 3)	7 (5.3 – 11.5)
Regionscore	1.5 (0 –3.75)	0 (0)	1 (0 –2)	5 (3 – 6.3)
Chemotherapy, n (%)	15 (65.2)	0 (0)	7 (70)	8 (80)
Surgical characteristics				

Table 1. Characteristics and perioperative parameters of the participants and the disease state (continued).

	All participants (n=23)	Benign (n=3)	EOC (n=10)	PC of EOC (n=10)
Explorative, n (%)	5 (21.7)	3 (100)	2 (20)	0 (0)
CR post chemotherapy, n (%)	14 (60.9)	0 (0)	6 (60)	8 (80)
CR in recurrent disease, n (%)	4 (17.3)	0 (0)	2 (20)	2 (20)
Anesthesia				
Intravenous and epidural, n (%)	23 (100)	3 (100)	10 (100)	10 (100)
Hypotensive event, n (%)	9 (39.1)	0 (0)	5 (50)	4 (40)
Norepinephrine, mg	0.3 (0.2 – 0.4)	0.3 (0.3 – x)	0.2 (0.15 – 0.3)	0.4 (0.2 –1.0)
Ephedrine, mg	10 (0 – 20.0)	0 (0)	10 (0 – 21.3)	12.5 (0 –21.3)
Per-operative parameters				
Heart rate, bpm	64 (57 – 71)	62 (57 – x)	65 (56.3 – 73.8)	64.5 (55 – 93)
Systolic pressure, mmHg	105 (81 – 130)	116 (66 – x)	93 (77.8 – 137)	107 (90 – 125)
Diastolic pressure, mmHg	55 (44 – 70)	67 (38 – x)	54.5 (44.3 – 76)	54 (44 – 66)
Mean pressure, mmHg	69 (54 – 84)	82 (49 – x)	65.5 (50 – 76)	70 (60 – 79)
Core temperature, c	36.1 (35.7 – 36.1)	35.9 (35.4 – x)	36.1 (35.6 – 36.6)	36.1 (35.9 – 36.4)
Hemoglobin, mmol/L	7.4 (6.8 – 7.9)	8.1 (7.2 – x)	7.7 (7.0 – 8.0)	6.9 (6.6 –7.8)
Hematocrit, fraction	0.35 (0.32 – 0.39)	0.39 (0.36 – x)	0.35 (0.34 – 0.40)	0.33 (0.31 –0.37)

Data are presented as medians and interquartile ranges unless indicated otherwise. Abbreviations: EOC, epithelial ovarian cancer; PC, peritoneal carcinomatosis; FIGO, international federation of Gynecology and Obstetrics; CR, cytoreductive, PCI, peritoneal cancer index; PAX8, paired box gene 8; X, upper interquartile range value was not available.

IDF imaging – qualitative analysis of angioarchitecture

IDF imaging of the microvasculature revealed extensive differences between the microvascular networks in peritoneum and peritoneal metastases (Figure 1A-D). The angioarchitecture in peritoneum without peritoneal metastases was characterized by an organized network structure and was comparable in all groups (benign, EOC without PC and EOC with PC) (Figure 1A-B). In all peritoneal metastases, a disorganized network of heterogeneous capillaries was observed (Figure 1C-D). The microvasculature surrounding metastases showed functional, parallel-aligned capillaries, that originated from the capillaries of normal peritoneum and were directed towards the metastases (Figure 1E-F).

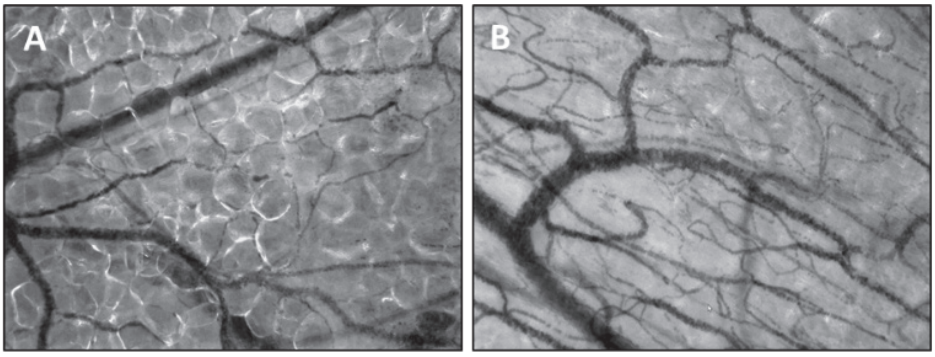

Normal peritoneum

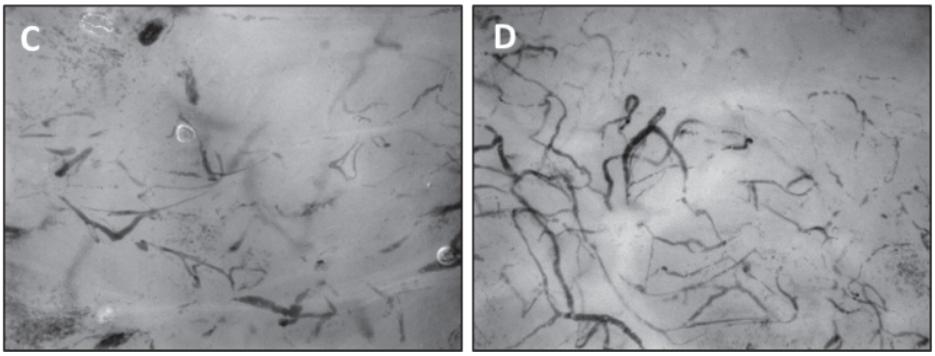

Peritoneal metastasis

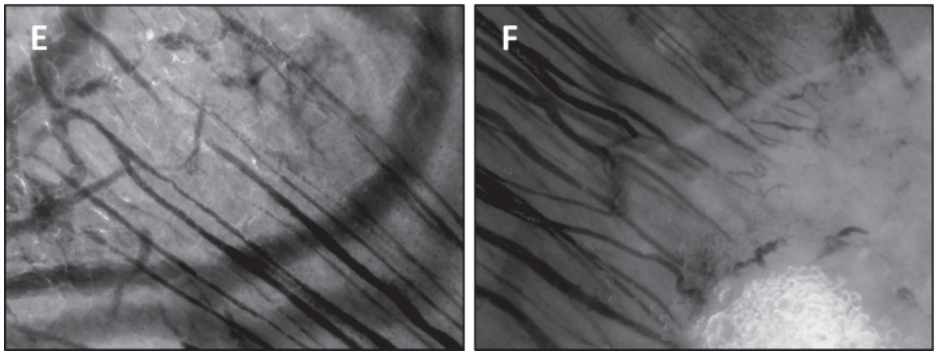

Figure 1. Screenshots from CytoCam – incident dark field imaging of the peritoneal microcirculation. Each image represents an imaged area of 1.55 x 1.16 mm. A, B. The microcirculation (black) in peritoneum with a macroscopically normal aspect showing continuous blood flow. The vessels were embedded in fat tissue and the angioarchitecture was characterized by an organized network of capillaries. C, D. The microcirculation within a peritoneal metastasis of EOC. The angioarchitecture was distinctly different from that in unaffected peritoneum. The blood flow in the microvasculature was either sluggish or absent. E, F. The microcirculation surrounding a peritoneal metastasis. E. Normal peritoneal microvasculature is indicated by NV. Parallel-aligned capillaries originate from the normal microvasculature and are directed towards a metastasis. F. Parallel-aligned capillaries that originate from the normal vasculature are directed towards a metastasis (M). Red line, boundary of the metastasis.

IDF imaging – quantitative analysis of microvascular parameters

Video clips of the microvasculature in peritoneum with a macroscopically normal aspect and of the microvasculature in peritoneal metastases are shown in the animation (Online Resource 1). Quantitative microvascular parameters are shown in Table 2. In peritoneum with a macroscopically-normal aspect, the microvasculature was characterized by a high perfusion rate, irrespective the presence of EOC and/or PC (Figure 2). In contrast, perfusion parameters (PPV and PVD) and TVD were significantly lower in metastases than in peritoneum with a macroscopically-normal aspect (Table 2; Figure 3). No differences in microvascular parameters were observed between imaging during primary cytoreductive surgery or after neo-adjuvant chemotherapy.

Table 2. Quantitative microvascular parameters.

	Benign	EOC, no PC	EOC, PC Macroscopically normal aspect peritoneum	EOC, PC Metastases	P value
Videos, n	17	55	32	14	
PPV, %	97.9 (95.3 – 100)	99.3 (90.8 – 100)	99.3* (92.3 – 100)	**25.7* (17.8 – 50.1)**	$p < 0.01$
PVD, mm/mm^2	7.9 (6.6 – 15.7)	11.4 (8.2 – 13.6)	9.8* (7.5 – 13.8)	**2.1* (0.5 – 3.2)**	$p < 0.01$
TVD, mm/mm^2	8.2 (7.0 – 17.6)	12.6 (9.5 – 14.0)	10.6* (8.4 – 13.9)	**7.2* (3.7 – 10.7)**	$p = 0.05$

Data are presented as medians and ranges between brackets. Abbreviations: EOC, epithelial ovarian cancer; PC, peritoneal carcinomatosis; PPV, percentage of perfused vessels; PVD, perfused vessel density; TVD, total vessel density. * Parameters were compared.

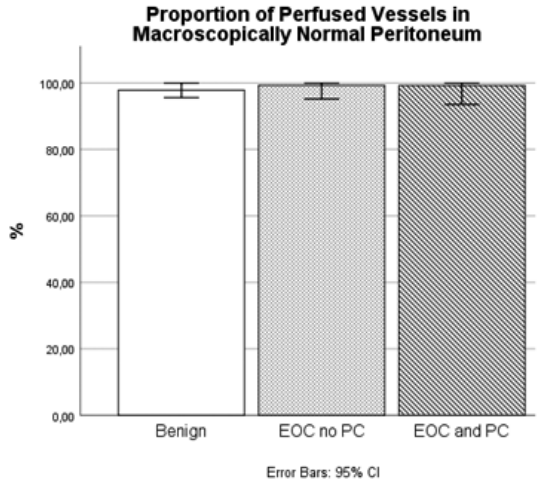

Figure 2. Proportion of perfused vessels in peritoneum with a macroscopically normal aspect in three groups of patients: 1. benign tumor (n=17 videos), 2. EOC without PC (n=55 videos) and 3. EOC with PC (n=32 videos). Abbreviations: EOC, epithelial ovarian cancer; PC, peritoneal carcinomatosis.

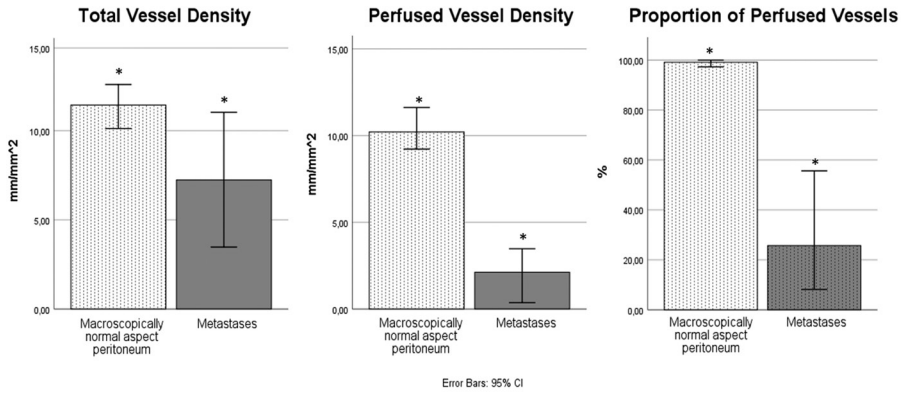

Figure 3. The microvascular parameters total vessel density, perfused vessel density and proportion of perfused vessels in peritoneum with a macroscopically normal aspect (n=104) compared to peritoneal metastases (n=14). Significant differences were observed for the perfusion parameters and are indicated with *.

Immunohistochemistry

In three different patients with high grade serous carcinoma, imaged tissue sites that were macroscopically determined to contain EOC metastases were biopsied, sectioned and stained (Figure 4). EOC cells were stained specifically with anti-PAX8 antibodies (27). All metastases indeed stained for PAX8 protein and all 3 metastases displayed high levels of VEGF, CD31-positive endothelial cells and expression of HIF-1α (Figure 4; metastases 1, 2 and 3). In all 3 metastases that had been biopsied, IDF imaging showed limited perfusion of the microvasculature. The control sample (peritoneum of patient with a benign ovarian tumor) did not stain for PAX8. Limited staining for VEGF, CD31 and HIF-1α was observed, especially in the endothelium of peritoneal micro vessels (Figure 4; normal peritoneum).

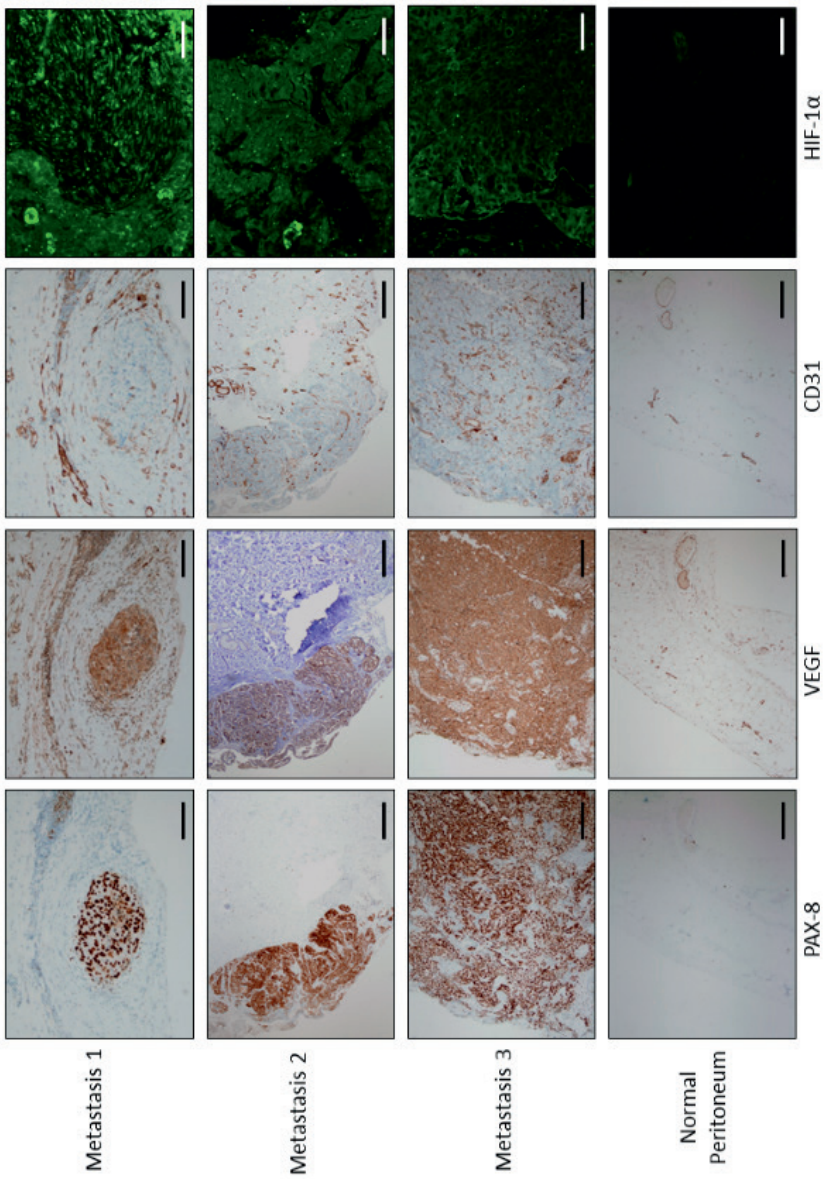

Figure 4. Immunohistochemical (IHC) staining of PAX8, VEGF, CD31 and HIF-1α was performed on paraffin sections of 3 IDF-imaged peritoneal high grade serous carcinoma metastases (metastases 1, 2 and 3). Chromogenic IHC-images of PAX8, VEGF and CD31, black bars = 100 μm. Fluorescence IHC-images of HIF-1α of an area that stained positive for PAX8, white bars = 25 μm. Abbreviations: PAX8, paired box gene 8; VEGF, vascular endothelial growth factor; CD31, cluster of differentiation 31; HIF-1α, hypoxia inducible factor 1α.

Whole mount 3D light sheet fluorescence microscopy

One of the imaged EOC peritoneal metastases was biopsied, cleared and immunohistochemically stained for CD31, and subsequently analyzed with light sheet fluorescence microscopy. Figure 5 shows the 3D image of the metastasis located in the submesothelial stroma of the peritoneum. The metastasis distorted the shape of the peritoneal elastic lamina (PEL), but did not penetrate it. However, as shown in Figure 6, capillaries from the submesothelial regions underneath the PEL were continuous with the capillaries of the metastasis. In other words, vascular sprouts were able to penetrate the PEL during angiogenesis, but EOC cells were not.

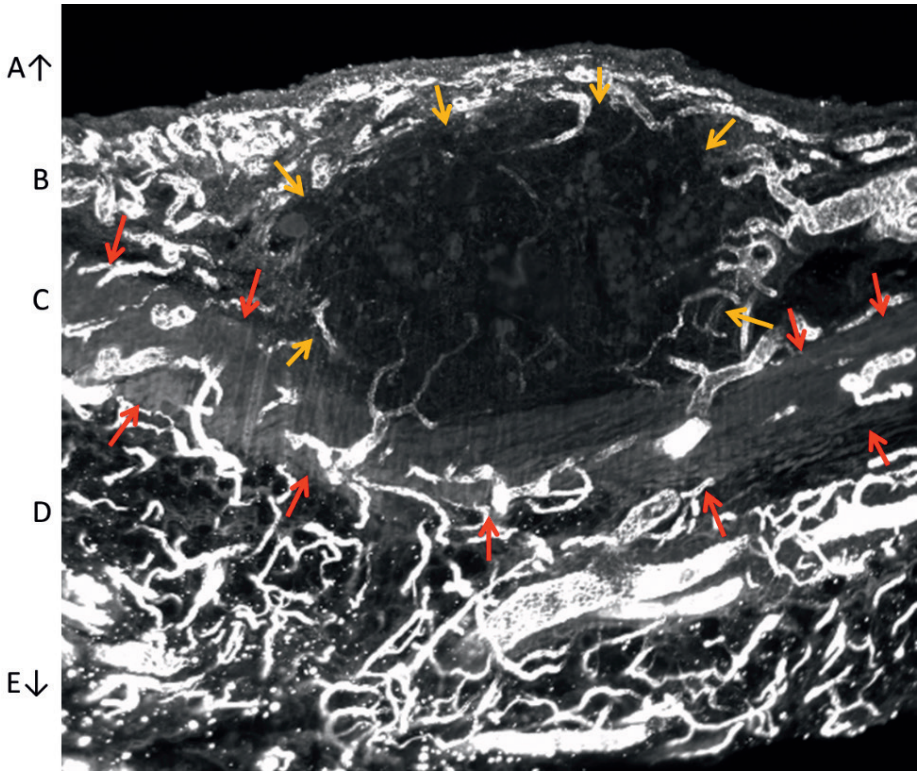

Figure 5. Light sheet fluorescence microscopy image of a peritoneal metastasis with CD31 staining. Blood vessels are shown in white. Boundaries of the metastasis are indicated by yellow arrows, and the boundaries of the elastic lamina (C) by red arrows. A, abdominal cavity; B, submesothelial stroma; C, elastic lamina; D, submesothelial stroma; E, abdominal wall. Bar = 200 µm.

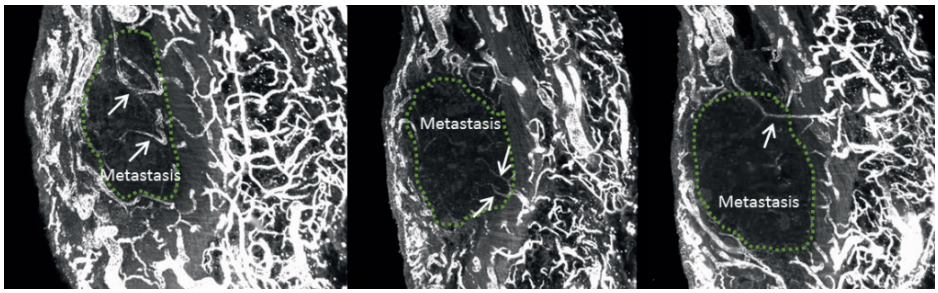

Figure 6. Light sheet fluorescence microscopy images of a peritoneal metastasis with CD31 staining. Arrows indicate vessels that originate from the submesothelial stroma, pass the elastic lamina, and invade the metastasis. Bar = 200 μm.

DISCUSSION

The results of our study suggest that 1) the perfusion of the microvasculature within peritoneal metastases of EOC is poor, 2) HIF-1α and VEGF expression are present in peritoneal metastases, 3) the microvascular networks of the peritoneum and EOC metastases are continuous through all peritoneal layers and 4) the intra-abdominal presence of EOC and/or PC does not affect the microvasculature in other unaffected regions of the peritoneum.

Tumor vasculature is known to differ widely between tumor types and to our knowledge, this is the first time that angioarchitecture and abnormalities in blood flow were studied and quantified *in vivo* in metastases of EOC (33). The perfusion of the microvasculature in peritoneal metastases of EOC is most likely limited by the disorganized network of aberrant vascular structures (34). Other theoretical explanations for the abnormal blood flow are the observed high levels of VEGF. High levels of VEGF can result in permeable and leaky vessels (8), which may further compromise perfusion. Since cancer and hemostasis are strongly related, thrombi in the microvasculature may also limit blood flow (35, 36). In the current study, we have observed vessels with absent flow in which individual erythrocytes could not be discriminated, which is possibly caused by the presence of thrombi (Figure 1C and 1D).

Our findings of the poor perfusion of the microvasculature in peritoneal metastases provide a possible explanation for the high peritoneal recurrence rate of EOC after IV-administered platinum-containing chemotherapy, which may be caused by ineffective delivery of insufficient concentrations of chemotherapy to peritoneal metastases (37). It is tempting to speculate that the findings of our current study also partially explain the

efficacy of (hyperthermic) intraperitoneal (IP) chemotherapy (HIPEC). It has been shown that (H)IPEC reduces the chance of recurrence and increases 5-year survival rates in patients with stage III EOC (38, 39). During this procedure, the peritoneum is exposed to heated (41 °C) chemotherapy for 1.5 hours. In case of poorly perfused microvasculature, the restricted blood flow may be less able to conduct heat and chemotherapy resulting in prolonged or more intense exposure in peritoneal metastases. The direct toxic effects of hyperthermia may be increased in this way, which is further intensified by the synergistic effect of chemotherapy (39).

We also hypothesized that a poorly perfused microvasculature in metastases may limit the exchange of oxygen, carbon dioxide and nutrients between the tissue and the vascular compartment, thus limiting expansive and invasive growth of EOC metastases into the peritoneum (40). Expression of HIF-1α suggests that metastases are in fact hypoxic. Oxygen delivery to tissue primarily depends on the microvasculature and occurs through the hemodynamic principles convection and diffusion. Convection is quantified by flow, and diffusion is quantified by the spatial arrangement of capillaries. The relatively high TVD but low perfusion parameters suggest that hypoxia in metastases is a convection/flow problem, rather than a diffusion/TVD problem (40).

Three dimensional imaging demonstrated vascular continuity between the vascular networks of the submesothelial stroma and the peritoneal metastasis, across the PEL. The metastasis seemed to distort the PEL rather than penetrate it (Figures 5 and 6), which is in line with other studies that have demonstrated that some metastases do not seem capable of penetrating the PEL, whereas other metastases do penetrate it (6). The findings of the current study suggest that blood vessel sprouts and in particular the tip cells of these sprouts invade the PEL. Proteolysis is needed for tissue invasion and tip cells are well equipped for these purposes (41). Elastin is particularly difficult to hydrolyze, and only a few proteases are able to do this (42). Apparently, angiogenesis through the PEL is possible, whereas invasion of the metastases through the PEL is more difficult.

Finally, an important finding of our study was that the presence of EOC does not affect the peritoneal vasculature in general (Figure 2). It is known that tumors can modify the microenvironment of the prospective metastatic site, in this case the peritoneum, to pre-create an environment more favorable for tumor survival and growth (43, 44). With IDF imaging, however, we did not observe an altered or increased vasculature in unaffected peritoneum, regardless the intra-abdominal presence of EOC or peritoneal metastases

elsewhere. This does not exclude preparation of the microenvironment by immunologic changes at a cellular level.

Strengths and limitations

This is the first study to assess and quantify the perfusion of the microvasculature in peritoneal metastases of EOC. *In vivo* imaging provided additional and crucial information, which cannot be obtained with the use of immunohistochemistry. Three-dimensional whole tumor imaging provided additional information on vascular structures connecting the vascular networks of the peritoneum and peritoneal metastases. The findings of this study generated hypotheses regarding pathophysiology and treatment of peritoneal carcinomatosis of EOC.

Limitations of this study include the limited focus depth of the CytoCam (max 300 μm), which can limit microvascular assessment of deeper vascular structures. However, the peritoneum is thin (approximately 50 μm in healthy subjects) and peritoneal metastases are small, thus very suitable for assessment with the CytoCam. Larger metastases may not allow full-depth assessment of their microvasculature. In these larger structures, it is likely that only the more superficial blood vessels are imaged. 3D imaging overcomes the limited focus depth, but provides no information on vessel perfusion. Another limitation of 3D imaging is that it requires clearing of the tissue, which is difficult in tumors. A limitation of CD31 staining is that endothelial cells are detected, also those which may not have formed capillaries yet. IDF imaging overcomes this limitation, because in the case of IDF imaging erythrocytes are visualized, which can only be present when there is flow, meaning that capillary formation must have occurred. It cannot be excluded that part of the observed effects is caused by neo-adjuvant chemotherapy. However, inter-participant differences of microvascular parameters did not occur and findings were consistent, irrespective of imaging during primary cytoreductive surgery or after neo-adjuvant chemotherapy. Also, the number of included participants was rather small, but because of the consistency of findings in the present study and our previous study (18), the differences are unlikely to be caused by coincidence.

The prevalence of cardiovascular risk factors in our study population was high, but comparable to the prevalence in the general population of similar age and gender (45). Cardiovascular disease can affect the microvasculature, but this effect would also be present in normal peritoneum and not exclusively in metastases. Therefore, it is unlikely

that differences between the microvasculature in metastases and normal peritoneum were caused by cardiovascular disease.

Finally, we visualized the vasculature in parietal peritoneum of the abdominal and pelvic wall. Although the microvascular anatomy is considered to be comparable in parietal and visceral peritoneum, future research is needed to investigate whether the vasculature in peritoneal metastases on the visceral peritoneum is similar. It is also interesting to investigate whether the microvasculature in peritoneal metastases of gastrointestinal tumors is similar, or whether our findings are specific for metastases of EOC. In addition, it should be investigated whether HIPEC treatment affects the peritoneal microvasculature and whether microvascular parameters of the peritoneum correlate with course of disease and response to treatment of PC.

CONCLUSION

We demonstrated that the perfusion of the microvasculature in peritoneal metastases of EOC is limited. Hypoperfusion may limit the therapeutic efficacy of IV chemotherapy and affect the behavior of EOC metastases on the peritoneum. Future studies should investigate whether microvascular parameters of the peritoneum correlate with disease outcome and response to therapy.

Acknowledgements
The authors thank Yasin Ince for technical support and assistance in graphic design, and Robert Evers for his assistance in sample preparation, staining and sectioning. We would also like to acknowledge the NKI-AVL Core Facility Molecular Pathology & Biobanking (CFMPB) for supplying NKI-AVL lab support.

Funding
This research did not receive any funding.

Conflicts of interest
Prof. Ince is listed as inventor of SDF imaging on related patents owned by the Academic Medical Center (AMC). He receives no royalties or benefits from this license. Braedius Medical, which is a company owned by a relative of Prof. Ince, has developed and designed a handheld microscope called Cytocam-IDF imaging. Prof. Ince has no

financial relationship with Braedius Medical of any sort (i.e., has never owned shares or received consultancy or speaker fees from Braedius Medical). Prof. Ince runs an internet site (https://microcirculationacademy.org) that offers services (e.g., training, courses, and analysis) related to clinical microcirculation. All other authors declare that they have no conflict of interest.

Author contributions

A.W. Kastelein, L.M.C. Vos, J.O.A.M. van Baal, J.J. Koning, C.J.F. van Noorden and C.A.R. Lok designed research, A.W. Kastelein, L.M.C. Vos, V.V.V. Hira, J.J. Koning, Z. Uz, C.J.F. van Noorden and C.A.R. Lok were involved in conception and design, analysis and interpretation of the data. A.W. Kastelein, L.M.C. Vos, R. Nieuwland, T.M. van Gulik, J. van Rheenen, C. Ince, J.P.W.R. Roovers, C.J.F. van Noorden and C.A.R. Lok were involved in drafting and revising the article. A.W. Kastelein is the guarantor and accepts full responsibility for the work.

Ethical approval

All procedures performed in studies involving human participants were in accordance with the ethical standards of the institutional and/or national research committee (METC Antoni van Leeuwenhoek, ref number N17IDF) and with the 1964 Helsinki declaration and its later amendments or comparable ethical standards.

REFERENCES

1. Jemal A, Bray F, Center MM, Ferlay J, Ward E, Forman D. Global cancer statistics. CA: a cancer journal for clinicians. 2011;61(2):69-90.
2. Siegel R, Ma J, Zou Z, Jemal A. Cancer statistics, 2014. CA: a cancer journal for clinicians. 2014;64(1):9-29.
3. Fagotti A, Gallotta V, Romano F, Fanfani F, Rossitto C, Naldini A, et al. Peritoneal carcinosis of ovarian origin. World Journal of Gastrointestinal Oncology. 2010;2(2):102-8.
4. Woopen H, Sehouli J. Current and future options in the treatment of malignant ascites in ovarian cancer. Anticancer research. 2009;29(8):3353-9.
5. Vaughan S, Coward JI, Bast RC, Jr., Berchuck A, Berek JS, Brenton JD, et al. Rethinking ovarian cancer: recommendations for improving outcomes. Nature reviews Cancer. 2011;11(10):719-25.
6. van Baal J, van Noorden CJF, Nieuwland R, Van de Vijver KK, Sturk A, van Driel WJ, et al. Development of Peritoneal Carcinomatosis in Epithelial Ovarian Cancer: A Review. The journal of histochemistry and cytochemistry : official journal of the Histochemistry Society. 2018;66(2):67-83.
7. van Baal JO, Van de Vijver KK, Nieuwland R, van Noorden CJ, van Driel WJ, Sturk A, et al. The histophysiology and pathophysiology of the peritoneum. Tissue Cell. 2017;49(1):95-105.
8. Kastelein AW, Vos LMC, de Jong KH, van Baal J, Nieuwland R, van Noorden CJF, et al. Embryology, anatomy, physiology and pathophysiology of the peritoneum and the peritoneal vasculature. Seminars in cell & developmental biology. 2019;92:27-36.
9. Hanahan D, Folkman J. Patterns and Emerging Mechanisms of the Angiogenic Switch during Tumorigenesis. Cell. 1996;86(3):353-64.
10. Gimbrone MA, Jr., Leapman SB, Cotran RS, Folkman J. Tumor dormancy in vivo by prevention of neovascularization. The Journal of experimental medicine. 1972;136(2):261-76.
11. Nowak-Sliwinska P, Alitalo K, Allen E, Anisimov A, Aplin AC, Auerbach R, et al. Consensus guidelines for the use and interpretation of angiogenesis assays. Angiogenesis. 2018.
12. Hillen F, Griffioen AW. Tumour vascularization: sprouting angiogenesis and beyond. Cancer Metastasis Reviews. 2007;26(3-4):489-502.
13. Carmeliet P, Jain RK. Angiogenesis in cancer and other diseases. Nature. 2000;407(6801):249-57.
14. Sandoval P, Jimenez-Heffernan JA, Rynne-Vidal A, Perez-Lozano ML, Gilsanz A, Ruiz-Carpio V, et al. Carcinoma-associated fibroblasts derive from mesothelial cells via mesothelial-to-mesenchymal transition in peritoneal metastasis. The Journal of pathology. 2013;231(4):517-31.
15. Gerber SA, Rybalko VY, Bigelow CE, Lugade AA, Foster TH, Frelinger JG, et al. Preferential attachment of peritoneal tumor metastases to omental immune aggregates and possible role of a unique vascular microenvironment in metastatic survival and growth. Am J Pathol. 2006;169(5):1739-52.

16. Masoumi Moghaddam S, Amini A, Morris D, Pourgholami M. Significance of vascular endothelial growth factor in growth and peritoneal dissemination of ovarian cancer2011. 143-62 p.
17. Ocak I, Kara A, Ince C. Monitoring microcirculation. Best practice & research Clinical anaesthesiology. 2016;30(4):407-18.
18. Uz Z, Kastelein AW, Milstein DMJ, Liu D, Rassam F, Veelo DP, et al. Intraoperative Incident Dark Field Imaging of the Human Peritoneal Microcirculation. Journal of vascular research. 2018;55(3):136-43.
19. de Bruin AF, Kornmann VN, van der Sloot K, van Vugt JL, Gosselink MP, Smits A, et al. Sidestream dark field imaging of the serosal microcirculation during gastrointestinal surgery. Colorectal disease : the official journal of the Association of Coloproctology of Great Britain and Ireland. 2016;18(3):O103-10.
20. Aykut G, Veenstra G, Scorcella C, Ince C, Boerma C. Cytocam-IDF (incident dark field illumination) imaging for bedside monitoring of the microcirculation. Intensive care medicine experimental. 2015;3(1):40.
21. Sherman H, Klausner S, Cook WA. Incident dark-field illumination: a new method for microcirculatory study. Angiology. 1971;22(5):295-303.
22. Massey MJ, Larochelle E, Najarro G, Karmacharla A, Arnold R, Trzeciak S, et al. The microcirculation image quality score: development and preliminary evaluation of a proposed approach to grading quality of image acquisition for bedside videomicroscopy. J Crit Care. 2013;28(6):913-7.
23. Hira VVV, Aderetti DA, van Noorden CJF. Glioma Stem Cell Niches in Human Glioblastoma Are Periarteriolar. The journal of histochemistry and cytochemistry : official journal of the Histochemistry Society. 2018;66(5):349-58.
24. Chambers R, Zweifach BW. Intercellular cement and capillary permeability. Physiol Rev. 1947;27(3):436-63.
25. De Backer D, Hollenberg S, Boerma C, Goedhart P, Buchele G, Ospina-Tascon G, et al. How to evaluate the microcirculation: report of a round table conference. Crit Care. 2007;11(5):R101.
26. Hira VVV, de Jong AL, Ferro K, Khurshed M, Molenaar RJ, Van Noorden CJF. Comparison of different methodologies and cryostat versus paraffin sections for chromogenic immunohistochemistry. Acta histochemica. 2019;121(2):125-34.
27. Laury AR, Perets R, Piao H, Krane JF, Barletta JA, French C, et al. A comprehensive analysis of PAX8 expression in human epithelial tumors. The American journal of surgical pathology. 2011;35(6):816-26.
28. Azaripour A, Lagerweij T, Scharfbillig C, Jadczak AE, Swaan BV, Molenaar M, et al. Three-dimensional histochemistry and imaging of human gingiva. Scientific reports. 2018;8(1):1647.
29. Wang D, Stockard CR, Harkins L, Lott P, Salih C, Yuan K, et al. Immunohistochemistry in the evaluation of neovascularization in tumor xenografts. Biotechnic & histochemistry : official publication of the Biological Stain Commission. 2008;83(3-4):179-89.

30. Hira VVV, Breznik B, Vittori M, Loncq de Jong A, Mlakar J, Oostra RJ, et al. Similarities Between Stem Cell Niches in Glioblastoma and Bone Marrow: Rays of Hope for Novel Treatment Strategies. The journal of histochemistry and cytochemistry : official journal of the Histochemistry Society. 2020;68(1):33-57.
31. Renier N, Wu Z, Simon DJ, Yang J, Ariel P, Tessier-Lavigne M. iDISCO: a simple, rapid method to immunolabel large tissue samples for volume imaging. Cell. 2014;159(4):896-910.
32. Ince C, Boerma EC, Cecconi M, De Backer D, Shapiro NI, Duranteau J, et al. Second consensus on the assessment of sublingual microcirculation in critically ill patients: results from a task force of the European Society of Intensive Care Medicine. Intensive Care Med. 2018;44(3):281-99.
33. Bergers G, Benjamin LE. Tumorigenesis and the angiogenic switch. Nature reviews Cancer. 2003;3(6):401-10.
34. Morikawa S, Baluk P, Kaidoh T, Haskell A, Jain RK, McDonald DM. Abnormalities in pericytes on blood vessels and endothelial sprouts in tumors. Am J Pathol. 2002;160(3):985-1000.
35. Van Noorden CJ, van Sluis GL, Spek CA. Experimental and clinical effects of anticoagulants on cancer progression. Thrombosis research. 2010;125 Suppl 2:S77-9.
36. Costa B, Eisemann T, Strelau J, Spaan I, Korshunov A, Liu HK, et al. Intratumoral platelet aggregate formation in a murine preclinical glioma model depends on podoplanin expression on tumor cells. Blood advances. 2019;3(7):1092-102.
37. Lane RJ, Khin NY, Pavlakis N, Hugh TJ, Clarke SJ, Magnussen J, et al. Challenges in chemotherapy delivery: comparison of standard chemotherapy delivery to locoregional vascular mass fluid transfer. Future oncology (London, England). 2018;14(7):647-63.
38. Jaaback K JN, Lawrie TA. Intraperitoneal chemotherapy for the initial management of primary epithelial ovarian cancer. Cochrane Database of Systematic Reviews. 2016.
39. van Driel WJ, Koole SN, Sikorska K, Schagen van Leeuwen JH, Schreuder HWR, Hermans RHM, et al. Hyperthermic Intraperitoneal Chemotherapy in Ovarian Cancer. The New England journal of medicine. 2018;378(3):230-40.
40. Jacob M, Chappell D, Becker BF. Regulation of blood flow and volume exchange across the microcirculation. Critical Care. 2016;20(1):319.
41. Friedl P, Alexander S. Cancer invasion and the microenvironment: plasticity and reciprocity. Cell. 2011;147(5):992-1009.
42. Yang J, Zhao HL, Tang BL, Chen XL, Su HN, Zhang XY, et al. Mechanistic insight into the elastin degradation process by the metalloprotease myroilysin from the deep-sea bacterium Myroides profundi D25. Marine drugs. 2015;13(3):1481-96.
43. Mikuła-Pietrasik J, Uruski P, Tykarski A, Książek K. The peritoneal "soil" for a cancerous "seed": a comprehensive review of the pathogenesis of intraperitoneal cancer metastases. Cellular and Molecular Life Sciences. 2018;75(3):509-25.
44. Gavalas NG, Liontos M, Trachana SP, Bagratuni T, Arapinis C, Liacos C, et al. Angiogenesis-related pathways in the pathogenesis of ovarian cancer. International journal of molecular sciences. 2013;14(8):15885-909.
45. Bots ML. Hart- en vaatziekten in Nederland. 2016.

9 | Summary

The microcirculation consists of the smallest blood vessels in the human body. These small blood vessels are essential for proper organ functioning and in processes such as wound healing and the development of cancer. The microcirculation can be visualized with *handheld vital microscopes*, allowing assessment of microcirculatory function and whether certain diseases or therapies affect this function. This thesis describes literature reviews and translational studies of different aspects of the microcirculation in patients with benign and malignant gynaecological diseases. We demonstrated that *incident dark field (IDF) imaging* is a suitable method to assess the microcirculation in these patients. The first part consists of four chapters that focus on the vaginal microcirculation, in the context of pelvic organ prolapse (POP) and vaginal POP surgery, vulvovaginal atrophy (VVA) and estrogen therapy. The second part of this thesis consists of three chapters that focus on the peritoneal microcirculation and its role in peritoneal carcinomatosis (PC) of epithelial ovarian cancer (EOC). We showed that in addition to the more common sublingual microcirculatory assessment, IDF imaging of the microcirculation can also be used for a myriad of purposes in gynaecology: assessment of vascular damage after vaginal surgery, assessment of angioarchitecture to measure the effect of estrogens, focal depth to measure epithelial thickness and to improve understanding of metastatic disease.

PART I THE VAGINAL MICROCIRCULATION

In **chapter 2**, we present a systematic literature review of preclinical and clinical research on the effect of estrogen on vaginal wound healing. Based on existing literature, we conclude that estrogens optimize surgical wound healing in the vagina, by increasing neovascularization, optimizing granulation formation, accelerating wound closure, enhancing collagen synthesis and increasing tissue strength. In addition, estrogen decreases the inflammatory response and reduces levels of TGF-β1. We hypothesize that such improved wound healing improves tissue quality, which may ultimately improve the outcome of POP surgery. However, in the included studies, outcome parameters were almost all evaluated *ex vivo* and/or in a highly subjective manner. In chapters 3, 4 and 5 we explore whether IDF imaging is a more objective, non-invasive and *in vivo* method to measure the effect of estrogens and surgery on the vaginal microvasculature and on the thickness of the vaginal epithelium. The great advantage of *in vivo* measurements over *ex vivo* measurements, is that function of the microcirculation can also be assessed. Proper functioning of the microvasculature is critical for oxygen supply to tissue.

In **chapter 3**, we describe the validation of focal depth measurements to measure epithelial thickness of the vaginal wall. To date, a non-invasive method to measure epithelial thickness of the vaginal wall is not available. Measuring epithelial thickness may be helpful in the diagnosis and treatment of VVA, to evaluate the effect of (new) treatments for VVA, and in wound healing, as demonstrated in chapter 2. Focal depth can be measured during microcirculatory assessment, as the distance between the surface of the mucosal membrane and the microcirculation. This study demonstrated good agreement between focal depth and epithelial thickness measured in histological slides, suggesting that focal depth measurements can be used as an accurate, noninvasive measure of epithelial thickness.

In **chapter 4**, the effects of estrogen therapy on the vaginal microcirculation are described. In chapter 2 we demonstrated that estrogens affect neoangiogenesis during vaginal wound healing. In this study, we demonstrated that treatment with estrogens has a distinct and measurable effect on angioarchitecture in women with VVA as well. Estrogen also has the potential to reverse the vascular alterations observed in women with VVA. We concluded that angioarchitecture most likely changes in response to a thicker epithelium, to enable oxygen supply to the avascular epithelial layer, and that estrogens do not necessarily increase capillary density. These results improved understanding of the working mechanism of estrogens. It also provided us with a quantitative, objective and non-invasive method to measure the effect of estrogens on the vaginal epithelium. This will have significant value for studies that evaluate the effect of estrogens or estrogen-replacing therapies such as vaginal laser therapy. Analysis of angioarchitecture may be combined with assessment of focal depth, as described in chapter 3.

In **chapter 5**, the effects of prolapse surgery on the vaginal microcirculation are described. The vaginal microcirculation was studied *in vivo* before and after vaginal POP surgery. Inter-individual differences with regard to perfusion and angioarchitecture were observed after seemingly identical surgical procedures, suggesting that some individuals are more susceptible to vascular trauma than others. However, regardless the vascular trauma directly after surgery, functional revascularization was observed in all patients after 6 weeks. The ability to quantify vascular trauma after surgery is crucial for future studies that investigate the relationship between vascular damage and surgical outcome and the potential of therapies such as estrogens to improve neovascularization and ultimately, the outcome of prolapse surgery. In this case, *in vivo* microcirculatory

assessment with IDF imaging will provide crucial information on vascular architecture and vascular function.

PART II THE PERITONEAL MICROCIRCULATION

In **chapter 6**, an overview of the literature on embryology, anatomy, physiology and pathophysiology of the peritoneum and the peritoneal vasculature is presented. The peritoneum is a complex structure with a variety of functions. The microvascular response in pathological processes such as adhesion formation, inflammation and cancer is important and remodeling of peritoneal vasculature occurs in many diseases. We concluded that the role of the peritoneal microcirculation in pathological conditions, especially in PC, is virtually unknown and requires further elucidation.

In **chapter 7**, we present a study in which intraoperative IDF imaging of the microcirculation was performed in healthy peritoneum. Imaging of the peritoneal membrane revealed a distinctive microvascular layout in which angioarchitecture was characterized by an organized network of capillaries, often flanked by fat cells. The peritoneal microcirculation was further characterized by a relatively low capillary density and adequate perfusion. The possibility of real-time and non-invasive assessment of the peritoneal microcirculation by quantification of vessel density and perfusion *in vivo* is promising for the study of many peritoneal conditions, including PC.

In **chapter 8**, we describe the peritoneal microcirculation in patients with EOC and PC. We demonstrated that peritoneal metastases of EOC were poorly perfused and hypoxic. We also used advanced 3-dimensional microscopy and showed that microvascular networks of peritoneum and EOC metastases were continuous through all peritoneal layers. The poor perfusion of EOC metastases may limit the therapeutic efficacy of intravenous chemotherapy, and subsequent hypoxia may affect the growth of metastases on the peritoneum. These findings are important for future research into new treatments for advanced ovarian cancer.

10 General discussion and future recommendations

There are at least 10,000 known diseases affecting humans, but for only a minority of these diseases, an effective treatment or cure is available. Development of effective treatments is a time consuming and expensive process. Therefore, (new) treatments and the clinical trials evaluating these treatments should preferably be based on well thought-out concepts, supported by basic science and translational research (1, 2). This reduces waste research, increases the chances of an efficacious intervention and successful implementation of these interventions in the future.

In translational research, knowledge from basic biology and clinical trials is applied to address medical needs, requiring skills and resources that are not readily available in a basic laboratory or preclinical research setting (1). Figure 1 shows the translational research spectrum, demonstrating that medical advances generally proceed from a basic science discovery to testing, to implementation and adoption by the larger medical community. However, movement on this scale is not unidirectional: results from a T3 of T4 study might reveal the need for more studies at the T2 level, or may indicate new pathways for research at the T0 level. Hereby, the goal of translational science is to keep the flow of ideas moving from laboratories and universities into the development of improved healthcare diagnostics, drugs, therapies and devices (3).

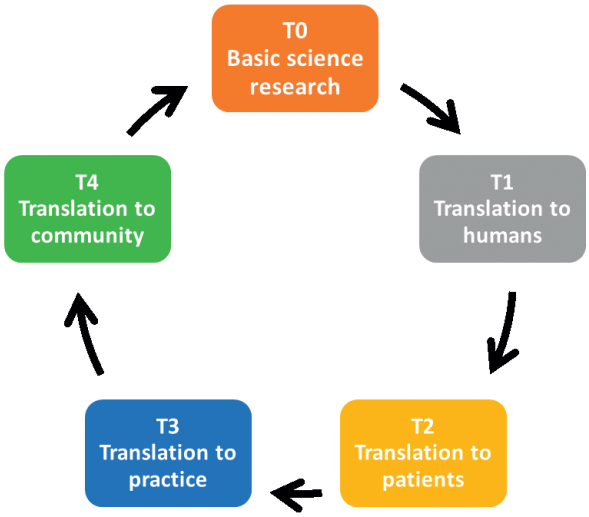

Figure 1. The four phases of the translational research spectrum.

Improved knowledge and understanding of the early phases of the translational research cycle will improve knowledge in the later phases. Understanding the basics will improve

interpretation of study results, enable selection of patients for therapy, and enhance development, implementation and adoption of new therapies. In this way, the T1 research performed in this thesis will contribute to the subsequent phases of the cycle. Unfortunately, the importance of translational research is not always acknowledged to the fullest extent, and traditionally, most research budget is available for patient-centered, clinical research.

Urogynaecology has traditionally been a practical specialty – basic science and translational research have not always been on research agendas, nor have they always formed the basis of implemented treatments. The over-hasty introduction of vaginal mesh is an illustrative example, with far-reaching consequences that may have been prevented with more elaborate basic science and translational research of aspects like textile properties of the mesh, host immune response and mechanical behavior (4). In addition, although the interest in translational medicine may have been more apparent in gynaecologic oncology, the peritoneum, despite its importance in ovarian cancer, has also been a 'forgotten' organ (5). Increasing translational knowledge of the vaginal and peritoneal microcirculation is thus indispensable, given the importance of the microcirculation for proper organ functioning and its key role in many physiological and pathophysiological processes.

In part I of this thesis, we improved basic knowledge of vaginal microvascular physiology and function, and explored the potential of microcirculatory assessment to objectify the effect of broadly-applied interventions, such as vaginal surgery and vaginal estrogen therapy. The results of chapter 2 demonstrated that estrogens can be beneficial for vaginal wound healing, but also that research into this topic is very limited. Consequently, estrogens are inconsistently prescribed before and after POP surgery, without consensus and without evidence of efficacy or treatment details such as dosage and duration. Also in the treatment of VVA, frequency and dosage are not based on convincing evidence, and measures to monitor treatment effect are almost all inaccurate, expensive and/or invasive (6). In the meantime, energy-based alternatives for estrogens such as vaginal laser and radiofrequency (7) are becoming increasingly popular and are introduced without sufficient (translational) knowledge of their working mechanism and their effect on vaginal physiology, microcirculation, and thus of their safety and efficacy (8-11).

We have demonstrated that estrogens change angioarchitecture rather than capillary density, and that angioarchitecture and also focal depth can be used as objective

measures of treatment effect, before and after POP surgery and also in the treatment of VVA. This implicates that measuring capillary density in histological slides to measure the effect of estrogen may not be useful. Microcirculatory assessment has other great advantages over existing tools (12), because of its non-invasive and objective character. To date, this assessment is mainly limited by the fact that analysis has to be performed manually, but recent developments in automated analysis are promising (13).

Microcirculatory assessment can also be used for the objective evaluation of the effect of aforementioned energy-based alternatives for estrogens. Focal depth and angioarchitecture are currently used as outcome measures in multiple preclinical and clinical studies. Other future applications of microcirculatory assessment in urogynaecology include evaluation of pelvic floor implants. Polypropylene vaginal mesh is currently heavily debated (14, 15), which has strongly stimulated research into the development of new materials (16). Such materials are preferably biodegradable and should stimulate angiogenesis, which is key for mesh-integration (17, 18). The angiogenic potential of implants can be increased by materials that for example release estrogens or VEGF, which is currently evaluated in *ex vivo* models such as the chorionic membrane of fertilized chicken eggs (19, 20). When these implants will be evaluated in T1 animal- or first-in-human studies, a method to non-invasively study neoangiogenesis *in vivo* should be available. The main limitation of IDF imaging for this application is focal depth, but it is currently being investigated whether light at another wavelength may increase the imaging depth. Other new techniques such as high definition ultrasound/power Doppler and photoacoustic imaging are also of interest for implant-related assessment of the microcirculation (21-23), and should be explored further (24).

In part II of this thesis, we used a similar approach to assess the peritoneal microcirculation. Our literature review demonstrated the importance of the peritoneal microcirculation in many intra-abdominal conditions, and that the number of studies performed to investigate the peritoneal microcirculation (especially in peritoneal carcinomatosis) is very limited. We used microcirculatory assessment to improve basic knowledge on one hand, and aimed to identify whether it can be used as 'biomarker' on the other hand, to monitor disease or select patients for (individualized) treatment.

In current treatment regimens for metastasized epithelial ovarian cancer, intravenous chemotherapy and VEGF-antagonists are widely applied, but the 5-year survival rates are still disappointing. Studies have mostly assessed the effect of these therapies on

survival rates, whereas the effects on the peritoneum and especially the peritoneal microcirculation, were studied to a much lesser extent. The studies that did investigate the microcirculation around peritoneal metastases of ovarian cancer, demonstrated normal or increased vasculature (25, 26). However, dynamic parameters such as flow were not investigated in these *ex vivo* studies, which is regrettable, because for tissue oxygenation, flow is equally important as capillary density (27). Thus, merely studying capillary density may lead to inaccurate and false conclusions.

In chapter 8 of this thesis, we described a very poor perfusion of the microcirculation in peritoneal metastases, suggesting that treatments that utilize or target the microvasculature, are not the most efficacious treatments. Our findings have generated important questions for future peritoneal carcinomatosis related research: why is the vasculature this dysfunctional in such small tumors, could hypoperfusion and hypoxia lead to restrictive tumor growth and can our findings explain the limited therapeutic efficacy of systemic chemotherapy and the increased therapeutic efficacy of hyperthermic intraperitoneal chemotherapy (HIPEC)?

Optimizing perfusion in peritoneal metastases may be a potential target for therapy, and may also partly explain the added value of HIPEC in patients with advanced ovarian cancer (as has recently been demonstrated in the OVHIPEC trial (28)). We hypothesize that hyperthermia causes vasodilation, which in turn improves blood flow in the microcirculation within peritoneal metastases. This may increase the uptake of chemotherapy, and enhance its efficacy. Also, intravenously administered chemotherapy may not reach peritoneal metastases due to the impaired blood flow, whereas HIPEC reaches the metastases by means of diffusion through the peritoneal membrane. Fundamental knowledge on the effects of HIPEC on the peritoneum and the peritoneal microcirculation is limited, and should be further expanded. A study is currently being performed in which peritoneal microcirculatory assessment is performed before, during and after HIPEC. This T1 translational research will also boost the subsequent phases: understanding *why* something is efficacious, will enhance implementation and adoption, which is currently not optimal for HIPEC.

It should also be determined whether microvascular parameters are related to clinical outcome: if microcirculatory assessment can be used to predict treatment response, it could possibly guide the personalized therapy of the future. This way, the perfusion status of the microcirculation in peritoneal metastases may determine dose, duration

and intravenous versus intraperitoneal drug delivery. Microvascular status may help predict whether patients will benefit from HIPEC, at what interval and at what dose. Additionally, our findings may also be interesting for other fields of oncology, and it would be interesting to explore whether similar findings are observed in peritoneal metastases of other (e.g. gastrointestinal) malignancies.

Altogether, this thesis has answered some of the fundamental, translational and clinical questions in different gynecological diseases, but it also generated new hypotheses and thus offers new research questions for future studies. We have provided overviews of evidence, generated new insight into pathophysiology and demonstrated that microcirculatory assessment can be used as objective, functional outcome measure of vaginal and peritoneal disease and associated treatments. Although traditionally most budget is available for clinical, patient-centered research, we demonstrated the value of translational medicine, which should always form the basis, to reduce waste research, enable individualized medicine of the future and protect patients from premature implementation of medical treatments (1).

REFERENCES

1. Choi PJ, Tubbs RS, Oskouian RJ. The Current Trend of the Translational Research Paradigm. Cureus. 2018;10(3):e2340-e.
2. Yu D. Translational research: current status, challenges and future strategies. Am J Transl Res. 2011;3(5):422-33.
3. Buffalo Uo. Clinical and Translational Science Institute [Available from: www.buffalo.edu.
4. Liang R, Knight K, Abramowitch S, Moalli PA. Exploring the basic science of prolapse meshes. Curr Opin Obstet Gynecol. 2016;28(5):413-9.
5. Reymond MA. Pleura and Peritoneum: the forgotten organs. Pleura Peritoneum. 2016;1(1):1-2.
6. Nilsson K, Risberg B, Heimer G. The vaginal epithelium in the postmenopause--cytology, histology and pH as methods of assessment. Maturitas. 1995;21(1):51-6.
7. Karcher C, Sadick N. Vaginal rejuvenation using energy-based devices. Int J Womens Dermatol. 2016;2(3):85-8.
8. Arunkalaivanan A, Kaur H, Onuma O. Laser therapy as a treatment modality for genitourinary syndrome of menopause: a critical appraisal of evidence. International urogynecology journal. 2017;28(5):681-5.
9. Mitchell CM. Seeing the light: the need for randomized trials of vaginal laser in postmenopausal women. Menopause (New York, NY). 2018;25(1):7-8.
10. Song S, Budden A, Short A, Nesbitt-Hawes E, Deans R, Abbott J. The evidence for laser treatments to the vulvo-vagina: Making sure we do not repeat past mistakes. The Australian & New Zealand journal of obstetrics & gynaecology. 2018;58(2):148-62.
11. Digesu GA, Tailor V, Preti M, Vieira-Baptista P, Tarcan T, Stockdale C, et al. The energy based devices for vaginal "rejuvenation," urinary incontinence, vaginal cosmetic procedures, and other vulvo-vaginal disorders: An international multidisciplinary expert panel opinion. Neurourology and urodynamics. 2019;38(3):1005-8.
12. Salvatore S, Leone Roberti Maggiore U, Athanasiou S, Origoni M, Candiani M, Calligaro A, et al. Histological study on the effects of microablative fractional CO2 laser on atrophic vaginal tissue: an ex vivo study. Menopause (New York, NY). 2015;22(8):845-9.
13. Hilty MP, Guerci P, Ince Y, Toraman F, Ince C. MicroTools enables automated quantification of capillary density and red blood cell velocity in handheld vital microscopy. Communications biology. 2019;2:217.
14. Dällenbach P. To mesh or not to mesh: a review of pelvic organ reconstructive surgery. International Journal of Women's Health. 2015;7:331-43.
15. Iyer S, Botros SM. Transvaginal mesh: a historical review and update of the current state of affairs in the United States. International urogynecology journal. 2017;28(4):527-35.
16. Mironska E, Chapple C, MacNeil S. Recent advances in pelvic floor repair. F1000Res. 2019;8.

17. Mangir N, Hillary CJ, Chapple CR, MacNeil S. Oestradiol-releasing Biodegradable Mesh Stimulates Collagen Production and Angiogenesis: An Approach to Improving Biomaterial Integration in Pelvic Floor Repair. European urology focus. 2019;5(2):280-9.
18. Shafaat S, Mangir N, Regureos SR, Chapple CR, MacNeil S. Demonstration of improved tissue integration and angiogenesis with an elastic, estradiol releasing polyurethane material designed for use in pelvic floor repair. Neurourology and urodynamics. 2018;37(2):716-25.
19. Mangir N, Raza A, Haycock JW, Chapple C, Macneil S. An Improved In Vivo Methodology to Visualise Tumour Induced Changes in Vasculature Using the Chick Chorionic Allantoic Membrane Assay. In Vivo. 2018;32(3):461-72.
20. Qutachi O, Bullock AJ, Gigliobianco G, MacNeil S. Spatiotemporal release of VEGF from biodegradable polylactic-co-glycolic acid microspheres induces angiogenesis in chick chorionic allantoic membrane assay. International journal of pharmaceutics. 2019;561:236-43.
21. Migda MS, Migda M, Słapa R, Mlosek RK, Migda B. The use of high-frequency ultrasonography in the assessment of selected female reproductive structures: the vulva, vagina and cervix. J Ultrason. 2019;19(79):261-8.
22. Huang C, Lowerison MR, Lucien F, Gong P, Wang D, Song P, et al. Noninvasive Contrast-Free 3D Evaluation of Tumor Angiogenesis with Ultrasensitive Ultrasound Microvessel Imaging. Scientific reports. 2019;9(1):4907.
23. Smith LM, Varagic J, Yamaleyeva LM. Photoacoustic Imaging for the Detection of Hypoxia in the Rat Femoral Artery and Skeletal Muscle Microcirculation. Shock (Augusta, Ga). 2016;46(5):527-30.
24. Kastelein AW, de Graaf BC, Latul YP, Verhorstert KWJ, Holthof J, Guler Z, et al. Ultra high frequency ultrasound: a promising technique to visualize pelvic floor meshes in vivo. Ultrasound Obstet Gynecol. 2020.
25. Sandoval P, Jimenez-Heffernan JA, Rynne-Vidal A, Perez-Lozano ML, Gilsanz A, Ruiz-Carpio V, et al. Carcinoma-associated fibroblasts derive from mesothelial cells via mesothelial-to-mesenchymal transition in peritoneal metastasis. The Journal of pathology. 2013;231(4):517-31.
26. Masoumi Moghaddam S, Amini A, Morris DL, Pourgholami MH. Significance of vascular endothelial growth factor in growth and peritoneal dissemination of ovarian cancer. Cancer and Metastasis Reviews. 2012;31(1):143-62.
27. Jacob M, Chappell D, Becker BF. Regulation of blood flow and volume exchange across the microcirculation. Critical Care. 2016;20(1):319.
28. van Driel WJ, Koole SN, Sikorska K, Schagen van Leeuwen JH, Schreuder HWR, Hermans RHM, et al. Hyperthermic Intraperitoneal Chemotherapy in Ovarian Cancer. The New England journal of medicine. 2018;378(3):230-40.

10

Appendices

Nederlandse samenvatting
List of co-authors and affiliations
PhD portfolio
Dankwoord
About the author

NEDERLANDSE SAMENVATTING

De microcirculatie bestaat uit de kleinste bloedvaten in het menselijk lichaam. Deze kleine bloedvaten zijn essentieel voor het functioneren van organen en allerlei processen in het lichaam, zoals bijvoorbeeld wondgenezing en de vorming van kanker. Microcirculatie kan in beeld worden gebracht met zogeheten *handheld* vitale microscopen, waarna de microcirculatie geanalyseerd kan worden. Zo kan bijvoorbeeld gemeten worden of de microcirculatie goed functioneert, en of bepaalde aandoeningen of therapieën de vorm en functie van de microcirculatie aantasten. Dit proefschrift beschrijft zowel literatuuronderzoek als translationeel onderzoek naar verschillende aspecten van de microcirculatie, in patiënten met benigne en maligne gynaecologische aandoeningen. Het eerste deel bestaat uit vier hoofdstukken die zich richten op de vaginale microcirculatie in de context van vaginale chirurgie, vaginale atrofie en oestrogeen therapie. Het tweede deel bestaat uit drie hoofdstukken die zich richten op de microcirculatie in het peritoneum (het buikvlies), in bredere zin en in de context van peritonitis carcinomatosa, een aandoening die vaak ontstaat bij patiënten met uitgezaaide eierstokkanker. We laten zien dat een bepaalde vorm van *handheld* vitale microscopie, namelijk *incident dark field* (IDF) *imaging*, een geschikte methode is om de microcirculatie bij gynaecologische aandoeningen in beeld te brengen. Het meten van de microcirculatie kan vervolgens voor verschillende doeleinden gebruikt worden. Voorbeelden zijn het meten van vaatschade na vaginale chirurgie, de beoordeling van vaatarchitectuur om het effect van behandelingen voor vaginale atrofie te objectiveren, het meten van de afstand tussen de oppervlakte van het vaginale slijmvlies en de microcirculatie (focusdiepte) om epitheeldikte te meten en tenslotte om onze kennis en inzichten over het peritoneum, in het bijzonder in het geval van uitgezaaide eierstokkanker, te vergroten. De opgedane kennis draagt uiteindelijk bij aan het ontwikkelen en verfijnen van behandelingen, en het analyseren van de microcirculatie biedt daarnaast een objectieve en nauwkeurige methode om het effect van deze behandelingen te evalueren.

DEEL I DE VAGINALE MICROCIRCULATIE

In **hoofdstuk 2** presenteren we een systematisch literatuuronderzoek waarin zowel preklinisch als klinisch onderzoek beschreven wordt naar het effect van oestrogenen op vaginale wondgenezing. Onze hypothese was dat oestrogenen vaginale wondgenezing bevorderen. Het verbeteren van vaginale wondgenezing kan mogelijk het succes van verzakkingschirurgie vergroten. Op basis van de bestaande literatuur concluderen we dat oestrogenen de vaginale wondgenezing bevorderen, onder meer door de vorming van

nieuwe bloedvaten te stimuleren. De zuurstofvoorziening in de wond wordt hierdoor beter, wat de productie van collageen bevordert, wat het weefsel steviger maakt. Oestrogenen zorgen daarnaast voor een verdikking van het epitheel, het sneller sluiten van een wond en minder ontsteking. Op basis van het beschikbare onderzoek is het niet mogelijk om uitspraken te doen over de beste dosering of de beste toedieningsweg van oestrogenen. Het is bovendien opvallend dat in al het beschikbare onderzoek, parameters zoals nieuwvorming van bloedvaten vrijwel allemaal *ex vivo* bepaald zijn, en dat er vaak sprake is van een hoge mate van subjectiviteit. In hoofdstukken 3, 4 en 5 wordt onderzocht of IDF imaging gebruikt kan worden om objectiever en bovendien *in vivo* vaginale epitheeldikte en het effect van oestrogenen en chirurgie op de vaginale microcirculatie te analyseren. Het grote voordeel van *in vivo* boven *ex vivo* onderzoek is dat ook de functie van bloedvaten onderzocht kan worden.

In **hoofdstuk 3** valideren we focusdiepte om epitheeldikte van de vaginawand te meten. Er is momenteel geen non-invasieve methode beschikbaar om epitheeldikte te meten, terwijl het meten van epitheeldikte erg waardevol kan zijn in de diagnose en behandeling van vaginale atrofie. Bovendien hebben we in hoofdstuk 2 gezien dat epitheeldikte een belangrijk onderdeel van wondgenezing is, waardoor het ook van waarde zou kunnen zijn om in deze setting epitheeldikte te meten. Focusdiepte kan gemeten worden tijdens het meten van de microcirculatie. Het is de afstand tussen het oppervlak van het vaginale slijmvlies en de microcirculatie in het dieper gelegen weefsel. De hypothese was dat focusdiepte een afspiegeling is van epitheeldikte. We hebben hiertoe focusdiepte metingen vergeleken met epitheeldikte metingen in biopten van vaginaal weefsel. De resultaten van dit onderzoek laten zien dat er goede overeenstemming is tussen focusdiepte en epitheeldikte. Dit betekent dat focusdiepte gebruikt kan worden als accurate, non-invasieve methode om epitheeldikte te meten. Oestrogeen behandeling heeft naast het effect op epitheeldikte, mogelijk ook een meetbaar effect op hoe de vaten eruit zien, de zogeheten architectuur van de microcirculatie. Dit is onderzocht in hoofdstuk 4.

In **hoofdstuk 4** beschrijven we het effect van oestrogenen op de vaginale microcirculatie. Hoofdstuk 2 heeft ons laten zien dat oestrogenen de vorming van nieuwe vaten stimuleert tijdens wondgenezing. Wij laten in dit hoofdstuk zien dat behandeling met oestrogenen ook een duidelijk en meetbaar effect heeft op de vaginale vaatarchitectuur in vrouwen met vaginale atrofie. We tonen daarnaast aan dat oestrogenen het vermogen hebben om de vaatveranderingen, zoals geobserveerd in vrouwen met vaginale atrofie, terug

te draaien. We concluderen dat de vaatarchitectuur waarschijnlijk verandert in respons op een dikker epitheel, en dat de vaatdichtheid niet per se lijkt te veranderen onder invloed van oestrogenen. Dit onderzoek heeft ons begrip van het werkingsmechanisme van oestrogenen vergroot, en biedt een kwantitatieve, objectieve en non-invasieve methode om het effect van oestrogenen op het vaginale epitheel te meten, wat van waarde kan zijn voor toekomstige studies die alternatieven voor oestrogeen therapieën onderzoeken, zoals vaginale laser therapie, in vrouwen met vaginale atrofie en/of na verzakkingschirurgie. Analyse van vaatarchitectuur kan dan gecombineerd worden met analyse van focusdiepte, zoals beschreven in hoofdstuk 3.

In **hoofdstuk 5** beschrijven we het effect van vaginale verzakkingschirurgie op de vaginale microcirculatie. De vaginale microcirculatie werd *in vivo* bestudeerd, voor en na verzakkingschirurgie. Interindividuele verschillen in perfusie (doorbloeding), en vaatarchitectuur na ogenschijnlijk identieke operaties wekken de indruk dat sommige individuen gemakkelijker vaatschade oplopen. Onafhankelijk van de vaatschade een dag na de operatie, zagen we dat functionele revascularisatie plaatsvond in alle proefpersonen na zes weken. De mogelijkheid om vaatschade na chirurgie te kwantificeren biedt mogelijkheden voor onderzoekers die de relatie tussen vaatschade en chirurgische uitkomst willen onderzoeken. Daarnaast kan het effect van oestrogenen op de vorming van nieuwe vaten tijdens wondgenezing, zoals beschreven in hoofdstuk 2, *in vivo* worden bestudeerd. Dit geeft naast informatie over de hoeveelheid bloedvaten, ook waardevolle informatie over de functie van de bloedvaten. Dergelijk onderzoek kan in de toekomst helpen om de ideale dosering en toedieningsweg van oestrogenen te onderzoeken, alsook de potentie van alternatieve therapieën om wondgenezing te bevorderen, zoals vaginale laser therapie.

DEEL II DE PERITONEALE MICROCIRCULATIE

In **hoofdstuk 6** presenteren we een overzicht van de beschikbare literatuur over de embryologie, anatomie, fysiologie en pathofysiologie van het peritoneum en de peritoneale microcirculatie. Het peritoneum is een complex orgaan met veel functies. In veel van deze functies en processen waarbij het peritoneum betrokken is, speelt de peritoneale microcirculatie een centrale rol. De respons van de microcirculatie op pathologische processen zoals verklevingen, ontsteking en kanker is belangrijk, en bijna alle peritoneale ziektes hebben effect op de peritoneale microcirculatie. Het blijkt echter dat de kennis over de peritoneale microcirculatie beperkt is. Zo concluderen we dat er te weinig bekend is over de rol van de peritoneale microcirculatie in naar het

peritoneum uitgezaaide kanker, zogeheten peritonitis carcinomatosa, en dat dit verdere verduidelijking vereist.

In **hoofdstuk 7** presenteren we een studie waarin IDF imaging is verricht tijdens grote buikoperaties, waarbij de microcirculatie van gezond peritoneum voor het eerst met deze techniek in beeld is gebracht. Dit onderzoek liet zien dat dat peritoneale microcirculatie een uitgesproken vaatarchitectuur heeft, en gekenmerkt wordt door een georganiseerd netwerk van bloedvaten. De peritoneale microcirculatie had in dit onderzoek een relatief lage vaatdichtheid en adequate perfusie. Het is onbekend of en hoe vaatdichtheid en vaatperfusie veranderen in het geval van peritonitis carcinomatosa. Dit is onderzocht in hoofdstuk 8.

In **hoofdstuk 8** beschrijven we de peritoneale microcirculatie in patiënten met eierstokkanker en peritonitis carcinomatosis. We laten zien dat er in peritoneale metastasen (uitzaaiingen) sprake is van slechte perfusie en hypoxie (onvoldoende zuurstof voorziening). Naast IDF imaging gebruiken we geavanceerde 3-dimensionale microscopie om in biopten van peritoneale metastases de continuïteit van de vaatnetwerken tussen de verschillende lagen van het peritoneum te beoordelen. Wij stellen dat de slechte perfusie van de microcirculatie in peritoneale metastases het therapeutisch effect van intraveneuze chemotherapie kan verminderen, en dat hypoxie de groei en/of invasiviteit van peritoneale metastasen kan beïnvloeden. Deze bevindingen bieden belangrijke aanknopingspunten voor toekomstig onderzoek naar nieuwe behandelingen voor uitgezaaide eierstokkanker.

LIST OF CO-AUTHORS AND AFFILIATIONS

J.O.A.M. van Baal	Centre for Gynaecologic Oncology Amsterdam, Antoni van Leeuwenhoek, Amsterdam, the Netherlands.
C.M. Diedrich	Department of Obstetrics and Gynaecology, Amsterdam UMC location AMC, Amsterdam, the Netherlands.
W.J. van Driel	Centre for Gynaecologic Oncology Amsterdam, Antoni van Leeuwenhoek, Amsterdam, the Netherlands.
Z. Guler Gocke	Department of Obstetrics and Gynaecology, Amsterdam UMC location AMC, Amsterdam, the Netherlands.
T.M. van Gulik	Department of Surgery, Amsterdam UMC location AMC, Amsterdam, the Netherlands
C.R. Hooijmans	Department for Health Evidence, Unit SYRCLE, Radboud University Medical Center, Nijmegen, the Netherlands.
V.V.V. Hira	Department of Genetic Toxicology and Cancer Biology, National Institute of Biology, Ljubjana, Slovenia
C. Ince	Department of Translational Physiology, Amsterdam UMC location AMC, Amsterdam, the Netherlands
	Department of Intensive Care, Erasmus University Medical Centre, Rotterdam, the Netherlands
C.H.J.R. Jansen	Department of Obstetrics and Gynaecology, Amsterdam UMC location AMC, Amsterdam, the Netherlands.
K.H. de Jong	Department of Medical Biology, Amsterdam UMC location AMC, Amsterdam, the Netherlands
J.J. Koning	Department of Molecular Cell Biology and Immunology, Amsterdam UMC, location VUMC, Amsterdam, the Netherlands
J. Limpens	Medical Library, Amsterdam UMC, location AMC, University of Amsterdam, Amsterdam, the Netherlands
C.A.R. Lok	Centre for Gynaecologic Oncology Amsterdam, Antoni van Leeuwenhoek, Amsterdam, the Netherlands
D. Lui	Department of Surgery, Amsterdam UMC location AMC, Amsterdam, the Netherlands

D.M. Milstein	Department of Oral and Maxillofacial Surgery, Amsterdam UMC location AMC, Amsterdam, the Netherlands
R. Nieuwland	Laboratory of Experimental Clinical Chemistry and Vesicle Observation Centre, Amsterdam UMC location AMC, Amsterdam, the Netherlands
C.J.F. van Noorden	Department of Medical Biology, Amsterdam UMC location AMC, Amsterdam, the Netherlands
	Department of Genetic Toxicology and Cancer Biology, National Institute of Biology, Ljubjana, Slovenia
F. Rassam	Department of Surgery, Amsterdam UMC location AMC, Amsterdam, the Netherlands
J. van Rheenen	Department of Molecular Pathology, The Netherlands Cancer Institute and Oncode Institute, Amsterdam, the Netherlands
J.P.W.R. Roovers	Department of Obstetrics and Gynaecology, Amsterdam UMC location AMC, Amsterdam, the Netherlands.
Z. Uz	Department of Surgery, Amsterdam UMC location AMC, Amsterdam, the Netherlands
	Department of Translational Physiology, Amsterdam UMC location AMC, Amsterdam, the Netherlands
D.P. Veelo	Department of Anesthesiology, Amsterdam UMC location AMC, Amsterdam, the Netherlands
F. Verri	Department of Obstetrics and Gynaecology, Amsterdam UMC location AMC, Amsterdam, the Netherlands.
E.V. Vodegel	Department of Obstetrics and Gynaecology, Amsterdam UMC location AMC, Amsterdam, the Netherlands.
L.M.C. Vos	Department of Obstetrics and Gynaecology, Amsterdam UMC location AMC, Amsterdam, the Netherlands.
L. de Waal	Department of Obstetrics and Gynaecology, Amsterdam UMC location AMC, Amsterdam, the Netherlands.
M.A. Weber	Department of Obstetrics and Gynaecology, Amsterdam UMC location AMC, Amsterdam, the Netherlands.
S.E. Zwolsman	Department of Obstetrics and Gynaecology, Amsterdam UMC location AMC, Amsterdam, the Netherlands.

PHD PORTFOLIO

Graduate School Courses	Year	Workload (ECTS)
Clinical monitoring of the microcirculation	2016	0.9
Laboratory Animal Science	2016	3.9
Basic Course Legislation and Organization (BROK)	2016	0.9
Scientific writing	2017	1.5
Practical Biostatistics	2017	1.1
Entrepeneurship in Health and Life Sciences	2017	1.5
Clinical Epidemiology	2019	0.9

Other courses	Year
ZonMw publiek-private samenwerkingsdag	2017
Interdisciplinaire Incontinentie en Prolaps Overleg Regio Amsterdam	2017-2019
Medical Business Masterclass: healthcare fundamentals & innovation	2018

Other	Year
Arts-onderzoeker WOMEN-UP project (Horizon 2020)	2016 – 2020
Arts-onderzoeker Coloplast RESTORELLE 522 study	2016 – 2020
Redacteur – Nederlands Tijdschrift voor Obstetrie en Gynaecologie	2017 – heden
Redactielid – de Jonge Specialist	2018 – 2020
Onderwijs coassistenten – Anatomie en Bekkenbodemproblematiek	2018 – 2020
Development course Toegepaste Gynaecologische Anatomie	2018
Development Massive Open Online Course urinary incontinence	2018
Kwaliteit waarborging hoofdstuk Gynaecologie – Compendium Geneeskunde	2019 – heden

(Inter)national conferences attended	Year	Workload (ECTS)
IUGA conference (Cape Town, South-Africa)	2016	0.5
EUGA conference (Amsterdam, Netherlands)	2016	0.5
IUGA conference (Vienna, Austria)	2018	0.5
EUGA conference (Milano, Italy)	2018	0.5
IUGA conference (Nashville, TN, USA)	2019	0.5
EUGA conference (Tel Aviv, Israel)	2019	0.5
IGO-Doelencongres (Rotterdam, Netherlands)	2019	0.5
IUGA conference (the Hague, Netherlands)	2020	0.5

Supervising	Year	Workload (ECTS)
Eva Vodegel, master thesis	2016	1.0
Laura de Waal, master thesis	2017	1.0
Laura Vos, master thesis	2018	1.0
Boris de Graaf, master thesis	2018	1.0
Nikki Stok, bachelor thesis	2018	1.0
Lotte Hollander, bachelor thesis	2018	1.0
Yani Latul, master thesis	2019	1.0

Oral presentations

A European project to develop an innovative treatment for stress urinary incontinence.
EUGA congress, Amsterdam, 2016.

The peritoneal microcirculation is dysfunctional in patients with peritoneal carcinomatosis of ovarian cancer.
Sectie XI bespreking, 2018, NKI-AvL.

Webbased bekkenfysiotherapie en serious gaming.
IGO-Doelencongres, 2019.

High definition ultrasound to study vaginal mesh.
EUGA congress, Tel Aviv, 2019.

Serious-game enhanced biofeedback-supported remotely-supervised self-management versus pelvic physiotherapy: a randomized controlled trial.
Presentation for European Commission, Brussels, 2019.
Long oral presentation, IUGA congress, 2020.
Winner Most Innovative Abstract Award, IUGA congress 2020.

Other presentations

Vaginal microcirculation to objectify wound healing after vaginal surgery.
Poster, EUGA congress, Vienna, 2018.

Anglès SA, Kastelein AW et al. Information and Communication Technologies (ICT) self-management system for pelvic floor muscle training: a pilot study in women with stress urinary incontinence.
Video abstract ICS 2017, EUGA 2017 and EUGA 2018.

Sistema De Automanejo Basado En Las Tecnologías De La Información Y La Comunicación (TIC) Para El Entrenamiento Muscular Del Suelo Pélvico: Un Estudio Piloto En Mujeres Con Incontinencia Urinaria De Esfuerzo.
Video abstract Congreso Nacional Suelo Pelvico de la S.E.G.O., Spain, 2018. Video abstract XV Congreso sociedad Iberoamericana de Neurourología y Uroginecología (SINUG), Sevilla, Spain, 2018.

Zwolsman SE, Kastelein AW et al. Heterogeneity of cost estimates in health economic evaluation research.
Oral poster presentation, EUGA congress, Vienna, 2018.

LIST OF PUBLICATIONS

Wiersma JJ, Meeuwese MC, van Miert JN, **Kastelein A**, Tijssen JP, Piek JJ, Trip MD. Diabetes mellitus type 2 is associated with higher levels of myeloperoxidase. *Med Sci Monit 2008 Aug;14(8):CR406-10.*

Kastelein AW, Oldenburger NY, van Pampus MG, Janszen EWM. Severe endocarditis and open-heart surgery during pregnancy. *BMJ Case Rep. 2016 Nov 25;2016.*

Kastelein AW, Dicker MFA, Opmeer BC, Angles S, Raatikainen KE, Alonso JF, Taut D, Airaksinen O, Cardozo LD, Roovers JPWR. Innovative Treatment Modalities for Urinary Incontinence: a European Survey Identifying Experience and Attitude of Healthcare Providers. *Int Urogynecol J. 2017 Nov;28(11): 1725-1731.*

Voogt MP, Opmeer BC, **Kastelein AW**, Jaspers MWM, Peute LW. Obstacles to successful implementation of eHealth applications into clinical practice. *Stud Health Technol Inform. 2018;247:521-525.*

Kastelein AW, Vos LMC, de Jong KH, van Baal JOAM, Nieuwland R, van Noorden CJF, Roovers JPWR, Lok CAR. Embryology, anatomy, physiology and pathophysiology of the peritoneum and the peritoneal vasculature. *Semin Cell Dev Biol. 2019 Aug;92:27-36.*

Uz Z, **Kastelein AW**, Milstein DM, Rassam F, Lui D, Veelo DP, Roovers JPWR, Ince C, van Gulik TM. Intraoperative Incident Dark Field imaging of the Human Peritoneal Microcirculation. *J Vasc Res 2018;55:136-143.*

Zwolsman S, **Kastelein A**, Daams J, Roovers JP, Opmeer BC. Heterogeneity of cost estimates in health economic evaluation research. A systematic review of stress urinary incontinence studies. *Int Urogynecol J. 2019 Jul;30(7):1045-1059.*

Diedrich CM, **Kastelein AW**, Verri F, Weber MA, Ince C, Roovers JPWR. Effects of topical estrogen therapy on the vaginal microcirculation in women with vulvovaginal atrophy. *Neurourol Urodyn. 2019 Jun;38(5):1298-1304.*

Kastelein AW, Diedrich CM, Jansen CHJR, Zwolsman SE, Ince C, Roovers JPWR. Validation of non-invasive focal depth measurements to determine epithelial thickness of the vaginal wall. *Menopause. 2019 Oct;26(10):1160-1165.*

Jansen CHJR, Kleinrouweler CE, **Kastelein AW,** Ruiter L, Mol BW, Pajkrt E, van Leeuwen E. Follow-up ultrasound in second trimester low-positioned anterior and posterior placentas – a prospective cohort study. *Ultrasound Obstet Gynecol. 2019 Oct 31.*

Kastelein AW, Diedrich CM, de Waal L, Ince C, Roovers JPWR. The vaginal microcirculation after prolapse surgery. *Neurourol Urodyn. 2020 Jan;39(1):331-338.*

Kastelein AW, Vos LMC, van Baal JOAM, Koning JJ, Hira VVV, Nieuwland R, van Driel WJ, Uz Z, van Gulik TM, Ince C, van Rheenen J, Roovers JPWR, van Noorden CJF, Lok CAR. Poor perfusion of the microvasculature in peritoneal carcinomatosis of ovarian cancer. *Clin Exp Metastasis. 2020 Apr;37(2):293-304.*

Jansen CHJR, **Kastelein AW,** Kleinrouweler CE, van Leeuwen E, de Jong KH, Pajkrt E, van Noorden CJF. Development of placental abnormalities in location and anatomy. *Acta Obstet Gynecol Scand. Feb 2020.*

Kastelein AW, de Graaf BC, Latul YP, Verhorstert KWJ, Holthof J, Guler Z, Roovers JPWR. Ultra high frequency ultrasound: a promising technique to visualize pelvic floor meshes in vivo. *Ultrasound Obstet Gynecol. 2020 Jul 4.*

Yetkin-Arik B, **Kastelein AW**, Jansen CHJR, Latul YP, Vittori M, Biri A, Kahraman K, Griffioen AW, Amant F, Lok CAR, Klaassen I, Schlingemann RO, van Noorden CJF. Angiogenesis in gynecological cancers and the options for anti-angiogenesis therapy. *Accepted for publication in BBA Reviews on Cancer.*

Mackova K, Mazzer AM, Mori Da Cunha MGMC, Hajkova Hympanova L, Urbankova I, **Kastelein AW**, Vodegel EV, Van der Linden K, Fehervary H, Guler Z, Roovers JP, Krofta L, Verhaeghe J, Deprest J. Vaginal Er:YAG LASER application in the menopausal ewe model: a randomized oestrogen and sham controlled trial. *BJOG. 2020 Oct 5.*

De Graaf BC, **Kastelein AW**, Vodegel EV, Anglès S, Baban A, Soler V, Alonso JF, Honegger G, Espuña-Pons M, Peute LW, Roovers JPWR. A novel therapy simulated usability approach for a pelvic floor muscle therapy eHealth intervention. *Submitted for publication*.

Vodegel EV, **Kastelein AW**, Hooijmans C, Jansen CHJR, Limpens JEJM, Zwolsman S, Roovers JPWR, Guler Gokce Z. The effects of estrogen on vaginal wound healing: a systematic review and meta-analysis. *Submitted for publication*.

Pope R, **Kastelein AW**, Nakhoma G, Chipungu E, Roovers JPWR. Microcirculation of vaginal and bladder tissue in the setting of vesicovaginal fistulae. *In progress*.

Angles SA, **Kastelein AW**, Tervo J, Opmeer BC, Airaksinen O, Roovers JPWR, Espuna M. Mobile and web-based self-management system for pelvic floor muscle training: a pilot study in women with stress urinary incontinence. *In progress*.

Kastelein AW, Angles SA, Tervo J, Opmeer BC, Raatikainen KE, Alonso JF, Taut D, Airaksinen O, Roovers JPWR, Espuna M. Serious-game enhanced biofeedback-supported remotely-supervised self-management versus pelvic physiotherapy: a randomized controlled trial. *In progress*.

DANKWOORD

Dit proefschrift was er niet geweest zonder de hulp van velen. Ik wil iedereen die op wat voor manier dan ook heeft bijgedragen heel hartelijk bedanken. Een aantal van hen in het bijzonder.

Mijn promotor, prof. dr. J.P.W.R. Roovers. Beste Jan-Paul, ik wil je ontzettend bedanken voor het vertrouwen en de kansen die je me geboden hebt. Toen ik net als onderzoeker was begonnen mocht ik mee naar Kaapstad en het werd een van de vele plekken ter wereld waar we samen zijn geweest, voor wetenschap maar ook voor een goed glas wijn. Je gedrevenheid is aanstekelijk en heeft er voor gezorgd dat ik onderzoek leuk ben gaan vinden. Je hebt me geleerd pragmatisch te zijn, hoofd en bijzaken te onderscheiden, om door te zetten en aan te pakken. Onze samenwerking zal gelukkig ook na dit proefschrift blijven bestaan en ik kijk daar naar uit.

Mijn promotor, prof. dr. ir. C. Ince. Beste Can, als zoekende jonge promovendus volgde ik een cursus microcirculatie bij je. Je enthousiasme voor het onderwerp werkte zeer motiverend en heeft er voor gezorgd dat ik ideeën heb omgezet in onderzoeksprojecten. Als ik later met een vraag bij je langskwam ging ik vaak na een uur weg met tien nieuwe ideeën. Bedankt voor de inspiratie en de introductie in de wereld van de microcirculatie.

Mijn copromotor, dr. C.A.R. Lok. Beste Christianne, ik had een idee voor onderzoek en werd aan jou voorgesteld. Het werd het begin van een hele prettige samenwerking. Ik wil je bedanken voor je enthousiasme, de mogelijkheid om in het AVL onderzoek te doen, de leerzame besprekingen en je hulp bij het tot stand komen van dit proefschrift. Zonder jou was het nooit op deze manier gelukt.

Geachte leden van de promotiecommissie. Dank voor uw bereidheid zitting te nemen in de promotiecommissie en uw kritische beoordeling van mijn proefschrift.

Ik wil graag alle medeauteurs bedanken die hebben bijgedragen aan de artikelen in dit proefschrift.

In het bijzonder Ron van Noorden, voor de zo prettige samenwerking en de leerzame correcties van mijn artikelen. Ik heb heel veel van je geleerd en ik hoop dat we nog

veel meer samen zullen schrijven. Daarnaast Jasper Koning, voor de hulp bij de 3D-microscopie en het enthousiasme voor ons onderzoek. Juliette van Baal, dat je openstond voor een nieuw idee en me hebt voorgesteld in het AVL. Yasin Ince, for all your help and the hours we spent together behind AVA and Photoshop. Zuhre Uz, voor de eerste lessen microcirculatie. Studenten wiens master- of bachelorthesis ik heb mogen begeleiden, en wiens werk heeft bijgedragen aan dit proefschrift, in het bijzonder Laura Vos en Laura de Waal.

Het AMC urogynaecologie onderzoeksteam. Theo, Bas, Marielle, Claudia, Alyde, Chantal, Fenne, Sandra, Zeliha, Eva, Kim, Yani en Lennart. Dank voor de inspirerende besprekingen, de congressen en de leuke team uitjes!

De gynaecologen, verloskundigen, verpleegkundigen, AIOS en ANIOS uit het Zaans Medisch Centrum en het OLVG Oost. Als ANIOS in het OLVG Oost wist ik zeker dat ik gynaecoloog wilde worden. In het bijzonder dank aan Eugenie Kaaijk en mijn mentor Erica Janszen, voor de begeleiding en supervisie tijdens het schrijven van mijn eerste artikel. Ook bijzonder dank aan Neriman Bayram, voor de eerste kennismaking met het vak als coassistent en als mijn huidige opleider.

Mijn kamergenoten en collega-vriendinnen, dank voor alle koppen thee, het samen lachen en huilen. In het bijzonder Maud, Annemijn, Charlotte, Chantal, Eva, Noor en Maddie. Annemijn in het bijzonder, vanwege onze fijne en zo complementaire samenwerking in de redactie van het NTOG.

Mijn anatomie docenten, collega's en vrienden, wat heb ik veel geleerd in de jaren op snijzaal en wat hebben we gelachen. Mijn anatomie kennis heeft enorm geholpen bij het schrijven van dit proefschrift. Roy, wat mooi dat wij elkaar nog zoveel zien!

Studiemaatjes, Olav, Rik, Eline, Merel en JW. We hebben heel wat uren samen in de collegezalen doorgebracht. Leuk dat we elkaar al die jaren zijn blijven zien. Het is ongelofelijk dat er dus zelfs zonder 1.1 een proefschrift kan komen.

Lieve Maud en familie Baars, een groot deel van mijn studententijd ben ik bij jullie over de vloer gekomen. Ik wil jullie bedanken voor de leuke jaren, de steun en het begrip voor mijn vaak inflexibele studie.

Ook al kom ik net om het hoekje kijken, toch wel mijn vrienden van het eerste uur. In het bijzonder Christiaan, Djurre, Floris, Jan-Willem, Jurriaan, Leon, Pim, Robbert, Rutger, Thijs en Thomas. De vakanties, wintersport, Sinterklaas en al het andere wat we gedeeld hebben. Christiaan, ik kan me onze eerste oud en nieuw samen nog goed herinneren. Ons samenwonen in Amsterdam heeft mijn eerste studiejaar niet veel goed gedaan, maar mij wel degelijk! Jup, bedankt voor je interesse en luisterend oor tijdens onze trainingssessies als ik even stoom moest afblazen van het onderzoek. Rut, ik ben blij dat jouw moeder destijds vond dat we vrienden moesten worden en dat ik naast je ben gaan zitten tijdens de Biologie les. En wat een goed idee om samen een boot te kopen.

Leon, jij moet natuurlijk in het bijzonder genoemd worden. Je bent niet alleen een hele goede vriend maar hebt ook een prachtig omslag voor dit proefschrift ontworpen waar ik heel erg blij mee bent. Je had aan 3 woorden genoeg. Bedankt!

Mijn paranimfen, Djurre en Lot.

Djurre, het begon met samen spijbelen op de middelbare school en eindigt voor ons allebei met een promotie. Is het toch allemaal nog redelijk goed gekomen! Bedankt voor je motiverende woorden en perspectief toen het aankwam op het afronden van dit proefschrift. Wat mooi dat je ondertussen vader bent geworden en wat ben ik blij met onze vriendschap.

Lot, wij leerden elkaar kennen tijdens de studie en in het OLVG was je al mijn steun en toeverlaat op de verloskamers. Wat leuk dat we daarna al die jaren bij elkaar op de kamer hebben gezeten en dat we vlak na elkaar promoveren. Oké, jij iets eerder dan ik, jij wint. Bedankt voor je hulp met statistiek als ik er weer eens niets van begreep, bedankt voor de blueberry muffins en die onuitstaanbare ballonnen op de kamer.

Mijn familie en schoonfamilie, in het bijzonder mijn oom Paul Reuwer. Ome Paul, zonder jouw enthousiaste verhalen over de gynaecologie was ik misschien wel nooit deze kant op gegaan. Je bent een voorbeeld voor me!

Ronald, Moran and Dani, thanks for welcoming me into your family! You have made me feel very welcome from day one. I'm very happy to know you guys!

Lieve zus, lieve Anna. Wat hebben wij een bijzondere band. Jij bent misschien wel mijn allerbeste vriend. Dankjewel dat je er altijd voor me bent, en dat we altijd elkaar hebben gehad, wat er ook gebeurde. Ik kan niet wachten tot ik oom word! Lieve Tom, wat ben ik blij dat jij mijn kleine zusje ten huwelijk hebt gevraagd. Ik kan me geen betere zwager voorstellen.

Lieve Annette en mijn kleine broertje en zusje Jonathan en Amélie, wat ben ik blij dat jullie er zijn. Ik kan niet wachten op al het leuks dat we ongetwijfeld nog met elkaar gaan meemaken.

Lieve Papa en Mama, ik heb alles aan jullie te danken. Bedankt voor het fijne gezin dat we waren, en dat jullie me altijd hebben gesteund, in alles, en in wat dan ook. Het voelt als vanzelfsprekend dat ik dit boek aan jullie opdraag. Papa, jouw carrière is altijd het grootste voorbeeld geweest. Bedankt voor je hulp, dat je altijd voor me klaar staat, en de motiverende woorden toen het aankwam op de keuze om te gaan promoveren. Mama, wat heb ik toch een geluk met een lieve moeder als jij. Als ik er in het leven even niet uitkom dan komen we er vaak samen wel uit. Dankjewel daarvoor.

Lieve Ash, mijn liefde en mijn rots in de branding. Jouw steun en geloof zijn geweldig. Zonder jou was dit niet gelukt. Ik hou van je.

ABOUT THE AUTHOR

Arnoud Willem Kastelein was born on 14 October 1987 in metropolitan Vancouver, Canada. He soon moved to The Netherlands where he lived in Assendelft and the small and picturesque village Hauwert. Arnoud attended local primary school *de Vijzel* and in 1997, he moved back to Vancouver where he attended *University Hill Elementary School*, laying the foundation for the English published in his thesis today. Later, Arnoud moved back to the Netherlands again to attend high school at the *OSG Westfriesland* in Hoorn. He started playing field hockey and after six years and numerous newly acquired friendships, Arnoud graduated from high school with ease.

After graduating in 2005, Arnoud moved to Málaga, Spain, to study at an international language school. In 2006, he started studying medicine at the University of Amsterdam. He developed a great interest in human anatomy and combined this with teaching, by working as a student assistant at the department of Anatomy. After his final rotation at the gynaecology department of the OLVG Oost, he also worked there as resident not in training (supervisor dr. E.M. Kaaijk). During this period, his choice for gynaecology was confirmed definitively.

In pursuit of his ambition to become a gynaecologist, Arnoud was glad to obtain a position as PhD-student in the research group of prof. dr. J.P.W.R. Roovers. Arnoud showed skills in scientific writing and his social abilities were useful in setting up a large, international randomized controlled trial. He (co-)authored many peer-reviewed articles outside the scope of this thesis and presented several of his research projects at national and international conferences, recently winning the prize for *Most Innovative Abstract* of the IUGA conference in 2020. During his PhD, he also developed a nationwide anatomy course for residents and joined the editorial board of the *NTOG* and *de Jonge Specialist*.

In 2020, Arnoud started his Obstetrics and Gynaecology residency program at the Amsterdam UMC (supervisor prof. dr. J.A.M. van der Post). He is currently working at the Zaans Medisch Centrum in Zaandam (supervisor dr. N. Bayram).

Arnoud lives in Amsterdam with his lovely girlfriend Ashika.